

2015

Organometallic complexes of tris(oxazoliny)borate and mixed N-heterocyclic carbene-oxazolinyborate: synthesis and catalysis

Songchen Xu
Iowa State University

Follow this and additional works at: <https://lib.dr.iastate.edu/etd>

 Part of the [Inorganic Chemistry Commons](#), and the [Organic Chemistry Commons](#)

Recommended Citation

Xu, Songchen, "Organometallic complexes of tris(oxazoliny)borate and mixed N-heterocyclic carbene-oxazolinyborate: synthesis and catalysis" (2015). *Graduate Theses and Dissertations*. 14441.
<https://lib.dr.iastate.edu/etd/14441>

This Dissertation is brought to you for free and open access by the Iowa State University Capstones, Theses and Dissertations at Iowa State University Digital Repository. It has been accepted for inclusion in Graduate Theses and Dissertations by an authorized administrator of Iowa State University Digital Repository. For more information, please contact digirep@iastate.edu.

Organometallic complexes of tris(oxazoliny)borate and mixed *N*-heterocyclic carbene–oxazolinyborate: Synthesis and catalysis

by

Songchen Xu

A dissertation submitted to the graduate faculty
in partial fulfillment of the requirements for the degree of

DOCTOR OF PHILOSOPHY

Major: Organic Chemistry

Program of Study Committee:
Aaron D. Sadow, Major Professor
Ning Fang
Javier Vela
L. Keith Woo
Yan Zhao

Iowa State University

Ames, Iowa

2015

Copyright © Songchen Xu, 2015. All rights reserved

To mom and dad

TABLE OF CONTENTS

	Page
ACKNOWLEDGEMENTS	v
ABSTRACT	ix
CHAPTER 1. INTRODUCTION	1
General Introduction	1
Thesis Organization	5
References	7
CHAPTER 2. OXYGEN INSERTION REACTIONS OF MIXED <i>N</i> - HETEROCYCLIC CARBENE–OXAZOLINYLBORATO ZINC ALKYL COMPLEXES	9
Abstract	9
Introduction	9
Results and Discussion	12
Conclusions	24
Acknowledgements	25
Experimental	25
Notes and References	32
CHAPTER 3. MIXED <i>N</i> -HETEROCYCLIC CARBENE– BIS(OXAZOLINYL)BORATO RHODIUM AND IRIDIUM COMPLEXES IN PHOTOCHEMICAL AND THERMAL OXIDATIVE ADDITION REACTIONS	37
Abstract	37
Introduction	38
Results and Discussion	42
Conclusions	86
Acknowledgements	88
Experimental	88
References	113

CHAPTER 4. CATALYTIC PARTIAL DEOXYGENATION OF ESTERS WITH AN OXAZOLINE-COORDINATED RHODIUM SILYLENE	120
Abstract.....	120
Introduction.....	121
Results and Discussion	123
Conclusions.....	139
Experimental.....	140
References.....	153
CHAPTER 5. ORGANOMETALLIC COMPLEXES OF BULKY AND OPTICALLY ACTIVE C_3 -SYMMETRIC TRIS(4 <i>S</i> -ISOPROPYL-5,5- DIMETHYL-2-OXAZOLINYL)PHENYLBORATE (To ^{P*})	159
Abstract.....	159
Introduction.....	160
Results and Discussion	162
Conclusions.....	184
Experimental.....	185
References.....	204
CHAPTER 6. CONCLUSION	209
APPENDIX A. X-RAY STRUCTURE OF THE IRIDIUM CYCLOOCTADIENE COMPLEX	213
APPENDIX B. X-RAY STRUCTURE OF THE IRIDIUM DICARBONYL COMPLEX	214

ACKNOWLEDGEMENTS

The past few years in graduate school have been a train ride full of bittersweet memories for me, as we boarded in 2008, anticipating an exciting adventure ahead, yet blissfully ignorant of the stumbling blocks along the way.

The journey starts with the successful syntheses of some compounds that launch the research onto the right track, and a beautiful view of an open prairie of hope under sunshine is seen outside the window. But it isn't always rainbows and butterflies out there. It begins to drizzle and the train slows down when the research enters the field where no one has explored. To make things worse, it starts to pour and the train is going uphill when the preliminary exam is coming to determine who still deserves to be onboard. But once it is over the hill, the feeling of accomplishment makes all the efforts worthwhile. However the train doesn't stay at the top for long, it accelerates as it goes downhill and the view gets blurry when I realize the clock is ticking and I'm still far away from the shore. The next few years feel like being stuck in the mountains, where there are countless fragile bridges to across, and endless dark tunnels to go through, as more result is needed to keep the research projects going toward publication. Then comes the final year, when I found myself in a vast snowy forest at a moonless night, and the train is going at full speed because it needs to get out of the woods before time runs out or it would be a train wreck. This is probably the darkest time of my life so far, so I'm truly thrilled to arrive at the destination of this journey safe and sound.

But I could never make it by myself. There are times when I doubt my capability of finishing this journey for I see passengers getting off the train halfway to the end, or reaching their destinations much sooner than I do, and there are times when I question my decision of boarding the train in the first place for I see others living their lives just fine without taking this trip. Sometimes I even want to jump off the train when it completely halts in the middle of nowhere or comes to a dead end after months of detouring. But I'm glad I didn't, and the following people that accompanied me alongside the journey are the reasons.

My advisor, Dr. Aaron D. Sadow, is the first person to whom I should give my gratitude, not only for all the knowledge of chemistry I learned from him, but also for teaching me how to think like a scientist, and how to be a successful one. I came to graduate school with a relatively weak background in chemistry, yet he was willing to take a chance on me by letting me join his group. Hence, I really appreciate his patience with me when I keep making the same mistake, his critiques in my writings and presentations, his guidance when I couldn't push my research forward, and his approval when I finally do. But most of all, I want to thank him for being strict with me on my research because now I understand that that's exactly what it takes to be a successful chemist. Lastly, I want to thank him for having faith in me, and for keeping this train from derailment.

I want to thank my POS committee members, Dr. Yan Zhao, Dr. Javier Vela, Dr. Keith Woo, and Dr. Ning Fang, for those insightful comments they made on my presentations on many occasions, and their valuable time spent on guiding my research.

To the members of the Sadow group, I wish I could stick around in the group until everyone I know has graduated, but I think it'll become illegal at some point, so to all of you, I want say thank you, and I'll miss the good time we had together. I learned so many things from the former group members, and they are part of the reason that I chose this group because they made it so lively and welcoming. To Dr. Andrew Pawlikowski, Dr. James Dunne, Dr. Steven Neal, Dr. Hung-An Ho, Dr. KaKing Yan, Dr. Debabrata Mukherjee, Dr. Kuntal Manna, and Dr. Barun Jana, thank you for helping me standing on my own feet in my early years here by showing me how to handle air-, moisture-, light-, temperature-, and sometimes shock-sensitive compounds and putting up with my never-ending questions about the whereabouts of the lab equipments. As for the present members of the group, it is your support and encouragement that keeps me motivated the whole time, and I also learned a lot from you. To Nicole Lampland, Naresh Eedugurala, Aradhana Pindwal, Zachary Weinstein, Jacob Fleckenstein, Regina Reinig, Bradley Schmidt, Abhranil Biswas, Kasuni Boteju, and Smita Patnaik, thank you for all those inspiring words during the time I need them the most, and teaching me how to use the new instruments again and again. To the undergraduate student that worked with me, Yitzhak Magoon, I can't thank you enough for figuring out the conditions for the deprotection step, and I apologize for not finishing our paper until very recently, and also the jokes I made about the pink backpack you used to carry. To the other members of the group, Megan Hovey, Yixin Ma, Marissa Kruse, Stephanie Smith, Brianna Upton, and Amy Jing Zhu, I'm equally grateful for your company.

To Dr. Arkady Ellern, thank you for solving all those crystal structures, and I know I had quite a few. To William C. Everett, Jeffery S. Boschen, and Dr. Theresa L.

Windus, thank you for the effort you put in the calculation. To Dr. Takeshi Kobayashi and Dr. Marek Pruski, thank you for your solid state NMR results. To Dr. Sarah Cady, and Dr. Shu Xu, thank you for setting up some of the experiments on the NMR spectrometers. To Regina Reinig and Bradley Schmidt, again, thank you for acquiring the cyclic voltammetry of my rhenium compound. To Lynette Edsall and Renee Harris, thank you for helping me out with my OPT status. To Dr. Joseph Burnett, and Dr. Tom Holme, thank you for those enlightening discussion of some general chemistry concepts. To Kirsten Johnson, and Anthony Gerten, thank you for helping me with the HPLC. To my friends I made here in Ames, Dahai Shao, Peng Xu, Dapeng Jing, Fanghao Hu, Xin Liu, Tianfu Wang, and Yan Gu, I'll miss all those laughter, discussions, and even arguments we had over dinners and road trips.

To my grandmother, Meizhong Tian, and my late grandfather, Pingyang Xu, thank you for those words of wisdom and years of nurture. Lastly, to my mother, Mingji Li, and my father, Long Xu, please forgive me for not being there for you all these years and I truly appreciate the sacrifices you made for me, and I'll never forget those heartfelt and encouraging words you said to me over the past few years. I love you, and I dedicate the following two hundred pages of thesis to you as my way of saying "Thank you".

It's actually Thanksgiving Day today when I'm writing these words, and I can't think of a better timing for doing this. Although the temperature is below zero outside right now, I feel quite warm, not just because the air-conditioning in the lab almost never breaks down, but also because I know on the new voyage I'm about to embark, with the experience I had here as a compass, I'll never be disoriented.

ABSTRACT

In order to enhance the reactivity of the organometallic complexes our group recently synthesized that bear the ligand of tris(oxazoliny)phenylborate, such as To^M and To^P (To^M = tris(4,4-dimethyl-2-oxazoliny)phenylborate; To^P = tris(4*S*-isopropyl-2-oxazoliny)phenylborate), the steric and electronic properties of the ligands are modified. The modification made to the ligand of To^M is replacing one of the three oxazoline rings in the ligand with an imidazole ring, which upon deprotonation forms a carbene moiety, hence increasing the electron-donating ability of the ligand. Therefore, a new set of mixed *N*-heterocyclic carbene–oxazoline scorpionate ligands, bis(4,4-dimethyl-2-oxazoliny)(1-*tert*-butylimidazolyl)phenylborate ($PhB(Ox^{Me_2})_2Im^{tBu}H$, Ox^{Me_2} = 4,4-dimethyl-2-oxazoline; $Im^{tBu}H$ = 1-*tert*-butylimidazole) and bis(4,4-dimethyl-2-oxazoliny)(1-mesitylimidazolyl)phenylborate ($PhB(Ox^{Me_2})_2Im^{Mes}H$, $Im^{Mes}H$ = 1-mesitylimidazole) are synthesized, followed by the isolation of a variety of the zinc, rhodium, and iridium complexes bearing these ligands. The zinc complexes, $\{PhB(Ox^{Me_2})_2Im^{Mes}\}ZnMe$, and $\{PhB(Ox^{Me_2})_2Im^{Mes}\}ZnEt$, are spectroscopically and crystallographically characterized, in which the zinc ethyl complex reacts with oxygen to provide an isolable mononuclear zinc ethylperoxide complex $\{PhB(Ox^{Me_2})_2Im^{Mes}\}ZnOOEt$. From the potassium salts of the ligands, a number of rhodium and iridium complexes are also synthesized, in which the rhodium dicarbonyl complex, $\{PhB(Ox^{Me_2})_2Im^{Mes}\}Rh(CO)_2$, and the iridium isocyanide complex, $\{PhB(Ox^{Me_2})_2Im^{Mes}\}Ir(CO)CN^tBu$, undergo oxidative addition of phenylsilane under

thermal conditions in darkness to give the corresponding metal silyl complexes, $\{\text{PhB}(\text{Ox}^{\text{Me}2})_2\text{Im}^{\text{Mes}}\}\text{RhH}(\text{SiH}_2\text{Ph})\text{CO}$ and $\{\text{PhB}(\text{Ox}^{\text{Me}2})_2\text{Im}^{\text{Mes}}\}\text{IrH}(\text{SiH}_2\text{Ph})\text{CN}^t\text{Bu}$, respectively, which demonstrates the enhanced activity of the ligand. Later, the rhodium silyl complex forms an electrophilic, coordinatively unsaturated rhodium silylene complex with Lewis acid, $\text{B}(\text{C}_6\text{F}_5)_3$, which catalyzes the deoxygenation reactions of carbonyl-containing compounds, especially esters, in the presence of phenylsilane.

The other modification is made to the ligand of To^{P} . In order to achieve high enantioselectivity in catalysis, the original oxazoline rings in To^{P} are replaced with the more sterically enhanced oxazolines, 4*S*-isopropyl-5,5-dimethyl-2-oxazoline, which has shown high enantioselectivity when incorporated in the intramolecular alkene hydroamination catalyst, $\{\text{PhB}(\text{C}_5\text{H}_4)(\text{Ox}^{\text{iPr,Me}2})_2\}\text{Zr}(\text{NMe}_2)_2$. The resulting ligand, tris(4*S*-isopropyl-5,5-dimethyl-2-oxazoliny)phenylborate ($\text{To}^{\text{P}*}$), is then synthesized from the natural amino acid, L-Valine. The rhenium and manganese carbonyl complexes, $\text{To}^{\text{P}*}\text{Re}(\text{CO})_3$ and $\text{To}^{\text{P}*}\text{Mn}(\text{CO})_3$, are spectroscopically and crystallographically characterized to assess the steric and electronic features of the ligand. The zinc hydride complex, $\text{To}^{\text{P}*}\text{ZnH}$, is then used as catalyst for cross-dehydrocoupling of silanes and alcohols and moderate enantioselectivity is achieved.

CHAPTER 1. INTRODUCTION

General Introduction

Recently, our group has synthesized a variety of organometallic complexes bearing the family of the tris(oxazolinyl)phenylborate ligand, To^M ,¹ To^P ,² and To^T (To^M = tris(4,4-dimethyl-2-oxazolinylphenyl)borate; To^P = tris(4*S*-isopropyl-2-oxazolinyl)phenylborate; To^T = tris(4*S*-*tert*-butyl-2-oxazolinyl)phenylborate),³ among which the zinc and the rhodium complexes, $To^M Zn$ and $To^M Rh$ for instance, are of particular interest because they both show remarkable reactivity toward other small molecules, and serve as outstanding catalysts for some important organic transformations.

One of the reactivity observed for the borate zinc alkyl complex $To^M ZnR$ ($R = Et$, $n-C_3H_7$, $i-C_3H_7$, and $t-Bu$), is the insertion of oxygen into the $Zn-C$ bond.⁴ The reaction takes place at room temperature, and the zinc alkyl peroxide complex $To^M ZnOOR$ is the only product formed with good to excellent yield. Interestingly, the relative reactivity of these zinc alkyl complexes toward oxygen insertion follows the trend of $To^M Zn*t*-Bu > To^M Zn*i*-Pr \approx To^M Zn*n*-Pr \approx To^M ZnEt$ in terms of the reaction rate, while $To^M ZnMe$ and $To^M ZnH$ remain inert even at higher temperature (120 °C) and higher oxygen pressure (100 psi). This relative reactivity partially deviates from the $Zn-E$ ($E = C$ or H) BDE's trend of $Zn-Me > Zn-Et > Zn-n-Pr > Zn-i-Pr > Zn-t-Bu > Zn-H$ as $To^M ZnH$ is expected to be more reactive. Kinetic study of the reaction between $To^M ZnEt$ and oxygen suggests a radical chain mechanism, which explains the inertness of $To^M ZnMe$ and $To^M ZnH$ toward oxygen as a lack of interaction of the complexes and $\cdot OOR$. Hence, an increase of

the electron density on the zinc center in $To^M ZnMe$ and $To^M ZnH$ would increase their reactivity toward oxygen insertion.

The need of the increase of the electron density on the metal center is also observed in the case of the borate rhodium and iridium carbonyl complexes $To^M Rh(CO)_2$ and $To^P Ir(CO)_2$ in oxidative addition of electrophiles, which is essentially involved in the C–H bond activation chemistry,⁵ and other catalytic chemistry such as hydrosilylation,⁶ and hydroacylation.⁷ Although $To^M Rh(CO)_2$ is more reactive than $TpRh(CO)_2$, $CpRh(CO)_2$, and some of their derivatives (Tp = tris(pyrazolyl)borate; Cp = cyclopentadienyl) in the photolytic alcohol decarbonylation which also involves oxidative addition of formyl C–H bonds,⁸ it gives a mixture of unidentified products when reacts with silanes under photolytic conditions, while $Tp^*Rh(CO)_2$ (Tp^* = tris(3,5-dimethylpyrazolyl)borate) forms $Tp^*RhH(SiEt_3)CO$ when exposed to Et_3SiH under the same conditions.⁹ In addition, when reacts with a strong electrophile such as $MeOTf$, instead of undergoing oxidative addition in which the methyl group is oxidatively added onto the metal center, $To^M Rh(CO)_2$,¹⁰ as well as $To^P Ir(CO)_2$,¹¹ gives the *N*-methylation product in which the methyl group ends up on the nitrogen atom of one of the three oxazoline rings.

Even though the electron richness of the metal center may not be the only factor responsible for the limited reactivity of the aforementioned borate metal complexes, a modification of the tris(oxazolyl)phenylborate ligand solely on its electronic property, while maintaining its *fac*-coordination mode, still mains intriguing because prior examples have shown a more electron-donating ligand could serve as the solution to the lack of reactivity of the metal center.¹² Among all the strong electron donors, *N*-

heterocyclic carbenes that derived from imidazole rings are preferred not only because are they proven increasing electron density on zinc,^{12a-d} rhodium,^{12e-f} and other metals,¹³ but also are they compatible with oxazoline rings and boron center.¹⁴ Moreover, the incorporation of *N*-heterocyclic carbene in the tris(oxazoliny)phenylborate by replacing one of the three oxazoline rings with an imidazole ring is synthetically accessible through Lewis acid-base interaction using the intermediate of the bis(oxazoliny)phenylborane also developed by our group (Figure 1).¹⁵ The synthetic route leads to a range of isoelectronic hybrid borate ligand as well. Furthermore, the mixed *N*-heterocyclic carbene-oxazoline borate ligand may offer new possibilities in catalysis.¹⁴

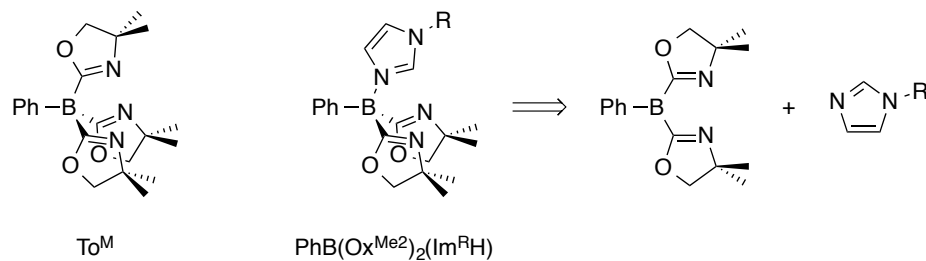


Figure 1. The incorporation of imidazole ring into the phenylborate ligand (To^M) and its reverse synthetic route.

The steric property of the tris(oxazoliny)phenylborate ligand is tunable as well. Oxazolines with different substituents on the 4- and/or 5- position, which originate from the corresponding amino acids used as starting materials for the synthesis, have been incorporated into the ligand, hence the aforementioned To^M , To^P , and To^T . Additionally, the incorporation of the enantiomerically enriched oxazolines creates the opportunity of generating highly enantioselective organometallic catalyst. The stereogenic centers on the

oxazoline ring, especially the one on the 4- position because of its proximity toward the metal center, may serve as an orientation exclusive fence on the catalyst that guides the coordination of the substrate onto the metal center in a certain direction, which as a result leads to highly enantioselective catalysis. In fact, excellent enantioselectivity has been observed in the catalytic hydroaminative cyclization of olefinic amines catalyzed by the zirconium complex $\{\text{PhB}(\text{C}_5\text{H}_4)(\text{Ox}^{\text{tPr,Me}_2})_2\}\text{Zr}(\text{NMe}_2)_2$,¹⁶ which incorporates the enantiomerically enriched 4*S*-isopropyl-5,5-dimethyl-2-oxazoline. This oxazoline moiety can also be observed elsewhere as key structural fragment of chiral catalysts responsible for enantioselective catalysis such as cyclopropanation,¹⁷ allylic oxidation,¹⁸ α -tosyloxylation,¹⁹ and Henry reaction (nitro Aldol reaction).²⁰ Therefore, the ligand of tris(4*S*-isopropyl-5,5-dimethyl-2-oxazoliny)phenylborate ($\text{To}^{\text{P}*}$) is added as a new member of the tris(oxazoliny)borate family as the sterically modification to To^{P} .

The following chapters of this thesis discuss in detail the steric and electronic properties of the aforementioned ligands, $\text{PhB}(\text{Ox}^{\text{Me}_2})_2(\text{Im}^{\text{tBuH}})$, $\text{PhB}(\text{Ox}^{\text{Me}_2})_2(\text{Im}^{\text{MesH}})$, and $\text{To}^{\text{P}*}$ (Ox^{Me_2} = 4,4-dimethyl-2-oxazoline; Im^{tBuH} = 1-*tert*-butylimidazole; Im^{MesH} = 1-mesitylimidazole), by comparing the characteristic spectroscopic and crystallographic data of the metal complexes bearing these ligands with other classic organometallic compounds bearing similar ones. In addition, the reactivity of the zinc, rhodium, and iridium complexes bearing the mixed *N*-heterocyclic carbene–oxazolinyborate or tris(4*S*-isopropyl-5,5-dimethyl-2-oxazoliny)phenylborate will also be discussed, as well as their catalytic ability toward deoxygenation of esters and cross-dehydrocoupling of silanes and alcohols.

Thesis Organization

This thesis is comprised of six chapters. Chapter 1 serves as a general introduction of the ideas behind the design of the oxazoline-based borate ligands involved in the following research results. Chapter 2 and 3 are journal articles slightly modified from their original published versions for the sake of coherence, while chapter 4 and 5 are manuscripts in progress, not yet published. The final chapter, chapter 6, concludes the property learnt about those oxazoline-based borate ligands, as well as the reactivity of the organometallic complexes bearing them.

Chapter 2 starts with the discussion of the synthesis of bis(4,4-dimethyl-2-oxazoliny)(1-mesitylimidazolyl)phenylborate ligand, followed by the synthesis of its zinc methyl and ethyl complexes. The discussion continues with their characterization and X-ray structures as well as their reactivity toward oxygen insertion. The discussion ends with the isolation of the zinc ethylperoxide complex and its X-ray structure features. William C. Everett and Dr. Theresa L. Windus contributed by providing the computational data, Dr. Arkady Ellern solved all the X-ray crystallographic structures, and Dr. Aaron D. Sadow was the corresponding author.

Chapter 3 introduces another mixed *N*-heterocyclic carbene–oxazolinyborate ligand, bis(4,4-dimethyl-2-oxazoliny)(1-*tert*-butylimidazolyl)phenylborate, as well as the LiCl-free forms of the two mixed ligands, which leads to the synthesis of a variety of rhodium and iridium complexes bearing these two ligands. Spectroscopic and crystallographic features of these complexes are then discussed and compared before the discussion of their reactivity, which includes the oxidative addition of primary silane to

the rhodium and iridium carbonyl complexes under thermal conditions. Dr. Kuntal Manna contributed by providing the work and data regarding complex **8** and **9**, Dr. Arkady Ellern solved all the X-ray crystallographic structures, and Dr. Aaron D. Sadow was the corresponding author.

Chapter 4 focuses on the structural identification of an electrophilic, coordinatively unsaturated rhodium silylene complex synthesized from the rhodium silyl complex in the previous chapter based on its characteristic spectroscopic data. The complex shows good catalytic ability toward the deoxygenation of carbonyl-containing compounds, especially esters. Jeffery S. Boschen and Dr. Theresa L. Windus contributed by providing the computational data, Dr. Takeshi Kobayashi and Dr. Marek Pruski contributed by providing the solid state NMR data, and Dr. Aaron D. Sadow was the corresponding author.

Chapter 5 switches the discussion to the third ligand of To^{P*} . The discussion starts with the organic synthesis of the chiral oxazoline, which leads to the synthesis of a series of salts of To^{P*} ligands with different counter ions. A variety of rhenium, manganese, and zinc complexes bearing To^{P*} has then been synthesized, and their characteristic spectroscopic and crystallographic features are discussed and compared. The discussion ends with the catalytic enantioselective cross-dehydrocoupling of silanes and alcohols catalyzed by the zinc hydride complex, $To^{P*}ZnH$. Yitzhak Magoon contributed to the synthesis of the chiral oxazoline, Regina R. Reinig and Bradley M. Schmidt contributed with the electrochemistry, Dr. Arkady Ellern solved all the X-ray crystallographic structures, and Dr. Aaron D. Sadow was the corresponding author.

References

1. Dunne, J. F.; Su, J.; Ellern, A.; Sadow, A. D. *Organometallics* **2008**, *27*, 2399-2401.
2. Baird, B.; Pawlikowski, A. V.; Su, J.; Wiench, J. W.; Pruski, M.; Sadow, A. D. *Inorg. Chem.* **2008**, *47*, 10208-10210.
3. Neal, S. R.; Ellern, A.; Sadow, A. D. *J. Organomet. Chem.* **2011**, *696*, 228-234.
4. Mukherjee, D.; Ellern, A.; Sadow, A. D. *J. Am. Chem. Soc.* **2012**, *134*, 13018-13026.
5. (a) Bergman, R. G. *Science* **1984**, *223*, 902-908. (b) Labinger, J. A.; Bercaw, J. E. *Nature* **2002**, *417*, 507-514.
6. Marciniak, B. *Hydrosilylation: A Comprehensive Review on Recent Advances*; Springer: Berlin, 2009.
7. (a) Bosnich, B. *Acc. Chem. Res.* **1998**, *31*, 667-674. (b) Leung, J. C.; Krische, M. *J. Chem. Sci.* **2012**, *3*, 2202-2209. (c) Roy, A. H.; Lenges, C. P.; Brookhart, M. J. *Am. Chem. Soc.* **2007**, *129*, 2082-2093.
8. Ho, H.-A.; Manna, K.; Sadow, A. D. *Angew. Chem., Int. Ed.* **2012**, *51*, 8607-8610.
9. Purwoko, A. A.; Lees, A. J. *Inorg. Chem.* **1996**, *35*, 675-682.
10. Ho, H.-A.; Dunne, J. F.; Ellern, A.; Sadow, A. D. *Organometallics* **2010**, *29*, 4105-4114.
11. Pawlikowski, A. V.; Gray, T. S.; Schoendorff, G.; Baird, B.; Ellern, A.; Windus, T. L.; Sadow, A. D. *Inorg. Chim. Acta* **2009**, *362*, 4517-4525.
12. (a) Arduengo, A. J. III; Dias, H. V. R.; Davidson, F.; Harlow, R. L. *J. Organomet. Chem.* **1993**, *462*, 13-18. (b) Wang, D.; Wurst, K.; Buchmeiser, M. R. *J.*

- Organomet. Chem.* **2004**, *689*, 2123-2130. (c) Jensen, T. R.; Schaller, C. P.; Hillmyer, M. A.; Tolman, W. B. *J. Organomet. Chem.* **2005**, *690*, 5881-5891. (d) Nelson, D. J.; Nolan, S. P. *Chem. Soc. Rev.* **2013**, *42*, 6723-6753. (e) Gigler, P.; Bechlars, B.; Herrmann, W. A.; Kühn, F. E. *J. Am. Chem. Soc.* **2011**, *133*, 1589-1596. (f) Schneider, N.; Finger, M.; Haferkemper, C.; Bellemin-Lapponnaz, S.; Hofman, P.; Gade, L. H. *Chem.–Eur. J.* **2009**, *15*, 11515-11529.
13. (a) Scepaniak, J. J.; Vogel, C. S.; Khusniyarov, M. M.; Heinemann, F. W.; Meyer, K.; Smith, J. M. *Science* **2011**, *331*, 1049-1052. (b) Nieto, I.; Bontchev, R. P.; Smith, J. M. *Eur. J. Inorg. Chem.* **2008**, 2476-2480. (c) Arrowsmith, M.; Hill, M. S.; Kociok-Köhn, G. *Organometallics* **2009**, *28*, 1730-1738.
14. (a) Gade, L. H.; César, V.; Bellemin-Lapponnaz, S. *Angew. Chem., Int. Ed.* **2004**, *43*, 1014-1017. (b) César, V.; Bellemin-Lapponnaz, S.; Gade, L. H. *Eur. J. Inorg. Chem.* **2004**, 3436-3444. (c) César, V.; Bellemin-Lapponnaz, S.; Wadepohl, H.; Gade, L. H. *Chem.–Eur. J.* **2005**, *11*, 2862-2873.
15. Dunne, J. F.; Manna, K.; Wiech, J. W.; Ellern, A.; Pruski, M.; Sadow A. D. *Dalton Trans.* **2010**, *39*, 641-653.
16. Manna, K.; Xu, S.; Sadow, A. D. *Angew. Chem., Int. Ed.* **2011**, *50*, 1865-1868.
17. Denmark, S. E.; Stavenger, R. A.; Faucher, A.-M.; Edwards, J. P. *J. Org. Chem.* **1997**, *62*, 3375-3389.
18. Dugal-Tessier, J.; Dake, G. R.; Gates, D. P. *Org. Lett.* **2010**, *12*, 4667-4669.
19. Guilbault, A.-A.; Basdevant, B.; Waine, V.; Legault, C. Y. *J. Org. Chem.* **2012**, *77*, 11283-11295.
20. Lang, K.; Park, J.; Hong, S. *J. Org. Chem.* **2010**, *75*, 6424-6435.

**CHAPTER 2. OXYGEN INSERTION REACTIONS OF MIXED N-
HETEROCYCLIC CARBENE–OXAZOLINYLBORATO ZINC ALKYL
COMPLEXES**

Modified from a paper published on *Dalton Transactions*

Songchen Xu, William C. Everett, Arkady Ellern, Theresa L. Windus, and Aaron D.

Sadow

Abstract

We report the synthesis of a new mixed oxazoline-carbene scorpionate ligand, bis(4,4-dimethyl-2-oxazoliny)(1-mesitylimidazolyl)phenylborate ($\text{PhB}(\text{Ox}^{\text{Me2}})_2\text{Im}^{\text{Mes}}$). Reactions of the protonated form $\text{PhB}(\text{Ox}^{\text{Me2}})_2(\text{Im}^{\text{Mes}}\text{H})$ with dialkylzinc compounds provide four-coordinate zinc alkyl complexes, and X-ray diffraction studies of the $\{\text{PhB}(\text{Ox}^{\text{Me2}})_2\text{Im}^{\text{Mes}}\}\text{ZnR}$ ($\text{R} = \text{Me}, \text{Et}$) compounds show significant structural distortions involving the R groups shifting away from the carbene donor. The reaction of $\{\text{PhB}(\text{Ox}^{\text{Me2}})_2\text{Im}^{\text{Mes}}\}\text{ZnEt}$ (**3**) and O_2 provides an isolable mononuclear zinc alkylperoxide $\{\text{PhB}(\text{Ox}^{\text{Me2}})_2\text{Im}^{\text{Mes}}\}\text{ZnOOEt}$ (**4**), which has been characterized by single crystal X-ray diffraction and ^{17}O NMR spectroscopy.

Introduction

Reactions of metal-carbon bonds and O_2 are important potential components of new approaches to green oxidative catalysis. Often these reactions can be complicated by

unselective product formation from overoxidation rather than formation of metallo-alkylperoxides that might be used as mediators of selective oxidation. This challenge affects organozinc chemistry, and the vigorous reactions of zinc alkyl compounds and oxygen are often difficult to control.¹ For example, reactions of ZnEt_2 and O_2 give $\text{Zn}(\text{OEt})_2$ or EtZnOEt , while ZnMe_2 and O_2 provide MeZnOMe , rather than $[\text{Zn}]\text{OOR}$.²⁻⁴ Lithium zincates, which can show enhanced reactivity in metalation in comparison to zinc alkyls,⁵ also react with O_2 to give bridging alkoxides.^{6,7} Only recently, the interaction of organozinc compounds and oxygen provided isolable and crystallographically characterized zinc alkylperoxide products, and this isolation often required carefully controlled preparative conditions.^{3,8-13} In addition, the products are generally multimetallic species with bridging alkoxide or alkylperoxide groups.

Recently, the synthesis of $\text{To}^{\text{M}}\text{ZnOOR}$ (To^{M} = tris(4,4-dimethyl-2-oxazoliny)phenylborate) by reaction of $\text{To}^{\text{M}}\text{ZnR}$ ($\text{R} = \text{Et}, n\text{-C}_3\text{H}_7, i\text{-C}_3\text{H}_7, t\text{-Bu}$) and O_2 was described.¹⁴ In contrast to these alkylzinc compounds, $\text{To}^{\text{M}}\text{ZnMe}$ and $\text{To}^{\text{M}}\text{ZnH}$ are inert to oxygen up to 120 °C and 100 psi of O_2 , even in the presence of reacting $\text{To}^{\text{M}}\text{ZnEt-O}_2$ mixtures. In addition, tris(pyrazolyl)borato zinc alkyls are inert to O_2 ,^{15,16} while $\text{Tp}^{t\text{-Bu}}\text{MgR}$ ($\text{Tp}^{t\text{-Bu}}$ = tris(3-*tert*-butyl)pyrazolylborate) react to give magnesium alkylperoxides.^{17,18} $\text{To}^{\text{M}}\text{MgMe}$ reacts with O_2 to give $\text{To}^{\text{M}}\text{MgOMe}$ species.¹⁹ $\{\text{HB}(3\text{-}t\text{Bupz})_2(5\text{-}t\text{Bupz})\}\text{AlEt}_2$ ($t\text{-Bupz} = \text{N}_2\text{C}_3\text{H}_2t\text{-Bu}$) forms uncharacterized products upon addition of excess O_2 .²⁰ On the basis of the pattern that suggests that To^{M} enhances the reactivity of Mg and Zn relative to $\text{Tp}^{t\text{-Bu}}$, we considered approaches to further enhance the reactivity of $\{\text{L}_2\text{X}\}\text{ZnMe}$ or $\{\text{L}_2\text{X}\}\text{ZnH}$ toward reaction with O_2 through modification of the ancillary ligand's electronic properties. However, strategies for this are not entirely

straightforward. First, the To^M ligand is currently the only ancillary ligand that has provided monometallic zinc alkylperoxides from zinc alkyls and O_2 . Second, in a comparative study, the infrared stretching frequencies of $Tp^*Re(CO)_3$ and $To^MRe(CO)_3$ suggest To^M is the stronger donor of the two, while the $E_{1/2}$ data indicates that $Tp^*Re(CO)_3$ is more easily oxidized than $To^MRe(CO)_3$.²¹ Furthermore, the electron-donating ability of tris(pyrazolyl)borates, at least in comparison to isoelectronic cyclopentadienide, is known to vary across the periodic table.²²

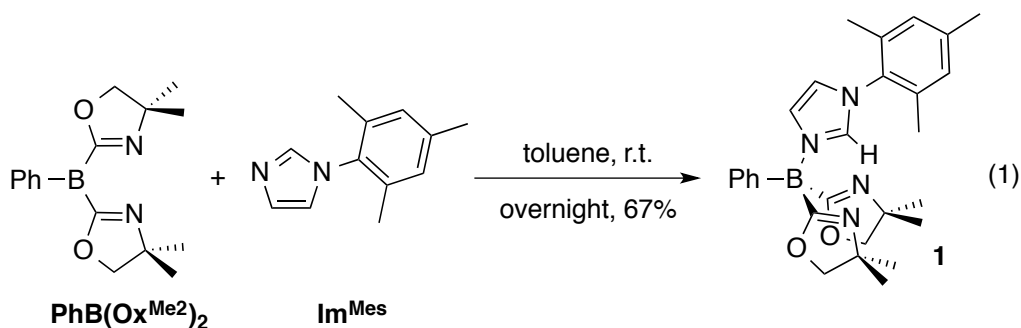
Some direction comes from the proposed pathway for O_2 insertion into Zn–C bonds. Kinetic evidence supporting a radical chain mechanism in the reaction of $To^M ZnEt$ and O_2 suggests that the inertness of $To^M ZnMe$ toward O_2 is related to the lack of interaction of $To^M ZnMe$ and $\cdot OOR$.¹⁴ We hypothesized that increasing the electron density on the zinc center could further increase the reactivity of zinc methyl and zinc hydride moieties. *N*-Heterocyclic carbenes (NHCs) are strong donors and should increase the electron density on the zinc center.²³⁻²⁶ Moreover, tris(carbene)borates^{27,28} are sufficiently strong donors to allow access to high oxidation state *3d* metal complexes,²⁹ such as a monometallic Fe(V) nitrido,³⁰ and bis(carbene)borates have been shown to stabilize low coordinate Ni(II) centers,³¹ and catalytic calcium and strontium centers.³² Mixed oxazolinylcarbene-coordinated rhodium complexes catalyze carbonyl hydrosilylation,³³⁻³⁵ and the combination of oxazolines and *N*-heterocyclic carbenes may offer new possibilities in catalysis. Furthermore, an *N*-heterocyclic carbene zinc dihydride complex was recently isolated and shown to react with carbon dioxide, whereas ZnH_2 is unstable with respect to its elemental components and reportedly inert toward CO_2 .³⁶

Hence, a modified tridentate monoanionic scorpionate ligand in which one oxazoline ring in To^{M} was replaced with an *N*-heterocyclic carbene, generated from *N*-substituted imidazolium, was sought to affect the aforementioned reactivity of $[\text{Zn}]\text{-Me}$ toward oxygen. Typically, *N*-heterocyclic carbenes coordinate to zinc(II) centers as neutral L-type ligands.^{23,24} However, *N*-borylation gives an overall uninegative charge to the bis(oxazoliny)(carbene)phenylborate, and the reaction of the imidazolium borate and dialkylzinc results in a metalation reaction to give zwitterionic complexes. Recently, a bis(carborane)-substituted NHC provided an interesting dianionic carbene ligand.³⁷

The present study describes the synthesis of the first example of a mixed oxazoline–carbene borate ligand, bis(oxazoliny)(carbene)phenylborate, its metalation chemistry with alkylzinc reagents to give tetracoordinate $\{\text{L}_2\text{X}\}\text{ZnR}$, and the reactions of $\{\text{L}_2\text{X}\}\text{ZnR}$ and O_2 to give the second example of an ancillary ligand that supports an isolable monomeric zinc alkylperoxide.

Results and Discussion

The compound $\text{PhB}(\text{Ox}^{\text{Me}_2})_2(\text{Im}^{\text{Mes}}\text{H})$ (**1**; $\text{Im}^{\text{Mes}}\text{H} = 1\text{-mesitylimidazolium}$; $\text{Ox}^{\text{Me}_2} = 4,4\text{-dimethyl-2-oxazoline}$) is synthesized in 67% yield by the reaction of bis(4,4-dimethyl-2-oxazoliny)phenylborane ($\text{PhB}(\text{Ox}^{\text{Me}_2})_2$)³⁸ and 1-mesitylimidazole (Im^{Mes})³⁹ in toluene (eq. 1). Previously, a related strategy for the synthesis of heteropodal multidentate oxazolinyborate ligands involved addition of sodium cyclopentadienide to $\text{PhB}(\text{Ox}^{\text{Me}_2})_2$ to provide the compound $\text{Na}[\text{PhB}(\text{Ox}^{\text{Me}_2})_2(\text{C}_5\text{H}_5)]$.⁴⁰ It appears that this ligand synthesis approach has some versatility in varying donor groups linked to oxazolines through a borate center.



This material is poorly soluble in toluene and benzene, but dissolves readily in acetonitrile. The ^1H NMR spectrum of the substance, acquired in acetonitrile- d_3 , contained a diagnostic downfield singlet at 8.15 ppm, which was assigned to the 2-H on the imidazolium ring. Signals at 1.24 (6 H) and 1.33 ppm (6 H) were assigned to oxazoline methyl groups and two singlets at 2.01 (6 H) and 2.33 ppm (3 H) were assigned to the mesityl group. For comparison, the ^1H NMR chemical shifts of Im^{Mes} appear at 7.06 (2-H), 1.58 (*ortho*-Mes), and 1.97 ppm (*para*-Mes) in acetonitrile- d_3 . These signals are distinct from those of **1**, and this provides convincing evidence that the imidazole is coordinated to the boron center even in a donor-solvent such as acetonitrile. Inequivalent oxazoline methyl groups indicate that the C_{2v} -symmetry of $\text{PhB}(\text{Ox}^{\text{Me}_2})_2$ is disrupted by coordination of the imidazole to the boron center. The ^{11}B NMR spectrum, also acquired in acetonitrile- d_3 , showed one singlet at -9.2 ppm. This result is consistent with a four-coordinate boron center. The $^{13}\text{C}\{^1\text{H}\}$ NMR spectrum, acquired in acetonitrile- d_3 , showed a sharp peak at 139.95 ppm and a broad peak at 179.53 ppm, which were assigned to the 2-C on the imidazolium ring and the 2-Cs on the oxazoline rings, respectively. Interestingly, the ^{15}N NMR chemical shifts for oxazoline and both imidazolium nitrogen atoms were obtained through ^1H - ^{15}N HMBC experiments. The oxazoline chemical shift (-139 ppm) was easily identified by correlations to its methyl

groups; both imidazolium nitrogen atoms correlated with the imidazolium 2-H, 4-H, and 5-H. One of the signals, at -202 ppm, is similar to ^{15}N NMR values of 1-alkyl substituted imidazolium salts. The other ^{15}N NMR chemical shift (-180 ppm) is further downfield than the signals from alkyl and aryl-substituted imidazoles,⁴¹ although this signal is similar to that reported for silver-coordinated *N*-heterocyclic carbenes.⁴² For comparison, the ^{15}N NMR chemical shifts of Im^{Mes} are -206 and -121 ppm for the 1-N and 3-N, respectively.

Crystals obtained from a concentrated toluene solution cooled to -30 °C were subjected to an X-ray diffraction study, verifying the connectivity of compound **1** as containing an imidazole coordinated to the boron center. A trace amount of benzene facilitates the crystallization, and two benzene molecules are included in the unit cell. The molecular structure is shown to be the centrosymmetric dimer $(\mathbf{1}\cdot\text{LiCl})_2$ (Figure 1); the two oxazolines of **1** are coordinated to a lithium cation, and each half of the dimer are related by a crystallographically imposed inversion center. As a result, the two imidazolium rings are located on opposite faces of the $(\text{LiCl})_2$ parallelogram.

The Li centers are four coordinate, and the N1-Li1-N2 angle of $93.7(1)^\circ$ and C11-Li1-C11# angle of $95.12(8)^\circ$ are much smaller than the N1-Li1-C11 or N2-Li1-C11 angles that range from $112.8(1)^\circ$ to $123.3(1)^\circ$. As expected based on VSEPR considerations, the Li1-C11-Li1# angles are acute ($84.88(8)^\circ$).

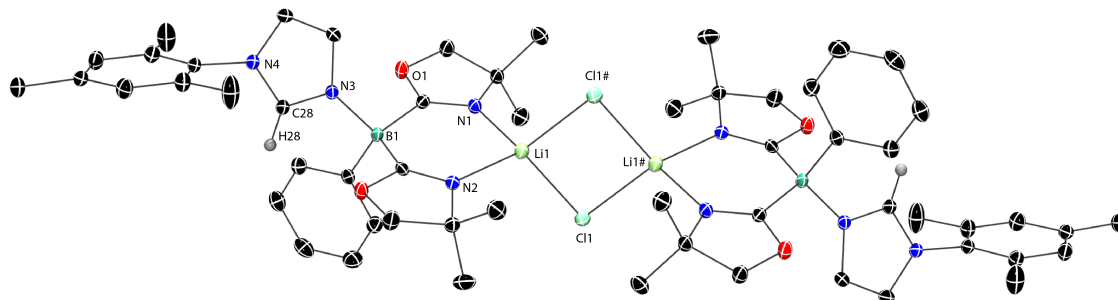
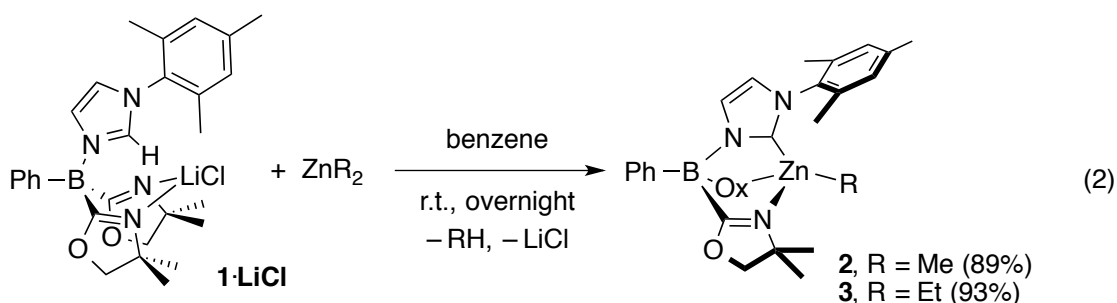


Figure 1. Rendered thermal ellipsoid diagram of $(\mathbf{1}\cdot\text{LiCl})_2$ with ellipsoids plotted at 35% probability. H28 atoms are illustrated, but all other H atoms and two co-crystallized benzene molecules are not depicted for clarity. Atoms with designator # related to the basic atom with transformation $2-x, 2-y, 2-z$. Selected interatomic distances (Å): Li1-N1, 2.070(3); Li1-N2, 2.079(3); Li1-Cl1, 2.371(2); Li1-Cl1#, 2.439(2). Selected interatomic angles (°): N1-Li1-N2, 93.7(1); Cl1-Li1-Cl1#, 95.12(8); N1-Li1-Cl1, 119.3(1); N1-Li1-Cl1#, 112.8(1); N2-Li1-Cl1, 114.7(1); N2-Li1-Cl1#, 123.3(1), Li1-Cl1-Li1#, 84.88(8).

LiCl is carried over in variable amounts from the reaction of $2\text{-LiOx}^{\text{Me}2}$ and PhBCl_2 for preparation of $[\text{PhB}(\text{Ox}^{\text{Me}2})_2]_n$, although $[\text{PhB}(\text{Ox}^{\text{Me}2})_2]_n$ may be purified from LiCl by repeated extractions with benzene or by column chromatography. The solution phase NMR spectroscopy above describes $\mathbf{1}\cdot\text{LiCl}$, likely with acetonitrile- d_3 coordinated to the lithium center. The presence of LiCl does not interfere in later metalation chemistry with dialkylzinc compounds, and $(\mathbf{1}\cdot\text{LiCl})_2$ may be used in further reactions described here. Although LiCl sometimes enhances metalation chemistry,^{5,43,44} typically the LiCl is associated with the base rather than the substrate. In fact, LiCl must be removed from $(\mathbf{1}\cdot\text{LiCl})_2$ for the successful deprotonation of $\mathbf{1}$ by more aggressive bases, such as PhCH_2K . That work will be described in Chapter 3. In addition, elemental

analysis data for $(\mathbf{1}\cdot\text{LiCl})_2$ was consistently high for carbon which may reflect slightly variable quantities of LiCl and coordinated donor in $\mathbf{1}$.

Compound $\mathbf{1}$ is readily metalated at the imidazolium 2-H by reaction with dialkylzinc compounds to give $\{\text{PhB}(\text{Ox}^{\text{Me}_2})_2\text{Im}^{\text{Mes}}\}\text{ZnR}$ ($\text{R} = \text{Me}$ ($\mathbf{2}$), Et ($\mathbf{3}$)) in 89 and 93% yield, respectively (eq. 2). The most convenient preparation involves the reaction of $(\mathbf{1}\cdot\text{LiCl})_2$ as a suspension in benzene with ZnMe_2 or ZnEt_2 . As the reaction proceeds and $\mathbf{2}$ or $\mathbf{3}$ are formed, LiCl is eliminated and the cloudy suspension becomes less opaque. Methane or ethane by-products are formed, and these species are detected by ^1H NMR spectroscopy in micromolar scale reactions performed in benzene- d_6 .



A singlet resonance at -0.52 ppm in the ^1H NMR spectrum of $\mathbf{2}$ in benzene- d_6 was assigned to a zinc methyl group on the basis of its upfield chemical shift and integration (3 H). The downfield imidazolium 2-H signal in $(\mathbf{1}\cdot\text{LiCl})_2$ was not observed in the spectra of $\mathbf{2}$ or $\mathbf{3}$, which suggested that the 2-C on the imidazolium had been metalated in both cases. The oxazoline groups are equivalent, as are the *ortho*-methyl groups on the mesityl ring. These data indicate that the compounds have effective C_s symmetry. Take compound $\mathbf{2}$ for example, two singlets in the alkyl region at 1.03 (6 H) and 1.08 ppm (6 H) assigned to the methyl groups on the oxazoline rings correlated in a $^1\text{H}-^{15}\text{N}$ HMBC

experiment to an ^{15}N NMR signal at -148 ppm (referenced to nitromethane). The zinc methyl ^1H NMR resonances also correlated with the oxazoline nitrogen, proving that both oxazolines are coordinated to the zinc center in solution. Three additional cross-peaks in the ^1H - ^{15}N HMBC experiment showed correlations between the imidazole 1-N (-190 ppm) and the ^1H NMR resonances assigned to *meta*- $\text{C}_6\text{H}_2\text{Me}_3$ (6.75 ppm) and the imidazole 4-H and 5-H (6.68 and 6.08 ppm). Two more cross-peaks between a ^{15}N NMR signal at -171 ppm, assigned to the 3-N bonded to the boron center, and the imidazole 4-H and 5-H completed the assignment of the nitrogen centers in **2**. Thus, the ^{15}N NMR chemical shift values for both oxazoline and imidazole groups change from those of $(\mathbf{1}\cdot\text{LiCl})_2$ upon metalation with zinc. In the $^{13}\text{C}\{^1\text{H}\}$ NMR spectrum, a signal at 186.02 ppm was assigned to the zinc-coordinated *N*-heterocyclic carbene. This chemical shift is essentially identical to that reported for $\text{HB}(\text{Im}^{t\text{-Bu}})_3\text{MgBr}$.²⁸ Similar ^{15}N and ^{13}C NMR data describing the ancillary mixed oxazoline-carbene borate ligand were obtained for compound **3**.

Compounds **2** and **3** are readily crystallized from concentrated benzene solutions at room temperature. Results from single crystal X-ray diffraction studies are presented in Figures 2 and 3. Interestingly, both **2** and **3** are solved in the space group *R3* (trigonal crystal system).

The distinguishing feature of the molecular structures of both compounds **2** and **3** is a distortion of the zinc alkyl group from the pseudo tetrahedral position where the ligand-zinc-carbon angles would be similar and the boron-zinc-carbon angles would be 180° . Instead, the B1-Zn1-C23 and B1-Zn1-C29 angles in **2** and **3** are $166.8(1)$ and $164.8(1)^\circ$, respectively. The large obtuse carbene-zinc-alkyl angles in **2** and **3** are

138.1(1) and 140.01(6)°, while the nitrogen-zinc-carbon angles range from 116–120°. The three angles from the donors on the ancillary ligand are similar in both mixed carbene–oxazolinyborato zinc methyl and ethyl compounds (ranging from 88–92°).

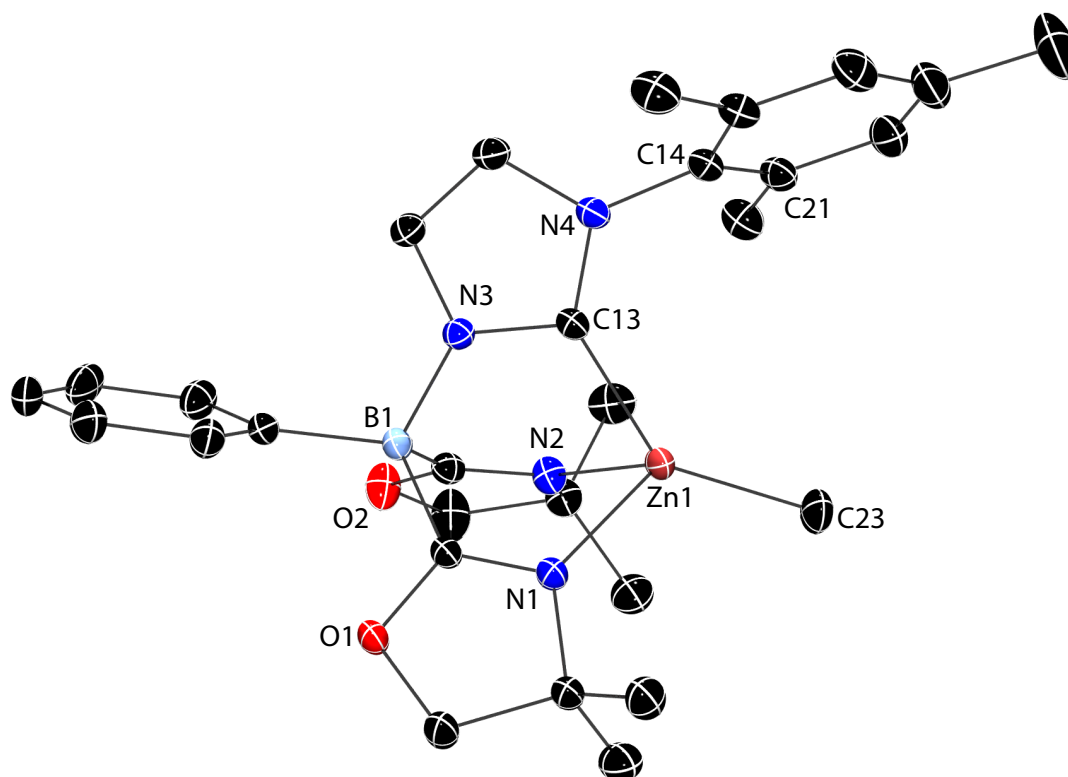


Figure 2. Rendered thermal ellipsoid diagram of $\{\text{PhB}(\text{Ox}^{\text{Me}_2})_2\text{Im}^{\text{Mes}}\}\text{ZnMe}$ (**2**) with ellipsoids at 35% probability. H atoms are not depicted for clarity. Selected interatomic distances (Å): Zn1-C13, 2.043(2); Zn1-N1, 2.104(2); Zn1-N2, 2.193(2); Zn1-C23, 1.978(2). Selected interatomic angles (°): B1-Zn1-C23, 166.8(1); C13-Zn1-C23, 138.1(1); N1-Zn1-C23, 116.08(9); N2-Zn1-C23, 120.1(1); N1-Zn1-N2, 88.79(7); C13-Zn1-N1, 92.74(7); C13-Zn1-N2, 88.27(7); C13-N4-C14-C21, 60.1(3).

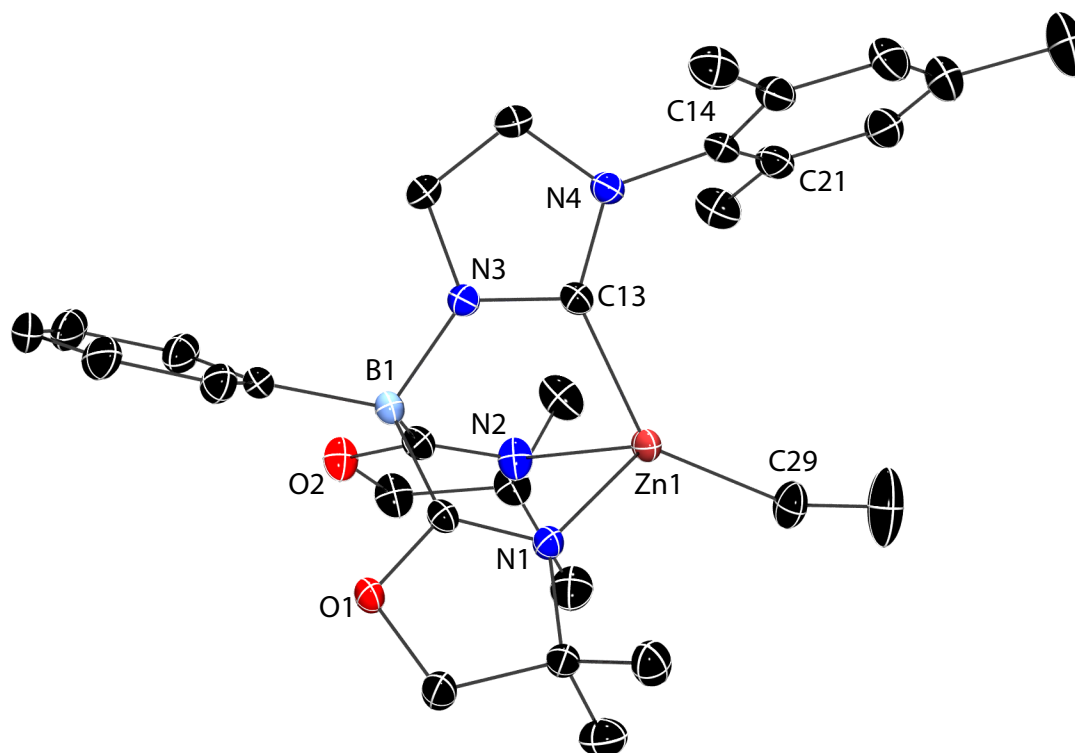


Figure 3. Rendered thermal ellipsoid diagram of $\{\text{PhB}(\text{Ox}^{\text{Me}_2})_2\text{Im}^{\text{Mes}}\}\text{ZnEt}$ (**3**) with ellipsoids at 35% probability. H atoms and 0.5 disordered pentane are not depicted for clarity. Selected interatomic distances (Å): Zn1-C13, 2.043(1); Zn1-N1, 2.125(1); Zn1-N2, 2.165(1); Zn1-C29, 1.979(2). Selected interatomic angles (°): B1-Zn1-C29, 164.8(1); C13-Zn1-C29, 140.01(6); N1-Zn1-C29, 118.04(6); N2-Zn1-C29, 115.94(6); N1-Zn1-N2, 88.61(5); C13-Zn1-N1, 92.25(5); C13-Zn1-N2, 88.36(5); C13-N4-C14-C21, 63.5(3).

The mesitylcarbene donor is much larger than the oxazoline donors, and the steric properties of $\text{PhB}(\text{Ox}^{\text{Me}_2})_2\text{Im}^{\text{Mes}}$ (solid angle, 6.26 steradians, 49.9%) are greater than those of To^{M} (solid angle, 5.51 steradians, 43.9%).^{45,46} The steric bulk of the mesitylcarbene donor might be responsible for the distortion. However, a few features argue against sterics as responsible for the unusual geometry. First, there are no

unfavorable interligand interactions, as determined by the above solid angle calculations. Second, the zinc–oxazoline and zinc–alkyl distances in **2** and **3** are similar to those in the C_{3v} -symmetric, undistorted $To^M ZnMe$ and $To^M ZnEt$.^{14,47} For example, the Zn–C_{alkyl} interatomic distances in **2** and **3** are 1.978(2) and 1.979(2) Å, whereas the distances are 1.972(1) and 1.994(2) Å in $To^M ZnMe$ and $To^M ZnEt$, respectively. The Zn–N interatomic distances in **2** and **3** range from 2.10–2.19 Å, whereas the Zn–N distances in $To^M ZnEt$ and $To^M ZnMe$ range from 2.06–2.10 Å. Thus, the coordination environment at zinc appears unremarkable with the exception of the unexpected alkyl ligand position.

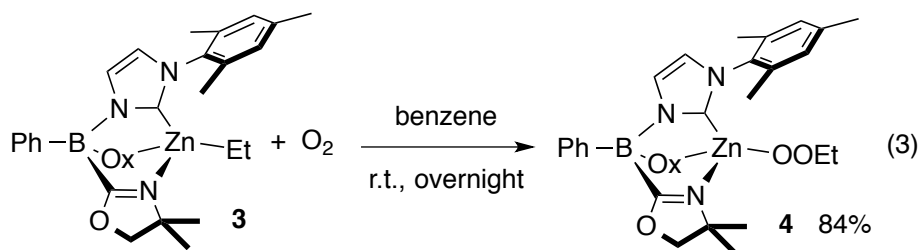
Additionally, the mesityl group is twisted with respect to the imidazole ring by approximately 60° in both **2** and **3**. The shortest H···H distance in **2** between a mesityl *ortho*-methyl and the zinc methyl is 2.83 Å (the C···C distance is 3.877 Å), and these are greater than the sum of the van der Waals radii of H and Me groups. In compound **3**, the ethyl ligand is oriented with the methyl group pointing into the open space resulting from the canted mesityl group. It is unreasonable that the mesityl ring would twist to form close contacts to an alkyl group on zinc, and then subsequently push the alkyl group into a distortion.

However, an electronic effect for the alkyl groups' unusual positions would also be surprising in the context of a metal-centered electronic distortion because compounds **2** and **3** are closed-shell, d^{10} complexes and unlikely to be distorted, even though the structural distortion of **2** and **3** is reminiscent of the tetragonal distortion of Cu(II) in spinels.⁴⁸ In addition, bending the ligand from a pseudo-tetrahedral position does not lower the overall symmetry of the complex.

To further probe these unusual structural features, the full structure of **2** was computationally optimized. In the gas-phase minimized structure, the methyl distortion is maintained (carbene-zinc-carbon angle, 139.4°), while the imidazole-mesityl torsion angle rotates to 84.3° (in comparison to 60.1° in the structure obtained by X-ray diffraction). From this, we conclude that the canted mesityl group does not relate to the distortion of the zinc's coordination sphere.

To further emphasize this point, the methyl position was straightened with both gas-phase and X-ray mesityl torsion angles of 84.3° and 60.1° . In both cases, the energy of the linear B-Zn-Me structures is higher by 0.9 and 1.2 kcal/mol, respectively, than structures with the observed B-Zn-Me angle of 167° . This small energy change related to the methyl position suggests that there are subtle electronic effects rather than steric effects in play and, indeed, it is difficult to identify any single electronic feature that is responsible for the distortion from pseudo- C_{3v} symmetry.

Compound **3** and O_2 (1 atm) react at room temperature overnight to give $\{\text{PhB}(\text{Ox}^{\text{Me}_2})_2\text{Im}^{\text{Mes}}\}\text{ZnOOEt}$ (**4**) (eq. 3), which is isolated as a white solid in 84% yield. Other possible products, including zinc ethoxy $\{\text{PhB}(\text{Ox}^{\text{Me}_2})_2\text{Im}^{\text{Mes}}\}\text{ZnOEt}$ or 2-*O*-imidazolone, were not detected in ^1H NMR spectra of crude reaction mixtures.



The reaction at the [Zn]-CH₂CH₃ is readily assessed by changes in the ¹H and ¹³C{¹H} NMR spectra acquired in benzene-*d*₆. The ¹H NMR signals for the CH₂CH₃ appeared at 0.44 ppm in **3** and 3.8 ppm in **4**. The ¹³C{¹H} NMR signals for the CH₂CH₃ was upfield of tetramethylsilane in the zinc alkyl starting material **3** at -1.48 ppm, and the signal in **4** was downfield in the ether region at 71.29 ppm. The 2-C signal in the ¹³C{¹H} NMR spectra of **3** (186.24 ppm) and **4** (181.45 ppm) were barely affected by exposure to oxygen. In addition, **3** was allowed to react with ¹⁷O-labelled O₂ to give **4**-¹⁷O₂. An ¹⁷O NMR spectrum acquired in benzene-*d*₆ contained two broad peaks at 328 and 165 ppm. The downfield resonance was assigned to the oxygen bonded to zinc (O_α), and the upfield resonance was then assigned to ZnOOEt (O_β); the difference Δ(δO) is 163 ppm (Δ(δO) = δO_α - δO_β). For comparison, the ¹⁷O NMR signals for To^MZnOOEt were detected at 319 and 169 ppm and have a smaller difference in chemical shift (Δ(δO) = 150 ppm),¹⁴ while the signals for Tp^{*t*-Bu}MgOOEt are even more separated (Δ(δO) = δO_α - δO_β = 407 - 130 = 277 ppm).^{17,18} Thus, the ¹⁷O chemical shifts of **4**-¹⁷O₂ are upfield for O_α and downfield for O_β with respect to the corresponding shifts in To^MZnOOEt.

Compound **4** crystallizes from a concentrated toluene solution at -30 °C. The solution to the single crystal X-ray diffraction study confirmed that O₂ inserted into the Zn-C bond (Figure 4). Most importantly, the formation of a ZnOOEt moiety is confirmed, and the zinc-carbene interaction is intact. The OOEt ligand is disordered over two positions, and the interatomic distances and angles must be cautiously interpreted; however, it is worth noting that the model places O3a and O3b at the same position, and this position gives the same type of distortion observed and described above for

compounds **2** and **3**. In addition, the C22-N4-C19-C12 torsion angle ($72.3(2)^\circ$) that describes the mesityl group position is larger than in **2** and **3**.

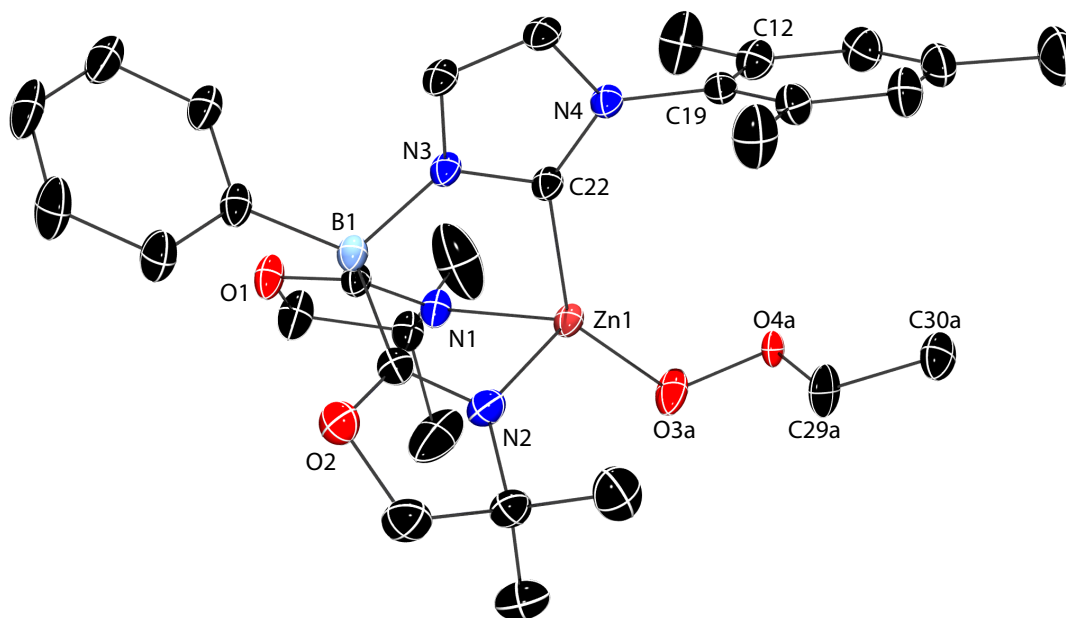


Figure 4. Rendered thermal ellipsoid diagram of $\{\text{PhB}(\text{Ox}^{\text{Me}_2})_2\text{Im}^{\text{Mes}}\}\text{ZnOOEt}$ (**4**) with ellipsoids plotted at 35% probability. The OOCC heavy atom positions are disordered over two positions, and only O3a, O4a, C29a, C30a atoms of the alkyl peroxide moiety are shown. The two positions for the OOEt group were refined using similarity restraints. However, O3a and O3b positions are identical. H atoms and a disordered toluene solvent molecule are not depicted for clarity.

As noted above, the alkyl ligands of **2** and **3** are distorted with respect to ideal positions. However, this distortion apparently did not translate into enhanced reactivity for the zinc methyl, at least with respect to the interaction of **2** and oxygen. In fact, compound **2** is stable under O_2 (1-3 atm) up to 60°C . The inert nature of the zinc methyl

in **2** follows the reactivity of $\text{To}^{\text{M}}\text{ZnMe}$ and $\text{To}^{\text{M}}\text{ZnH}$, which, as noted above, also are inert toward reaction with O_2 .

We were unable to isolate $\{\text{PhB}(\text{Ox}^{\text{Me}_2})_2\text{Im}^{\text{Mes}}\}\text{ZnOO}t\text{-Bu}$ from the reaction of **3** and $t\text{-BuOOH}$. Even though a small amount of ethane was detected by ^1H NMR spectroscopy in micromolar scale reactions performed in benzene- d_6 , the majority of **3** remained unreacted at room temperature over 1 day. After 2 days at room temperature, a signal at 10.86 ppm assigned to a 2H-imidazolium moiety was observed as part of the major product suggesting protonation of the carbene.

Conclusions

We have described the preparation of a new heteroleptic monoanionic scorpionate ligand that contains two oxazoline donors and one *N*-heterocyclic carbene donor. There are some similarities between the tris(oxazolinyl)borate To^{M} and the bis(oxazolinyl)(carbene)borate in the facile metalation reactions of $\text{H}[\text{ligand}]$ by dialkylzinc reagents. Both ligands support four-coordinate monoalkyl zinc compounds. In addition, both $\text{To}^{\text{M}}\text{ZnMe}$ and $\{\text{PhB}(\text{Ox}^{\text{Me}_2})_2\text{Im}^{\text{Mes}}\}\text{ZnMe}$ compounds are inert toward O_2 , whereas both $\text{To}^{\text{M}}\text{ZnEt}$ and $\{\text{PhB}(\text{Ox}^{\text{Me}_2})_2\text{Im}^{\text{Mes}}\}\text{ZnEt}$ react with O_2 to give isolable zinc alkylperoxides. Unlike $\text{To}^{\text{M}}\text{ZnEt}$, $\{\text{PhB}(\text{Ox}^{\text{Me}_2})_2\text{Im}^{\text{Mes}}\}\text{ZnEt}$ does not provide an isolable $[\text{Zn}]\text{OO}t\text{-Bu}$ in its reaction with $t\text{-BuOOH}$. The ancillary ligand $\text{PhB}(\text{Ox}^{\text{Me}_2})_2\text{Im}^{\text{Mes}}$ is only the second example of a ligand that supports a monometallic zinc alkylperoxide formed from O_2 . Notably, the carbene moiety is inert toward O_2 as well as any $\cdot\text{OOR}$ present during the radical chain process that gives $\{\text{PhB}(\text{Ox}^{\text{Me}_2})_2\text{Im}^{\text{Mes}}\}\text{ZnOOEt}$. Additionally, a significant and systematic structural distortion of the compounds

$\{\text{PhB}(\text{Ox}^{\text{Me}_2})_2\text{Im}^{\text{Mes}}\}\text{ZnX}$ has been observed, where the X group (Me, Et, OOEt) is distorted away from the carbene ligand in three structures determined by X-ray crystallographic diffraction studies. However, this distortion, or the substitution of an oxazoline in the $\text{To}^{\text{M}}\text{ZnR}$ compounds with a carbene donor does not appear to affect the reactivity of zinc methyl or ethyl toward O_2 , either by increasing the reactivity of the zinc methyl or decreasing the reactivity of the zinc ethyl toward O_2 .

Acknowledgements

This research was supported by the U.S. Department of Energy, Office of Basic Energy Sciences, Division of Chemical Sciences, Geosciences, and Biosciences through the Ames Laboratory Catalysis and Chemical Physics programs. The Ames Laboratory is operated for the U.S. Department of Energy by Iowa State University under Contract No. DE-AC02-07CH11358. This research was also supported by an allocation of advance computing resources provided by the National Science Foundation (A.D.S. and T.L.W). The computations were performed on Kraken at the National Institute for Computational Sciences.

Experimental

General synthetic procedures. All reactions were performed under a dry argon atmosphere using standard Schlenk techniques or under a nitrogen atmosphere in a glovebox, unless otherwise indicated. Benzene, toluene, and pentane were dried and deoxygenated using an IT PureSolv system. Benzene- d_6 was heated to reflux over Na/K alloy and vacuum transferred. Acetonitrile- d_3 was heated to reflux over CaH_2 and

vacuum transferred. $[\text{PhB}(\text{Ox}^{\text{Me}_2})_2]_n$,³⁸ and 1-mesitylimidazole³⁹ were synthesized according to literature procedures. Dimethylzinc solution (2.0 M in toluene) was purchased from Sigma-Aldrich and transferred to a flask equipped with a resealable Teflon valve for storage inside a glovebox. Diethylzinc was purchased from Strem Chemicals, Inc., and stored inside a glovebox in its original Swagelok cylinder.

^1H , $^{13}\text{C}\{^1\text{H}\}$, ^{11}B , and ^{17}O NMR spectra were collected on an Avance II 600 MHz NMR spectrometer. ^{15}N chemical shifts were determined by ^1H - ^{15}N HMBC experiments on an Avance II 600 MHz NMR spectrometer. ^{15}N chemical shifts were originally referenced to an external liquid NH_3 standard and recalculated to the CH_3NO_2 chemical shift scale by adding -381.9 ppm. Infrared spectra were recorded on a Bruker Vertex spectrometer. Elemental analyses were performed using a Perkin-Elmer 2400 Series II CHN/S in the Iowa State Chemical Instrumentation Facility.

$\text{PhB}(\text{Ox}^{\text{Me}_2})_2(\text{Im}^{\text{Mes}}\text{H})\text{LiCl}$ (1·LiCl). $[\text{PhB}(\text{Ox}^{\text{Me}_2})_2(\text{LiCl})]_n$ (1.175 g, 3.598 mmol) was suspended in toluene (15 mL), and 1-mesitylimidazole (0.625 g, 3.36 mmol) was added to give a transparent brown solution. The reaction mixture was stirred at room temperature overnight. The product, as a white precipitate, was observed after 6 h. The resulting suspension was allowed to settle in a centrifuge over 7 min at 4000 rpm, and the top clear brown solution was decanted. The precipitate was washed with toluene (3×5 mL) and dried *in vacuo* to afford the product as a white solid (1.144 g, 2.232 mmol, 66.8%). ^1H NMR (acetonitrile- d_3 , 600 MHz): δ 8.15 (s, 1 H, 2H- $\text{N}_2\text{C}_3\text{H}_3\text{Mes}$), 7.31-7.18 (m, 7 H, C_6H_5 , 4- and 5H- $\text{N}_2\text{C}_3\text{H}_3\text{Mes}$), 7.07 (s, 2 H, *m*- $\text{C}_6\text{H}_2\text{Me}_3$), 3.74 (m, 4 H, $\text{CNCMe}_2\text{CH}_2\text{O}$), 2.33 (s, 3 H, *p*- $\text{C}_6\text{H}_2\text{Me}_3$), 2.01 (s, 6 H, *o*- $\text{C}_6\text{H}_2\text{Me}_3$), 1.33 (s, 6 H, $\text{CNCMe}_2\text{CH}_2\text{O}$), 1.24 (s, 6 H, $\text{CNCMe}_2\text{CH}_2\text{O}$). $^{13}\text{C}\{^1\text{H}\}$ NMR (acetonitrile- d_3 , 150

MHz): δ 180 (br, CNCMe₂CH₂O), 147 (br, *ipso*-C₆H₅), 139.95 (2C-N₂C₃H₃Mes), 135.85 (*ipso*-C₆H₂Me₃), 133.33 (*o*-C₆H₅), 132.79 (*o*-C₆H₂Me₃), 130.18 (*m*-C₆H₂Me₃), 129.92 (*p*-C₆H₂Me₃), 128.49 (*m*-C₆H₅), 127.09 (4,5C-N₂C₃H₃Mes), 126.26 (*p*-C₆H₅), 123.12 (4,5C-N₂C₃H₃Mes), 78.30 (CNCMe₂CH₂O), 68.14 (CNCMe₂CH₂O), 28.72 (CNCMe₂CH₂O), 28.52 (CNCMe₂CH₂O), 21.17 (*p*-C₆H₂Me₃), 17.51 (*o*-C₆H₂Me₃). ¹¹B NMR (acetonitrile-*d*₃, 128 MHz): δ -9.2. ¹⁵N{¹H} NMR (acetonitrile-*d*₃, 71 MHz): δ -139 (CNCMe₂CH₂O), -180 (N₂C₃H₃Mes), -202 (N₂C₃H₃Mes). IR (KBr, cm⁻¹): 3164 w, 2962 m, 2927 w, 1658 s (CN), 1546 m, 1461 w, 1135 s, 990 m, 969 m, 767 m. Anal. Calcd for C₂₈H₃₅BCILiN₄O₂: C, 65.58; H, 6.88; N, 10.93. Found: C, 67.76; H, 7.04; N, 10.56. Mp, 127-130 °C.

{PhB(Ox^{Me2})₂Im^{Mes}}ZnMe (2). PhB(Ox^{Me2})₂(Im^{Mes}H)LiCl (**1**·LiCl, 0.351 g, 0.684 mmol) was suspended in benzene (10 mL), and a 2.0 M solution of ZnMe₂ (0.380 mL, 0.760 mmol) in toluene was added. The white suspension was stirred at room temperature overnight. The suspension was filtered, and the solvent was removed under reduced pressure to afford a white solid, which was triturated with pentane (2 × 10 mL) and dried *in vacuo* (0.336 g, 0.611 mmol, 89.3%). ¹H NMR (benzene-*d*₆, 600 MHz): δ 8.45 (d, ³J_{HH} = 7.2 Hz, 2 H, *o*-C₆H₅), 7.55 (t, ³J_{HH} = 7.2 Hz, 2 H, *m*-C₆H₅), 7.40 (t, ³J_{HH} = 7.2 Hz, 1 H, *p*-C₆H₅), 6.75 (s, 2 H, *m*-C₆H₂Me₃), 6.62 (s, 1 H, N₂C₃H₂Mes), 6.06 (s, 1 H, N₂C₃H₂Mes), 3.55 (d, ²J_{HH} = 7.8 Hz, 2 H, CNCMe₂CH₂O), 3.53 (d, ²J_{HH} = 7.8 Hz, 2 H, CNCMe₂CH₂O), 2.09 (s, 3 H, *p*-C₆H₂Me₃), 1.97 (s, 6 H, *o*-C₆H₂Me₃), 1.08 (s, 6 H, CNCMe₂CH₂O), 1.03 (s, 6 H, CNCMe₂CH₂O), -0.52 (s, 3 H, ZnCH₃). ¹³C{¹H} NMR (benzene-*d*₆, 150 MHz): δ 189 (br, CNCMe₂CH₂O), 186 (br, 2C-N₂C₃H₂Mes), 143.39 (*ipso*-C₆H₅), 138.29 (*p*-C₆H₂Me₃), 137.40 (*o*-C₆H₂Me₃), 137.01 (*o*-C₆H₅), 135.26 (*ipso*-

C₆H₂Me₃), 129.47 (*m*-C₆H₂Me₃), 127.75 (*m*-C₆H₅), 127.23 (*p*-C₆H₅), 124.61 (4,5C-N₂C₃H₂Mes), 119.01 (4,5C-N₂C₃H₂Mes), 80.46 (CNCMe₂CH₂O), 66.14 (CNCMe₂CH₂O), 28.40 (CNCMe₂CH₂O), 28.31 (CNCMe₂CH₂O), 21.36 (*p*-C₆H₂Me₃), 18.19 (*o*-C₆H₂Me₃), -16.91 (ZnCH₃). ¹¹B NMR (benzene-*d*₆, 128 MHz): δ -9.9. ¹⁵N{¹H} NMR (benzene-*d*₆, 71 MHz): δ -148 (CNCMe₂CH₂O), -171 (3N-N₂C₃H₂Mes), -190 (1N-N₂C₃H₂Mes). IR (KBr, cm⁻¹): 3123 w, 3076 w, 2956 s, 2926 m, 2891 m, 2824 w, 1594 s (CN), 1491 m, 1461 m, 1268 s, 1193 m, 1183 m, 1158 s, 1108 w, 1015 w, 951 m, 819 m, 704 m, 669 m, 640 m, 523 w. Anal. Calcd for C₂₉H₃₇BN₄O₂Zn: C, 63.55; H, 6.78; N, 10.19. Found: C, 63.77; H, 6.72; N, 10.77. Mp, 173-176 °C.

{PhB(Ox^{Me2})₂Im^{Mes}}ZnEt (3). PhB(Ox^{Me2})₂(Im^{Mes}H)LiCl (**1**·LiCl, 0.740 g, 1.44 mmol) was suspended in benzene (10 mL), and ZnEt₂ (0.165 mL, 1.61 mmol) was added. The white suspension was stirred at room temperature overnight. The suspension was filtered, the solvent was removed under reduced pressure, and the resulting white solid was triturated with pentane (2 × 10 mL), and dried *in vacuo* (0.754 g, 1.34 mmol, 92.7%). ¹H NMR (benzene-*d*₆, 600 MHz): δ 8.45 (d, ³J_{HH} = 7.2 Hz, 2 H, *o*-C₆H₅), 7.55 (t, ³J_{HH} = 7.2 Hz, 2 H, *m*-C₆H₅), 7.40 (t, ³J_{HH} = 7.2 Hz, 1 H, *p*-C₆H₅), 6.79 (s, 2 H, *m*-C₆H₂Me₃), 6.61 (s, 1 H, N₂C₃H₂Mes), 6.05 (s, 1 H, N₂C₃H₂Mes), 3.54 (m, 4 H, CNCMe₂CH₂O), 2.12 (s, 3 H, *p*-C₆H₂Me₃), 1.96 (s, 6 H, *o*-C₆H₂Me₃), 1.31 (m, 3 H, ZnCH₂CH₃), 1.07 (s, 6 H, CNCMe₂CH₂O), 1.04 (s, 6 H, CNCMe₂CH₂O), 0.44 (m, 2 H, ZnCH₂CH₃). ¹³C{¹H} NMR (benzene-*d*₆, 150 MHz): δ 189 (br, CNCMe₂CH₂O), 186.24 (2C-N₂C₃H₂Mes), 144 (br, *ipso*-C₆H₅), 138.47 (*p*-C₆H₂Me₃), 137.75 (*o*-C₆H₂Me₃), 136.90 (*o*-C₆H₅), 135.56 (*ipso*-C₆H₂Me₃), 129.44 (*m*-C₆H₂Me₃), 127.74 (*m*-C₆H₅), 127.20 (*p*-C₆H₅), 124.81 (4,5C-N₂C₃H₂Mes), 118.89 (4,5C-N₂C₃H₂Mes), 80.34 (CNCMe₂CH₂O), 66.09

(CNCMe₂CH₂O), 28.50 (CNCMe₂CH₂O), 28.28 (CNCMe₂CH₂O), 21.37 (*p*-C₆H₂Me₃), 18.06 (*o*-C₆H₂Me₃), 14.45 (ZnCH₂CH₃), -1.48 (ZnCH₂CH₃). ¹¹B NMR (benzene-*d*₆, 128 MHz): δ -10.0. ¹⁵N{¹H} NMR (benzene-*d*₆, 71 MHz): δ -148 (CNCMe₂CH₂O), -170 (3N-N₂C₃H₂Mes), -190 (1N-N₂C₃H₂Mes). IR (KBr, cm⁻¹): 3132 w, 3008 w, 2971 s, 2927 s, 2885 s, 2852 m, 1592 s (CN), 1492 m, 1464 m, 1398 w, 1366 w, 1269 s, 1193 m, 1183 m, 1157 s, 1109 w, 1010 w, 963 s, 822 w, 744 m, 704 m, 672 m, 641 m. Anal. Calcd for C₃₀H₃₉BN₄O₂Zn: C, 63.90; H, 6.97; N, 9.94. Found: C, 64.07; H, 6.81; N, 10.32. Mp, 199-201 °C.

{PhB(Ox^{Me2})₂Im^{Mes}}ZnOOEt (4). A benzene solution (15 mL) of {PhB(Ox^{Me2})₂Im^{Mes}}ZnEt (**3**, 0.700 g, 1.24 mmol) was degassed with “freeze-pump-thaw” cycles (3×), and then oxygen was added (1 atm). The solution was allowed to stir at room temperature overnight. Evaporation of the mixture to dryness gave a white solid. The crude product was dissolved in a minimal amount of toluene, and the solution was cooled to -30 °C to produce colorless crystals. The crystals were isolated by filtration, washed with pentane (2 × 2 mL) and dried *in vacuo* (0.621 g, 1.04 mmol, 84.0%). ¹H NMR (benzene-*d*₆, 600 MHz): δ 8.4 (2 H, *o*-C₆H₅), 7.5 (m, 2 H, *m*-C₆H₅), 7.4 (m, 1 H, *p*-C₆H₅), 6.7 (s, 2 H, *m*-C₆H₂Me₃), 6.6 (s, 1 H, N₂C₃H₂Mes), 6.0 (s, 1 H, N₂C₃H₂Mes), 3.8 (m, 2 H, ZnOOCH₂CH₃), 3.6 (m, 4 H, CNCMe₂CH₂O), 2.1 (s, 3 H, *p*-C₆H₂Me₃), 2.0 (s, 6 H, *o*-C₆H₂Me₃), 1.3 (s, 6 H, CNCMe₂CH₂O), 1.2 (s, 6 H, CNCMe₂CH₂O), 1.1 (m, 3 H, ZnOOCH₂CH₃). ¹³C{¹H} NMR (benzene-*d*₆, 150 MHz): δ 189 (br, CNCMe₂CH₂O), 181.45 (2C-N₂C₃H₂Mes), 142 (br, *ipso*-C₆H₅), 138.38 (*p*-C₆H₂Me₃), 136.93 (*o*-C₆H₂Me₃), 136.84 (*o*-C₆H₅), 135.23 (*ipso*-C₆H₂Me₃), 129.44 (*m*-C₆H₂Me₃), 127.74 (*m*-C₆H₅), 127.32 (*p*-C₆H₅), 124.99 (4,5C-N₂C₃H₂Mes), 119.48 (4,5C-N₂C₃H₂Mes), 80.77

(CNCMe₂CH₂O), 71.29 (ZnOOCH₂CH₃), 65.9 (CNCMe₂CH₂O), 28.18 (CNCMe₂CH₂O), 28.04 (CNCMe₂CH₂O), 21.21 (*p*-C₆H₂Me₃), 18.00 (*o*-C₆H₂Me₃), 14.62 (ZnOOCH₂CH₃). ¹¹B NMR (benzene-*d*₆, 128 MHz): δ -10.0. ¹⁵N{¹H} NMR (benzene-*d*₆, 71 MHz): δ -150 (CNCMe₂CH₂O), -169 (N₂C₃H₂Mes), -190 (N₂C₃H₂Mes). ¹⁷O NMR (benzene-*d*₆, 81 MHz): δ 328 (ZnOOCH₂CH₃), 165 (ZnOOCH₂CH₃). IR (KBr, cm⁻¹): 3133 w, 2966 s, 2927 m, 2888 m, 1610 s (CN), 1462 m, 1276 w, 1179 m, 1154 s, 1065 m, 968 s, 853 w, 849 w, 734 m, 704 m. Anal. Calcd for C₃₀H₃₉BN₄O₄Zn: C, 60.47; H, 6.60; N, 9.40. Found: C, 60.98; H, 6.64; N, 8.92. Mp, 138-141 °C.

X-ray crystallography. Single-crystal X-ray diffraction experiments for **1-4** were carried out on a Bruker diffractometer with an APEX II CCD detector using graphite monochromated MoK α radiation with a detector distance of 50.6 mm. Full-sphere data collection with exposure of 30 s per frame were made with ω scans in the range 0-180° at $\phi = 0, 120, \text{ and } 240^\circ$. A semi-empirical absorption correction was based on a fit of a spherical harmonic function to the empirical transmission surface as sampled by multiple equivalent measurements⁴⁹ using SADABS software.⁵⁰ The experiment was optimized to collect data to a resolution of 0.71 Å, however, the datasets have been truncated to obtain the statistically relevant resolution. The positions of metal atoms were found by direct methods. The remaining atoms were located in an alternating series of least-squares cycles and difference Fourier maps. All non-hydrogen atoms were refined in the full-matrix anisotropic approximation. All hydrogen atoms were placed in the structure factor calculation at idealized positions and were allowed to ride on the neighboring atoms with relative isotropic displacement coefficients. All calculations were performed using the BRUKER APEX II software suite.⁵¹

SQUEEZE was used to treat diffuse electron density in solvent accessible voids for structures **1-3**.⁵² Crystallographic data and structure refinement parameters for **1-4** are summarized in Table 1.

Table 1. Crystallographic data for compounds **1-4**.

	1·LiCl	2	3	4
Chemical formula	C ₃₇ H ₄₄ BClLiN ₄ O ₄	C ₂₉ H ₃₇ BN ₄ O ₂ Zn	C _{32.5} H ₄₅ BN ₄ O ₂ Zn	C _{33.5} H ₄₇ BN ₄ O ₄ Zn
Formula weight	629.96	549.81	599.91	645.93
Crystal system	Triclinic	Trigonal	Trigonal	Monoclinic
Unit-cell dimensions	$a = 11.152(1) \text{ \AA}$ $b = 12.661(1) \text{ \AA}$ $c = 13.378(1) \text{ \AA}$ $\alpha = 85.243(2)^\circ$ $\beta = 69.278(1)^\circ$ $\gamma = 88.683(2)^\circ$	$a = b = 29.159(2) \text{ \AA}$ $c = 19.403(3) \text{ \AA}$ $\alpha = \beta = 90^\circ$ $\gamma = 120^\circ$	$a = b = 28.780(3) \text{ \AA}$ $c = 20.259(2) \text{ \AA}$ $\alpha = \beta = 90^\circ$ $\gamma = 120^\circ$	$a = 9.497(1) \text{ \AA}$ $b = 26.859(3) \text{ \AA}$ $c = 13.405(2) \text{ \AA}$ $\alpha = \gamma = 90^\circ$ $\beta = 96.814(2)^\circ$
Volume	1760.5(3) Å ³	14287(2) Å ³	14542(2) Å ³	3395.0(7) Å ³
Space group	<i>P1</i>	<i>R3</i>	<i>R3</i>	<i>P12₁/n1</i>
<i>Z</i>	2	18	18	4
Reflections collected	19082	53056	53004	44529
Independent reflections	8984	8974	8740	7785
<i>R</i> _{int}	0.0261	0.0303	0.0356	0.0327
<i>R</i> <i>I</i> > 2σ(<i>I</i>)	$R_1 = 0.0424$ $wR_2 = 0.0963$	$R_1 = 0.0415$ $wR_2 = 0.1480$	$R_1 = 0.0314$ $wR_2 = 0.0839$	$R_1 = 0.0448$ $wR_2 = 0.1329$
<i>R</i> _{all}	$R_1 = 0.0610$ $wR_2 = 0.1062$	$R_1 = 0.0553$ $wR_2 = 0.1602$	$R_1 = 0.0432$ $wR_2 = 0.0878$	$R_1 = 0.0537$ $wR_2 = 0.1398$

DFT calculations. All calculations were performed with the NWChem computational chemistry software.⁵³ Density functional theory with the B3LYP

functional was used for single point energy calculations, geometry optimization and frequency calculations.⁵⁴⁻⁵⁶ The 6-311G(d,p) basis set was used for H, C, N, O, and B.⁵⁷ The Stuttgart 1997 relativistic small core basis set with effective core potential was used for Zn.⁵⁸

Notes and References

^a 1605 Gilman Hall, Department of Chemistry, Iowa State University, Ames, IA 50011, USA

† Electronic Supplementary Information (ESI) available: Experimental data and spectra for compounds **1**·LiCl, **2-4**. Crystallographic data files (995354-995357) are available from the CCDC. Computational coordinates and energies. See DOI: 10.1039/b000000x/

1. D. Seyferth, *Organometallics*, 2001, **20**, 2940-2955.
2. J. Maury, L. Feray, S. Bazin, J.-L. Clément, S. R. A. Marque, D. Siri and M. P. Bertrand, *Chem.–Eur. J.*, 2011, **17**, 1586-1595.
3. J. Lewiński, W. Marciniak, J. Lipkowski and I. Justyniak, *J. Am. Chem. Soc.*, 2003, **125**, 12698-12699.
4. S. Jana, R. J. F. Berger, R. Fröhlich, T. Pape and N. W. Mitzel, *Inorg. Chem.*, 2007, **46**, 4293-4297.
5. A. R. Kennedy, J. Klett, R. E. Mulvey and D. S. Wright, *Science*, 2009, **326**, 706-708.
6. A. E. H. Wheatley, *New J. Chem.*, 2004, **28**, 435-443.
7. A. E. H. Wheatley, *Chem. Soc. Rev.*, 2001, **30**, 265-273.

8. J. Lewiński, Z. Ochal, E. Bojarski, E. Tratkiewicz, I. Justyniak and J. Lipkowski, *Angew. Chem. Int. Ed.*, 2003, **42**, 4643-4646.
9. J. Lewiński, K. Suwała, M. Kubisiak, Z. Ochal, I. Justyniak and J. Lipkowski, *Angew. Chem. Int. Ed.*, 2008, **47**, 7888-7891.
10. J. Lewiński, W. Śliwiński, M. Dranka, I. Justyniak and J. Lipkowski, *Angew. Chem. Int. Ed.*, 2006, **45**, 4826-4829.
11. J. Lewiński, K. Suwała, T. Kaczorowski, M. Galezowski, D. T. Gryko, I. Justyniak and J. Lipkowski, *Chem. Commun.*, 2009, 215-217.
12. N. Hollingsworth, A. L. Johnson, A. Kingsley, G. Kociok-Köhn and K. C. Molloy, *Organometallics*, 2010, **29**, 3318-3326.
13. M. Kubisiak, K. Zelga, I. Justyniak, E. Tratkiewicz, T. Pietrzak, A. R. Keeri, Z. Ochal, L. Hartenstein, P. W. Roesky and J. Lewiński, *Organometallics*, 2013, **32**, 5263-5265.
14. D. Mukherjee, A. Ellern and A. D. Sadow, *J. Am. Chem. Soc.*, 2012, **134**, 13018-13026.
15. I. B. Gorrell, A. Looney and G. Parkin, *J. Chem. Soc., Chem. Commun.*, 1990, 220-222.
16. A. Looney, R. Han, I. B. Gorrell, M. Cornebise, K. Yoon, G. Parkin and A. L. Rheingold, *Organometallics*, 1995, **14**, 274-288.
17. R. Han and G. Parkin, *J. Am. Chem. Soc.*, 1990, **112**, 3662-3663.
18. R. Han and G. Parkin, *J. Am. Chem. Soc.*, 1992, **114**, 748-757.
19. D. Mukherjee, N. L. Lampland, K. Yan, J. F. Dunne, A. Ellern and A. D. Sadow, *Chem. Commun.*, 2013, **49**, 4334-4336.

20. M. H. Chisholm, N. W. Eilerts and J. C. Huffman, *Inorg. Chem.*, 1996, **35**, 445-450.
21. K. Wu, D. Mukherjee, A. Ellern, A. D. Sadow and W. E. Geiger, *New J. Chem.*, 2011, **35**, 2169-2178.
22. D. M. Tellers, S. J. Skoog, R. G. Bergman, T. B. Gunnoe and W. D. Harman, *Organometallics*, 2000, **19**, 2428-2432.
23. A. J. Arduengo III, H. V. R. Dias, F. Davidson and R. L. Harlow, *J. Organomet. Chem.*, 1993, **462**, 13-18.
24. D. Wang, K. Wurst and M. R. Buchmeiser, *J. Organomet. Chem.*, 2004, **689**, 2123-2130.
25. T. R. Jensen, C. P. Schaller, M. A. Hillmyer and W. B. Tolman, *J. Organomet. Chem.*, 2005, **690**, 5881-5891.
26. D. J. Nelson and S. P. Nolan, *Chem. Soc. Rev.*, 2013, **42**, 6723-6753.
27. R. Fränkel, U. Kernbach, M. Bakola-Christianopoulou, U. Plaia, M. Suter, W. Ponikwar, H. Nöth, C. Moinet and W. P. Fehlhammer, *J. Organomet. Chem.*, 2001, **617-618**, 530-545.
28. I. Nieto, F. Cervantes-Lee and J. M. Smith, *Chem. Commun.*, 2005, 3811-3813.
29. J. M. Smith, *Comments Inorg. Chem.*, 2008, **29**, 189-233.
30. J. J. Scepaniak, C. S. Vogel, M. M. Khusniyarov, F. W. Heinemann, K. Meyer and J. M. Smith, *Science*, 2011, **331**, 1049-1052.
31. I. Nieto, R. P. Bontchev and J. M. Smith, *Eur. J. Inorg. Chem.*, 2008, 2476-2480.

32. M. Arrowsmith, M. S. Hill and G. Kociok-Köhn, *Organometallics*, 2009, **28**, 1730-1738.
33. L. H. Gade, V. César and S. Bellemin-Laponnaz, *Angew. Chem. Int. Ed.*, 2004, **43**, 1014-1017.
34. V. César, S. Bellemin-Laponnaz and L. H. Gade, *Eur. J. Inorg. Chem.*, 2004, 3436-3444.
35. V. César, S. Bellemin-Laponnaz, H. Wadepohl and L. H. Gade, *Chem.–Eur. J.*, 2005, **11**, 2862-2873.
36. A. Rit, T. P. Spaniol, L. Maron and J. Okuda, *Angew. Chem. Int. Ed.*, 2013, **52**, 4664-4667.
37. A. El-Hellani and V. Lavallo, *Angew. Chem. Int. Ed.*, 2014, **53**, 4489-4493.
38. J. F. Dunne, K. Manna, J. W. Wiench, A. Ellern, M. Pruski and A. D. Sadow, *Dalton Trans.*, 2010, **39**, 641-653.
39. G. Occhipinti, V. R. Jensen, K. W. Törnroos, N. Å. Frøystein and H.-R. Bjørsvik, *Tetrahedron*, 2009, **65**, 7186-7194.
40. K. Manna, A. Ellern and A. D. Sadow, *Chem. Commun.*, 2010, **46**, 339-341.
41. A. Lyčka, R. Doleček, P. Šimůnek and V. Macháček, *Magn. Reson. Chem.*, 2006, **44**, 521-523.
42. U. J. Scheele, M. Georgiou, M. John, S. Dechert and F. Meyer, *Organometallics*, 2008, **27**, 5146-5151.
43. A. Hernán-Gómez, E. Herd, E. Hevia, A. R. Kennedy, P. Knochel, K. Koszinowski, S. M. Manolikakes, R. E. Mulvey and C. Schnegelsberg, *Angew. Chem. Int. Ed.*, 2014, **53**, 2706-2710.

44. R. Campbell, D. Cannon, P. García-Álvarez, A. R. Kennedy, R. E. Mulvey, S. D. Robertson, J. Saßmannshausen and T. Tuttle, *J. Am. Chem. Soc.*, 2011, **133**, 13706-13717.
45. I. A. Guzei and M. Wendt, *Dalton Trans.*, 2006, 3991-3999.
46. I. A. Guzei and M. Wendt, *Solid-G*, UW-Madison, WI, USA, 2004.
47. D. Mukherjee, R. R. Thompson, A. Ellern and A. D. Sadow, *ACS Catal.*, 2011, **1**, 698-702.
48. D. Reinen, M. Atanasov, G. Nikolov and F. Steffens, *Inorg. Chem.*, 1988, **27**, 1678-1686.
49. R. Blessing, *Acta Cryst. A*, 1995, **51**, 33-38.
50. G. Sheldrick, *Acta Cryst. A*, 2008, **64**, 112-122.
51. Bruker Apex II Software Suite, Madison WI USA, 2008.
52. A. L. Spek, *J. Appl. Cryst.*, 2003, **36**, 7-13.
53. M. Valiev, E. J. Bylaska, N. Govind, K. Kowalski, T. P. Straatsma, H. J. J. Van Dam, D. Wang, J. Nieplocha, E. Apra, T. L. Windus and W. A. de Jong, *Comput. Phys. Commun.*, 2010, **181**, 1477-1489.
54. A. D. Becke, *J. Chem. Phys.*, 1993, **98**, 5648-5652.
55. C. T. Lee, W. T. Yang and R. G. Parr, *Phys. Rev. B*, 1988, **37**, 785-789.
56. S. H. Vosko, L. Wilk and M. Nusair, *Can. J. Phys.*, 1980, **58**, 1200-1211.
57. R. Krishnan, J. S. Binkley, R. Seeger and J. A. Pople, *J. Chem. Phys.*, 1980, **72**, 650-654.
58. M. Dolg, U. Wedig, H. Stoll and H. Preuss, *J. Chem. Phys.*, 1987, **86**, 866-872.

**CHAPTER 3. MIXED N-HETEROCYCLIC CARBENE–
BIS(OXAZOLINYLBORATO RHODIUM AND IRIIDIUM COMPLEXES IN
PHOTOCHEMICAL AND THERMAL OXIDATIVE ADDITION REACTIONS**

Modified from a paper published on *Organometallics*

Songchen Xu, Kuntal Manna, Arkady Ellern, and Aaron D. Sadow

Abstract

In order to facilitate oxidative addition chemistry of *fac*-coordinated rhodium(I) and iridium(I) compounds, carbene–bis(oxazoliny)phenylborate proligands have been synthesized and reacted with organometallic precursors. Two proligands, $\text{PhB}(\text{Ox}^{\text{Me}2})_2(\text{Im}^{\text{tBu}}\text{H})$ (H[1]; $\text{Ox}^{\text{Me}2}$ = 4,4-dimethyl-2-oxazoline; $\text{Im}^{\text{tBu}}\text{H}$ = 1-*tert*-butylimidazole) and $\text{PhB}(\text{Ox}^{\text{Me}2})_2(\text{Im}^{\text{Mes}}\text{H})$ (H[2]; $\text{Im}^{\text{Mes}}\text{H}$ = 1-mesitylimidazole) are deprotonated with potassium benzyl to generate K[1] and K[2], and these potassium compounds serve as reagents for the synthesis of a series of rhodium and iridium complexes. Cyclooctadiene and dicarbonyl compounds $\{\text{PhB}(\text{Ox}^{\text{Me}2})_2\text{Im}^{\text{tBu}}\}\text{Rh}(\eta^4\text{-C}_8\text{H}_{12})$ (**3**), $\{\text{PhB}(\text{Ox}^{\text{Me}2})_2\text{Im}^{\text{Mes}}\}\text{Rh}(\eta^4\text{-C}_8\text{H}_{12})$ (**4**), $\{\text{PhB}(\text{Ox}^{\text{Me}2})_2\text{Im}^{\text{Mes}}\}\text{Rh}(\text{CO})_2$ (**5**), $\{\text{PhB}(\text{Ox}^{\text{Me}2})_2\text{Im}^{\text{Mes}}\}\text{Ir}(\eta^4\text{-C}_8\text{H}_{12})$ (**6**), and $\{\text{PhB}(\text{Ox}^{\text{Me}2})_2\text{Im}^{\text{Mes}}\}\text{Ir}(\text{CO})_2$ (**7**) are synthesized along with $\text{To}^{\text{M}}\text{M}(\eta^4\text{-C}_8\text{H}_{12})$ (M = Rh (**8**); M = Ir (**9**); To^{M} = tris(4,4-dimethyl-2-oxazoliny)phenylborate). The spectroscopic and structural properties and reactivity of this series of compounds show electronic and steric effects of substituents on the imidazole (*tert*-butyl vs. mesityl), effects of replacing an oxazoline in To^{M} with a

carbene donor, and the influence of the donor ligand (CO vs. C₈H₁₂). The reactions of K[**2**] and [M(μ -Cl)(η^2 -C₈H₁₄)₂]₂ (M = Rh, Ir) provide { κ^4 -PhB(Ox^{Me2})₂Im^{Mes'}CH₂}Rh(μ -H)(μ -Cl)Rh(η^2 -C₈H₁₄)₂ (**10**) and {PhB(Ox^{Me2})₂Im^{Mes}}IrH(η^3 -C₈H₁₃) (**11**). In the former compound, a spontaneous oxidative addition of a mesityl *ortho*-methyl to give a mixed-valent dirhodium species is observed, while the iridium compound forms a monometallic allyl hydride. Photochemical reactions of dicarbonyl compounds **5** and **7** result in C–H bond oxidative addition providing the compounds { κ^4 -PhB(Ox^{Me2})₂Im^{Mes'}CH₂}RhH(CO) (**12**) and {PhB(Ox^{Me2})₂Im^{Mes}}IrH(Ph)CO (**13**). In **12**, oxidative addition results in cyclometalation of the mesityl *ortho*-methyl similar to **10** whereas the iridium compound reacts with the benzene solvent to give a rare crystallographically characterized *cis*-[Ir](H)(Ph) complex. Alternatively, the rhodium carbonyl **5** or iridium isocyanide {PhB(Ox^{Me2})₂Im^{Mes}}Ir(CO)CN^tBu (**15**) reacts with PhSiH₃ in the dark to form the silyl compound {PhB(Ox^{Me2})₂Im^{Mes}}RhH(SiH₂Ph)CO (**14**) or {PhB(Ox^{Me2})₂Im^{Mes}}IrH(SiH₂Ph)CN^tBu (**17**). These examples demonstrate the enhanced thermal reactivity of {PhB(Ox^{Me2})₂Im^{Mes}}-supported iridium and rhodium carbonyl compounds in comparison to tris(oxazolinyl)borate, tris(pyrazolyl)borate, and cyclopentadienyl-supported compounds.

Introduction

Oxidative addition is an essential part of the rich chemistry of low-valent rhodium and iridium compounds, playing a central role in C–H bond activation chemistry¹ and a large range of catalytic chemistry including hydrogenation,² hydrosilylation,³ hydroformylation,⁴ and hydroacylation.⁵ Decarbonylation of aldehydes also involves

oxidative addition of formyl C–H bonds.⁶ Recently, we described a rhodium(I)-catalyzed alcohol and aldehyde decarbonylation reaction that involves oxidative addition of formyl C–H bonds.⁷ The $\text{To}^{\text{M}}\text{Rh}(\text{CO})_2$ or $\text{To}^{\text{M}}\text{Rh}(\text{H})_2\text{CO}$ (To^{M} = tris(4,4-dimethyl-2-oxazoliny)phenylborate) catalysts require photochemical activation, presumably to generate low-coordinate rhodium centers through CO dissociation. Photochemical CO dissociation is also required for C–H bond oxidative addition mediated by *fac*-coordinated Tp and Cp rhodium dicarbonyl compounds (Tp = tris(pyrazolyl)borate; Cp = cyclopentadienyl) in the classic early examples of hydrocarbon metalation. Despite this similarity, $\text{TpRh}(\text{CO})_2$, $\text{CpRh}(\text{CO})_2$, and a few of their substituted derivatives are inactive or less active in comparison to $\text{To}^{\text{M}}\text{Rh}(\text{CO})_2$ in the photocatalytic alcohol decarbonylation.

Conversely, $\text{To}^{\text{M}}\text{Rh}^{\text{I}}$ and $\text{To}^{\text{M}}\text{Ir}^{\text{I}}$ compounds are less reactive in a number of oxidative additions than Tp, Cp, and phosphine-coordinated monovalent group 9 compounds that are valuable catalysts for many synthetic transformations. For example, only a few polar C–X bonds are reactive toward $\text{To}^{\text{M}}\text{Rh}(\eta^4\text{-C}_8\text{H}_{12})$, and the iridium congeners are unreactive toward oxidative addition of electrophiles such as hydrogen and silanes. In contrast, cyclopentadienyl and tris(pyrazolyl)borate rhodium and iridium compounds have provided the seminal examples of oxidative addition of inert methyl, methylene and methane C–H bonds.⁸ Instead of oxidative addition, reactions of $\text{To}^{\text{M}}\text{Rh}(\text{CO})_2$,⁹ $\text{To}^{\text{M}}\text{Ir}(\text{CO})_2$, and $\text{To}^{\text{P}}\text{Ir}(\text{CO})_2$ ¹⁰ (To^{P} = tris(4*S*-isopropyl-2-oxazoliny)phenylborate) with strong electrophiles such as MeOTf result in *N*-methylation of the nitrogen atom on one of the three oxazoline rings. $\text{To}^{\text{M}}\text{Rh}(\text{CO})_2$ reacts with benzene upon photolysis to give $\text{To}^{\text{M}}\text{RhH}(\text{Ph})\text{CO}$, but reactions of silanes give

mixtures of unidentified products, while $\text{To}^{\text{M}}\text{Ir}(\text{CO})_2$ is inert toward benzene and silanes under a range of photochemical and thermal conditions. For comparison, $\text{Tp}^*\text{Rh}(\text{CO})_2$ ($\text{Tp}^* = \text{tris}(3,5\text{-dimethylpyrazolyl})\text{borate}$) oxidatively adds the Si–H bond in Et_3SiH under photolytic conditions to give $\text{Tp}^*\text{RhH}(\text{SiEt}_3)\text{CO}$,¹¹ the photochemical C–H bond oxidative addition chemistry of $\text{Tp}^*\text{Rh}(\text{CO})_2$ noted above is well known. Likewise, $\text{CpRh}(\eta^2\text{-C}_2\text{H}_4)_2$ also reacts with silanes via oxidative addition under photochemical activation.¹² Thermal C–H bond additions in these systems are observed mainly with olefin leaving groups.¹³ A number of factors might be responsible for the reduced reactivity of $\text{To}^{\text{M}}\text{M}$ compounds in oxidative additions of nonpolar bonds including the ancillary ligand's steric properties, its coordination mode, its conformation, and its effect on the electronic properties of the metal center. For example, the varying coordination of tris(pyrazolyl)borate between bidentate and tridentate modes is intimately related to the oxidative addition of C–H bonds.¹⁴⁻¹⁶ While these factors may or may not directly impact catalytic decarbonylation reactivity (or other catalytic processes that invoke oxidative addition), new isoelectronic *fac*-coordinating ligand derivatives may facilitate oxidative additions and/or provide improved catalysis.

In this context, the oxazolinyborate framework remains appealing (despite the limited oxidative addition chemistry of tris(oxazoliny)borate group 9 compounds) because it allows the synthesis of a range of isoelectronic hybrid ligands through the intermediate $\text{PhB}(\text{Ox}^{\text{R}})_2$. Thus, the electron-donating ability of To^{M} may be modified by substituting an oxazoline by an imidazole to provide mixed carbene–bis(oxazoliny)borate ligands. *N*-Heterocyclic carbene donors, derived from imidazole rings, are good electron-donating ligands,¹⁷ and in Chapter 2 we reported the

monoanionic ligand bis(4,4-dimethyl-2-oxazoliny)(1-mesitylimidazolyl)phenylborate ($[\text{PhB}(\text{Ox}^{\text{Me}_2})_2\text{Im}^{\text{Mes}}]^-$) as a supporting ligand for zinc alkylperoxides.¹⁸ The presence of the borate group in oxazolinyborates appears to increase the oxazoline group's electron donation ability,¹⁹ and this may also extend to *N*-borylated carbenes. In addition, ligands based on *N*-borylated imidazoles have proven successes in stabilizing high-valent metal centers. Smith and co-workers have demonstrated the electron-donating ability of the tris(imidazol-2-ylidene)phenylborate ligand in the syntheses of four-coordinated iron(IV) nitrido complexes²⁰ and a cationic iron(V).²¹ Furthermore, a rhodium catalyst supported by a mixed carbene–oxazoline ligand was proposed to allow access to a rhodium silylene in a carbonyl hydrosilylation.^{22,23} On the basis of these examples, we began to prepare and investigate the reaction chemistry of rhodium and iridium complexes coordinated by mixed oxazoline–carbene ligands.

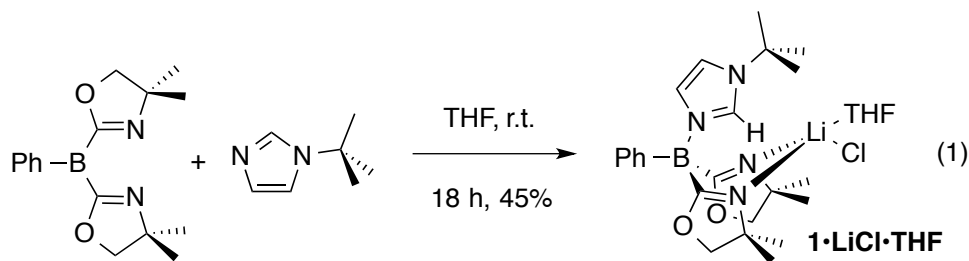
The current contribution reports the synthesis and structures of carbene–bis(oxazoliny)borate ligands as their potassium salts and as a series of group 9 compounds for study in oxidative addition chemistry. In particular, the rhodium and iridium compounds $[\text{M}(\mu\text{-Cl})(\text{CO})_2]_2$, $[\text{M}(\mu\text{-Cl})(\eta^4\text{-C}_8\text{H}_{12})]_2$, and $[\text{M}(\mu\text{-Cl})(\eta^2\text{-C}_8\text{H}_{14})]_2$ react with the anionic carbene–bis(oxazoliny)borate proligands to provide group 9 starting materials. Analysis of the spectroscopic and structural features of the ligands and the series of compounds reveals steric and electronic effects of the *N*-borylated carbene donor in comparison to related tris(oxazoliny)borate and tris(pyrazolyl)borate compounds. These steric and electronic features were considered in the context of their importance to the oxidative addition chemistry. Furthermore, the resulting compounds show intra- and intermolecular reactivity in oxidative addition of C–H and Si–H bonds

under thermal and photochemical conditions that is distinct from the well-known chemistry of cyclopentadienyl and tris(pyrazolyl)borato metal dicarbonyls.

Results and Discussion

Synthesis and characterization of bis(4,4-dimethyl-2-oxazolinyl)(1-*tert*-butylimidazolyl)phenylborate $\text{PhB}(\text{Ox}^{\text{Me}_2})_2(\text{Im}^{\text{tBu}}\text{H})\text{LiCl}(\text{THF})$ ($\text{H}[1]\cdot\text{LiCl}\cdot\text{THF}$).

The compound $\text{PhB}(\text{Ox}^{\text{Me}_2})_2(\text{Im}^{\text{tBu}}\text{H})\text{LiCl}(\text{THF})$ ($\text{H}[1]\cdot\text{LiCl}\cdot\text{THF}$; $\text{Im}^{\text{tBu}}\text{H}$ = 1-*tert*-butylimidazole, Ox^{Me_2} = 4,4-dimethyl-2-oxazoline) is prepared by combination of $\text{PhB}(\text{Ox}^{\text{Me}_2})_2$ ²⁴ and 1-*tert*-butylimidazole in THF at room temperature (eq. 1). In this compound, the imidazole binds to the boron center through a Lewis acid–base interaction, and the presence of LiCl comes from the preparation of $\text{PhB}(\text{Ox}^{\text{Me}_2})_2$.²⁴



Compound $\text{H}[1]\cdot\text{LiCl}\cdot\text{THF}$ precipitates from the yellow THF solution as an analytically pure white solid in 45% yield after stirring overnight. Compound $\text{H}[1]\cdot\text{LiCl}\cdot\text{THF}$ is slightly soluble in benzene, but very soluble in acetonitrile, and the latter solvent is preferable for NMR spectral characterization. The ^1H NMR spectrum of $\text{H}[1]\cdot\text{LiCl}\cdot\text{THF}$ contained two singlets and one multiplet assigned to the oxazoline methyl and methylene groups, respectively. This pattern suggests a C_s -symmetric structure, as is

expected for an imidazole–borane adduct. Signals at 1.58 (9 H) and 8.09 (1 H) ppm were assigned to the *tert*-butyl and 2-H on the imidazolium, respectively. The ^{11}B NMR spectrum revealed one singlet signal at -9.4 ppm; for comparison, the ^{11}B NMR chemical shift of $\text{PhB}(\text{Ox}^{\text{Me}_2})_2$ as an acetonitrile adduct (in acetonitrile- d_3) was observed at -8.1 ppm,²⁴ whereas the borate center in $\text{H}[\text{To}^{\text{M}}]$ was observed at -17.2 ppm.²⁵ Natural abundance ^{15}N NMR data was obtained through ^1H – ^{15}N HMBC experiments and differentiated the nitrogen atoms on the imidazolium and oxazoline rings. The 1-N imidazolium signal at -178 ppm was correlated with the ^1H NMR signals assigned to the *tert*-butyl group while the 3-N signal at -184 ppm correlated only with 4-H and 5-H. The heteronuclear ^1H – ^{15}N correlation experiment also revealed the magnetic equivalence of the oxazoline rings, as both methyl signals were correlated to a single ^{15}N NMR signal at -138 ppm.

An X-ray quality crystal of $\text{H}[\mathbf{1}] \cdot \text{LiCl} \cdot \text{NCCD}_3$ is obtained by slow evaporation of acetonitrile- d_3 at room temperature. The adduct formation of the imidazole–borane and the presence of LiCl and acetonitrile- d_3 as an additional two-electron donor are verified by an X-ray diffraction study (Figure 1). In the solid-state structure, both oxazolines coordinate to the lithium center through the nitrogen atoms. The pseudotetrahedral coordination sphere of the lithium ion is completed by chloride and an acetonitrile ligand, which apparently replaced the THF ligand. The boron center is also pseudotetrahedral. For comparison, $(\text{PhB}(\text{Ox}^{\text{Me}_2})_2(\text{Im}^{\text{Mes}}\text{H})\text{LiCl})_2$ ($(\text{H}[\mathbf{2}] \cdot \text{LiCl})_2$, $\text{Im}^{\text{Mes}}\text{H} = 1$ -mesitylimidazole) crystallizes as a dimer with bridging chloride ligands.¹⁸

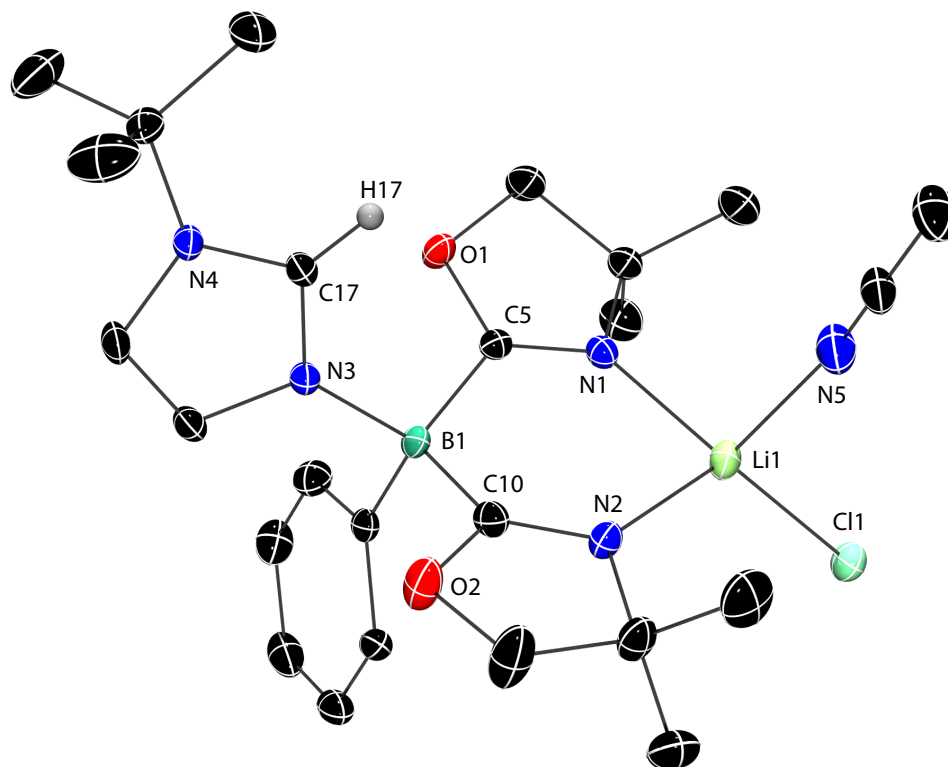
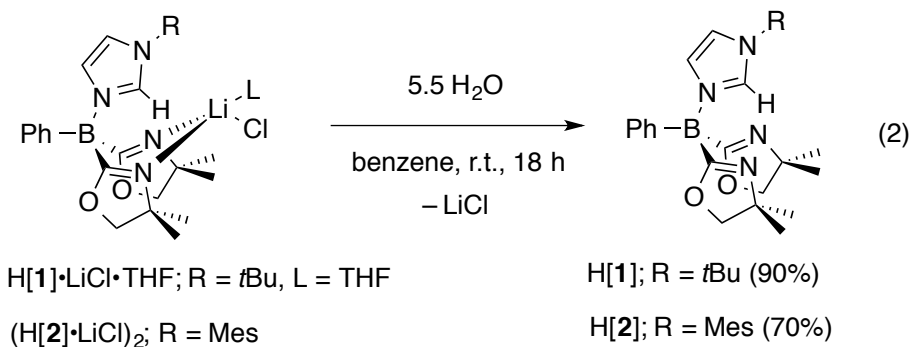


Figure 1. Rendered thermal ellipsoid plot of $\text{PhB}(\text{Ox}^{\text{Me}_2})_2(\text{Im}^{\text{tBu}}\text{H})\text{LiCl}(\text{NCCD}_3)$ ($\text{H}[1]\cdot\text{LiCl}\cdot\text{NCCD}_3$) with ellipsoids at 35% probability. H and D atoms are not plotted for clarity except for the H17 on the imidazolium C17. Selected interatomic distances (Å): B1-C5, 1.620(4); B1-C10, 1.607(4); B1-N3, 1.594(3); Li1-N1, 2.057(5); Li1-N2, 2.052(5); Li1-N5, 2.118(6). Selected interatomic angles (°): C5-B1-C10, 111.6(2); C5-B1-N3, 109.1(2); C10-B1-N3, 109.6(2); N1-Li1-N2, 93.5(2).

Syntheses and characterizations of proligands $\text{PhB}(\text{Ox}^{\text{Me}_2})_2(\text{Im}^{\text{tBu}}\text{H})$ (H[1]) and $\text{PhB}(\text{Ox}^{\text{Me}_2})_2(\text{Im}^{\text{Mes}}\text{H})$ (H[2]) and their deprotonation. Attempts to deprotonate $\text{H}[1]\cdot\text{LiCl}\cdot\text{THF}$ and $(\text{H}[2]\cdot\text{LiCl})_2$ by reaction with *n*BuLi, KCH_2Ph , $\text{LiN}(\text{SiMe}_3)_2$, or $\text{LiN}(\text{CHMe}_2)_2$ do not provide the desired lithium or potassium borates $[1]^-$ or $[2]^-$ in the solvents benzene, toluene, diethyl ether, and tetrahydrofuran over a range of appropriate

temperatures. We hypothesized that the LiCl adduct might be interfering with reactions with bases, even though LiCl often enhances the reactivity of alkyl magnesium, zinc, and copper reagents toward metalations.²⁶ In addition, $(\text{H}[\mathbf{2}]\cdot\text{LiCl})_2$ and ZnR_2 ($\text{R} = \text{Me}, \text{Et}$) react to give $\{\mathbf{2}\}\text{ZnR}$, and the LiCl present in the starting material precipitates during those reactions.¹⁸

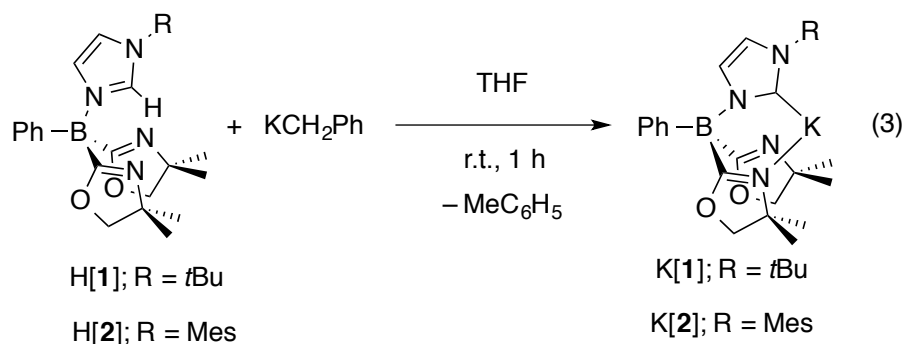
Purification of compound $\text{H}[\mathbf{1}]\cdot\text{LiCl}\cdot\text{THF}$ or $(\text{H}[\mathbf{2}]\cdot\text{LiCl})_2$ from their LiCl adducts is accomplished by the addition of excess water to their benzene suspensions. In both cases, an analytically pure white solid is isolated in good yield (eq. 2), and this isolated product is sufficiently dry for reactions with strong bases such as KCH_2Ph . Flame tests of $\text{H}[\mathbf{1}]$ or $\text{H}[\mathbf{2}]$ gave blue flames in contrast to the red color observed for the tests of $\text{H}[\mathbf{1}]\cdot\text{LiCl}\cdot\text{THF}$ or $(\text{H}[\mathbf{2}]\cdot\text{LiCl})_2$.



The solubility of $\text{H}[\mathbf{1}]$ or $\text{H}[\mathbf{2}]$ in benzene, toluene, tetrahydrofuran and diethyl ether noticeably increased relative to their LiCl adducts. In contrast to the broad spectrum of $\text{H}[\mathbf{1}]\cdot\text{LiCl}\cdot\text{THF}$ acquired in benzene- d_6 , the spectrum of $\text{H}[\mathbf{1}]$ contained sharp, well-defined resonances with distinct chemical shifts. For example, the 2-H signal in $\text{H}[\mathbf{1}]$ and $\text{H}[\mathbf{1}]\cdot\text{LiCl}\cdot\text{THF}$ were 9.55 and 8.09 ppm, respectively. The ^{15}N NMR chemical shift value

for the oxazoline was slightly downfield in H[1] at -125 ppm in comparison to -138 ppm for H[1]·LiCl·THF. In addition, the ν_{CN} band in the IR spectrum for H[1]·LiCl·THF at 1624 cm^{-1} was at higher energy than for H[1] at 1605 cm^{-1} .

Deprotonation of H[1] or H[2] to generate the potassium complex K[1] or K[2] is readily accomplished with potassium benzyl in THF (eq. 3).



A micromolar-scale reaction of H[1] and potassium benzyl in tetrahydrofuran-*d*₈ forms a white precipitate in ca. 20 min. A ¹H NMR spectrum of the solution showed the formation of toluene and concomitant disappearance of the 2-H imidazole signal at 9.46 ppm. The resulting product is sparingly soluble in THF, and only a few key oxazoline, imidazole, and phenyl ¹H NMR signals could be assigned. The ¹¹B NMR spectrum contained one signal at -11.6 ppm, which was slightly upfield of H[1] (-9.4 ppm). Attempts to isolate the white precipitate typically afforded mixtures of K[1] and H[1] despite careful air- and moisture-free manipulations. Therefore, the most efficient synthetic protocols employ K[1] generated *in situ*.

K[2], also generated by the reaction of KCH₂Ph and H[2], is soluble in THF. The formation of toluene confirmed the expected deprotonation. The 2-H imidazole signal at

8.84 ppm in H[2] was absent in the product's ^1H NMR spectrum, which is distinct from that of H[2]. Although attempts to isolate K[2] provided mixtures contaminated with H[2], a crystal of K[2] was fortuitously obtained from a crystallization in benzene at room temperature. An X-ray diffraction study revealed the 2-C (C22 in Figure 2) bonded to a K center that affirmed the proposed deprotonation and the proposed connectivity of K[2].

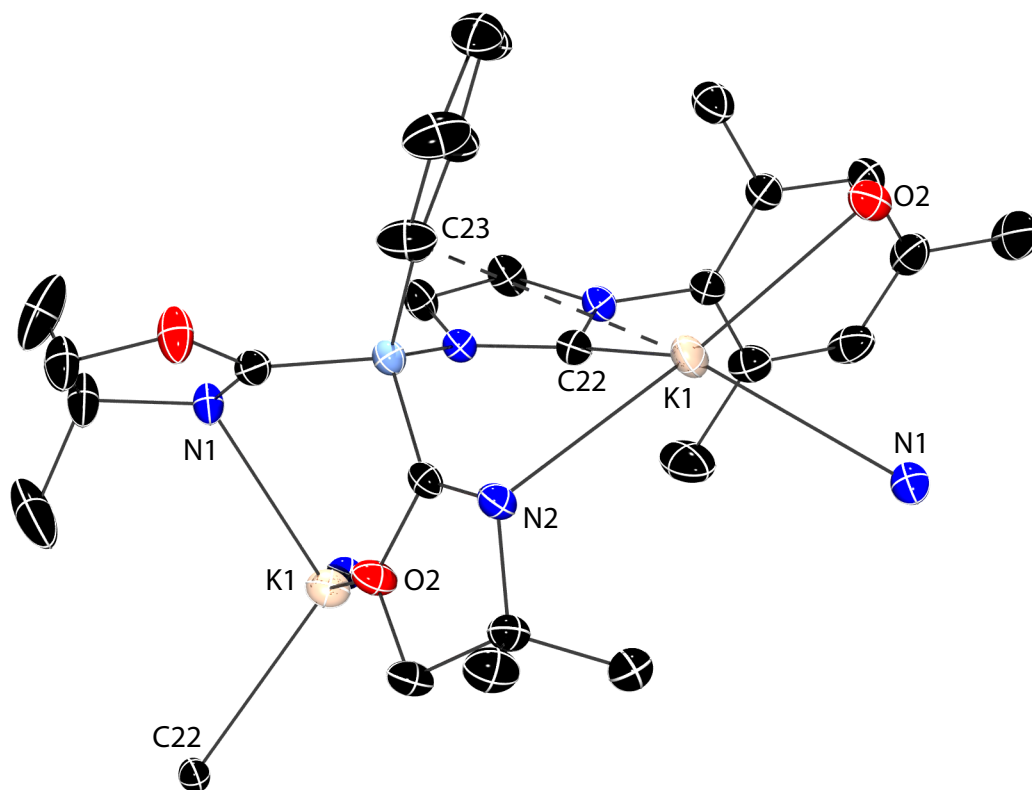
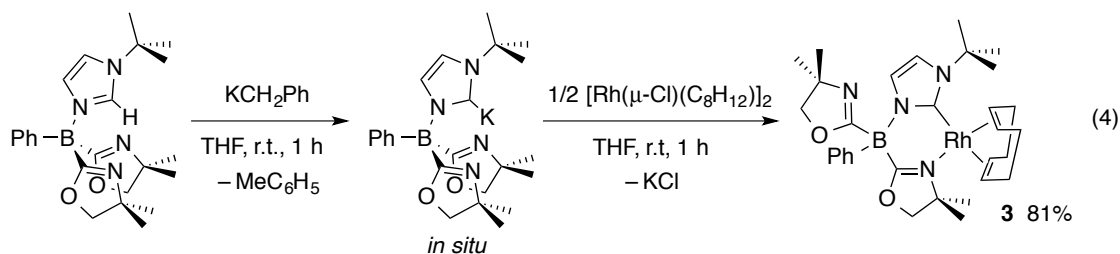


Figure 2. Rendered thermal ellipsoid plot of $\text{K}[\text{PhB}(\text{Ox}^{\text{Me}_2})_2\text{Im}^{\text{Mes}}]$ (K[2]). Ellipsoids are plotted at 35% probability, and H atoms are not illustrated for clarity. Selected interatomic distances (Å): K1-N1, 2.861(2); K1-O2, 2.697(1); K1-C22, 2.991(2); K1-N2, 2.732(2); K1-C23, 3.373(2).

The resulting interesting structure (Figure 2) is a polymeric chain of alternating potassium cations and $[2]^-$, with each potassium atom coordinated to five atoms on two ligands: the *ipso*-carbon of the phenyl group (C23), the NHC carbon (C22), and an oxazoline nitrogen (N2) of one ligand and to one oxazoline nitrogen (N1) and one oxazoline oxygen (O2) of the next $[2]$ in the polymer chain. The oxazoline ring that contains N2 and O2 is bridging between two crystal-symmetry-related potassium atoms. Although $K[2]$ may be crystallized, its isolation is challenging, and it is most conveniently prepared and used *in situ*.

Synthesis and characterization of rhodium(I) and iridium(I) compounds containing $[1]^-$ and $[2]^-$. A series of rhodium and iridium compounds have been prepared using $[M(\mu\text{-Cl})(\eta^4\text{-C}_8\text{H}_{12})_2]_2$, $[M(\mu\text{-Cl})(\eta^2\text{-C}_8\text{H}_{14})_2]_2$, and $[M(\mu\text{-Cl})(\text{CO})_2]_2$ (M = Rh, Ir) as starting materials. A notable difference between $[1]^-$ and $[2]^-$ is observed, in that $[2]^-$ readily provides a rich reactivity on rhodium and iridium, whereas only a single rhodium compound containing $[1]^-$ as an ancillary ligand is isolable using these starting materials. In all other cases tested, $H[1]$ is the major isolated product from reactions of $K[1]$ and the rhodium or iridium salts.

Upon addition of the rhodium precursor $[\text{Rh}(\mu\text{-Cl})(\eta^4\text{-C}_8\text{H}_{12})_2]_2$ to a pink suspension of *in situ* generated $K[1]$, the precipitate dissolves immediately to give a red solution (eq. 4).



The ^1H NMR spectrum of **3**, acquired in benzene- d_6 , indicates that the two oxazoline groups are inequivalent. Correlations between the oxazoline methyl groups and nitrogen in a ^1H - ^{15}N HMBC experiment revealed two distinct chemical shifts for the oxazoline nitrogen. The ^{15}N signal at -183 ppm was assigned to a coordinated oxazoline, while the signal at -123 ppm was assigned to a noncoordinated group based on its similarity to the ^{15}N NMR chemical shift of 2H-4,4-dimethyl-2-oxazoline.²⁴ Both imidazole nitrogen centers were detected in this experiment at -172 (1-N) and -181 ppm (3-N) and distinguished by a cross-peak from the latter to the *tert*-butyl ^1H NMR signal (Table 1). Coordination of the carbene to rhodium was supported by a doublet resonance at 181.1 ppm ($^1J_{\text{RhC}} = 50$ Hz) in the $^{13}\text{C}\{^1\text{H}\}$ NMR spectrum. Additionally, two ν_{CN} bands in the IR spectrum (acquired in KBr) provided support for coordinated (1570 cm^{-1}) and noncoordinated oxazoline (1613 cm^{-1}).

Table 1. Key spectroscopic data from rhodium and iridium compounds.

Compound	ν_{CO} (cm^{-1} , KBr)	$\delta^{13}\text{C}$ of C_8H_{12} or $(\text{CO})_2$	$\delta^{15}\text{N}_{\text{oxazoline}}$
$\{\mathbf{1}\}\text{Rh}(\eta^4\text{-C}_8\text{H}_{12})$ (3)	n.a.	88.61 (7.2 Hz), 88.36 (8.1 Hz), 79.68 (13.7 Hz), 69.13 (12.8 Hz)	$-183, -123$

Table 1 continued.

Compound	ν_{CO} (cm ⁻¹ , KBr)	$\delta^{13}\text{C}$ of C ₈ H ₁₂ or (CO) ₂	$\delta^{15}\text{N}_{\text{oxazoline}}$
{2}Rh(η^4 -C ₈ H ₁₂) (4)	n.a.	90.72 (7.7 Hz), 87.89 (7.8 Hz), 75.22 (12.9 Hz), 70.84 (13.1 Hz)	-182, -125
{2}Rh(CO) ₂ (5)	2063, 1993	176.20 (45.0 Hz)	-153
{2}Ir(η^4 -C ₈ H ₁₂) (6)	n.a.	75.66, 72.66, 59.95, 56.37	-188, -124
{2}Ir(CO) ₂ (7)	2053, 1979	179.08	-156
To ^M Rh(CO) ₂ ^a	κ^2 : 2070, 2010, 1997; κ^3 : 2048, 1968	188.42 (66.6 Hz)	-163
To ^M Ir(CO) ₂ ^b	2066, 1989	176.63	-167
Tp [*] Rh(CO) ₂ ^c	2052, 1974	n.a.	n.a.
To ^M Rh(η^4 -C ₈ H ₁₂) (8)	n.a.	79.33, 75.65	-169, -161
To ^M Ir(η^4 -C ₈ H ₁₂) (9)	n.a.	62.77, 59.25	-193, -155
{PhMeBpz ^{Me} }Rh(CO) ₂ ^d	2078, 2012	185.1 (67.6 Hz)	-149
{Acac}Rh(CO) ₂ ^e	2083, 2015	n.a.	n.a.
[(DEAM-MbBI)Rh(CO) ₂][BF ₄] ^f	2084, 2026	179.96, 179.93 (45 Hz)	n.a.
{BDI-3}Ir(CO) ₂ ^g	2054, 1986	198.50	n.a.

^a See ref. 9. ^b See ref. 10. ^c See ref. 27. ^d PhMeBpz^{Me} = bis(3-methylpyrazolyl)methylphenylborate; see ref. 32. ^e Acac = acetyl acetonate; see ref. 31. ^f DEAM-MbBI = *trans*-9,10-dihydro-9,10-ethanoanthracene-11,12-bis(1-methyl)benzimidazolidine-2-ylidene; see ref. 33. ^g BDI-3 = *N,N'*-bis(2,6-diisopropylphenyl)-2,4-diketimate; see ref. 34.

A single-crystal X-ray diffraction study supports the connectivity and coordination geometry suggested by the solution-phase data (Figure 3). The structure will be discussed below in comparison with $\{2\}$ -coordinated rhodium and iridium compounds.

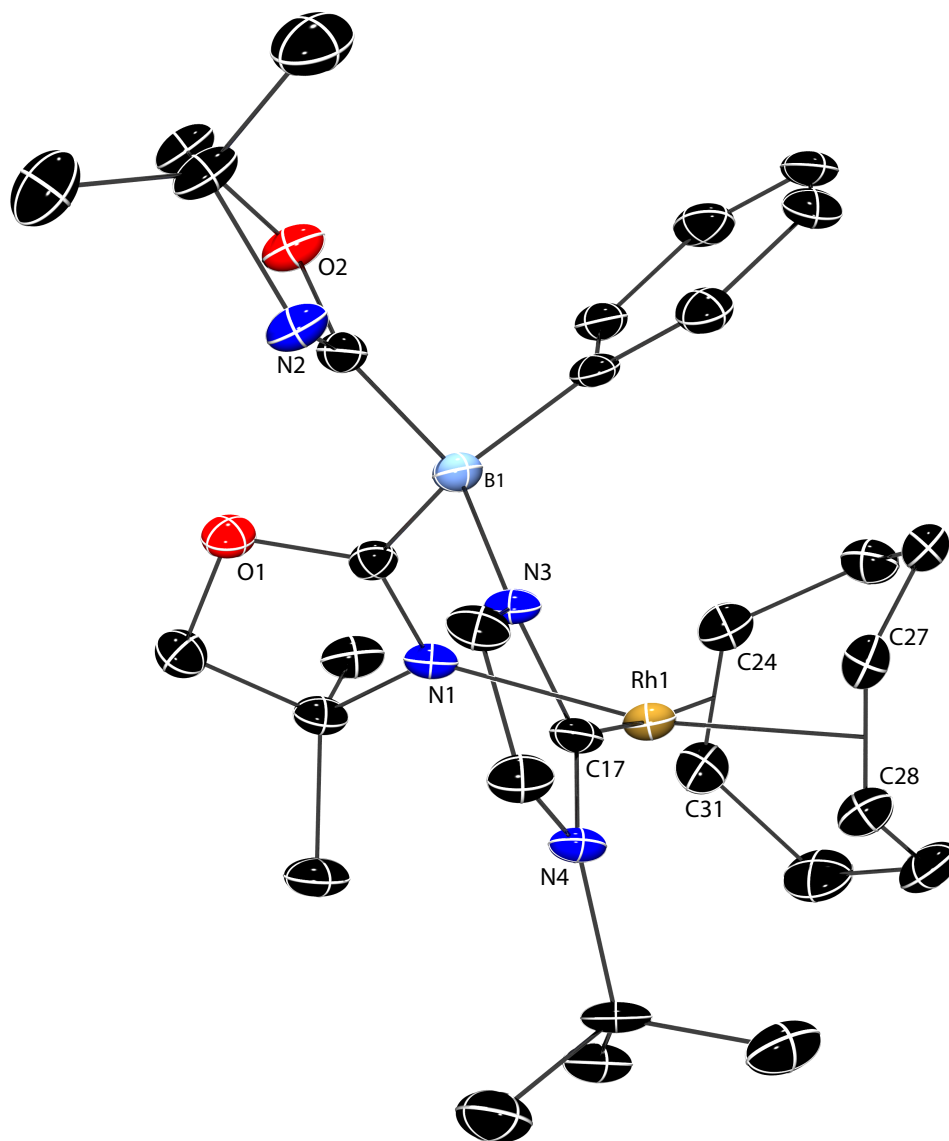
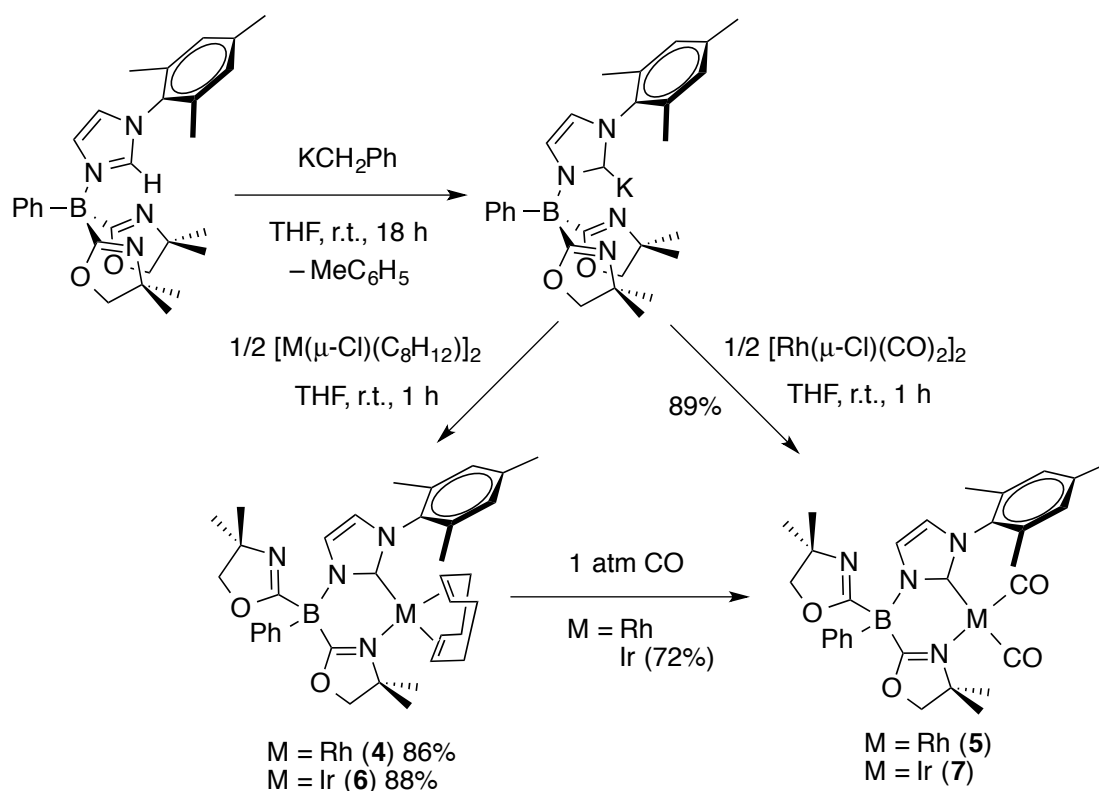


Figure 3. Rendered thermal ellipsoid plot of $\{\text{PhB}(\text{Ox}^{\text{Me}_2})_2\text{Im}^{\text{tBu}}\}\text{Rh}(\eta^4\text{-C}_8\text{H}_{12})$ (**3**) with ellipsoids at 35% probability. H atoms are not plotted for clarity. Selected interatomic

distances (Å) and angle (°): Rh1-N1, 2.121(4); Rh1-C17, 2.063(5); Rh1-C24, 2.208(4); Rh1-C27, 2.116(5); Rh1-C28, 2.147(5); Rh1-C31, 2.173(5); N1-Rh1-C17, 83.0(2).

The syntheses of the red, mesityl-substituted carbene compound $\{\text{PhB}(\text{Ox}^{\text{Me}_2})_2\text{Im}^{\text{Mes}}\}\text{Rh}(\eta^4\text{-C}_8\text{H}_{12})$ (**4**) and the yellow dicarbonyl analogue (**5**) follow that of the ^tBu-substituted carbene complex **3** (Scheme 1).



Scheme 1. Preparation of $\{\text{PhB}(\text{Ox}^{\text{Me}_2})_2\text{Im}^{\text{Mes}}\}\text{M}(\eta^4\text{-C}_8\text{H}_{12})$ (M = Rh (**4**), Ir (**6**)) and $\{\text{PhB}(\text{Ox}^{\text{Me}_2})_2\text{Im}^{\text{Mes}}\}\text{M}(\text{CO})_2$ (M = Rh (**5**), Ir (**7**)).

As in **3**, the inequivalent oxazoline groups in **4** do not exchange on the ^1H NMR time scale at room temperature. In addition, the methyl groups from the mesityl are

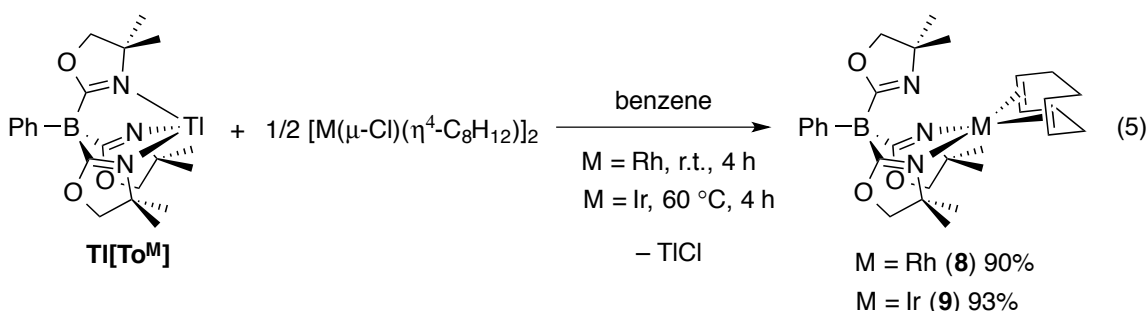
inequivalent and the compound appears C_1 symmetric. Thus, seven singlet resonances (3 H each) were observed, assigned to seven inequivalent methyl groups, and these were distinguished with $^1\text{H}-^{13}\text{C}$ HMBC and $^1\text{H}-^{15}\text{N}$ HMBC experiments (see Table 1).

Compound **5** is obtained as a yellow solid from the reaction of 2 equiv. of K[**2**] and $[\text{Rh}(\mu\text{-Cl})(\text{CO})_2]_2$ at room temperature. The spectroscopy of **5** suggests its structure has higher symmetry than the C_1 -symmetric cyclooctadiene-substituted **3** and **4**. Thus, the mesityl group produced only three total ^1H NMR signals for methyl and arene hydrogens, and the two oxazolines in **5** appeared equivalent. The oxazoline methyl signals appeared as two singlets in ^1H NMR spectra of **5** acquired from room temperature to 195 K in toluene- d_8 . Although the signals broadened as the temperature decreased suggesting an exchange process, resolution of the signals into four resonances (expected for a four-coordinated structure) was not observed. A $^1\text{H}-^{15}\text{N}$ HMBC experiment revealed one nitrogen signal at -153 ppm correlated to the two oxazoline methyl resonances. In contrast, the solid-state infrared spectrum of **5** (precipitated from pentane, KBr) contained two ν_{CN} bands at 1564 and 1626 cm^{-1} . An IR spectrum of **5** dissolved in benzene contained two broad ν_{CN} bands ranging from 1530 to 1560 cm^{-1} , and from 1620 to 1650 cm^{-1} . The broad IR signals in the ν_{CN} region suggest the oxazoline exchange process occurs at a rate on the order of the IR time scale. Thus, carbonyl compound **5** is highly fluxional in solution, but only one oxazoline is coordinated in the solid state.

The related iridium compound $\{\text{PhB}(\text{Ox}^{\text{Me}2})_2\text{Im}^{\text{Mes}}\}\text{Ir}(\eta^4\text{-C}_8\text{H}_{12})$ (**6**) is prepared from $[\text{Ir}(\mu\text{-Cl})(\eta^4\text{-C}_8\text{H}_{12})]_2$ and *in situ* generated K[**2**] analogously to the rhodium congener. Addition of 1 atm of CO to **6** affords $\{\text{PhB}(\text{Ox}^{\text{Me}2})_2\text{Im}^{\text{Mes}}\}\text{Ir}(\text{CO})_2$ (**7**). As expected, the spectroscopic properties and structures of the rhodium and iridium

compounds are similar. Thus, the oxazoline groups of **6**, like its rhodium analogue **4**, were inequivalent on the ^1H NMR time scale, while the oxazoline moieties of the dicarbonyl compounds **5** and **7** appeared to be equivalent because of a rapid exchange process. The reaction of **4** and 1 atm of CO also provides **5**; however, the corresponding reaction of the *tert*-butyl-based carbene compound **3** and CO (1 atm) results in a mixture of unidentified species and cyclooctadiene.

To complete the series for comparison, $\text{To}^{\text{M}}\text{M}(\eta^4\text{-C}_8\text{H}_{14})$ ($\text{M} = \text{Rh}$ (**8**), Ir (**9**)) are synthesized by reaction of $\text{Ti}[\text{To}^{\text{M}}]$ and $[\text{M}(\mu\text{-Cl})(\eta^4\text{-C}_8\text{H}_{12})_2]$ in benzene (eq. 5). The use of $\text{Ti}[\text{To}^{\text{M}}]$ is important for formation of $\text{To}^{\text{M}}\text{M}(\eta^4\text{-C}_8\text{H}_{14})$, as $\text{Li}[\text{To}^{\text{M}}]$ provided a dimeric lithium chloride adduct.¹⁰ Moreover, the spectroscopy of $\text{To}^{\text{M}}\text{M}(\eta^4\text{-C}_8\text{H}_{14})$ is complicated in comparison to $\{\text{PhB}(\text{Ox}^{\text{Me}_2})_2\text{Im}^{\text{R}}\}\text{M}(\eta^4\text{-C}_8\text{H}_{14})$.



The room-temperature ^1H NMR spectra of **8** and **9** contained three singlets assigned to the methyl groups and three slightly broad singlets for the methylene groups of the oxazolines. The three methyl signals are consistent with C_s -symmetric structures, but the singlet methylene signals suggest that the To^{M} ligand's coordination mode is dynamic. In the solid state, infrared spectroscopy provided evidence for the bidentate coordination mode, as indicated by two ν_{CN} bands corresponding to coordinated

oxazolines (**8**: 1567 cm⁻¹; **9**: 1558 cm⁻¹) and noncoordinated oxazolines (**8**: 1611 cm⁻¹; **9**: 1607 cm⁻¹). These NMR data suggest a slow dynamic exchange process between the pendent oxazoline and the two coordinated oxazolines that occurs close to the ¹H NMR time scale in solution at room temperature. In contrast, the oxazoline groups in previously reported dicarbonyl compounds To^MM(CO)₂ (M = Rh, Ir) are rapidly exchanging at room temperature.^{7,10} Previously, the denticities of tris(pyrazolyl)borato group **9** compounds have been correlated to ¹⁰³Rh NMR chemical shifts,²⁷ ¹¹B NMR chemical shifts,²⁸ and ν_{BH} stretching frequencies in the IR spectra,²⁹ but the latter two methods do not provide insight in the phenyl-oxazolinyborate systems.

Four olefinic ¹³C NMR signals were detected and assigned to the C₈H₁₂ group in compounds **3**, **4**, and **6**; four signals result from the C₁-symmetry of the compounds (see Table 1). In contrast, the ¹³C{¹H} spectra for C_s-symmetric To^MM(η⁴-C₈H₁₂) contained only two olefinic resonances as the result of C_s symmetry. The chemical shifts were further upfield in the iridium complexes than in the rhodium analogues for both To^M and PhB(Ox^{Me2})₂Im^{Mes}-supported compounds. The comparison between C₈H₁₂ olefinic resonances in To^M and PhB(Ox^{Me2})₂Im^{Mes}-supported complexes reveal a common set of upfield chemical shifts as well as an additional downfield set of olefinic chemical shifts for {**1**}- and {**2**}-supported compounds. There were also two sets of two olefinic signals observed in the ¹H NMR spectra, and the downfield set of ¹H NMR resonances correlated to the downfield ¹³C NMR signals in ¹H-¹³C HMQC experiments. The downfield ¹H and ¹³C chemical shifts were assigned to the olefin ligand *trans* to the NHC donor, while the upfield signals were assigned to the olefin ligand *trans* to the oxazoline donor based on their similarity to the olefinic chemical shifts in the To^MM(η⁴-C₈H₁₂) compounds. These

assignments were further supported by NOESY experiments on compound **4**. In particular, the downfield ^1H NMR signals assigned to cyclooctadiene at 4.48 and 4.67 ppm showed through-space correlations to the oxazoline methyl signals, and from that the downfield ^1H NMR signals were assigned as *cis* to the oxazoline and *trans* to the carbene. The upfield ^1H NMR signals at 3.11 and 3.52 ppm exhibited through-space correlations to the two *ortho*-methyl groups on the NHC-mesityl ring in the NOESY experiment, and these signals and the corresponding upfield ^{13}C NMR signals were assigned as *trans* to oxazoline. Satisfyingly, two out of the four cyclooctadiene olefinic signals at 4.48 and 3.52 ppm correlated to the *meta*- C_6H_5 in the NOESY experiment, and these data placed those two hydrogen atoms *syn* with the pseudoaxial phenyl group on boron. The other two olefinic hydrogens were *anti* with the phenyl group, and no cross-peak was detected.

In the rhodium $\text{PhB}(\text{Ox}^{\text{Me}_2})_2\text{Im}^{\text{R}}$ cyclooctadiene compounds, the $^1J_{\text{RhC}}$ values are larger for the upfield signals (12–14 Hz) than for downfield, *trans*-to-NHC olefinic signals (7–8 Hz). This effect was previously observed.³⁰ Unfortunately, the $^{13}\text{C}\{^1\text{H}\}$ NMR signals in $\text{To}^{\text{M}}\text{Rh}(\eta^4\text{-C}_8\text{H}_{12})$ for the diene are broad, and the coupling constants could not be measured.

The CO stretching frequencies in the four-coordinate complexes **5** and **7** appeared at lower energy than those in corresponding $\kappa^2\text{-To}^{\text{M}}\text{M}(\text{CO})_2$ compounds (measured on four-coordinate square planar compounds in a KBr matrix), which supports the expectation that $\text{PhB}(\text{Ox}^{\text{Me}_2})_2\text{Im}^{\text{Mes}}$ is more electron-donating than To^{M} . The five-coordinate rhodium complex $\text{Tp}^*\text{Rh}(\text{CO})_2$ has CO bonds that are lower energy than **5**, but that compound is 18 electron.²⁷ Better comparisons are with four-coordinate

compounds such as $\{\text{Acac}\}\text{Rh}(\text{CO})_2$ or $\{\text{PhMeBp}^{\text{Me}}\}\text{Rh}(\text{CO})_2$, which show higher energy CO stretching frequencies.^{31,32} The ν_{CO} bands for cationic bis(carbene) rhodium dicarbonyl compounds appear at even higher energy.³³ The carbonyl stretching frequencies of **7** and strongly electron-donating diketimate iridium dicarbonyls are similar, suggesting similar electron-donating capabilities of zwitterionic $\text{PhB}(\text{Ox}^{\text{Me}_2})\text{Im}^{\text{Mes}}$ (as a bidentate ligand) to the monoanionic diketimate ligands.³⁴

The upfield nitrogen signals observed in the $^1\text{H}-^{15}\text{N}$ HMBC experiments of compounds **3**, **4**, and **6** were assigned to the coordinated oxazoline nitrogen. The downfield ^{15}N cross-peak was assigned to the noncoordinated oxazoline because that signal was closer to the chemical shift of the oxazoline nitrogen in H[1] and H[2] (−125 ppm). Although the two nitrogen chemical shift values in the cyclooctadiene compounds **4** and **6** were different from the ones observed in the carbonyl compounds **5** and **7** (−153 and −156 ppm, respectively), the average values of the former are very close (−154 ppm, **4**; −156 ppm, **6**) to those of **5** and **7**. This similarity is attributed to the chemical averaging of signals in **5** and **7** that results from the fluxionality of the carbonyl compounds. The $^{13}\text{C}\{^1\text{H}\}$ NMR signals for the carbene 2-C for the series of compounds range from 178 to 187 ppm without a clear affect of metal center or other ligand (CO, cyclooctadiene).

X-ray quality crystals of all five $\text{PhB}(\text{Ox}^{\text{Me}_2})_2\text{Im}^{\text{R}}$ -supported compounds **3**, **4**, **5**, **6**, and **7** are obtained from pentane at $-30\text{ }^\circ\text{C}$. The conformations of cyclooctadiene-coordinated compounds **3**, **4**, and **6** are similar to one another, as are the structural features of the dicarbonyls **5** and **7**. Thermal ellipsoid-rendered representations for rhodium compounds **3**, **4**, and **5** are shown in Figures 3, 4, and 5, while illustrations of iridium complexes **6** and **7** are available in Appendix. The molecular structure of

$\text{To}^{\text{M}}\text{Rh}(\eta^4\text{-C}_8\text{H}_{12})$ (**8**) is shown in Figure 6. In all six compounds, the metal center is coordinated in the square planar geometry that is expected for monovalent group 9 compounds. To achieve this geometry, the $\text{PhB}(\text{Ox}^{\text{Me}_2})_2\text{Im}^{\text{Mes}}$ ligand coordinates in a bidentate fashion through the NHC and one of the two oxazoline donors. The bidentate-coordinated $\text{PhB}(\text{Ox}^{\text{Me}_2})_2\text{Im}^{\text{Mes}}$ ligand forms a boat-like conformation with the boron and metal centers occupying the "bow" and "stern" positions. A similar boat conformation is obtained in the crystal structure of *tert*-butyl-substituted complex **3** (shown above in Figure 3) and To^{M} -supported compound **8**.

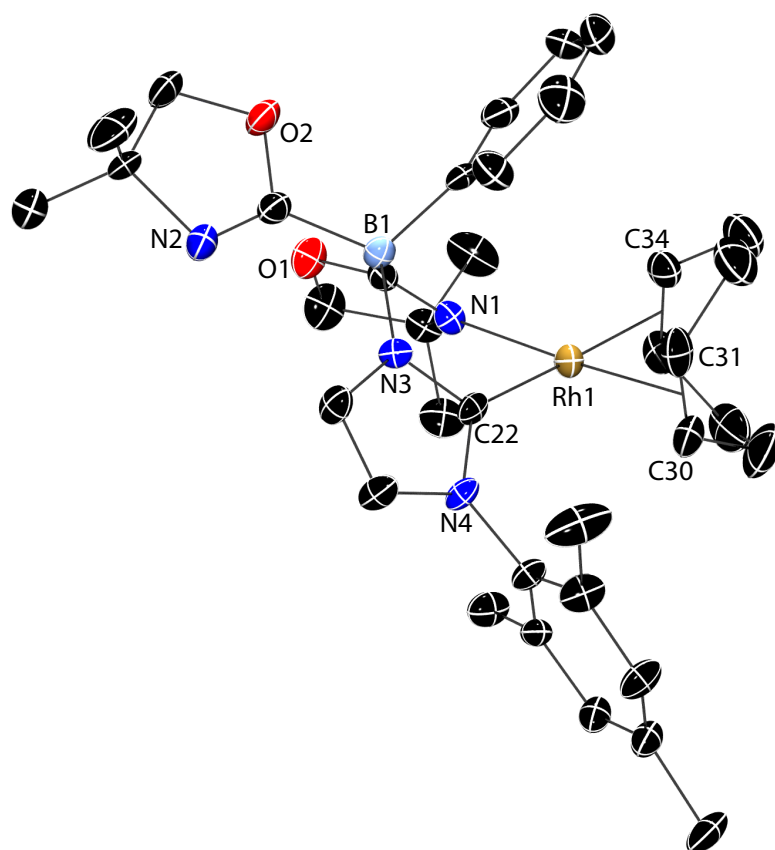


Figure 4. Rendered thermal ellipsoid plot of $\{\text{PhB}(\text{Ox}^{\text{Me}_2})_2\text{Im}^{\text{Mes}}\}\text{Rh}(\eta^4\text{-C}_8\text{H}_{12})$ (**4**). The ellipsoids are plotted at 35% probability, and H atoms are not illustrated for clarity.

Selected interatomic distances (Å) and angle (°): Rh1-N1, 2.132(6); Rh1-C22, 2.051(7); Rh1-C30, 2.139(8); Rh1-C31, 2.105(8); Rh1-C34, 2.198(7); Rh1-C35, 2.189(7); C22-Rh1-N1, 84.6(2).

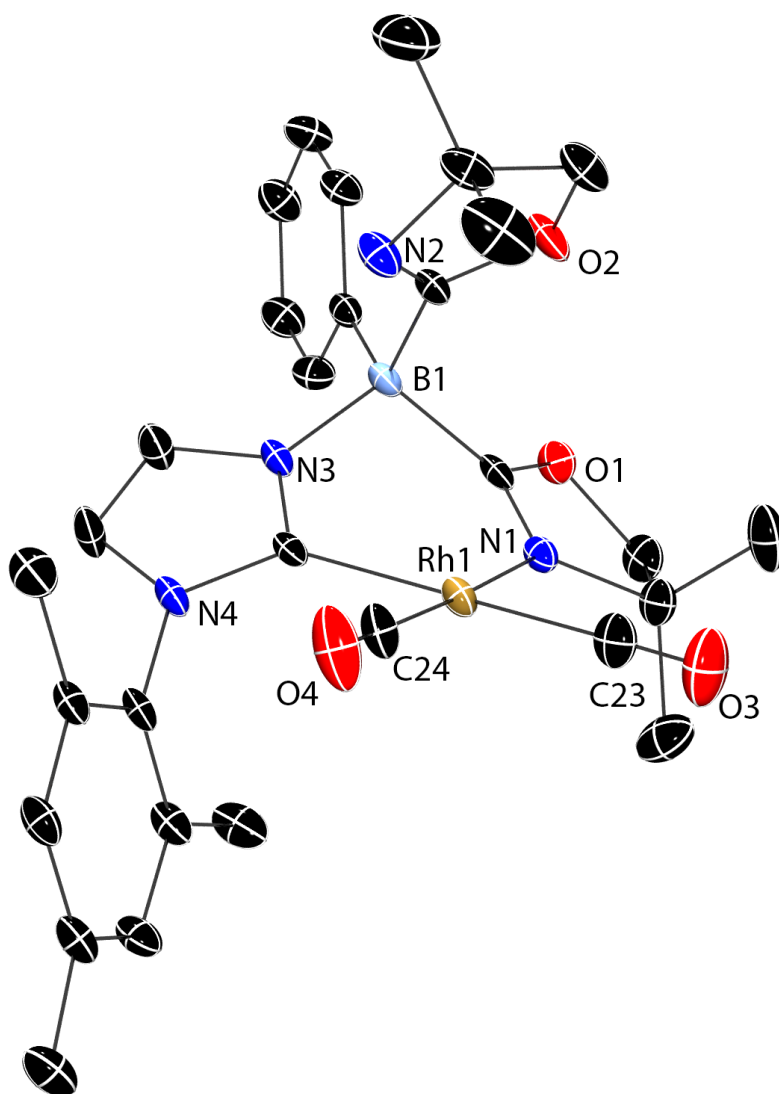


Figure 5. Rendered thermal ellipsoid plot of $\{\text{PhB}(\text{Ox}^{\text{Me}2})_2\text{Im}^{\text{Mes}}\}\text{Rh}(\text{CO})_2$ (**5**) at 35% probability. H atoms are not included in the depiction for clarity. Selected interatomic distances (Å): Rh1-N1, 2.087(2); Rh1-C22, 2.062(3), Rh1-C23, 1.896(4); Rh1-C24,

1.836(3). Selected interatomic angles ($^{\circ}$): C22-Rh1-N1, 87.4(1); N1-Rh1-C23, 96.0(1); C23-Rh1-C24, 85.3(1); C24-Rh1-C22, 91.3(1).

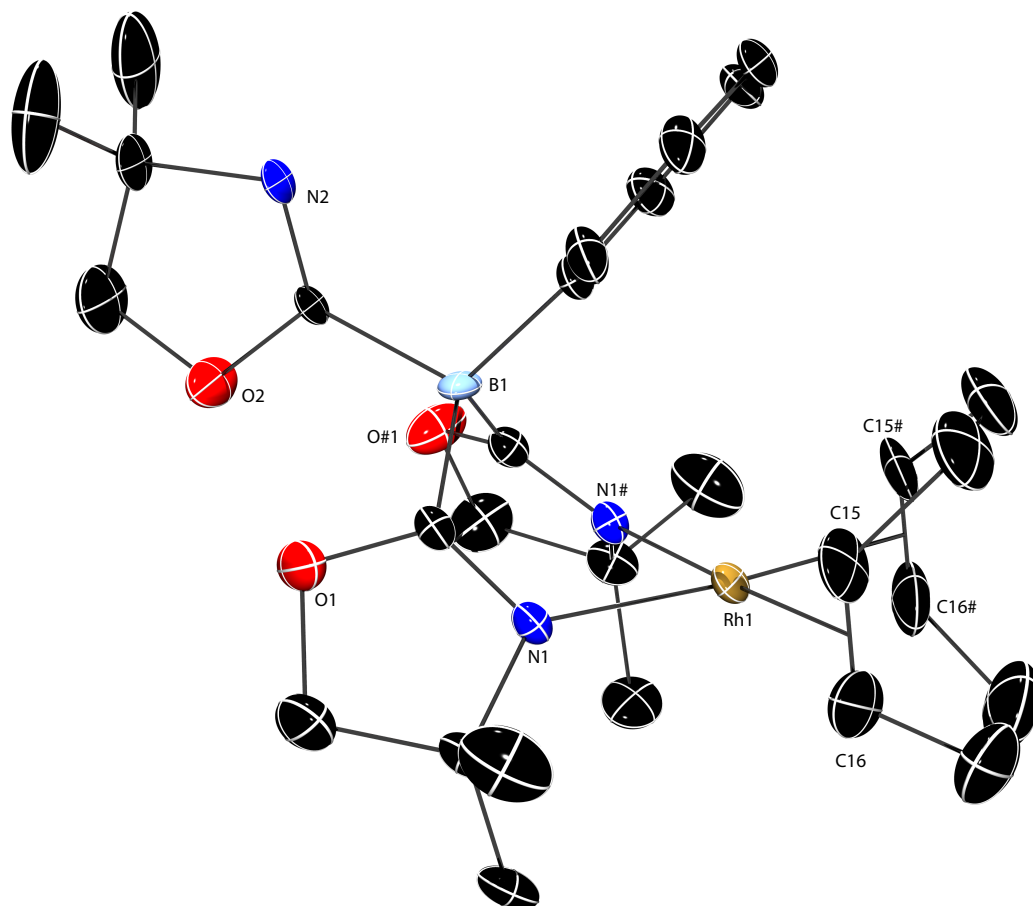


Figure 6. Rendered thermal ellipsoid plot of $\text{To}^{\text{M}}\text{Rh}(\eta^4\text{-C}_8\text{H}_{12})$ (**8**). Ellipsoids are plotted at 35% probability, and H atoms are not illustrated for clarity. Selected interatomic distances (\AA) and angle ($^{\circ}$): Rh1–N1, 2.116(6); Rh1–C15, 2.099(9); Rh1–C16, 2.12(1); N1–Rh1–N1#1, 84.4(3).

The six-membered boat conformation places the pendent oxazoline and phenyl groups bonded to boron in either axial or equatorial positions. The boat conformation

results in steric interactions between the axial group on boron and the other ligand(s) on the metal center. Interestingly, the pendent oxazoline is axial and points toward the metal center in the two carbonyl compounds **5** and **7**, while in the cyclooctadiene compounds **3**, **4**, and **6**, the phenyl ring occupies the axial position and the oxazoline group points away from the metal center. The combination of bulky cyclooctadiene on the metal center and nonplanar 4,4-dimethyl-2-oxazoline in the axial position likely would result in unfavorable steric interactions. For this reason, the conformation that places the planar phenyl group in the axial position is more favorable for the cyclooctadiene-coordinated compounds. Because the CO ligands have significantly diminished steric demand in comparison to cyclooctadiene, the carbonyl compounds can adopt a conformation in which the pendent oxazoline group is axial and points at the metal center. Presumably, a weak interaction between the metal center and the axial oxazoline might favor that conformation; however, the Rh1-N2 and Rh1-O2 distances in **5** are 3.713 and 4.213 Å and probably too long for a meaningful interaction (the sum of van der Waal radii of Rh–N and Rh–O are 3.6 and 3.5 Å).³⁵ A related conformation was reported from the results of single-crystal X-ray diffraction studies of $\text{Tp}^{3R,5R}\text{Rh}(\text{CO})_2$ (R = Me or CF₃) and $\text{Tp}^{4-t\text{Bu}-3,5-\text{Me}_2}\text{Rh}(\text{CO})_2$, in which the noncoordinated pyrazolyl is located in the axial position of the boat, above the coordination plane of the rhodium center; however, in the pyrazolylborate case, the pyrazolyl plane and square plane are orthogonal.^{16,36} $\text{Tp}^*\text{Ir}(\eta^4\text{-C}_8\text{H}_{12})$ adopts a conformation in the solid state in which the noncoordinated pyrazole is axial, but this is attributed to steric repulsions of the 5-methyl groups.³⁷ This literature compound is fluxional. Moreover, the coordination of the ancillary ligand in $\text{Tp}^*\text{Rh}(\text{CO})_2$

is proposed to be $\kappa^{2.5}$, and this configuration is suggested to be essential for the C–H bond oxidative addition chemistry of that complex.

In fact, an interesting pattern emerges upon analysis of the ancillary ligands' solid-state conformations in comparison to the fluxionality of the complexes. As noted above, carbonyl compounds **5** and **7** are fluxional from 190 to 298 K, whereas the cyclooctadiene compounds are not fluxional at room temperature. Thus, the conformations in the solid state and the rates of oxazoline exchange are similarly partitioned by the ancillary cyclooctadiene or carbon monoxide ligands. Likewise, the $\text{To}^{\text{M}}\text{Rh}(\eta^4\text{-C}_8\text{H}_{12})$ (**8**) is nonfluxional at room temperature (400 MHz) while $\text{To}^{\text{M}}\text{Rh}(\text{CO})_2$ is highly fluxional under the same conditions.

The $\text{M}-\text{C}_{\text{NHC}}$ distances in compounds **3-7** are equivalent within 3σ and apparently the imidazole *N*-substituent and the ancillary ligand do not influence this interaction (Table 2). Also, the $\text{M}-\text{N}_{\text{oxazoline}}$ distances are similar in compounds **3-8**. A large and systematic *trans* influence of the NHC donor is observed, such that the metal–carbon bonds *trans* to the carbene moiety are longer than the bonds *trans* to oxazoline donor. This observation is consistent with observations for carbene-imine-supported compounds, in which the *trans* influence of carbene is greater than that of the imine donor.³⁸

Table 2. Characteristic interatomic distances in compounds **3-8**.

Compound	$\text{M}-\text{C}_{\text{NHC}}^a$	$\text{M}-\text{N}^a$	$\text{M}-\text{C}_{\text{trans to NHC}}^a$	$\text{M}-\text{C}_{\text{trans to N}}^a$
$\{\mathbf{1}\}\text{Rh}(\eta^4\text{-C}_8\text{H}_{12})$ (3)	2.063(5)	2.121(4)	2.208(4) 2.173(5)	2.116(5) 2.147(5)
$\{\mathbf{2}\}\text{Rh}(\eta^4\text{-C}_8\text{H}_{12})$ (4)	2.051(7)	2.132(6)	2.198(7) 2.189(7)	2.139(8) 2.105(8)

Table 2 continued.

Compound	M–C _{NHC} ^a	M–N ^a	M–C _{trans to NHC} ^a	M–C _{trans to N} ^a
{2}Rh(CO) ₂ (5)	2.062(3)	2.087(2)	1.896(4)	1.836(2)
{2}Ir(η ⁴ -C ₈ H ₁₂) (6)	2.069(3)	2.116(2)	2.192(3) 2.161(3)	2.124(3) 2.126(3)
{2}Ir(CO) ₂ (7)	2.075(3)	2.085(2)	1.891(3)	1.836(3)
To ^M Rh(η ⁴ -C ₈ H ₁₂) (8)	n.a.	2.116(6)	n.a.	2.099(9) 2.12(1)

^a In angstrom (Å).

Cyclooctene group 9 precursors give nonanalogous Rh(III) and Ir(III) products. Interestingly, the products obtained from reactions of *in situ* generated K[2] with [Rh(μ-Cl)(η²-C₈H₁₄)₂]₂ or [Ir(μ-Cl)(η²-C₈H₁₄)₂]₂ are not isostructural, although both transformations involve formation of trivalent metal centers through oxidative addition reactions. The reaction of K[2] with 0.5 equiv. of the rhodium starting material gives a red-brown solid that is difficult to purify. Recrystallization of the reaction product provides an interesting asymmetric dimer {κ⁴-PhB(Ox^{Me2})₂Im^{Mes'}CH₂}Rh(μ-H)(μ-Cl)Rh(η²-C₈H₁₄)₂ (10), in which only one PhB(Ox^{Me2})₂Im^{Mes} ligand is present per two rhodium centers even though two equiv. of K[2] were allowed to react with [Rh(μ-Cl)(η²-C₈H₁₄)₂]₂ in the initial exploratory experiments. An upfield signal in the ¹H NMR spectrum at –21.70 ppm revealed that a rhodium hydride formed, and the doublet of doublets splitting pattern indicated that the hydride interacts inequivalently with two rhodium centers (¹J_{RhH} = 30 and 18 Hz). Four singlet resonances at 1.90, 1.28, 1.23, and 1.10 ppm were assigned to four inequivalent oxazoline methyl groups based on 2D NMR correlation spectroscopy and suggested a C₁-symmetric product. In addition, cyclooctene

resonances were evident in the ^1H and $^{13}\text{C}\{^1\text{H}\}$ NMR spectra. Although the product is asymmetric, only two mesityl-derived signals at 2.23 and 2.08 ppm (3 H each) were observed. The missing mesityl methyl group was transformed into a Rh-CH₂-Aryl moiety via a cyclometalation event and appeared as a multiplet at 2.80 ppm (2 H). Further evidence for cyclometalation was provided by a ^1H - ^{13}C HMQC experiment, which showed a correlation between this ^1H NMR signal and a doublet in the $^{13}\text{C}\{^1\text{H}\}$ NMR spectrum at 12.78 ppm ($^1J_{\text{RhC}} = 21$ Hz). The carbene is coordinated to a rhodium center based on its appearance as a doublet in the $^{13}\text{C}\{^1\text{H}\}$ NMR spectrum at 175.98 ppm ($^1J_{\text{RhC}} = 50$ Hz).

In addition, both of the oxazoline groups are coordinated to rhodium. This assignment was based upon their ^{15}N NMR chemical shifts of -162 and -178 ppm, which were upfield of noncoordinated oxazoline (~ -125 ppm). Moreover, the groups disposed *trans* to these oxazolines are clearly not identical based on the different ^{15}N NMR chemical shifts of the oxazolines. The *trans* ligands, however, could not be assigned because cross-peaks to the other ligands bonded to rhodium, such as the upfield hydride signal, were not detected in the ^1H - ^{15}N HMBC experiment. Thus, the PhB(Ox^{Me2})₂Im^{Mes'}CH₂ ligand is coordinated in a tetradentate fashion to rhodium having undergone a cyclometalation, a hydride is formed, the compound contains at least two rhodium centers, and cyclooctene ligands are present. Ultimately, the identity of **10** was clarified by a single-crystal X-ray diffraction study (Figure 7), and this allowed a rational ratio of reactants for a more efficient preparation based on the product's constitution (Scheme 2). The same product is obtained after longer reaction times (18 h) or heating at 60 °C.

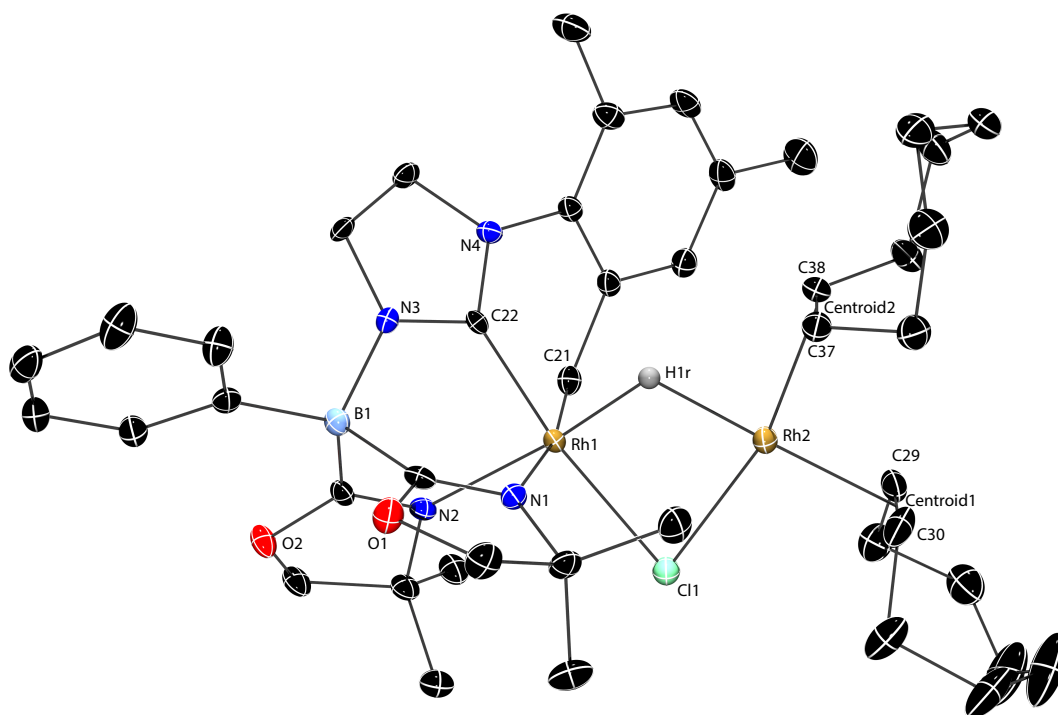
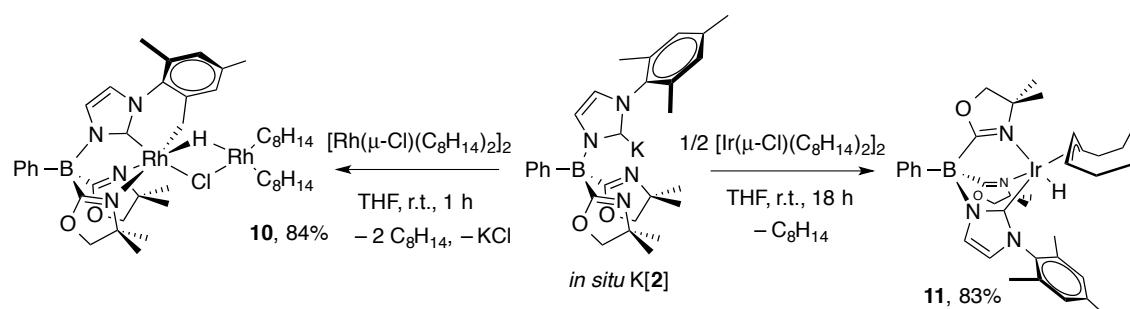


Figure 7. Rendered thermal ellipsoid plot of $\{\kappa^4\text{-PhB(Ox}^{\text{Me}_2})_2\text{Im}^{\text{Mes}'}\text{CH}_2\}\text{Rh}(\mu\text{-H})(\mu\text{-Cl})\text{Rh}(\eta^2\text{-C}_8\text{H}_{14})_2$ (**10**) with ellipsoids depicted at 35% probability. A disordered pentane and hydrogen atoms are not included in the representation, with the exception of the rhodium hydride, which was located in the Fourier difference map and refined isotropically. Selected interatomic distances (Å): Rh1-N1, 2.221(3); Rh1-N2, 2.110(3); Rh1-C21, 2.069(4); Rh1-C22, 1.941(4); Rh1-Cl1, 2.434(1); Rh1-H1r, 1.61(4); Rh1-Rh2, 2.8586(5); Rh2-Cl1, 2.363(1); Rh2-H1r, 1.81(5); Rh2-C29, 2.155(5); Rh2-C30, 2.154(5); Rh2-C37, 2.150(3); Rh2-C38, 2.158(3). Selected interatomic angles (°): N1-Rh1-N2, 83.5(1); C22-Rh1-N1, 89.5(1); C22-Rh1-N2, 87.2(1); C22-Rh1-C21, 82.2(1); C22-Rh1-Rh2, 121.5(1); C21-Rh1-Rh2, 87.5(1); Rh2-Rh1-Cl1, 52.29(3); N1-Rh1-Cl1, 97.32(8); N2-Rh1-Cl1, 98.69(8); Rh1-Cl1-Rh2, 73.13(3); Rh1-Rh2-Cl1, 54.59(3).

Compound **10** has a unique structure that features two inequivalent rhodium centers with bridging hydride and chloride ligands. One rhodium center is bonded to six ligands, the C–H bond-cleaved mesityl methylene group, two oxazolines, the carbene, and bridging hydride and chloride groups; the other rhodium atom is bonded to two η^2 -cyclooctene in addition to the bridging ligands. The overall valence requirements of the Rh₂ dimer is four, creating possible valence assignments of the rhodium atoms as either Rh(I)/Rh(III) or Rh(II)/Rh(II). The Rh–Rh distance is 2.8586(5) Å, which is significantly longer than the distance in Rh₂(OAc)₄ of 2.386 Å.³⁹ In addition, **10** contains one six-coordinate rhodium center in a distorted octahedral configuration, while the second rhodium is four-coordinate square planar. The Rh1-Rh2 axis splits the bridging H and Cl ligands. Moreover, the Rh1-Cl1 (2.434(1) Å) and Rh2-Cl1 (2.363(1) Å) distances are inequivalent, as are the Rh1-H1r (1.61(4) Å) and Rh2-H1r (1.81(5) Å) distances. On the basis of these data, it is more appropriate to assign six-coordinate Rh1 as trivalent and Rh2 as monovalent, following an approach applied previously.⁴⁰ A search of the Cambridge Structural Database revealed eight dirhodium compounds bridged by chloride and hydride; however these were all symmetrical Rh(III)/Rh(III) dimers. Unlike most Rh(II)–Rh(II) compounds in which the square planar coordination is orthogonal to the Rh–Rh vector, the Rh(I) coordination plane contains the Rh–Rh vector. In addition, cyclometalations of IMes and I^tBu (IMes = 1,3-bis(2,3,5-trimethylphenyl)imidazole-2-ylidene; I^tBu = *N,N*-di(*tert*-butyl)imidazol-2-ylidene) are reported for their reactions with the same rhodium precursor used for **10**, namely [Rh(μ -Cl)(η^2 -C₈H₁₄)₂]₂.⁴¹ Cyclometalation of tris(pyrazolyl)borate rhodium and iridium are discussed below.



Scheme 2. Contrasting reactions of $[\text{M}(\mu\text{-Cl})(\eta^2\text{-C}_8\text{H}_{14})_2]_2$ ($\text{M} = \text{Rh}, \text{Ir}$) with *in situ* generated $\text{K}[2]$.

In contrast, the iridium system forms a yellow compound $\{\text{PhB}(\text{Ox}^{\text{Me}_2})_2\text{Im}^{\text{Mes}}\}\text{IrH}(\eta^3\text{-C}_8\text{H}_{13})$ (**11**) from $\text{K}[2]$ and $[\text{Ir}(\mu\text{-Cl})(\eta^2\text{-C}_8\text{H}_{14})_2]_2$ after stirring overnight (Scheme 2). Compound **11** is C_1 symmetric rather than C_s -symmetric, as evidenced by seven methyl resonances in the ^1H NMR spectrum. A resonance at -27.49 ppm was assigned to an iridium hydride, while a triplet at 4.90 ppm ($^3J_{\text{HH}} = 7.2$ Hz, 1 H), a quartet at 4.09 ($^3J_{\text{HH}} = 8.4$ Hz, 1 H), and a multiplet at 3.43 ppm (1 H, overlapped with CH_2 of oxazoline ring) were assigned to the allyl protons on the C–H bond activated cyclooctene ring. The symmetry of the molecule suggests that the hydride is not *trans* to the carbene, as this configuration would produce a C_s -symmetric species. Instead, one of the oxazoline ligands is disposed *trans* to the iridium hydride, as evidenced by a correlation between the nitrogen signal at -184 ppm and the hydride resonance in a ^1H – ^{15}N HMBC experiment. Unfortunately, signals associated with imidazole nitrogen were not detected in the ^1H – ^{15}N HMBC spectrum.

There are a few other reported iridium allyl hydrides formed through metalation of an olefin upon coordination of a monoanionic tridentate *fac*-coordinating ligand, and these include $\{\text{PhB}(\text{CH}_2\text{PR}_2)_3\}$ ($\text{R} = \text{Ph}, i\text{-C}_3\text{H}_7$),^{42,43} Tp ,⁴⁴ and To^{M} .⁴⁵ $\text{Cp}^*\text{RhH}(\text{C}_3\text{H}_5)$ is

formed by photolysis of $\text{Cp}^*\text{Rh}(\eta^2\text{-C}_3\text{H}_6)_2$,⁴⁶ and the iridium analogue is synthesized by reduction of $\text{Cp}^*\text{Ir}(\eta^3\text{-C}_3\text{H}_5)\text{Cl}$.⁴⁷ The hydride resonance of **11** at -27.49 ppm appeared further upfield than the other iridium allyl hydride compounds following the trend $\{\text{PhB}(\text{CH}_2\text{PPh}_2)_3\}\text{IrH}(\eta^3\text{-C}_8\text{H}_{13})$ (at -12.55 ppm)⁴² $>$ $\{\text{PhB}(\text{CH}_2\text{P}^i\text{Pr}_2)_3\}\text{IrH}(\eta^3\text{-C}_8\text{H}_{13})$ (at -15.3 ppm)⁴³ $>$ $\{\text{PhB}(\text{CH}_2\text{P}^i\text{Pr}_2)_3\}\text{IrH}(\eta^3\text{-C}_3\text{H}_5)$ (at -15.60 ppm) $>$ $\text{Cp}^*\text{IrH}(\eta^3\text{-C}_3\text{H}_5)$ (at -16.7 ppm) $>$ $\text{TpIrH}(\eta^3\text{-C}_8\text{H}_{13})$ (at -18.10 ppm).⁴⁴ Attempts to synthesize $\text{To}^{\text{M}}\text{IrH}(\eta^3\text{-C}_8\text{H}_{13})$ were unsuccessful with $\text{K}[\text{To}^{\text{M}}]$ or $\text{Li}[\text{To}^{\text{M}}]$, but $\text{Tl}[\text{To}^{\text{M}}]$ gives the product ($\delta_{\text{IrH}} = -28.54$ ppm).⁴⁵ $\text{To}^{\text{M}}\text{RhH}(\eta^3\text{-C}_8\text{H}_{13})$ has a comparable hydride doublet at -24.27 ppm (in benzene- d_6 , $^1J_{\text{RhH}} = 11.6$ Hz).⁴⁵ In addition, a unique feature of **11** is that the ligands *trans* to the allyl group are inequivalent.

X-ray quality crystals of **11** are obtained from a concentrated benzene solution at room temperature. A single-crystal X-ray diffraction study of **11** confirms the C_1 -symmetry of the complex and the configuration that disposes one of the oxazolines and the hydride ligand *trans* (Figure 8). The Ir–N distance *trans* to hydride (Ir1–N1, 2.286(2) Å) is elongated compared to the Ir–N bond *trans* to the allyl group (Ir1–N2, 2.125(2) Å). This is presumably due to the strong *trans* influence of the hydride ligand, as also observed in $\{\text{PhB}(\text{CH}_2\text{PPh}_2)_3\}\text{IrH}(\eta^3\text{-C}_8\text{H}_{13})$. Moreover, the allylic coordination of C_8H_{13} to the iridium center is also affected by the inequivalent donors. Within the $[\text{Ir}](\eta^3\text{-C}_8\text{H}_{13})$ interaction of **11**, the iridium–carbon distances vary (Ir1–C29, 2.183(3) Å); Ir1–C30, 2.110(3); Ir1–C31, 2.278(4) Å). The allylic carbon (C31) *cis* to the oxazoline and pseudo-*trans* to the carbene has the longest iridium–carbon distance, whereas the carbon pseudo-*trans* to oxazoline is ca. 0.1 Å shorter. The mesityl group on the NHC is rotated to accommodate the C_8H_{13} group (C22–N4–C13–C14, 88.38°), while the oxazoline methyl

groups are directed toward the C₈H₁₃ ligand. Thus, the inequivalent allyl bonding may be a combination of complementary steric and electronic influences. The related Ir–C distances in {PhB(CH₂PPh₂)₃}IrH(η^3 -C₈H₁₃) are longer than in **11** at 2.302(9), 2.176(8) and 2.261(9) Å.

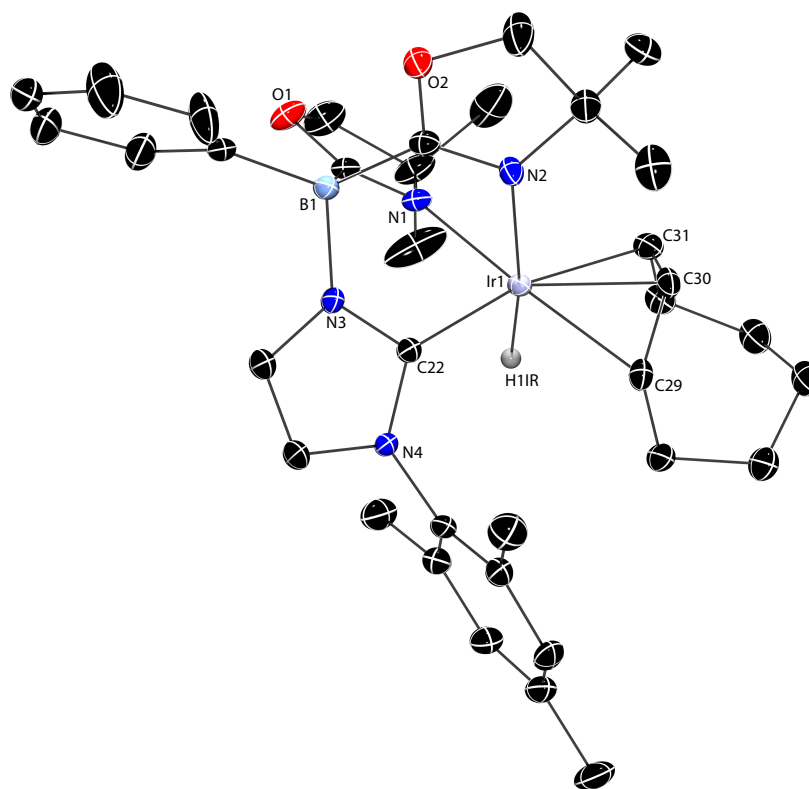
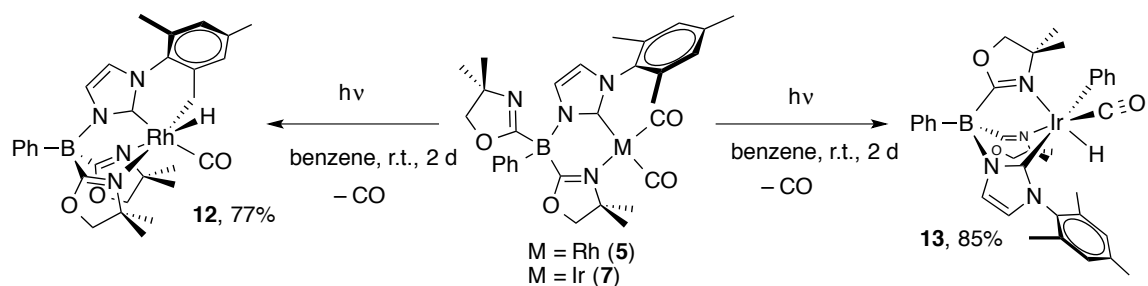


Figure 8. Rendered thermal ellipsoid plot of {PhB(Ox^{Me2})₂Im^{Mes}}IrH(η^3 -C₈H₁₃) (**11**) with ellipsoids at 35% probability. H atoms are not plotted for clarity with the exception of the iridium hydride, which was located objectively on a difference Fourier map. Selected interatomic distances (Å): Ir1–N1, 2.286(2); Ir1–N2, 2.125(2); Ir1–C22, 2.029(3); Ir1–H11R, 1.55(3); Ir1–C29, 2.183(3); Ir1–C30, 2.110(3); Ir1–C31, 2.278(4). Selected interatomic angles (°): C22–Ir1–N1, 85.8(1); C22–Ir1–N2, 85.5(1); C22–Ir1–C29, 103.2(1); C22–Ir1–C30, 137.8(1); C22–Ir1–C31, 167.7(1); N1–Ir1–N2, 82.46(9).

Photochemical intra- and intermolecular oxidative addition reactions of $\{\text{PhB}(\text{Ox}^{\text{Me}_2})_2\text{Im}^{\text{Mes}}\}\text{M}(\text{CO})_2$ ($\text{M} = \text{Rh}$ (5**), Ir (**7**)).** The metal dicarbonyl compounds **5** and **7** react under photolytic conditions in a Rayonet reactor (254 nm) to give inequivalent products. Photolysis of **5** in benzene- d_6 for 2 d provides cyclometalated rhodium hydride $\{\kappa^4\text{-PhB}(\text{Ox}^{\text{Me}_2})_2(\text{Im}^{\text{Mes}'}\text{CH}_2)\}\text{RhH}(\text{CO})$ as a yellow solid in 77% yield (**12**, Scheme 3). Compound **12** is persistent in solution even after extended photolysis, and the hydride resonance at -14.21 ppm ($^1J_{\text{RhH}} = 23.4$ Hz) was observed in the ^1H NMR spectrum even at long reaction times in benzene- d_6 . Unlike the symmetric-appearing fluxional starting material, the product's overall C_1 -symmetry was indicated by the observation of six methyl signals for inequivalent oxazolines and the cyclometalated mesityl group. The diastereotopic cyclometalated CH_2 resonances appeared as a virtual triplet at 2.78 ppm.



Scheme 3. Divergent photochemical reactivity of rhodium and iridium congeners of $\{\text{PhB}(\text{Ox}^{\text{Me}_2})_2\text{Im}^{\text{Mes}}\}\text{M}(\text{CO})_2$.

In a ^1H - ^{15}N HMBC experiment, two methyl signals at 0.90 and 1.02 ppm and the rhodium hydride provided cross-peaks to the same oxazoline nitrogen signal at -162

ppm. On the basis of this through-rhodium correlation, the rhodium hydride is assigned as *trans* to one of the oxazoline donors. The other two upfield methyl signals at 0.72 and 0.83 ppm (3 H each) correlated to a nitrogen signal at -171 ppm. The IR spectrum (KBr) contained bands at 2015 and 2064 cm^{-1} assigned to the carbonyl and hydride vibrations, respectively. An additional two absorptions at 1587 and 1568 cm^{-1} were assigned to the oxazoline ν_{CN} . Light yellow crystals of **12** are obtained from a pentane solution cooled at $-30\text{ }^{\circ}\text{C}$. A single crystal X-ray diffraction study confirms the proposed structure and reveals that the NHC and carbonyl ligands are disposed in a *trans* configuration, as are the mesityl-derived benzyl ligand and an oxazoline (Figure 9). The hydride (H1r), which was located and refined isotropically, is *trans* to one of the oxazolines; the Rh1-H1r distance is ca. 0.2 \AA shorter than in the bridging hydride of dirhodium compound **10**.

The resulting compound contains three types of carbon-based ligands coordinated to rhodium in a meridional fashion: an NHC, a carbonyl, and a benzyl group. The Rh–C distance associated with the benzyl ligand (Rh1-C21, $2.103(3)\text{ \AA}$) is longer than the benzyl in **10** (Figure 7, Rh1-C21, $2.069(4)\text{ \AA}$) and the previously reported Rh(IMes)(H)(IMes')Cl ($2.079(2)\text{ \AA}$).^{41c} The intramolecular C–H bond activation on the substituent of the imidazole ring has been reported for thermal activation for both rhodium and iridium complexes.^{41,48} In addition, thermal and photolytic conditions can lead to intramolecular C–H bond cleavage of tris(pyrazolyl)borate ligands in rhodium and iridium compounds.⁴⁹ For instance, optically active $\text{Tp}^{\text{Menth}}\text{Rh}(\text{CO})_2$ ($\text{Tp}^{\text{Menth}} = \text{tris}(7R\text{-isopropyl-}4R\text{-methyl-}4,5,6,7\text{-tetrahydroindazolyl)borate}$) undergoes cyclometalation upon photolysis.^{49a}

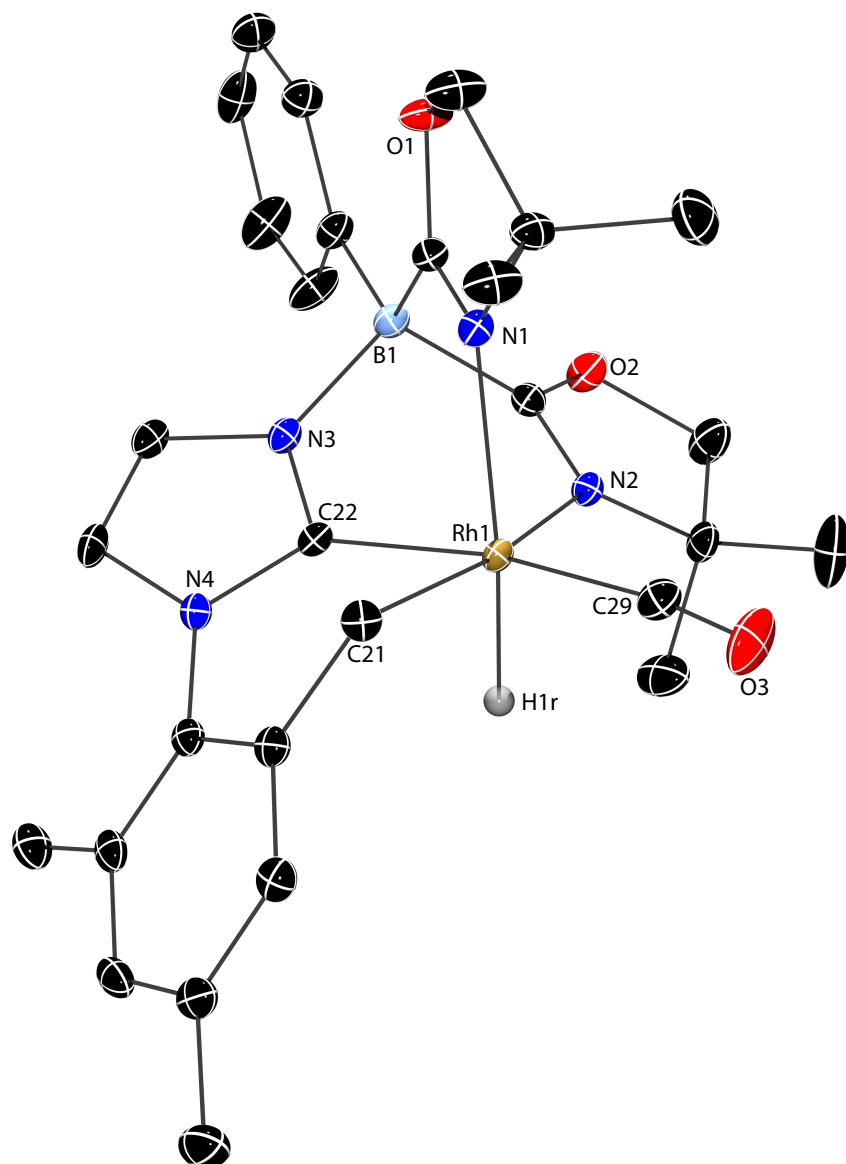


Figure 9. Rendered thermal ellipsoid plot of $\{\kappa^4\text{-PhB(Ox}^{\text{Me}_2}\text{)}_2\text{Im}^{\text{Mes}'\text{CH}_2}\text{RhH(CO)}$ (**12**) with ellipsoids at 35% probability. With the exception of the hydrogen bonded to rhodium, which was located in the Fourier difference map and refined isotropically, H atoms are not plotted for clarity. Selected interatomic distances (Å): Rh1-N1, 2.191(2); Rh1-N2, 2.147(2); Rh1-C21, 2.106(3); Rh1-C22, 2.016(3); Rh1-C29, 1.882(3); Rh1-H1r, 1.44(3). Selected interatomic angles (°): C22-Rh1-N1, 85.05(8); C22-Rh1-N2, 86.76(9); N1-Rh1-N2, 83.04(8); C22-Rh1-C21, 81.0(1); C21-Rh1-C29, 89.5(1).

In contrast to the intramolecular C–H bond oxidative addition observed with rhodium, the iridium dicarbonyl (**7**) reacts under photolytic conditions over 2 d with the benzene solvent to give an intermolecular metalated product $\{\text{PhB}(\text{Ox}^{\text{Me}_2})_2\text{Im}^{\text{Mes}}\}\text{IrH}(\text{Ph})\text{CO}$ (**13**) in 85% yield (Scheme 3). Further UV photolysis of isolated **13** leads to a complicated mixture of unidentified species. In addition, compound **7** decomposes in methylene chloride under photolytic conditions, and apparently the cyclometalated iridium analogue of **12** is not accessible under these conditions. Although the photolytic chemistry is not clean in methylene chloride, the benzene-activated product **13** is persistent in methylene chloride- d_2 . In the ^1H NMR spectrum of **13** in methylene chloride- d_2 , a singlet at -16.51 ppm was assigned to the iridium hydride. All seven methyl groups were inequivalent in the C_1 symmetric complex. The ^1H – ^{15}N HMBC experiment showed a correlation between the hydride and the nitrogen signal at -182 ppm, suggesting that this oxazoline ring is *trans* to hydride. However, a ^1H – ^{13}C HMBC experiment revealed two strong cross-peaks between the hydride and carbon signals at 139.32 and 171.70 ppm and a faint correlation to a ^{13}C NMR signal at 170.07 ppm. The signal at 139.32 ppm was assigned to *ipso*- IrC_6H_5 , while the signal at 170.07 ppm, which also correlated to the 4-H and 5-H signals of the $\text{N}_2\text{C}_3\text{H}_2\text{Mes}$, was assigned to the carbene carbon on the imidazole ring, and the signal at 171.70 ppm was assigned to the carbon atom in the carbonyl group. These multiple correlations to the iridium hydride resonance complicate the assignments of the iridium center's configuration, although the carbonyl, phenyl group, and hydride are most likely *fac* disposed.

The iridium center's configuration in **13** is unambiguously determined by a single-crystal X-ray diffraction study (Figure 10), which shows that the phenyl and NHC ligands are *trans*, one oxazoline and the hydride are *trans*, and the second oxazoline and carbonyl are *trans* in an overall distorted octahedral geometry. This configuration is remarkable because all the other monometallic rhodium(III) and iridium(III) compounds reported in this chapter contain the neutral donor ligand *trans* to the NHC. In cyclometalated **12**, the NHC and metalated mesityl are geometrically required to be *cis* because the groups are connected through the multidentate ligand. However, in the silyl compounds described below, that geometric constraint is lifted but the carbene and the two electron-donor π -acid ligands remain *trans*.

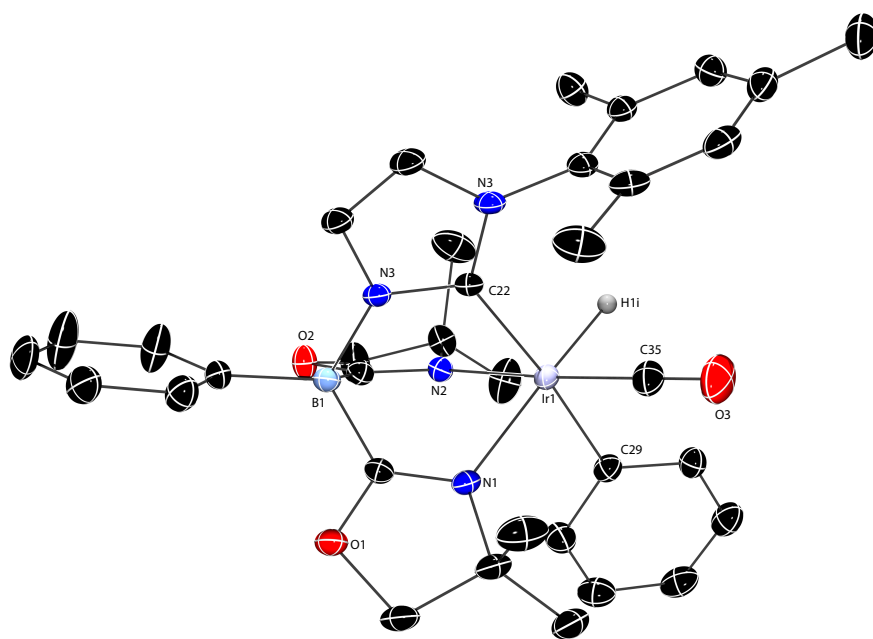


Figure 10. Rendered thermal ellipsoid plot of $\{\text{PhB}(\text{Ox}^{\text{Me}_2})_2\text{Im}^{\text{Mes}}\}\text{IrH}(\text{Ph})\text{CO}$ (**13**) with ellipsoids at 35% probability. H atoms are not plotted for clarity. The Ir1-H11 was located in the Fourier difference map and fixed without refinement. Selected interatomic

distances (Å): Ir1-C22, 2.84(4); Ir1-N1, 2.182(3); Ir1-N2, 2.136(3); Ir1-C29, 2.101(4); Ir1-C35, 1.813(5); Ir1-H1i, 1.67. Selected interatomic angles (°): C22-Ir1-N1, 85.1(1); C22-Ir1-N2, 84.0(1); N1-Ir1-N2, 85.8(1); C22-Ir1-C35, 97.4(2); C29-Ir1-C35, 88.6(2); C29-Ir1-C35, 88.6(2); C22-Ir1-C29, 173.9(1).

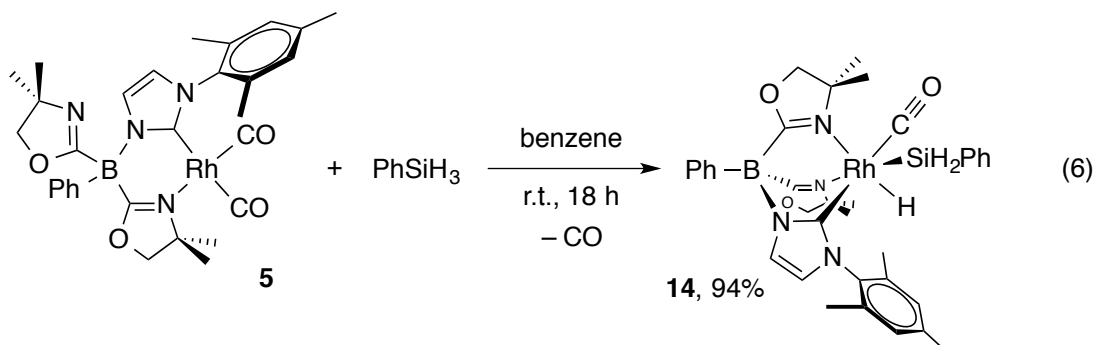
Compound **13** is one of the few examples of crystallographically characterized rhodium or iridium complexes with the hydride, the hydrocarbyl, and a third ancillary group *fac*-coordinated to the metal. To the best of our knowledge, the only other example is the carbene-stabilized compound $\text{Tp}^*\text{IrH}(\text{C}_6\text{H}_5)(\text{C}_5\text{H}_3\text{MeNH})$ ($\text{C}_5\text{H}_3\text{MeNH}$ = pyridylidene),⁵⁰ in which the hydride, the phenyl, and the pyridylidene are *fac*-coordinated to iridium and formed from heterolytic addition of H_2 to an iridium(III) 2-pyridyl phenyl compound and not from C–H bond oxidative addition. The air-stable iridium vinyl hydride $\{\text{HBPf}_3\}\text{IrH}(\text{C}_2\text{H}_3)\text{CO}$ (HBPf_3 = tris(3-trifluoromethyl-5-methylpyrazol-1-yl)borate) is also stabilized relative to its monovalent $\eta^2\text{-C}_2\text{H}_4$ isomer.^{13a} For comparison in the $\text{To}^{\text{M}}\text{Rh}(\text{CO})_2$ -catalyzed photochemical decarbonylation chemistry in benzene- d_6 , extensive H/D exchange suggests that reversible C–H oxidative addition/reductive elimination occurs from $\text{To}^{\text{M}}\text{RhH}(\text{Ph})\text{CO}$. Likewise $\text{To}^{\text{M}}\text{RhH}(\eta^3\text{-C}_8\text{H}_{13})$ reacts by reductive elimination in the presence of alcohols.⁴⁵ The cyclopentadienyl rhodium(III) alkyl hydride compounds are also unstable with respect to hydrocarbon reductive elimination and form dimeric $\text{Cp}_2\text{Rh}_2(\text{CO})_3$.⁵¹ Typically, rhodium and iridium hydrocarbyl hydride compounds such as $\text{Tp}^*\text{RhH}(\text{Ph})\text{CO}$ that are formed from C–H bond oxidative addition are converted into halide complexes for isolation.^{8,52}

Examples of *trans*-[Ir](H)Ph are more common, presumably because C–H reductive elimination is less facile with *trans*-disposed ligands.⁵³

Thus, in two instances, the rhodium precursor reacts via cyclometalation of the *ortho*-methyl of the mesityl-imidazole, whereas the iridium congener reacts with the C–H bond of a substrate (either benzene or cyclooctene). We have not yet observed the reductive elimination reaction of either of the cyclometalated rhodium compounds into a tridentate monoanionic *C,N,N*-coordinating ligand, and a few reactions provide compound **12**. The tendency for **10** and **12** to form from a few different conditions and a few starting materials may reflect a thermodynamic preference of the cyclometalated structure for rhodium with $\text{PhB}(\text{Ox}^{\text{Me}_2})_2\text{Im}^{\text{Mes}}$. Attempts to generate the cyclometalated iridium analogue have been unsuccessful.

Thermal oxidative addition of phenylsilane: Synthesis and characterization of $\{\text{PhB}(\text{Ox}^{\text{Me}_2})_2\text{Im}^{\text{Mes}}\}\text{RhH}(\text{SiH}_2\text{Ph})\text{CO}$ (14**).** Complex **5** and PhSiH_3 react at room temperature to give a clean and isolable rhodium silyl complex $\{\text{PhB}(\text{Ox}^{\text{Me}_2})_2\text{Im}^{\text{Mes}}\}\text{RhH}(\text{SiH}_2\text{Ph})\text{CO}$ (**14**). The yellow-brown solution leads to the isolation of **14** as a brown solid after evaporation of solvent and volatiles (eq. 6). In contrast, $\text{To}^{\text{M}}\text{Rh}(\text{CO})_2$ and PhSiH_3 are the only species detected by ^1H NMR spectroscopy even at elevated temperature (60 °C) for extended time (24 h). In addition, the rhodium cyclooctadiene compounds **3** and **4** remain unchanged after heating at 120 °C in the presence of PhSiH_3 , Ph_2SiH_2 , PhMeSiH_2 , and Mes_2SiH_2 . Also, the reaction of iridium carbonyl congener **7** and PhSiH_3 affords a mixture of unidentified products. Secondary silanes such as Mes_2SiH_2 , Ph_2SiH_2 , and PhMeSiH_2 do not react with **5** even at

elevated temperature. In fact, the lack of phenylsilane redistribution and/or polymerization is unusual given the tendency for rhodium to catalyze these processes.^{54,55}



The reaction of eq. 6 occurs under ambient light and in the dark, and it is complete after 1 h at 60 °C in the dark. This reactivity also contrasts with the reactions of $\text{Cp}^{\text{R}}\text{Rh}(\text{CO})_2$ ($\text{Cp}^{\text{R}} = \text{C}_5\text{H}_5, \text{C}_5\text{H}_4\text{Me}, \text{C}_5\text{Me}_5$) and Et_3SiH , which require photolytically activated CO dissociation.⁵⁶ Most likely, CO dissociation requires hydrosilane preassociation because **5** persists in benzene and thermal C–H bond activation (e.g. of benzene solvent) by **5** is not detected. Although thermal C–H bond oxidative addition chemistry of Tp^*RhL_2 monovalent systems is known, such reactivity typically requires a labile ligand such as ethylene.⁵⁷

Evidence for phenylsilane oxidative addition was provided by a rhodium hydride resonance at -13.22 ppm in the ^1H NMR spectrum, which appeared as a doublet of doublets resulting from rhodium and silicon-hydride coupling ($^1J_{\text{RhH}} = 21$ Hz; $^3J_{\text{HH}} = 1.2$ Hz). As in the C_1 -symmetric compounds described above, a combination of 1D NMR and 2D correlation spectroscopy suggested that oxazoline and hydride are disposed *trans*. Two doublets at 4.43 and 4.91 ppm (1 H each; $^2J_{\text{HH}} = 6.0$ Hz; $^1J_{\text{SiH}} = 170$ and 188 Hz)

were assigned to the diastereotopic silicon hydrides. The $^{13}\text{C}\{^1\text{H}\}$ NMR spectrum of **14** contained a doublet at 194.53 ppm that was assigned to the carbene 2-C ($^1J_{\text{RhC}} = 51$ Hz). Likewise, the carbonyl carbon signal appeared as a doublet at 178.39 ppm ($^1J_{\text{RhC}} = 41$ Hz). The IR spectrum (KBr) showed a broad peak at 1593 cm^{-1} associated with the CN stretching mode, peaks at 2064 and 2016 cm^{-1} assigned to the ν_{RhH} and ν_{CO} , and one band at 1998 cm^{-1} for the ν_{SiH} . The ν_{CO} and ν_{RhH} were assigned by comparison with the cyclometalated Rh(III) hydrido carbonyl **12** which contains a RhH and carbonyl and similar IR peaks at 2064 and 2015 cm^{-1} but lacks both the SiH_2Ph group and the IR band at 1998 cm^{-1} and by comparison with the IR spectrum of $\text{Tp}^*\text{RhH}(\text{SiEt}_3)\text{CO}$, which contained absorptions at 2086 (ν_{RhH}) and 2020 cm^{-1} (ν_{CO}).¹¹

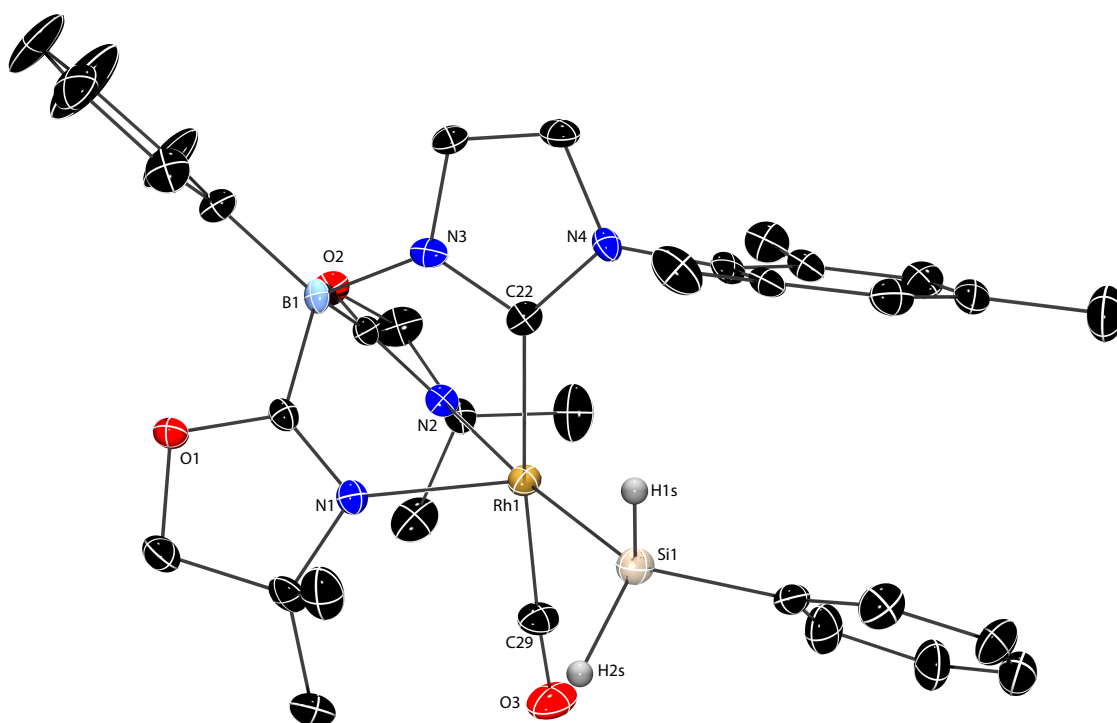
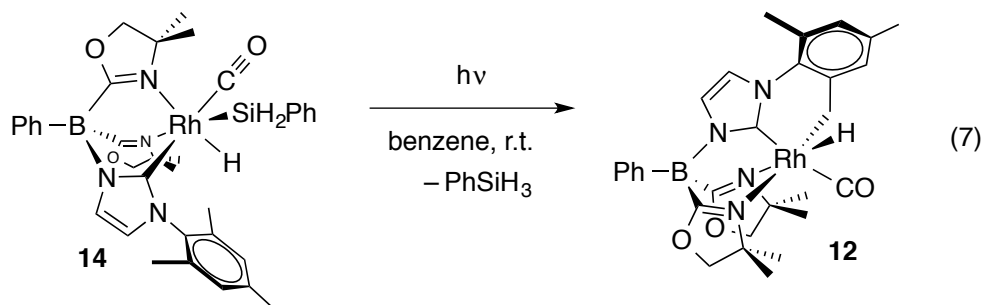


Figure 11. Rendered thermal ellipsoid plot of $\{\text{PhB}(\text{Ox}^{\text{Me}_2})_2\text{Im}^{\text{Mes}}\}\text{RhH}(\text{SiH}_2\text{Ph})\text{CO}$ (**14**) with ellipsoids drawn at 35% probability. A cocrystallized toluene solvent molecule and

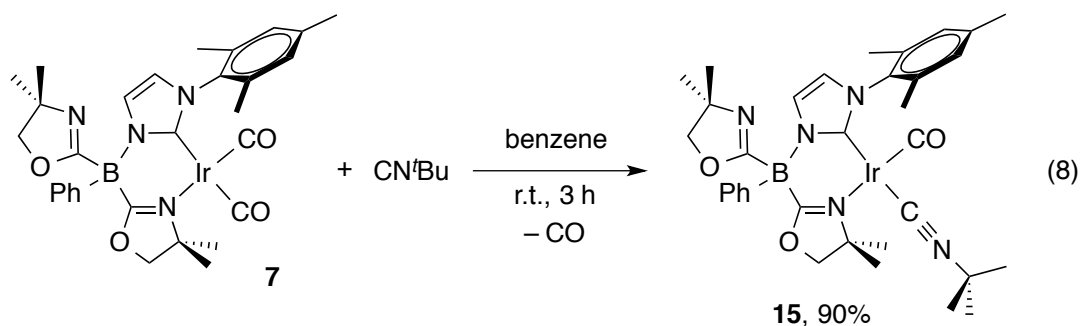
H atoms, with the exception the SiH, are not plotted for clarity. The H1s and H2s were located objectively in a difference Fourier map and refined isotropically; however, the H1r was placed in a calculated position with Rh1-H1r of 1.61 Å, its temperature factor was set based on the rhodium atom, and is not included in the illustration. Selected interatomic distances (Å): Rh1-N1, 2.184(5); Rh1-N2, 2.206(5); Rh1-C22, 2.068(5); Rh1-C29, 1.857(7); Rh1-Si1, 2.328(2). Selected interatomic angles (°): C22-Rh1-N1, 85.7(2); C22-Rh1-N2, 84.2(2); N1-Rh1-N2, 85.2(2); N1-Rh1-C29, 99.4(3); N2-Rh1-C29, 97.3(2); N1-Rh1-Si1, 99.9(2); C22-Rh1-Si1, 95.1(2).

X-ray quality crystals of **14** are obtained from a concentrated pentane solution at –30 °C, and an ORTEP diagram is shown in Figure 11. The coordination environment of the rhodium center in **14** is related to that of cyclometalated **12**, with *trans* carbene/carbonyl ligands and *trans* oxazoline/hydride ligands; however, the cyclometalated mesityl of **12** is replaced with a silyl ligand in **14**. The strong *trans* influence of the silyl group on the rhodium-oxazoline interaction in **14** is evidenced by the longer Rh1-N2 distance of 2.206(5) Å versus the Rh1-N1 distance of 2.184(5) Å in **12**. The other rhodium–ligand distances (Rh1-CO, Rh1-N1_{oxazoline}, Rh1-C22_{NHC}) are similar for **12** and **14**.

Photolysis of **14** at 254 nm results in elimination of PhSiH₃ and formation of the cyclometalated **12** (eq. 7). On a micromolar scale, the process takes 2 days to finish, which is as slow as the formation of **12** from **5**. This process appears to involve a sequence of reductive elimination of a Si–H bond followed by oxidative addition of the C–H bond on the basis of photolysis of **14-d**₃, which gives unlabeled **12**.



Synthesis and characterization of $\{\text{PhB}(\text{Ox}^{\text{Me}_2})_2\text{Im}^{\text{Mes}}\}\text{Ir}(\text{CO})\text{CN}^t\text{Bu}$ (15). As noted above and in contrast to $\{\text{PhB}(\text{Ox}^{\text{Me}_2})_2\text{Im}^{\text{Mes}}\}\text{Rh}(\text{CO})_2$ (5), the reaction of iridium congener 7 and PhSiH_3 provides a mixture of products. Because 5 likely reacts with PhSiH_3 through an associative substitution that precedes oxidative addition, the substitution of CO with other ligands was tested for the iridium compound. Complex 7 reacts with *tert*-butyl isocyanide in benzene to give $\{\text{PhB}(\text{Ox}^{\text{Me}_2})_2\text{Im}^{\text{Mes}}\}\text{Ir}(\text{CO})\text{CN}^t\text{Bu}$ (15, eq. 8). Under the photolytic conditions in which the iridium dicarbonyl reacts with benzene, compound 15 decomposes to H[2].



The oxazoline groups appeared equivalent in ^1H NMR spectra of 15 acquired from 195 K to room temperature. The integration of the *tert*-butyl peak (9 H, relative to

oxazoline methyl peaks being 6 H each) shows that only one carbonyl moiety is replaced by the isocyanide group. An ^{15}N NMR signal at -196 ppm was assigned to the isocyanide nitrogen on the basis of its correlation to the *tert*-butyl signal in a ^1H - ^{15}N HMBC experiment. In the ^{15}N dimension, one signal (-154 ppm) correlated to the oxazoline protons and two signals (-176 and -188 ppm) correlated to imidazole protons. The IR spectrum (KBr) contained characteristic bands assigned to isocyanide (2144 cm^{-1}), CO (1973 cm^{-1}), and oxazoline ν_{CN} (1616 and 1579 cm^{-1}). Although the NMR and IR spectra suggest that compound **15** is four-coordinate square planar containing an axial noncoordinated oxazoline, the stereochemical disposition of the isocyanide group (*cis* or *trans* to NHC) was unknown.

X-ray quality crystals of **15** are obtained from a pentane solution cooled to -30 °C (Figure 12), and the single-crystal X-ray diffraction study reveals that the isocyanide ligand is disposed *trans* to the NHC donor. The $\text{PhB}(\text{Ox}^{\text{Me}_2})\text{Im}^{\text{Mes}}$ ligand's conformation is similar to that of the dicarbonyl compounds, and this conformation was suggested by the fluxionality of the oxazoline donors as discussed above. The Ir-CN^{*t*}Bu distance (*trans* to carbene, Ir1-C29, $1.955(2)$ Å) is longer than the Ir-CO distance (*trans* to oxazoline, Ir1-C35, $1.817(2)$ Å). In addition, the Ir-CO distance in **15** is shorter than in **7** (*trans* to oxazoline, Ir1-C30, $1.836(3)$ Å).

Although oxazoline groups rapidly exchange in **15**, the substitution reaction of the carbonyl *trans* to the NHC donor is remarkably stereoselective and only one stereoisomer is obtained. The selectivity suggests an associative substitution, as is typical in reactions of square planar d^8 compounds, but may also be related to unfavorable steric interactions between the mesityl substituent on the imidazole ring and the *tert*-butyl isocyanide in the

unobserved stereoisomer. Still, this substitution reaction demonstrates the stronger *trans* effect of the carbene donor with respect to oxazoline, while the crystallographically determined structures of starting materials and products show the *trans* influence of the NHC donor.

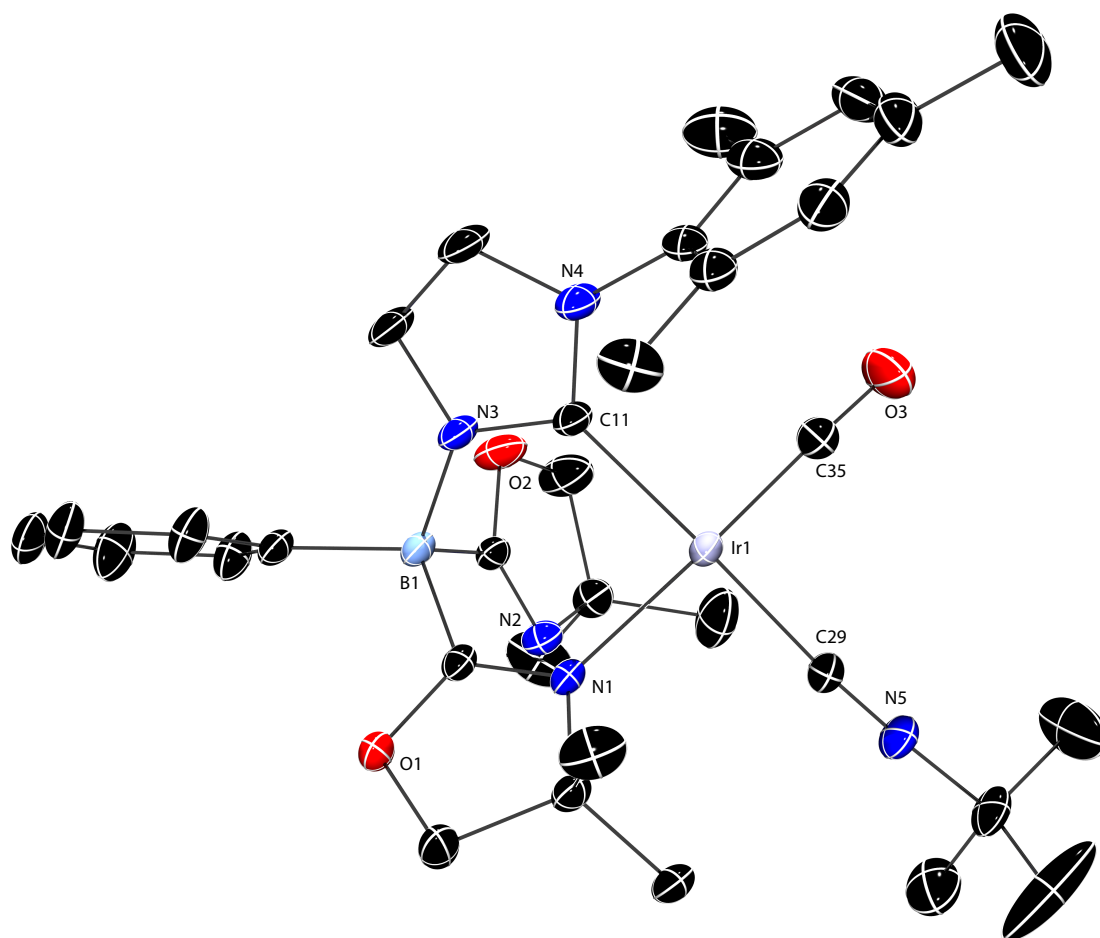
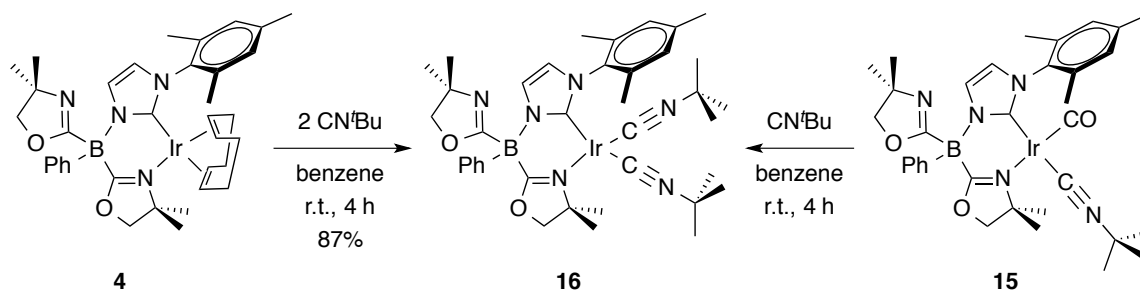


Figure 12. Rendered thermal ellipsoid plot of $\{\text{PhB}(\text{Ox}^{\text{Me}_2})_2\text{Im}^{\text{Mes}}\}\text{Ir}(\text{CO})\text{CN}^t\text{Bu}$ (**15**) with ellipsoids at 35% probability. A disordered benzene solvent molecule and H atoms are not plotted for clarity. Selected interatomic distances (Å): Ir1-C11, 2.052(2); Ir1-N1, 2.099(2); Ir1-C29, 1.955(2); Ir1-C35, 1.817(2). Selected interatomic angles (°): C11-Ir1-N1, 85.22(7); N1-Ir1-C29, 94.12(7); C29-Ir1-C35, 87.05(9); C35-Ir1-C11, 93.41(9).

The reaction of excess *tert*-butyl isocyanide and **7** results in the replacement of both carbonyl groups to give $\{\text{PhB}(\text{Ox}^{\text{Me}_2})_2\text{Im}^{\text{Mes}}\}\text{Ir}(\text{CN}^t\text{Bu})_2$ (**16**). Because **7** is prepared from **4**, it is more convenient to add 2 equiv. of CN^tBu to **4** to more directly obtain **16** (Scheme 4).

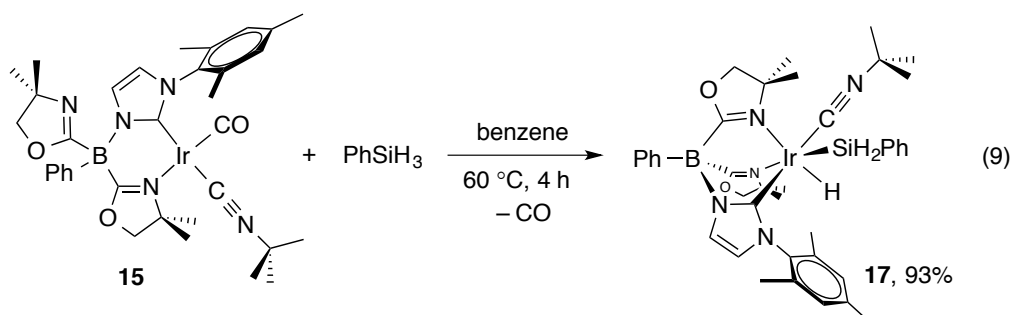


Scheme 4. Synthesis of $\{\text{PhB}(\text{Ox}^{\text{Me}_2})_2\text{Im}^{\text{Mes}}\}\text{Ir}(\text{CN}^t\text{Bu})_2$ (**16**).

As in the dicarbonyl compounds, compound **16** is fluxional, and apparently rapid processes exchange oxazoline groups and isocyanide groups. Two oxazoline methyl singlets at 1.38 and 1.35 ppm (6 H each) were observed in the ^1H NMR spectrum that correlated to the oxazoline nitrogen signal at -154 ppm in a $^1\text{H}-^{15}\text{N}$ HMBC experiment. The *tert*-butyl isocyanide ligands exhibited one broad peak at 0.96 ppm (18 H), compared to a sharp singlet at 0.73 ppm in the ^1H NMR spectrum of **15**. The chemical shift of the *tert*-butyl group in **16** and free *tert*-butyl isocyanide were identical, and that signal increased in intensity upon addition of excess *tert*-butyl isocyanide, indicating that free and coordinated isocyanide undergo rapid exchange. The ^1H NMR spectrum of isolated **16** also contained a broad signal, and the two inequivalent isocyanides are not distinguished. However, both exchange processes are slower than the vibrational time

scale because symmetric and asymmetric $\nu_{\text{C-N}}$ bands were observed in the solid state (2124 and 2029 cm^{-1}) and in solution (2120 and 2028 cm^{-1}). In addition, coordinated and noncoordinated oxazoline bands are observed in the solid state (1616 and 1581 cm^{-1}) and in solution at 1617 and 1587 cm^{-1} . The solution-phase IR spectrum of **16** with 2 equiv. of *tert*-butyl isocyanide revealed the $\nu_{\text{C-N}}$ signals from **16** and an additional band from noncoordinated isocyanide at 2134 cm^{-1} . In addition, the two oxazoline ν_{CN} absorptions of the mixture of CN^tBu and **16** appeared at 1610 and 1564 cm^{-1} . These bands are lower in energy than the oxazoline ν_{CN} peaks in **16** alone, and perhaps this results from a transient associative interaction of CN^tBu and **16** in the mixture.

Thermal oxidative addition of phenylsilane: Synthesis and characterization of $\{\text{PhB}(\text{Ox}^{\text{Me}_2})_2\text{Im}^{\text{Mes}}\}\text{IrH}(\text{SiH}_2\text{Ph})\text{CN}^t\text{Bu}$ (17**).** In contrast to the mixture obtained in reactions of iridium dicarbonyl **7** and silanes, compound **15** reacts with phenylsilane at elevated temperature to give an isolable iridium silyl complex $\{\text{PhB}(\text{Ox}^{\text{Me}_2})_2\text{Im}^{\text{Mes}}\}\text{IrH}(\text{SiH}_2\text{Ph})\text{CN}^t\text{Bu}$ (**17**; eq. 9). Remarkably, the carbonyl is replaced by the silyl and hydride ligands, rather than the isocyanide ligand, and the final crystallographically determined structure reveals that the isocyanide is *trans* to the carbene moiety.



As in the rhodium(III) carbonyl analogue, the hydride resonance at -18.76 ppm correlated with a nitrogen signal at -189 ppm in a $^1\text{H}-^{15}\text{N}$ HMBC experiment to establish their *trans* disposition. In the ^1H NMR spectrum, the diastereotopic SiH's appeared as doublet resonances at 4.10 and 4.61 ppm ($^1J_{\text{SiH}} = 169$ and 155 Hz; $^2J_{\text{HH}} = 3.6$ Hz). This observation is consistent with the formation of a stereogenic iridium center in a C_1 -symmetric product. Moreover, the *tert*-butyl resonance at 0.92 ppm revealed that the isocyanide is not replaced in the reaction.

X-ray quality crystals of **17** are obtained from a concentrated benzene solution at room temperature, and the results are depicted in Figure 13. The *trans* hydride-oxazoline configurational assignment suggested by $^1\text{H}-^{15}\text{N}$ correlation is confirmed by the diffraction experiment. Furthermore, the isocyanide and NHC donor are mutually *trans*.

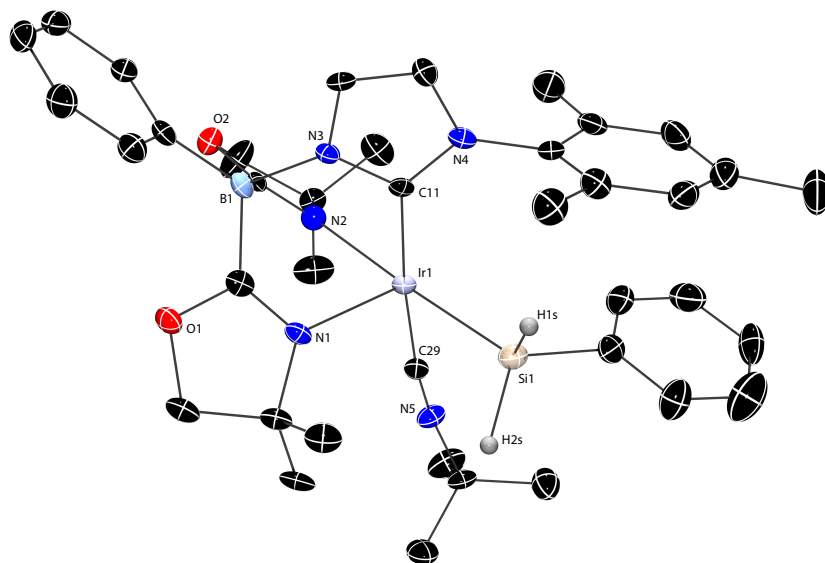


Figure 13. Rendered thermal ellipsoid plot of $\{\text{PhB}(\text{Ox}^{\text{Me}2})_2\text{Im}^{\text{Mes}}\}\text{IrH}(\text{SiH}_2\text{Ph})\text{CN}^t\text{Bu}$ (**17**) with ellipsoids at 35% probability. H1s and H2s on Si1 are located objectively in the

Fourier difference map, refined isotropically, and included in the plot. All other H atoms are placed in calculated positions, and the location of the H atom on Ir1 is not determined. Selected interatomic distances (Å): Ir1-N1, 2.191(5); Ir1-N2, 2.198(5); Ir1-C11, 2.060(8); Ir1-C29, 1.943(8); Ir1-Si1, 2.336(2). Selected interatomic angles (°): C11-Ir1-N1, 86.5(2); C11-Ir1-N2, 84.4(2); N1-Ir1-N2, 83.0(2); N1-Ir1-C29, 97.9(3); N2-Ir1-C29, 98.4(3); N1-Ir1-Si1, 101.8(1); C11-Ir1-Si1, 97.5(2).

Conclusions

This work has demonstrated that the substitution of an oxazoline donor in the tris(oxazolinyl)phenylborate ligand $\text{PhB}(\text{Ox}^{\text{Me}_2})_3$ for an *N*-heterocyclic carbene donor in $\text{PhB}(\text{Ox}^{\text{Me}_2})_2\text{Im}^{\text{Mes}}$ has a significant effect on the reactivity of iridium and rhodium compounds. This effect has been evaluated through the comparison of the reactivity of a series of compounds supported by the related tris(oxazolinyl)borate ligand, as well as tris(pyrazolyl)borate and cyclopentadienyl-coordinated group 9 metal complexes. The enhanced reactivity imparted by the $\text{PhB}(\text{Ox}^{\text{Me}_2})_2\text{Im}^{\text{Mes}}$ ligand is demonstrated by the thermal displacement of CO during the oxidative addition of Si–H bonds to rhodium(I) and iridium(I) centers. For comparison, oxidative additions of C–H and Si–H bonds to $\text{To}^{\text{M}}\text{Rh}(\text{CO})_2$, $\text{TpRh}(\text{CO})_2$, and $\text{CpM}(\text{CO})_2$ require photochemically mediated CO dissociation. However, C–H bond activation by $\{\text{PhB}(\text{Ox}^{\text{Me}_2})_2\text{Im}^{\text{Mes}}\}\text{M}(\text{CO})_2$ requires photochemical activation, as well as higher energy and more intense light than the corresponding photochemical reactions of $\text{Tp}^*\text{Rh}(\text{CO})_2$. Currently, we are exploring the potential application of these compounds in catalytic thermal decarbonylation reactions given the enhanced reactivity toward CO dissociation. Thermal C–H oxidative additions

that involve displacement of CO might facilitate transformations involving carbonylation of hydrocarbons or decarbonylations of oxygenates.

Presumably, the mechanisms of thermal oxidative addition of Si–H bonds and photochemical C–H bonds are different, and this is suggested by the inequivalent configurations of the products. In particular, photo-induced benzene metalation provides an [Ir](H)Ph species with Ph and NHC disposed *trans*, whereas thermal oxidative addition of Si–H gives [M](H)SiH₂Ph with both hydride and silyl ligands *trans* to weaker oxazoline donors. The reactivity of PhB(Ox^{Me2})₂Im^{Mes}-supported compounds may be attributed to the electron-donating ability of the carbene donor, which manifests itself in low energy ν_{CO} stretching frequencies, systematic changes in ¹H and ¹³C NMR chemical shifts and ¹J_{RhH} coupling constants, the *trans* influence evident in monovalent species, and the observed stereoselective substitution chemistry. The first point, regarding the electron-donating ability of the carbene-containing ligand, is that the CO stretching frequencies of the dicarbonyl compounds **5** and **7** appeared at similar energy β -diketiminato dicarbonyl compounds and at lower energy than those of κ^2 -To^MRh(CO)₂ and κ^2 -To^MIr(CO)₂. Within the mixed oxazoline–carbene borate ligand, the carbene donor exhibits a stronger *trans* influence than the oxazoline. Interestingly, substitution reactions of **7** also show that the carbene donor has a greater *trans* effect on the substitution of CO donors than the oxazoline donor, as evidenced by reactions of **7** and isocyanide as well as the photochemical reaction of **7** and benzene. Detailed mechanistic investigations of thermal oxidative addition reactions of PhSiH₃ and **5** or **15**, as well as application of these compounds in catalytic Si–H addition chemistry, are currently underway.

In addition, the synthetic aspects of this work demonstrate the breadth and initial limitations of heavier group 9 centers supported by $\text{PhB}(\text{Ox}^{\text{Me}_2})_2\text{Im}^{\text{R}}$ monoanionic ligands. The mesityl-imidazole substitution provides a range of compounds that are promising for future transformations, mechanistic investigations, and catalysis, whereas the chemistry of the *tert*-butyl-imidazole derivative is currently limited. This limitation of $\text{PhB}(\text{Ox}^{\text{Me}_2})_2\text{Im}^{\text{tBu}}$ in rhodium and iridium chemistry is unexpected, given the successful application of bulkier $\text{PhB}(\text{Im}^{\text{tBu}})_3$ as a supporting ligand for smaller first-row metal centers such as iron.^{20a} Alternative synthetic approaches for $\text{PhB}(\text{Ox}^{\text{Me}_2})_2\text{Im}^{\text{tBu}}\text{H}$ metalation reactions and other substitutions of oxazoline are currently under investigation based on the initial reaction chemistry reported here.

Acknowledgements

This research was supported by the U.S. Department of Energy, Office of Basic Energy Sciences, Division of Chemical Sciences, Geosciences, and Biosciences through the Ames Laboratory (Contract No. DE-AC02-07CH11358).

Experimental

General procedures. All reactions were performed under a dry argon atmosphere using standard Schlenk techniques or under a nitrogen atmosphere in a glovebox, unless otherwise indicated. Benzene, toluene, methylene chloride, pentane, and tetrahydrofuran were dried and deoxygenated using an IT PureSolv system. Benzene-*d*₆, toluene-*d*₈, and tetrahydrofuran-*d*₈ were heated to reflux over Na/K alloy and vacuum transferred. Acetonitrile-*d*₃ and methylene chloride-*d*₂ were heated to reflux over CaH₂ and vacuum

transferred. $[\text{PhB}(\text{Ox}^{\text{Me}_2})_2]_n$,²⁴ 1-*tert*-butylimidazole,⁵⁸ 1-mesitylimidazole,⁵⁹ $[\text{PhB}(\text{Ox}^{\text{Me}_2})_2(\text{Im}^{\text{Mes}}\text{H})\text{LiCl}]_2$ ($(\text{H}[2]\cdot\text{LiCl})_2$),¹⁸ $\text{Ti}[\text{To}^{\text{M}}]$,⁹ $[\text{Rh}(\mu\text{-Cl})(\eta^4\text{-C}_8\text{H}_{12})]_2$,⁶⁰ $[\text{Rh}(\mu\text{-Cl})(\eta^2\text{-C}_8\text{H}_{14})]_2$,⁶¹ $[\text{Rh}(\mu\text{-Cl})(\text{CO})_2]_2$,⁶² $[\text{Ir}(\mu\text{-Cl})(\eta^4\text{-C}_8\text{H}_{12})]_2$, and $[\text{Ir}(\mu\text{-Cl})(\eta^2\text{-C}_8\text{H}_{14})]_2$ ⁶³ were synthesized according to literature procedures. *tert*-Butyl isocyanide and phosphorus pentoxide were purchased from Sigma-Aldrich and stored inside a glovebox. Anhydrous sodium sulfate was purchased from Fisher Scientific and predried at 180 °C before use. Potassium benzyl was synthesized by reacting potassium *tert*-butoxide with *n*BuLi in toluene. Phenylsilane was synthesized by reduction of trichlorophenylsilane with LiAlH_4 .

^1H , $^{13}\text{C}\{^1\text{H}\}$, ^{11}B , ^{15}N and ^{29}Si NMR spectra were collected on Avance II 600 or 700 MHz NMR spectrometers. NMR signals (^1H , ^{13}C , and ^{15}N) were assigned based on COSY, HMQC and HMBC experiments. ^{15}N chemical shifts were determined by ^1H - ^{15}N HMBC experiments. ^{15}N chemical shifts were originally referenced to an external liquid NH_3 standard and recalculated to the CH_3NO_2 chemical shift scale by adding -381.9 ppm. ^{29}Si chemical shifts were determined by ^1H - ^{29}Si HMQC experiments and calibrated to an external standard of PhSiH_3 in a capillary (at -59 ppm). Infrared spectra were recorded on a Bruker Vertex spectrometer. Elemental analyses were performed using a PerkinElmer 2400 Series II CHN/S in the Iowa State Chemical Instrumentation Facility. Photolyses were performed in sealed storage vessels placed in a Rayonet photochemical reactor (model RPR-100) at an operating temperature of 35 °C at 254 nm and intensity of 1.65×10^{16} photon $\cdot\text{s}^{-1}\text{cm}^{-3}$.

$\text{PhB}(\text{Ox}^{\text{Me}_2})_2(\text{Im}^{\text{tBu}}\text{H})\text{LiCl}(\text{THF})$ ($\text{H}[1]\cdot\text{LiCl}\cdot\text{THF}$). A 100 mL Schlenk flask was charged with $[\text{PhB}(\text{Ox}^{\text{Me}_2})_2]_n$ (2.50 g, 8.80 mmol) and tetrahydrofuran (20 mL). 1-

tert-Butylimidazole (1.09 g, 8.78 mmol) was added, and the solution was stirred at room temperature for 18 h. The clear yellow solution became cloudy after ca. 3 h. The resulting yellow suspension was filtered, and the solid was washed with pentane (2 × 20 mL) and dried *in vacuo* to afford the product as a yellowish solid (1.61 g, 3.96 mmol, 45.1%). ¹H NMR (acetonitrile-*d*₃, 600 MHz): δ 8.09 (s, 1 H, 2H-N₂C₃H₃CMe₃), 7.49 (s, 1 H, 4,5H-N₂C₃H₃CMe₃), 7.25-7.13 (m, 6 H, C₆H₅ (5 H) and 4,5H-N₂C₃H₃CMe₃ (1 H)), 3.71 (m, 4 H, CNCMe₂CH₂O), 3.63 (m, 4 H, THF), 1.79 (m, 4 H, THF), 1.58 (s, 9 H, CMe₃), 1.36 (s, 6 H, CNCMe₂CH₂O), 1.26 (s, 6 H, CNCMe₂CH₂O). ¹³C{¹H} NMR (acetonitrile-*d*₃, 150 MHz): δ 180 (br, CNCMe₂CH₂O), 148 (br, *ipso*-C₆H₅), 136.18 (2C-N₂C₃H₃CMe₃), 133.31 (*o*-C₆H₅), 128.28 (*m*-C₆H₅), 127.10 (*p*-C₆H₅), 126.67 (4,5C-N₂C₃H₃CMe₃), 119.39 (4,5C-N₂C₃H₃CMe₃), 78.05 (CNCMe₂CH₂O), 68.26 (THF), 68.18 (CNCMe₂CH₂O), 59.22 (CMe₃), 29.96 (CMe₃), 28.70 (CNCMe₂CH₂O), 28.58 (CNCMe₂CH₂O), 26.19 (THF). ¹¹B NMR (acetonitrile-*d*₃, 192 MHz): δ -9.4. ¹⁵N{¹H} NMR (acetonitrile-*d*₃, 61 MHz): δ -138 (CNCMe₂CH₂O), -178 (1N-N₂C₃H₃CMe₃), -184 (3N-N₂C₃H₃CMe₃). IR (KBr, cm⁻¹): 3089 w, 2964 m, 2928 m, 2883 m, 1624 s (CN), 1251 m, 1191 m, 1126 s, 991 m, 751 m. Anal. Calcd for C₂₇H₄₁BClLiN₄O₃: C, 62.14; H, 7.73; N, 10.74. Found: C, 62.11; H, 7.79; N, 10.72. Mp, 218-221 °C.

PhB(Ox^{Me2})₂(Im^{tBu}H) (H[1]). A 100 mL round-bottom flask was charged with PhB(Ox^{Me2})₂(Im^{tBu}H)LiCl(THF) (H[1]·LiCl·THF, 0.842 g, 1.61 mmol) and bench grade benzene (50 mL) in air. Water (160 μL, 8.88 mmol) was added, and the white suspension was stirred at room temperature in air for 18 h. The mixture became noticeably more transparent after ca. 3 h. The white suspension was stirred with Na₂SO₄ and then filtered, and the benzene solvent was evaporated to give a white solid. The white solid was

redissolved in dry benzene (15 mL) in the glovebox and dried over P₂O₅ for 18 h. The mixture was filtered, and the solvent was evaporated. Trituration with pentane and drying *in vacuo* afforded the product as a white solid (0.591 g, 1.45 mmol, 89.9%). Spectral data are given in benzene-*d*₆, as well as in tetrahydrofuran-*d*₈ for comparison with the deprotonated product K[1]. ¹H NMR (benzene-*d*₆, 600 MHz): δ 9.55 (s, 1 H, 2H-N₂C₃H₃CMe₃), 8.02 (d, ³J_{HH} = 7.2 Hz, 2 H, *o*-C₆H₅), 7.58 (s, 1 H, 4,5H-N₂C₃H₃CMe₃), 7.40 (t, ³J_{HH} = 7.2 Hz, 2 H, *m*-C₆H₅), 7.22 (t, ³J_{HH} = 6.6 Hz, 1 H, *p*-C₆H₅), 6.11 (s, 1 H, 4,5H-N₂C₃H₃CMe₃), 3.73 (d, ²J_{HH} = 7.8 Hz, 2 H, CNCMe₂CH₂O), 3.68 (d, ²J_{HH} = 7.8 Hz, 2 H, CNCMe₂CH₂O), 1.29 (s, 6 H, CNCMe₂CH₂O), 1.28 (s, 6 H, CNCMe₂CH₂O), 0.68 (s, 9 H, CMe₃). ¹H NMR (tetrahydrofuran-*d*₈, 600 MHz): δ 9.46 (s, 1 H, 2H-N₂C₃H₃CMe₃), 7.38 (d, ³J_{HH} = 7.2 Hz, 2 H, *o*-C₆H₅), 7.34 (s, 1 H, 4,5H-N₂C₃H₃CMe₃), 7.29 (s, 1 H, 4,5H-N₂C₃H₃CMe₃), 7.02 (t, ³J_{HH} = 7.2 Hz, 2 H, *m*-C₆H₅), 6.96 (t, ³J_{HH} = 7.2 Hz, 1 H, *p*-C₆H₅), 3.6 (br, 4 H, CNCMe₂CH₂O, overlapping with tetrahydrofuran-*d*₈), 1.60 (s, 9 H, CMe₃), 1.16 (s, 6 H, CNCMe₂CH₂O), 1.15 (s, 6 H, CNCMe₂CH₂O). ¹³C{¹H} NMR (benzene-*d*₆, 150 MHz): δ 179 (br, CNCMe₂CH₂O), 150 (br, *ipso*-C₆H₅), 136.91 (2C-N₂C₃H₃CMe₃), 134.33 (*o*-C₆H₅), 127.90 (*m*-C₆H₅), 127.76 (4,5C-N₂C₃H₃CMe₃), 126.48 (*p*-C₆H₅), 116.10 (4,5C-N₂C₃H₃CMe₃), 77.66 (CNCMe₂CH₂O), 68.00 (CNCMe₂CH₂O), 56.67 (CMe₃), 29.59 (CNCMe₂CH₂O), 29.45 (CMe₃), 29.44 (CNCMe₂CH₂O). ¹³C{¹H} NMR (tetrahydrofuran-*d*₈, 150 MHz): δ 178 (br, CNCMe₂CH₂O), 149 (br, *ipso*-C₆H₅), 137.44 (2C-N₂C₃H₃CMe₃), 134.02 (*o*-C₆H₅), 127.33 (4,5C-N₂C₃H₃CMe₃), 127.06 (*m*-C₆H₅), 125.59 (*p*-C₆H₅), 116.94 (4,5C-N₂C₃H₃CMe₃), 77.46 (CNCMe₂CH₂O), 67.94 (CNCMe₂CH₂O), 57.91 (CMe₃), 29.94 (CMe₃), 29.13 (CNCMe₂CH₂O), 29.07 (CNCMe₂CH₂O). ¹¹B NMR (benzene-*d*₆, 192

MHz): δ -8.8. ^{11}B NMR (tetrahydrofuran- d_8 , 192 MHz): δ -9.4. $^{15}\text{N}\{^1\text{H}\}$ NMR (benzene- d_6 , 61 MHz): δ -125 (CNCMe₂CH₂O), -177 (3N-N₂C₃H₃CMe₃), -186 (1N-N₂C₃H₃CMe₃). $^{15}\text{N}\{^1\text{H}\}$ NMR (tetrahydrofuran- d_8 , 61 MHz): δ -125 (CNCMe₂CH₂O), -183 (N₂C₃H₃CMe₃). IR (KBr, cm⁻¹): 3138 w, 3049 w, 2964 s, 2881 w, 1605 s (CN), 1423 w, 1359 w, 1259 m, 1189 m, 1114 s, 1017 m, 969 m, 801 w, 731 w, 697 w, 658 w. Anal. Calcd for C₂₃H₃₃BN₄O₂: C, 67.65; H, 8.15; N, 13.72. Found: C, 67.96; H, 8.11; N, 13.68. Mp, 120-123 °C.

K[PhB(Ox^{Me2})₂Im^{tBu}] (K[1]). This material was most conveniently generated *in situ*. Compound H[1] (0.0223 g, 0.0546 mmol) and potassium benzyl (0.072 g, 0.055 mmol) were allowed to react in tetrahydrofuran- d_8 (0.50 mL). Instantaneously, a clear brown solution formed, which turned red and cloudy in 5 min. ^1H NMR (tetrahydrofuran- d_8 , 600 MHz): δ 7.9 (br, 1 H, 5H-N₂C₃H₂CMe₃), 7.43-6.86 (m, C₆H₅, 4H-N₂C₃H₂CMe₃, and toluene), 3.5 (br, 4 H, CNCMe₂CH₂O), 2.31 (s, 9 H, CMe₃), 1.51 (s, 6 H, CNCMe₂CH₂O), 1.1 (br, 6 H, CNCMe₂CH₂O). $^{13}\text{C}\{^1\text{H}\}$ NMR (tetrahydrofuran- d_8 , 150 MHz): δ 135.18 (2C-N₂C₃H₂CMe₃), 129.01 (4,5C-N₂C₃H₂CMe₃), 126.39 (4,5C-N₂C₃H₂CMe₃), 76.97 (CNCMe₂CH₂O), 30.73 (CMe₃), 28.89 (CNCMe₂CH₂O), 28.79 (CNCMe₂CH₂O). ^{11}B NMR (tetrahydrofuran- d_8 , 192 MHz): δ -11.6.

PhB(Ox^{Me2})₂(Im^{Mes}H) (H[2]). The procedure for preparation of H[2] follows the one for H[1] described above, using [PhB(Ox^{Me2})₂(Im^{Mes}H)LiCl]₂ ([H[2]·LiCl]₂, 1.052 g, 2.051 mmol), 50 mL bench grade benzene, and water (203 μL , 11.3 mmol). The white solid product was obtained in good yield (0.675 g, 1.44 mmol, 70.0%). ^1H NMR (benzene- d_6 , 600 MHz): δ 9.06 (s, 1 H, 2H-N₂C₃H₃Mes), 8.04 (d, $^3J_{\text{HH}} = 7.2$ Hz, 2 H, *o*-C₆H₅), 7.74 (s, 1 H, 4,5H-N₂C₃H₃Mes), 7.42 (t, $^3J_{\text{HH}} = 7.2$ Hz, 2 H, *m*-C₆H₅), 7.25 (t, $^3J_{\text{HH}}$

= 7.2 Hz, 1 H, *p*-C₆H₅), 6.48 (s, 2 H, *m*-C₆H₂Me₃), 5.83 (s, 1 H, 4,5H-N₂C₃H₃Mes), 3.73 (d, ²J_{HH} = 7.8 Hz, 2 H, CNCMe₂CH₂O), 3.69 (d, ²J_{HH} = 7.8 Hz, 2 H, CNCMe₂CH₂O), 1.99 (s, 3 H, *p*-C₆H₂Me₃), 1.67 (s, 6 H, *o*-C₆H₂Me₃), 1.23 (s, 12 H, CNCMe₂CH₂O). ¹H NMR (tetrahydrofuran-*d*₈, 600 MHz): δ 8.84 (s, 1 H, 2H-N₂C₃H₃Mes), 7.49 (m, 3 H, *o*-C₆H₅ (2 H) and 4,5H-N₂C₃H₃Mes (1 H)), 7.09 (m, 3 H, *m*-C₆H₅ (2 H) and 4,5H-N₂C₃H₃Mes (1 H)), 7.04 (m, 3 H, *p*-C₆H₅ (1 H) and *m*-C₆H₂Me₃ (2 H)), 3.6 (br, 4 H, CNCMe₂CH₂O), 2.33 (s, 3 H, *p*-C₆H₂Me₃), 2.07 (s, 6 H, *o*-C₆H₂Me₃), 1.15 (s, 6 H, CNCMe₂CH₂O), 1.14 (s, 6 H, CNCMe₂CH₂O). ¹³C{¹H} NMR (benzene-*d*₆, 150 MHz): δ 179 (br, CNCMe₂CH₂O), 149 (br, *ipso*-C₆H₅), 140.71 (2C-N₂C₃H₃Mes), 139.97 (*p*-C₆H₂Me₃), 135.37 (*ipso*-C₆H₂Me₃), 134.50 (*o*-C₆H₅), 132.74 (*o*-C₆H₂Me₃), 129.69 (*m*-C₆H₂Me₃), 128.00 (*m*-C₆H₅), 127.79 (4,5C-N₂C₃H₃Mes), 126.65 (*p*-C₆H₅), 119.48 (4,5C-N₂C₃H₃Mes), 77.94 (CNCMe₂CH₂O), 67.84 (CNCMe₂CH₂O), 29.56 (CNCMe₂CH₂O), 29.33 (CNCMe₂CH₂O), 21.21 (*p*-C₆H₂Me₃), 17.47 (*o*-C₆H₂Me₃). ¹³C{¹H} NMR (tetrahydrofuran-*d*₈, 150 MHz): δ 179 (br, CNCMe₂CH₂O), 149 (br, *ipso*-C₆H₅), 141.45 (2C-N₂C₃H₃Mes), 140.68 (*p*-C₆H₂Me₃), 136.05 (*ipso*-C₆H₂Me₃), 134.53 (*o*-C₆H₅), 133.62 (*o*-C₆H₂Me₃), 130.00 (*m*-C₆H₂Me₃), 127.43 (4,5C-N₂C₃H₃Mes), 127.38 (*m*-C₆H₅), 126.05 (*p*-C₆H₅), 120.49 (4,5C-N₂C₃H₃Mes), 77.96 (CNCMe₂CH₂O), 67.94 (CNCMe₂CH₂O), 29.20 (CNCMe₂CH₂O), 29.08 (CNCMe₂CH₂O), 21.09 (*p*-C₆H₂Me₃), 17.58 (*o*-C₆H₂Me₃). ¹¹B NMR (benzene-*d*₆, 192 MHz): δ -8.3. ¹¹B NMR (tetrahydrofuran-*d*₈, 192 MHz): δ -11.0. ¹⁵N{¹H} NMR (benzene-*d*₆, 61 MHz): δ -125 (CNCMe₂CH₂O), -174 (3N-N₂C₃H₃Mes), -206 (1N-N₂C₃H₃Mes). ¹⁵N{¹H} NMR (tetrahydrofuran-*d*₈, 61 MHz): δ -127 (CNCMe₂CH₂O), -176 (3N-N₂C₃H₃Mes), -207 (1N-N₂C₃H₃Mes). IR (KBr, cm⁻¹): 3166 m, 3133 m, 3068 w, 2963 s, 1606 s (CN), 1532 s, 1133 s, 1066 s, 907 s, 801 m, 737

s, 707 s. Anal. Calcd for $C_{28}H_{35}BN_4O_2$: C, 71.49; H, 7.50; N, 11.91. Found: C, 71.73; H, 7.48; N, 12.08. Mp, 149-152 °C.

K[PhB(Ox^{Me2})₂Im^{Mes}] (K[2]). As with K[1], K[2] is most conveniently generated *in situ*, and the data given here are from an *in situ* reaction. An X-ray quality crystal was obtained from benzene solution at room temperature; however, spectroscopic analysis of the supernatant revealed both H[2] and K[2]. H[2] (0.0257 g, 0.0546 mmol) and potassium benzyl (0.0072 g, 0.055 mmol) were allowed to react in tetrahydrofuran-*d*₈ (0.50 mL) to give a transparent brown solution. ¹H NMR (tetrahydrofuran-*d*₈, 600 MHz): δ 8.43 (s, 1 H, N₂C₃H₂Mes), 7.52 (d, ³J_{HH} = 7.2 Hz, 2 H, *o*-C₆H₅), 7.00 (t, ³J_{HH} = 7.2 Hz, 2 H, *m*-C₆H₅), 6.91 (t, ³J_{HH} = 7.2 Hz, 1 H, *p*-C₆H₅), 6.86 (s, 2 H, *m*-C₆H₂Me₃), 6.61 (s, 1 H, N₂C₃H₂Mes), 3.47 (d, ²J_{HH} = 7.8 Hz, 2 H, CNCMe₂CH₂O), 3.44 (d, ²J_{HH} = 7.2 Hz, 2 H, CNCMe₂CH₂O), 2.26 (s, 3 H, *p*-C₆H₂Me₃), 1.99 (s, 6 H, *o*-C₆H₂Me₃), 1.09 (s, 6 H, CNCMe₂CH₂O), 1.07 (s, 6 H, CNCMe₂CH₂O). ¹³C{¹H} NMR (tetrahydrofuran-*d*₈, 150 MHz): δ 183 (br, CNCMe₂CH₂O), 156 (br, *ipso*-C₆H₅), 141.62 (*p*-C₆H₂Me₃), 136.63 (*ipso*-C₆H₂Me₃), 136.42 (*o*-C₆H₂Me₃), 135.21 (*o*-C₆H₅), 129.07 (*m*-C₆H₂Me₃), 126.81 (4,5C-N₂C₃H₂Mes), 126.53 (*m*-C₆H₅), 124.58 (*p*-C₆H₅), 116.09 (4,5C-N₂C₃H₂Mes), 77.07 (CNCMe₂CH₂O), 67.95 (CNCMe₂CH₂O), 29.01 (CNCMe₂CH₂O), 28.94 (CNCMe₂CH₂O), 21.10 (*p*-C₆H₂Me₃), 18.32 (*o*-C₆H₂Me₃). ¹¹B NMR (tetrahydrofuran-*d*₈, 192 MHz): δ -11.6. ¹⁵N{¹H} NMR (tetrahydrofuran-*d*₈, 61 MHz): δ -134 (CNCMe₂CH₂O), -170 (N₂C₃H₂Mes), -189 (N₂C₃H₂Mes).

{PhB(Ox^{Me2})₂Im^{tBu}}Rh(η⁴-C₈H₁₂) (3). The compound PhB(Ox^{Me2})₂(Im^{tBu}H) (H[1], 0.127 g, 0.312 mmol) was dissolved in tetrahydrofuran (10 mL), and potassium benzyl (0.0495 g, 0.380 mmol) was added. This combination provided a transparent, but

dark red solution, which became a pink opaque suspension upon stirring for 1 h at room temperature. Addition of $[\text{Rh}(\mu\text{-Cl})(\eta^4\text{-C}_8\text{H}_{12})]_2$ (0.0768 g, 0.156 mmol) gave a dark brown mixture that was stirred for 1 h at room temperature. The solvent was removed *in vacuo*, and the residual solid was extracted with benzene (2×5 mL). The benzene extracts were combined, filtered, and evaporated to dryness. Trituration with pentane and *in vacuo* drying afforded the product as a yellow solid (0.156 g, 0.252 mmol, 80.8%). ^1H NMR (benzene- d_6 , 600 MHz): δ 8.9 (br, 1 H, $\text{N}_2\text{C}_3\text{H}_2\text{CMe}_3$), 7.83 (d, $^3J_{\text{HH}} = 7.2$ Hz, 2 H, *o*- C_6H_5), 7.43 (t, $^3J_{\text{HH}} = 7.2$ Hz, 2 H, *m*- C_6H_5), 7.27 (t, $^3J_{\text{HH}} = 7.2$ Hz, 1 H, *p*- C_6H_5), 6.65 (s, 1 H, $\text{N}_2\text{C}_3\text{H}_2\text{CMe}_3$), 4.93 (m, 1 H, C_8H_{12}), 4.35 (m, 1 H, C_8H_{12}), 3.66 (d, $^2J_{\text{HH}} = 7.2$ Hz, 1 H, $\text{CN}(\text{Rh})\text{CMe}_2\text{CH}_2\text{O}$), 3.58 (d, $^2J_{\text{HH}} = 8.4$ Hz, 1 H, $\text{CN}(\text{Rh})\text{CMe}_2\text{CH}_2\text{O}$), 3.5 (br, 3 H, $\text{CNCMe}_2\text{CH}_2\text{O}$ (1 H) and C_8H_{12} (2 H)), 3.30 (d, $^2J_{\text{HH}} = 8.4$ Hz, 1 H, $\text{CN}(\text{Rh})\text{CMe}_2\text{CH}_2\text{O}$), 2.31 (m, 1 H, C_8H_{12}), 1.98 (m, 1 H, C_8H_{12}), 1.84 (m, 1 H, C_8H_{12}), 1.61 (s, 9 H, CMe_3), 1.45 (m, 1 H, C_8H_{12}), 1.40 (m, 1 H, C_8H_{12}), 1.33 (s, 3 H, $\text{CNCMe}_2\text{CH}_2\text{O}$), 1.23 (s, 3 H, $\text{CNCMe}_2\text{CH}_2\text{O}$), 1.12 (m, 2 H, C_8H_{12}), 0.90 (s, 3 H, $\text{CN}(\text{Rh})\text{CMe}_2\text{CH}_2\text{O}$), 0.84 (s, 3 H, $\text{CN}(\text{Rh})\text{CMe}_2\text{CH}_2\text{O}$), 0.78 (m, 1 H, C_8H_{12}). $^{13}\text{C}\{^1\text{H}\}$ NMR (benzene- d_6 , 150 MHz): δ 189 (br, $\text{CN}(\text{Rh})\text{CMe}_2\text{CH}_2\text{O}$), 181.06 (d, $^1J_{\text{RhC}} = 49.8$ Hz, 2C- $\text{N}_2\text{C}_3\text{H}_2\text{CMe}_3$), 179 (br, $\text{CNCMe}_2\text{CH}_2\text{O}$), 154 (br, *ipso*- C_6H_5), 133.74 (*o*- C_6H_5), 128.92 (4,5C- $\text{N}_2\text{C}_3\text{H}_2\text{CMe}_3$), 127.89 (*m*- C_6H_5), 125.72 (*p*- C_6H_5), 117.62 (4,5C- $\text{N}_2\text{C}_3\text{H}_2\text{CMe}_3$), 88.61 (d, $^1J_{\text{RhC}} = 7.2$ Hz, C_8H_{12}), 88.36 (d, $^1J_{\text{RhC}} = 8.1$ Hz, C_8H_{12}), 80.29 ($\text{CN}(\text{Rh})\text{CMe}_2\text{CH}_2\text{O}$), 79.68 (d, $^1J_{\text{RhC}} = 13.7$ Hz, C_8H_{12}), 77.13 ($\text{CNCMe}_2\text{CH}_2\text{O}$), 69.13 (d, $^1J_{\text{RhC}} = 12.8$ Hz, C_8H_{12}), 68.29 ($\text{CNCMe}_2\text{CH}_2\text{O}$), 68.05 ($\text{CN}(\text{Rh})\text{CMe}_2\text{CH}_2\text{O}$), 56.85 (CMe_3), 32.84 (CMe_3), 32.27 (C_8H_{12}), 31.69 (C_8H_{12}), 29.59 (C_8H_{12}), 29.38 ($\text{CNCMe}_2\text{CH}_2\text{O}$), 29.24 ($\text{CNCMe}_2\text{CH}_2\text{O}$), 28.39 ($\text{CN}(\text{Rh})\text{CMe}_2\text{CH}_2\text{O}$), 28.28

(CN(Rh)CMe₂CH₂O), 27.46 (C₈H₁₂). ¹¹B NMR (benzene-*d*₆, 192 MHz): δ -8.0. ¹⁵N{¹H} NMR (benzene-*d*₆, 61 MHz): δ -123 (CNCMe₂CH₂O), -172 (1N-N₂C₃H₂CMe₃), -181 (3N-N₂C₃H₂CMe₃), -183 (CN(Rh)Me₂CH₂O). IR (KBr, cm⁻¹): 3128 w, 2962 s, 2928 s, 2870 s, 2823 m, 1613 s (CN), 1570 s (CN), 1463 m, 1370 m, 1262 m, 1197 s, 1152 s, 1123 m, 1019 m, 998 m, 977 s, 965 s, 734 s, 703 s, 688 w. Anal. Calcd for C₃₁H₄₄BN₄O₂Rh: C, 60.21; H, 7.17; N, 9.06. Found: C, 60.00; H, 7.65; N, 9.35. Mp, 201-202 °C.

{PhB(Ox^{Me2})₂Im^{Mes}}Rh(η⁴-C₈H₁₂) (4). PhB(Ox^{Me2})₂(Im^{Mes}H) (H[2], 0.102 g, 0.217 mmol) and potassium benzyl (0.0341 g, 0.262 mmol) were allowed to react in tetrahydrofuran (10 mL) to give a transparent, yet dark red solution that was stirred at room temperature for 1 h. Addition of [Rh(μ-Cl)(η⁴-C₈H₁₂)₂] (0.0535 g, 0.109 mmol) provided a dark brown solution that was stirred at room temperature for 1 h. A solid residue was obtained by evaporation of the volatile materials. Extraction with benzene (2 × 5 mL), evaporation of the benzene, trituration with pentane, and drying gave **4** as a yellow solid (0.127 g, 0.187 mmol, 86.2%). ¹H NMR (benzene-*d*₆, 600 MHz): δ 9.59 (s, 1 H, N₂C₃H₂Mes), 7.74 (d, ³J_{HH} = 7.2 Hz, 2 H, *o*-C₆H₅), 7.42 (t, ³J_{HH} = 7.2 Hz, 2 H, *m*-C₆H₅), 7.24 (t, ³J_{HH} = 7.2 Hz, 1 H, *p*-C₆H₅), 6.84 (s, 1 H, *m*-C₆H₂Me₃), 6.62 (s, 1 H, *m*-C₆H₂Me₃), 6.32 (s, 1 H, N₂C₃H₂Mes), 4.67 (m, 1 H, C₈H₁₂), 4.48 (m, 1 H, C₈H₁₂), 3.75 (d, ²J_{HH} = 7.8 Hz, 1 H, CNCMe₂CH₂O), 3.66 (d, ²J_{HH} = 7.8 Hz, 1 H, CN(Rh)CMe₂CH₂O), 3.57 (d, ²J_{HH} = 7.8 Hz, 1 H, CNCMe₂CH₂O), 3.52 (m, 1 H, C₈H₁₂), 3.31 (d, ²J_{HH} = 8.4 Hz, 1 H, CN(Rh)CMe₂CH₂O), 3.11 (m, 1 H, C₈H₁₂), 2.39 (s, 3 H, *o*-C₆H₂Me₃), 2.12 (s, 3 H, *p*-C₆H₂Me₃), 1.93 (m, 1 H, C₈H₁₂), 1.87 (s, 3 H, *o*-C₆H₂Me₃), 1.57 (m, 1 H, C₈H₁₂), 1.52 (m, 1 H, C₈H₁₂), 1.40 (s, 3 H, CNCMe₂CH₂O), 1.38 (m, 1 H,

C_8H_{12}), 1.23 (s, 3 H, $CNCMe_2CH_2O$), 1.19 (m, 4 H, C_8H_{12}), 1.02 (s, 3 H, $CN(Rh)CMe_2CH_2O$), 0.87 (s, 3 H, $CN(Rh)CMe_2CH_2O$). $^{13}C\{^1H\}$ NMR (benzene- d_6 , 150 MHz): δ 191 (br, $CN(Rh)CMe_2CH_2O$), 179.90 (d, $^1J_{RhC} = 51.5$ Hz, $2C-N_2C_3H_2Mes$), 178 (br, $CNCMe_2CH_2O$), 155 (br, *ipso*- C_6H_5), 138.53 (*p*- $C_6H_2Me_3$), 137.93 (*o*- $C_6H_2Me_3$), 136.14 (*ipso*- $C_6H_2Me_3$), 135.33 (*o*- $C_6H_2Me_3$), 133.72 (*o*- C_6H_5), 129.46 (*m*- $C_6H_2Me_3$), 129.37 (*m*- $C_6H_2Me_3$), 127.69 ($4,5C-N_2C_3H_2Mes$), 127.61 (*m*- C_6H_5), 125.67 (*p*- C_6H_5), 120.63 ($4,5C-N_2C_3H_2Mes$), 90.72 (d, $^1J_{RhC} = 7.7$ Hz, C_8H_{12}), 87.89 (d, $^1J_{RhC} = 7.8$ Hz, C_8H_{12}), 81.24 ($CNCMe_2CH_2O$), 77.00 ($CN(Rh)CMe_2CH_2O$), 75.22 (d, $^1J_{RhC} = 12.9$ Hz, C_8H_{12}), 70.84 (d, $^1J_{RhC} = 13.1$ Hz, C_8H_{12}), 68.40 ($CNCMe_2CH_2O$), 68.26 ($CN(Rh)CMe_2CH_2O$), 31.96 (C_8H_{12}), 31.32 (C_8H_{12}), 30.15 (C_8H_{12}), 29.50 ($CNCMe_2CH_2O$), 29.27 ($CNCMe_2CH_2O$), 28.63 ($CN(Rh)CMe_2CH_2O$), 28.00 (C_8H_{12}), 27.74 ($CN(Rh)CMe_2CH_2O$), 21.31 (*p*- $C_6H_2Me_3$), 20.52 (*o*- $C_6H_2Me_3$), 18.54 (*o*- $C_6H_2Me_3$). ^{11}B NMR (benzene- d_6 , 192 MHz): δ -8.8. $^{15}N\{^1H\}$ NMR (benzene- d_6 , 61 MHz): δ -125 ($CNCMe_2CH_2O$), -176 ($N_2C_3H_2Mes$), -182 ($CN(Rh)CMe_2CH_2O$), -191 ($N_2C_3H_2Mes$). IR (KBr, cm^{-1}): 3041 w, 2960 s, 2925 s, 2873 s, 2829 w, 1613 m (CN), 1576 m (CN), 1459 m, 1394 m, 1310 m, 1191 s, 1123 w, 1011 m, 990 s, 810 m, 731 s, 700 m. Anal. Calcd for $C_{36}H_{46}BN_4O_2Rh$: C, 63.54; H, 6.81; N, 8.23. Found: C, 63.43; H, 7.12; N, 8.27. Mp, 246-248 °C.

$\{PhB(Ox^{Me_2})_2Im^{Mes}\}Rh(CO)_2$ (5). $PhB(Ox^{Me_2})_2(Im^{Mes}H)$ (H[2], 0.308 g, 0.655 mmol) and potassium benzyl (0.0939 g, 0.721 mmol) were allowed to react in tetrahydrofuran (10 mL) to form K[2] as above. $[Rh(\mu-Cl)(CO)_2]_2$ (0.127 g, 0.328 mmol) was added to provide a dark green solution. The solution was stirred at room temperature for 1 h, the solvent was removed *in vacuo*, and the residue was extracted with benzene (2

× 5 mL). The benzene extracts were combined, filtered, and evaporated to give a solid. The solid was triturated with pentane and dried *in vacuo* to afford the product as a yellowish green solid (0.366 g, 0.583 mmol, 89.0%). ¹H NMR (benzene-*d*₆, 600 MHz): δ 7.82 (m, 3 H, *o*-C₆H₅ (2 H) and N₂C₃H₂Mes (1 H)), 7.43 (t, ³J_{HH} = 7.2 Hz, 2 H, *m*-C₆H₅), 7.27 (t, ³J_{HH} = 7.2 Hz, 1 H, *p*-C₆H₅), 6.74 (s, 2 H, *m*-C₆H₂Me₃), 6.20 (s, 1 H, N₂C₃H₂Mes), 3.60 (m, 4 H, CNCMe₂CH₂O), 2.08 (s, 3 H, *p*-C₆H₂Me₃), 2.02 (s, 6 H, *o*-C₆H₂Me₃), 1.16 (s, 6 H, CNCMe₂CH₂O), 1.12 (s, 6 H, CNCMe₂CH₂O). ¹³C {¹H} NMR (benzene-*d*₆, 150 MHz): δ 188 (br, CNCMe₂CH₂O), 186 (br, 2C-N₂C₃H₂Mes), 176.20 (d, ¹J_{RhC} = 45.0 Hz, CO), 149 (br, *ipso*-C₆H₅), 139.17 (*ipso*-C₆H₂Me₃), 137.36 (*p*-C₆H₂Me₃), 136.45 (*o*-C₆H₂Me₃), 134.70 (*o*-C₆H₅), 129.69 (*m*-C₆H₂Me₃), 127.84 (*m*-C₆H₅), 127.01 (4,5C-N₂C₃H₂Mes), 126.75 (*p*-C₆H₅), 120.50 (4,5C-N₂C₃H₂Mes), 78.94 (CNCMe₂CH₂O), 67.94 (CNCMe₂CH₂O), 29.03 (CNCMe₂CH₂O), 28.80 (CNCMe₂CH₂O), 21.37 (*p*-C₆H₂Me₃), 18.91 (*o*-C₆H₂Me₃). ¹¹B NMR (benzene-*d*₆, 192 MHz): δ -8.8. ¹⁵N {¹H} NMR (benzene-*d*₆, 61 MHz): δ -153 (CNCMe₂CH₂O), -173 (3N-N₂C₃H₂Mes), -189 (1N-N₂C₃H₂Mes). IR (KBr, cm⁻¹): 3124 w, 3071 w, 3050 w, 2964 m, 2925 m, 2872 w, 2063 s (CO), 1993 s (CO), 1959 w, 1626 m (CN), 1564 m (CN), 1490 m, 1459 m, 1434 m, 1407 w, 1367 w, 1347 w, 1319 w, 1283 m, 1250 w, 1189 m, 1163 m, 1131 w, 1021 m, 988 w, 963 m, 853 w, 732 m, 701 m. Anal. Calcd for C₃₀H₃₄BN₄O₄Rh: C, 57.35; H, 5.45; N, 8.92. Found: C, 57.36; H, 5.55; N, 9.38. Mp, 132-135 °C.

{PhB(Ox^{Me2})₂Im^{Mes}}Ir(η⁴-C₈H₁₂) (6). PhB(Ox^{Me2})₂(Im^{Mes}H) (H[2], 0.307 g, 0.653 mmol) and potassium benzyl (0.102 g, 0.783 mmol) were stirred in tetrahydrofuran (10 mL) at room temperature for 1 h. [Ir(μ-Cl)(η⁴-C₈H₁₂)]₂ (0.219 g, 0.326 mmol) was

added to give a transparent red solution that was stirred at room temperature for 1 h. The product was isolated following the procedure described for compound **4**, giving a red solid (0.442 g, 0.574 mmol, 87.9%). ^1H NMR (benzene- d_6 , 600 MHz): δ 9.44 (s, 1 H, $\text{N}_2\text{C}_3\text{H}_2\text{Mes}$), 7.61 (d, $^3J_{\text{HH}} = 7.2$ Hz, 2 H, $o\text{-C}_6\text{H}_5$), 7.37 (t, $^3J_{\text{HH}} = 7.2$ Hz, 2 H, $m\text{-C}_6\text{H}_5$), 7.20 (t, $^3J_{\text{HH}} = 7.2$ Hz, 1 H, $p\text{-C}_6\text{H}_5$), 6.80 (s, 1 H, $m\text{-C}_6\text{H}_2\text{Me}_3$), 6.63 (s, 1 H, $m\text{-C}_6\text{H}_2\text{Me}_3$), 6.35 (s, 1 H, $\text{N}_2\text{C}_3\text{H}_2\text{Mes}$), 4.35 (m, 1 H, C_8H_{12}), 4.08 (m, 1 H, C_8H_{12}), 3.73 (d, $^2J_{\text{HH}} = 7.8$ Hz, 1 H, $\text{CNCMe}_2\text{CH}_2\text{O}$), 3.66 (d, $^2J_{\text{HH}} = 8.4$ Hz, 1 H, $\text{CN}(\text{Ir})\text{CMe}_2\text{CH}_2\text{O}$), 3.56 (d, $^2J_{\text{HH}} = 7.8$ Hz, 1 H, $\text{CNCMe}_2\text{CH}_2\text{O}$), 3.33 (d, $^2J_{\text{HH}} = 8.4$ Hz, 1 H, $\text{CN}(\text{Ir})\text{CMe}_2\text{CH}_2\text{O}$), 3.20 (m, 1 H, C_8H_{12}), 2.90 (m, 1 H, C_8H_{12}), 2.27 (s, 3 H, $o\text{-C}_6\text{H}_2\text{Me}_3$), 2.11 (s, 3 H, $p\text{-C}_6\text{H}_2\text{Me}_3$), 1.92 (s, 3 H, $o\text{-C}_6\text{H}_2\text{Me}_3$), 1.81 (m, 1 H, C_8H_{12}), 1.54 (m, 1 H, C_8H_{12}), 1.38 (s, 3 H, $\text{CNCMe}_2\text{CH}_2\text{O}$), 1.32 (m, 1 H, C_8H_{12}), 1.21 (s, 6 H, $\text{CNCMe}_2\text{CH}_2\text{O}$ (3 H) and C_8H_{12} (3 H)), 1.03 (s, 4 H, $\text{CN}(\text{Ir})\text{CMe}_2\text{CH}_2\text{O}$ (3 H) and C_8H_{12} (1 H)), 0.92 (s, 4 H, $\text{CN}(\text{Ir})\text{CMe}_2\text{CH}_2\text{O}$ (3 H) and C_8H_{12} (1 H)). $^{13}\text{C}\{^1\text{H}\}$ NMR (benzene- d_6 , 150 MHz): δ 193 (br, $\text{CN}(\text{Ir})\text{CMe}_2\text{CH}_2\text{O}$), 178.33 (2C- $\text{N}_2\text{C}_3\text{H}_2\text{Mes}$), 177 (br, $\text{CNCMe}_2\text{CH}_2\text{O}$), 154 (br, $ipso\text{-C}_6\text{H}_5$), 138.31 ($ipso\text{-C}_6\text{H}_2\text{Me}_3$), 138.10 ($p\text{-C}_6\text{H}_2\text{Me}_3$), 136.09 ($o\text{-C}_6\text{H}_2\text{Me}_3$), 135.40 ($o\text{-C}_6\text{H}_2\text{Me}_3$), 133.18 ($o\text{-C}_6\text{H}_5$), 129.41 ($m\text{-C}_6\text{H}_2\text{Me}_3$), 129.35 ($m\text{-C}_6\text{H}_2\text{Me}_3$), 127.62 ($m\text{-C}_6\text{H}_5$), 127.05 (4,5C- $\text{N}_2\text{C}_3\text{H}_2\text{Mes}$), 125.61 ($p\text{-C}_6\text{H}_5$), 121.05 (4,5C- $\text{N}_2\text{C}_3\text{H}_2\text{Mes}$), 82.32 ($\text{CN}(\text{Ir})\text{CMe}_2\text{CH}_2\text{O}$), 77.05 ($\text{CNCMe}_2\text{CH}_2\text{O}$), 75.66 (C_8H_{12}), 72.66 (C_8H_{12}), 69.29 ($\text{CN}(\text{Ir})\text{CMe}_2\text{CH}_2\text{O}$), 68.36 ($\text{CNCMe}_2\text{CH}_2\text{O}$), 59.95 (C_8H_{12}), 56.37 (C_8H_{12}), 33.16 (C_8H_{12}), 31.52 (C_8H_{12}), 30.48 (C_8H_{12}), 29.48 ($\text{CNCMe}_2\text{CH}_2\text{O}$), 29.24 ($\text{CNCMe}_2\text{CH}_2\text{O}$), 29.19 (C_8H_{12}), 28.73 ($\text{CN}(\text{Ir})\text{CMe}_2\text{CH}_2\text{O}$), 27.46 ($\text{CN}(\text{Ir})\text{CMe}_2\text{CH}_2\text{O}$), 21.32 ($p\text{-C}_6\text{H}_2\text{Me}_3$), 20.44 ($o\text{-C}_6\text{H}_2\text{Me}_3$), 18.56 ($o\text{-C}_6\text{H}_2\text{Me}_3$). ^{11}B NMR (benzene- d_6 , 192 MHz): δ -9.0. $^{15}\text{N}\{^1\text{H}\}$ (benzene- d_6 , 61 MHz): δ -124

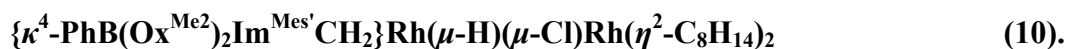
(CNCMe₂CH₂O), -178 (N₂C₃H₂Mes), -188 (CN(Ir)CMe₂CH₂O), -192 (N₂C₃H₂Mes). IR (KBr, cm⁻¹): 2960 s, 2923 s, 2872 m, 1611 m (CN), 1564 m (CN), 1461 m, 1384 m, 1363 m, 1194 m, 1134 m, 994 m, 965 m, 732 m, 701 m, 677 m. Anal. Calcd for C₃₆H₄₆BIrN₄O₂: C, 56.17; H, 6.02; N, 7.28. Found: C, 56.03; H, 6.36; N, 7.33. Mp, 242-245 °C.

{PhB(Ox^{Me2})₂Im^{Mes}}Ir(CO)₂ (7). {PhB(Ox^{Me2})₂Im^{Mes}}Ir(η⁴-C₈H₁₂) (6, 0.407 g, 0.529 mmol) was dissolved in benzene (10 mL), the clear red solution was degassed three times, and the vessel was charged with 1 atm CO. The solution turned yellow after 5 minutes. The flask was sealed, and the solution was stirred at room temperature for 3 h. The volatile materials were evaporated under reduced pressure, and the residue was triturated with pentane and dried *in vacuo* to afford the product as a yellow solid (0.273 g, 0.380 mmol, 71.8%). ¹H NMR (benzene-*d*₆, 600 MHz): δ 7.81 (d, ³J_{HH} = 7.8 Hz, 2 H, *o*-C₆H₅), 7.52 (s, 1 H, N₂C₃H₂Mes), 7.43 (t, ³J_{HH} = 7.2 Hz, 2 H, *m*-C₆H₅), 7.27 (t, ³J_{HH} = 7.2 Hz, 1 H, *p*-C₆H₅), 6.74 (s, 2 H, *m*-C₆H₂Me₃), 6.16 (s, 1 H, N₂C₃H₂Mes), 3.61 (d, ²J_{HH} = 8.4 Hz, 2 H, CNCMe₂CH₂O), 3.58 (d, ²J_{HH} = 8.4 Hz, 2 H, CNCMe₂CH₂O), 2.08 (s, 3 H, *p*-C₆H₂Me₃), 2.02 (s, 6 H, *o*-C₆H₂Me₃), 1.18 (s, 6 H, CNCMe₂CH₂O), 1.13 (s, 6 H, CNCMe₂CH₂O). ¹³C {¹H} NMR (benzene-*d*₆, 150 MHz): δ 187 (br, CNCMe₂CH₂O), 179 (br, CO), 176.07 (2C-N₂C₃H₂Mes), 149 (br, *ipso*-C₆H₅), 139.43 (*p*-C₆H₂Me₃), 136.97 (*ipso*-C₆H₂Me₃), 136.53 (*o*-C₆H₂Me₃), 134.77 (*o*-C₆H₅), 129.75 (*m*-C₆H₂Me₃), 127.96 (*m*-C₆H₅), 126.96 (*p*-C₆H₅), 126.69 (4,5C-N₂C₃H₂Mes), 120.99 (4,5C-N₂C₃H₂Mes), 79.19 (CNCMe₂CH₂O), 68.75 (CNCMe₂CH₂O), 28.94 (CNCMe₂CH₂O), 28.58 (CNCMe₂CH₂O), 21.38 (*p*-C₆H₂Me₃), 18.95 (*o*-C₆H₂Me₃). ¹¹B NMR (benzene-*d*₆, 192 MHz): δ -8.7. ¹⁵N {¹H} NMR (benzene-*d*₆, 61 MHz): δ -156 (CNCMe₂CH₂O), -173 (3N-

$\text{N}_2\text{C}_3\text{H}_2\text{Mes}$), -187 ($1\text{N-N}_2\text{C}_3\text{H}_2\text{Mes}$). IR (KBr, cm^{-1}): 2964 w, 2872 w, 2053 s (CO), 1979 s (CO), 1612 w, 1551 w (CN), 1461 w, 1361 w, 1292 w, 1188 w, 967 m, 732 m, 703 m. Anal. Calcd for $\text{C}_{30}\text{H}_{34}\text{BIrN}_4\text{O}_4$: C, 50.21; H, 4.78; N, 7.81. Found: C, 50.84; H, 4.97; N, 8.47. Mp, 143-146 °C.

To^MRh(η^4 -C₈H₁₂) (8). $\text{Ti}[\text{To}^{\text{M}}]$ (0.440 g, 0.749 mmol) and $[\text{Rh}(\mu\text{-Cl})(\eta^4\text{-C}_8\text{H}_{12})]_2$ (0.189 g, 0.384 mmol) were allowed to react in benzene (20 mL) for 4 h at room temperature. The reaction mixture was filtered, the filtrate was evaporated, and the residue was extracted with benzene. The solvent was removed under reduced pressure to afford the product as a yellow solid (0.205 g, 0.345 mmol, 90.3%). ¹H NMR (benzene-*d*₆, 700 MHz): δ 7.77 (d, ³*J*_{HH} = 6.4 Hz, 2 H, *o*-C₆H₅), 7.44 (t, ³*J*_{HH} = 7.6 Hz, 2 H, *m*-C₆H₅), 7.29 (t, ³*J*_{HH} = 7.6 Hz, 1 H, *p*-C₆H₅), 4.2 (br, 2 H, C₈H₁₂), 4.0 (br, 2 H, C₈H₁₂), 3.75 (s, 2 H, CNCMe₂CH₂O), 3.57 (s, 2 H, CNCMe₂CH₂O), 3.46 (s, 2 H, CNCMe₂CH₂O), 2.0 (br, 2 H, C₈H₁₂), 1.3 (br, 10 H C₈H₁₂ (4 H) and CNCMe₂CH₂O (6 H)), 1.08 (s, 8 H, C₈H₁₂ (2 H) and CNCMe₂CH₂O (6 H)), 0.72 (s, 6 H, CNCMe₂CH₂O). ¹³C{¹H} NMR (benzene-*d*₆, 175 MHz): δ 193 (br, CNCMe₂CH₂O), 135.41 (*o*-C₆H₅), 127.83 (*m*-C₆H₅), 125.57 (*p*-C₆H₅), 81.79 (CNCMe₂CH₂O), 79.34 (C₈H₁₂), 77.40 (CNCMe₂CH₂O), 75.65 (C₈H₁₂), 68.47 (CNCMe₂CH₂O), 67.62 (CNCMe₂CH₂O), 30.83 (C₈H₁₂), 29.51 (CNCMe₂CH₂O and C₈H₁₂), 28.14 (CNCMe₂CH₂O), 27.56 (CNCMe₂CH₂O). ¹¹B NMR (benzene-*d*₆, 192 MHz): δ -16.3. IR (KBr, cm^{-1}): 3063 w, 3042 w, 2999 m, 2963 s, 2927 s, 2879 s, 2834 m, 1611 m (CN), 1567 s (CN), 1485 w, 1461 m, 1432 w, 1387 w, 1365 m, 1335 w, 1303 w, 1276 s, 1252 m, 1194 s, 1155 m, 1130 w, 995 s, 968 s, 894 w, 874 w, 838 w, 816 w, 775 w, 729 m, 704 m. Anal. Calcd for $\text{C}_{29}\text{H}_{41}\text{BN}_3\text{O}_3\text{Rh}$: C, 58.70; H, 6.96; N, 7.08. Found: C, 58.57; H, 6.77; N, 7.01. Mp, 180-185 °C (dec).

To^MIr(η^4 -C₈H₁₂) (9). Compound **9** was prepared following the procedure for the rhodium analogue, with TI[To^M] (0.700 g, 1.19 mmol) and [Ir(μ -Cl)(η^4 -C₈H₁₂)]₂ (0.411 g, 0.611 mmol) providing **9** (0.758 g, 1.11 mmol, 93.3%). ¹H NMR (benzene-*d*₆, 700 MHz): δ 7.62 (d, ³J_{HH} = 6.4 Hz, 2 H, *o*-C₆H₅), 7.39 (t, ³J_{HH} = 7.2 Hz, 2 H, *m*-C₆H₅), 7.24 (t, ³J_{HH} = 7.2 Hz, 1 H, *p*-C₆H₅), 4.1 (br, 2 H, C₈H₁₂), 3.7 (br, 4 H, CNCMe₂CH₂O (2 H) and C₈H₁₂ (2 H)), 3.59 (s, 2 H, CNCMe₂CH₂O), 3.49 (s, 2 H, CNCMe₂CH₂O), 1.9 (br, 2 H, C₈H₁₂), 1.34 (s, 6 H, CNCMe₂CH₂O), 1.2 (br, 4 H, C₈H₁₂), 1.06 (s, 6 H, CNCMe₂CH₂O), 0.9 (br, 2 H, C₈H₁₂), 0.81 (s, 6 H, CNCMe₂CH₂O). ¹³C{¹H} NMR (benzene-*d*₆, 175 MHz): δ 194 (br, CNCMe₂CH₂O), 153 (br, *ipso*-C₆H₅), 134.83 (*o*-C₆H₅), 127.75 (*m*-C₆H₅), 125.45 (*p*-C₆H₅), 82.98 (2 CNCMe₂CH₂O overlapped), 77.41 (CNCMe₂CH₂O), 68.62 (2 CNCMe₂CH₂O overlapped), 63.13 (C₈H₁₂), 59.61 (C₈H₁₂), 31.54 (2 C₈H₁₂ overlapped), 30.26 (C₈H₁₂), 29.51 (CNCMe₂CH₂O), 28.16 (CNCMe₂CH₂O), 27.15 (CNCMe₂CH₂O). ¹¹B NMR (benzene-*d*₆, 192 MHz): δ -16.4. IR (KBr, cm⁻¹): 3063 w, 3036 w, 3000 m, 2965 s, 2928 s, 2881 s, 2835 m, 1607 m (CN), 1558 s (CN), 1462 m, 1433 w, 1388 w, 1370 m, 1329 w, 1284 s, 1254 w, 1198 s, 1158 s, 1131 m, 1002 s, 967 s, 892 w, 875 w, 839 w, 817 w, 785 w, 739 m, 704 m. Anal. Calcd for C₂₉H₄₁BIrN₃O₃: C, 51.02; H, 6.05; N, 6.16. Found: C, 51.00; H, 5.53; N, 6.03. Mp, 175-180 °C.



PhB(Ox^{Me₂})₂(Im^{Mes¹}H) (H[2], 0.107 g, 0.228 mmol) was deprotonated with potassium benzyl (0.0365 g, 0.280 mmol) in tetrahydrofuran (10 mL) as above, [Rh(μ -Cl)(η^2 -C₈H₁₄)₂]₂ (0.164 g, 0.228 mmol) was added, and the dark brown solution was stirred at room temperature for 1 h. The volatile materials were evaporated *in vacuo*, and the residue was extracted with benzene (2 × 5 mL). The benzene extracts were combined,

filtered, and evaporated. The residue was triturated with pentane and dried *in vacuo* to afford the product as a yellow solid (0.179 g, 0.192 mmol, 84.2%). ^1H NMR (benzene- d_6 , 600 MHz): δ 8.55 (d, $^3J_{\text{HH}} = 7.2$ Hz, 2 H, *o*-C₆H₅), 7.60 (t, $^3J_{\text{HH}} = 7.2$ Hz, 2 H, *m*-C₆H₅), 7.47 (s, 1 H, 3H-C₆H₂(CH₂Rh)Me₂), 7.44 (t, $^3J_{\text{HH}} = 7.2$ Hz, 1 H, *p*-C₆H₅), 6.79 (s, 1 H, N₂C₃H₂Mes'), 6.59 (s, 1 H, 5H-C₆H₂(CH₂Rh)Me₂), 6.56 (s, 1 H, N₂C₃H₂Mes'), 4.3 (br, 1 H, C₈H₁₄), 3.67 (m, 4 H, CNCMe₂CH₂O (1 H) and C₈H₁₄ (3 H)), 3.30 (d, $^2J_{\text{HH}} = 7.8$ Hz, 1 H, CNCMe₂CH₂O), 3.02 (m, 1 H, C₈H₁₄), 3.0 (br, 2 H, CHCMe₂CH₂O (1 H) and C₈H₁₄ (1 H)), 2.80 (m, 4 H, CNCMe₂CH₂O (1 H), C₈H₁₄ (1 H), and CH₂Rh (2 H)), 2.42 (m, 1 H, C₈H₁₄), 2.23 (s, 3 H, *p*-C₆H₂(CH₂Rh)Me₂), 2.08 (s, 3 H, *o*-C₆H₂(CH₂Rh)Me₂), 1.90 (s, 3 H, CNCMe₂CH₂O), 1.75 (m, 1 H, C₈H₁₄), 1.57 (m, 5 H, C₈H₁₄), 1.39 (m, 9 H, C₈H₁₄), 1.28 (s, 3 H, CNCMe₂CH₂O), 1.23 (s, 3 H, CNCMe₂CH₂O), 1.17 (m, 3 H, C₈H₁₄), 1.10 (s, 3 H, CNCMe₂CH₂O), 1.04 (m, 2 H, C₈H₁₄), -21.70 (dd, 1 H, $^1J_{\text{RhH}} = 30$ and 18 Hz). $^{13}\text{C}\{^1\text{H}\}$ NMR (benzene- d_6 , 150 MHz): δ 187 (br, CNCMe₂CH₂O), 184 (br, CNCMe₂CH₂O), 175.98 (d, $^1J_{\text{RhC}} = 50.1$ Hz, 2C-N₂C₃H₂Mes'), 150.61 (*ipso*-C₆H₂(CH₂Rh)Me₂), 143 (br, *ipso*-C₆H₅), 136.77 (*o*-C₆H₅), 136.60 (2C and 6C-C₆H₂(CH₂Rh)Me₂), 135.53 (4C-C₆H₂(CH₂Rh)Me₂), 128.92 (5C-C₆H₂(CH₂Rh)Me₂), 127.91 (*m*-C₆H₅), 127.31 (3C-C₆H₂(CH₂Rh)Me₂), 127.07 (*p*-C₆H₅), 124.55 (4,5C-N₂C₃H₂Mes'), 119.58 (4,5C-N₂C₃H₂Mes'), 81.06 (CNCMe₂CH₂O), 80.78 (d, $^1J_{\text{RhC}} = 10.8$ Hz, C₈H₁₄), 80.39 (CNCMe₂CH₂O), 75.99 (d, $^1J_{\text{RhC}} = 11.6$ Hz, C₈H₁₄), 71.57 (d, $^1J_{\text{RhC}} = 11.4$ Hz, C₈H₁₄), 69.36 (d, $^1J_{\text{RhC}} = 12.2$ Hz, C₈H₁₄), 69.18 (CNCMe₂CH₂O), 68.58 (CNCMe₂CH₂O), 33.0 (br, C₈H₁₄), 31.8 (br, C₈H₁₄), 31.7 (br, C₈H₁₄), 30.1 (br, C₈H₁₄), 29.9 (br, C₈H₁₄), 29.88 (C₈H₁₄), 29.55 (CNCMe₂CH₂O), 29.31 (CNCMe₂CH₂O), 29.1 (br, C₈H₁₄), 28.31 (CNCMe₂CH₂O), 28.0 (br, C₈H₁₄), 27.3 (br, C₈H₁₄), 27.23 (C₈H₁₄), 27.16

(C₈H₁₄), 26.71 (C₈H₁₄), 25.44 (CNCMe₂CH₂O), 21.47 (*p*-C₆H₂(CH₂Rh)Me₂), 20.34 (*o*-C₆H₂(CH₂Rh)Me₂), 12.78 (¹J_{RhH} = 21.2 Hz, RhCH₂). ¹¹B NMR (benzene-*d*₆, 192 MHz): δ -9.6. ¹⁵N{¹H} NMR (benzene-*d*₆, 61 MHz): δ -162 (CNCMe₂CH₂O), -178 (CNCMe₂CH₂O). IR (KBr, cm⁻¹): 2956 m, 2921 s, 2849 m, 1582 s (CN), 1559 w (CN), 1480 m, 1464 m, 1413 m, 1354 s, 1278 m, 1187 s, 1166 m, 967 s, 888 w, 850 w, 837 w, 821 w, 743 w, 728 w, 703 s, 670 w, 645 w. Anal. Calcd for C₄₄H₆₂BClN₄O₂Rh₂: C, 56.76; H, 6.71; N, 6.02. Found: C, 57.11; H, 6.78; N, 6.44. Mp, 189-192 °C.

{PhB(Ox^{Me2})₂Im^{Mes}}IrH(η³-C₈H₁₃) (11). PhB(Ox^{Me2})₂(Im^{Mes}H) (H[2], 0.0914 g, 0.194 mmol) was deprotonated with potassium benzyl (0.0317 g, 0.243 mmol) in tetrahydrofuran (10 mL). [Ir(μ-Cl)(η²-C₈H₁₄)₂]₂ (0.0871 g, 0.0972 mmol) was added and the dark brown solution was stirred at room temperature for 18 h. The solvent was removed *in vacuo*, and the residue was extracted with benzene (2 × 5 mL). The benzene extracts were combined, filtered, and evaporated to give a solid, which was triturated with pentane and dried *in vacuo* to afford the product as a yellow solid (0.124 g, 0.161 mmol, 83.0%). ¹H NMR (benzene-*d*₆, 600 MHz): δ 8.49 (d, ³J_{HH} = 7.2 Hz, 2 H, *o*-C₆H₅), 7.57 (t, ³J_{HH} = 7.2 Hz, 2 H, *m*-C₆H₅), 7.41 (t, ³J_{HH} = 7.2 Hz, 1 H, *p*-C₆H₅), 6.85 (s, 1 H, N₂C₃H₂Mes), 6.78 (s, 1 H, *m*-C₆H₂Me₃), 6.70 (s, 1 H, *m*-C₆H₂Me₃), 6.09 (s, 1 H, N₂C₃H₂Mes), 4.90 (t, ³J_{HH} = 7.2 Hz, 1 H, CH(CH)₂(CH₂)₅), 4.09 (q, ³J_{HH} = 8.4 Hz, 1 H, CH(CH)₂(CH₂)₅), 3.85 (d, ²J_{HH} = 8.4 Hz, 1 H, CNCMe₂CH₂O *trans* to C₈H₁₃), 3.69 (d, ²J_{HH} = 8.4 Hz, 1 H, CNCMe₂CH₂O *trans* to C₈H₁₃), 3.43 (m, 2 H, CNCMe₂CH₂O *trans* to H (1 H) and CH(CH)₂(CH₂)₅ (1 H)), 3.34 (d, ²J_{HH} = 8.4 Hz, 1 H, CNCMe₂CH₂O *trans* to H), 2.58 (m, 1 H, C₈H₁₃), 2.43 (m, 1 H, C₈H₁₃), 2.19-2.17 (m, 4 H, C₆H₂Me₃ (3 H) and C₈H₁₃ (1 H)), 2.10 (s, 3 H, C₆H₂Me₃), 2.00 (s, 3 H, C₆H₂Me₃), 1.55 (m, 3 H, C₈H₁₃), 1.24

(s, 3 H, CNCMe₂CH₂O *trans* to C₈H₁₃), 1.20 (m, 3 H, C₈H₁₃), 1.09 (s, 3 H, CNCMe₂CH₂O *trans* to C₈H₁₃), 0.84 (s, 3 H, CNCMe₂CH₂O *trans* to H), 0.76 (s, 3 H, CNCMe₂CH₂O *trans* to H), 0.70 (m, 1 H, C₈H₁₃), -27.49 (s, 1 H, IrH). ¹³C{¹H} NMR (benzene-*d*₆, 150 MHz): δ 186 (br, CNCMe₂CH₂O), 184 (br, CNCMe₂CH₂O), 164.12 (2C-N₂C₃H₂Mes), 144 (br, *ipso*-C₆H₅), 139.73 (*o*-C₆H₂Me₃), 139.70 (*o*-C₆H₂Me₃), 138.19 (*ipso*-C₆H₂Me₃), 137.17 (*o*-C₆H₅), 136.87 (*p*-C₆H₂Me₃), 129.70 (*m*-C₆H₂Me₃), 129.19 (4,5C-N₂C₃H₂Mes), 127.62 (*m*-C₆H₅), 127.10 (*p*-C₆H₅), 124.19 (*m*-C₆H₂Me₃), 120.23 (4,5C-N₂C₃H₂Mes), 89.26 (C₈H₁₃), 82.99 (CNCMe₂CH₂O *trans* to H), 80.70 (CNCMe₂CH₂O *trans* to C₈H₁₃), 69.42 (CNCMe₂CH₂O *trans* to C₈H₁₃), 69.36 (CNCMe₂CH₂O *trans* to H), 54.82 (C₈H₁₃), 48.43 (C₈H₁₃), 38.57 (C₈H₁₃), 37.52 (C₈H₁₃), 31.56 (C₈H₁₃), 31.50 (C₈H₁₃), 31.38 (C₈H₁₃), 28.45 (CNCMe₂CH₂O *trans* to H), 28.23 (CNCMe₂CH₂O *trans* to H), 28.18 (CNCMe₂CH₂O *trans* to C₈H₁₃), 28.12 (CNCMe₂CH₂O *trans* to C₈H₁₃), 27.03 (C₈H₁₃), 21.36 (*o*-C₆H₂Me₃), 18.51 (*p*-C₆H₂Me₃), 18.50 (*o*-C₆H₂Me₃). ¹¹B NMR (benzene-*d*₆, 192 MHz): δ -10.5. ¹⁵N{¹H} NMR (benzene-*d*₆, 61 MHz): δ -184 (CNCMe₂CH₂O, *trans* to H), -196 (CNCMe₂CH₂O *trans* to C₈H₁₃). IR (KBr, cm⁻¹): 3126 w, 2960 s, 2922 s, 2245 s (IrH), 1585 s (CN), 1567 m (CN), 1490 m, 1456 m, 1404 s, 1338 s, 1324 m, 1261 m, 1186 s, 1161 m, 1020 m, 993 m, 972 m, 927 w, 853 w, 823 w, 745 m, 704 s, 672 m, 643 m. Anal. Calcd for C₃₆H₄₈BIrN₄O₂: C, 56.02; H, 6.27; N, 7.26. Found: C, 56.25; H, 5.89; N, 7.23. Mp, 183-185 °C.

{κ⁴-PhB(Ox^{Me2})₂Im^{Mes}CH₂}RhH(CO) (12). A 10 mL benzene solution of {PhB(Ox^{Me2})Im^{Mes}}Rh(CO)₂ (**5**, 0.144 g, 0.230 mmol) was exposed to UV light in a Rayonet reactor for 2 d. The reaction mixture was evaporated to dryness, and the solid residue was triturated with pentane and dried *in vacuo* to provide the brown product

(0.106 g, 0.177 mmol, 77.0%). ^1H NMR (benzene- d_6 , 600 MHz): δ 8.54 (d, $^3J_{\text{HH}} = 7.8$ Hz, 2 H, *o*-C₆H₅), 7.62 (t, $^3J_{\text{HH}} = 7.8$ Hz, 2 H, *m*-C₆H₅), 7.45 (t, $^3J_{\text{HH}} = 7.2$ Hz, 1 H, *p*-C₆H₅), 7.18 (s, 1 H, 5H-C₆H₂(CH₂Rh)Me₂), 6.84 (s, 1 H, N₂C₃H₂Mes'), 6.63 (s, 1 H, N₂C₃H₂Mes'), 6.61 (s, 1 H, 3H-C₆H₂(CH₂Rh)Me₂), 3.67 (d, $^2J_{\text{HH}} = 8.4$ Hz, 1 H, CNCMe₂CH₂O), 3.44 (m, 2 H, CNCMe₂CH₂O), 3.38 (d, $^2J_{\text{HH}} = 8.4$ Hz, 1 H, CNCMe₂CH₂O), 2.78 (m, 2 H, CH₂Rh), 2.15 (s, 3 H, *o*-C₆H₂(CH₂Rh)Me₂), 1.92 (s, 3 H, *p*-C₆H₂(CH₂Rh)Me₂), 1.02 (s, 3 H, CNCMe₂CH₂O *trans* to H), 0.90 (s, 3 H, CNCMe₂CH₂O *trans* to H), 0.83 (s, 3 H, CNCMe₂CH₂O *trans* to CH₂), 0.72 (s, 3 H, CNCMe₂CH₂O *trans* to CH₂), -14.21 (d, $^1J_{\text{RhH}} = 23.4$ Hz, 1 H, RhH). $^{13}\text{C}\{^1\text{H}\}$ NMR (benzene- d_6 , 150 MHz): δ 197.06 (d, $^1J_{\text{RhC}} = 52.5$ Hz, CO), 186 (br, CNCMe₂CH₂O), 185.74 (d, $^1J_{\text{RhC}} = 40.2$ Hz, 2C-N₂C₃H₂Mes'), 185 (br, CNCMe₂CH₂O), 148.64 (2C-C₆H₂(CH₂Rh)Me₂), 143 (br, *ipso*-C₆H₅), 137.15 (4,6C-C₆H₂(CH₂Rh)Me₂), 137.14 (4,6C-C₆H₂(CH₂Rh)Me₂), 136.68 (*o*-C₆H₅), 136.28 (*ipso*-C₆H₂(CH₂Rh)Me₂), 129.01 (3C-C₆H₂(CH₂Rh)Me₂), 127.98 (*m*-C₆H₅), 127.45 (*p*-C₆H₅), 126.06 (5C-C₆H₂(CH₂Rh)Me₂), 123.97 (4,5C-N₂C₃H₂Mes'), 119.40 (4,5C-N₂C₃H₂Mes'), 80.35 (CNCMe₂CH₂O *trans* to H), 79.77 (CNCMe₂CH₂O *trans* to CH₂), 67.87 (CNCMe₂CH₂O *trans* to H), 66.70 (CNCMe₂CH₂O *trans* to CH₂), 28.71 (CNCMe₂CH₂O *trans* to H), 28.00 (CNCMe₂CH₂O *trans* to CH₂), 27.93 (CNCMe₂CH₂O *trans* to CH₂), 27.32 (CNCMe₂CH₂O *trans* to H), 21.29 (*o*-C₆H₂(CH₂Rh)Me₂), 20.39 (*p*-C₆H₂(CH₂Rh)Me₂), 6.58 (d, $^1J_{\text{RhC}} = 20.6$ Hz, CH₂Rh). ^{11}B NMR (benzene- d_6 , 192 MHz): δ -9.7. $^{15}\text{N}\{^1\text{H}\}$ NMR (benzene- d_6 , 61 MHz): δ -162 (CNCMe₂CH₂O *trans* to H), -171 (CNCMe₂CH₂O *trans* to CH₂), -183 (N₂C₃H₂Mes'), -188 (N₂C₃H₂Mes'). IR (KBr, cm⁻¹): 2976 m, 2929 m, 2892 w, 2064 m (RhH), 2015 s (CO), 1967 w, 1587 m (CN), 1568 m (CN), 1479 m, 1430 m, 1362 m,

1274 m, 1164 m, 968 m, 957 m, 819 w, 705 m. Anal. Calcd for $C_{29}H_{34}BN_4O_3Rh$: C, 58.02; H, 5.71; N, 9.33. Found: C, 58.46; H, 5.51; N, 9.42. Mp, 196-199 °C.

{PhB(Ox^{Me2})₂Im^{Mes}}IrH(Ph)CO (13). A 10 mL benzene solution of {PhB(Ox^{Me2})₂Im^{Mes}}Ir(CO)₂ (7, 0.0930 g, 0.130 mmol) was irradiated with UV light in a Rayonet reactor for 2 d. The volatile materials were evaporated, and the residue was triturated with pentane and dried *in vacuo* to afford the product as a brown solid (0.0843 g, 0.110 mmol, 84.6%). ¹H NMR (methylene chloride-*d*₂, 600 MHz): δ 8.04 (d, ³J_{HH} = 7.2 Hz, 2 H, *o*-BC₆H₅), 7.39 (m, 4 H, *m*-BC₆H₅ (2 H) and IrC₆H₅ (2 H)), 7.32 (t, ³J_{HH} = 7.2 Hz, 1 H, *p*-BC₆H₅), 7.07 (s, 1 H, *m*-C₆H₂Me₃), 7.00 (s, 1 H, *m*-C₆H₂Me₃), 6.8 (br, 3 H, N₂C₃H₂Mes (1 H) and IrC₆H₅ (2 H)), 6.69 (m, 2 H, N₂C₃H₂Mes (1 H) and IrC₆H₅ (1 H)), 4.24 (d, ²J_{HH} = 7.8 Hz, 1 H, CNCMe₂CH₂O), 4.17 (d, ²J_{HH} = 8.4 Hz, 1 H, CNCMe₂CH₂O), 3.92 (d, ²J_{HH} = 8.4 Hz, 1 H, CNCMe₂CH₂O), 3.80 (d, ²J_{HH} = 8.4 Hz, 1 H, CNCMe₂CH₂O), 2.39 (s, 3 H, *p*-C₆H₂Me₃), 2.05 (s, 3 H, *o*-C₆H₂Me₃), 1.94 (s, 3 H, *o*-C₆H₂Me₃), 0.94 (s, 3 H, CNCMe₂CH₂O *trans* to H), 0.89 (s, 6 H, CNCMe₂CH₂O), 0.54 (s, 3 H, CNCMe₂CH₂O *trans* to CO), -16.51 (s, 1 H, IrH). ¹³C{¹H} NMR (methylene chloride-*d*₂, 150 MHz): δ 188 (br, CNCMe₂CH₂O), 185 (br, CNCMe₂CH₂O), 171.70 (CO), 170.07 (2C-N₂C₃H₂Mes), 144 (br, IrC₆H₅), 143.44 (IrC₆H₅), 143.26 (*ipso*-BC₆H₅), 139.32 (*ipso*-IrC₆H₅), 139.30 (*p*-C₆H₂Me₃), 139.16 (*ipso*-C₆H₂Me₃), 136.99 (*o*-C₆H₂Me₃), 136.58 (*o*-C₆H₂Me₃), 136.18 (*o*-BC₆H₅), 129.34 (*m*-C₆H₂Me₃), 129.25 (*m*-C₆H₂Me₃), 127.46 (*m*-BC₆H₅), 127.16 (*p*-BC₆H₅), 124.31 (4,5C-N₂C₃H₂Mes), 122.67 (IrC₆H₅), 120.92 (4,5C-N₂C₃H₂Mes), 80.22 (CNCMe₂CH₂O *trans* to H), 79.78 (CNCMe₂CH₂O *trans* to CO), 70.24 (CNCMe₂CH₂O), 70.09 (CNCMe₂CH₂O), 29.47 (CNCMe₂CH₂O *trans* to H), 29.40 (CNCMe₂CH₂O *trans* to CO), 26.29 (CNCMe₂CH₂O *trans* to H), 25.45

(CNCMe₂CH₂O *trans* to CO), 21.45 (*p*-C₆H₂Me₃), 18.85 (*o*-C₆H₂Me₃), 18.13 (*o*-C₆H₂Me₃). ¹¹B NMR (methylene chloride-*d*₂, 192 MHz): δ -10.0. ¹⁵N{¹H} NMR (benzene-*d*₆, 61 MHz): δ -182 (CNCMe₂CH₂O *trans* to H), -193 (CNCMe₂CH₂O *trans* to CO). IR (KBr, cm⁻¹): 3139 w, 3046 w, 2969 m, 2925 m, 2885 w, 2177 m (IrH), 1999 s (CO), 1578 m (CN), 1558 m (CN), 1404 m, 1291 m, 1205 m, 1183 m, 1162 m, 967 m, 744 m, 704 m. Anal. Calcd for C₃₅H₄₀BIrN₄O₃: C, 54.75; H, 5.25; N, 7.30. Found: C, 54.84; H, 5.17; N, 7.23. Mp, 281-282 °C.

{PhB(Ox^{Me2})₂Im^{Mes}}RhH(SiH₂Ph)CO (14). PhSiH₃ (70.0 μL, 0.567 mmol) was allowed to react with {PhB(Ox^{Me2})₂Im^{Mes}}Rh(CO)₂ (**5**, 0.351 g, 0.559 mmol) in benzene (10 mL) at room temperature for 18 h. The volatiles were removed *in vacuo*, and the brown residue was triturated with pentane and dried to give a brown solid (0.372 g, 0.525 mmol, 94.1%). ¹H NMR (benzene-*d*₆, 600 MHz): δ 8.41 (d, ³J_{HH} = 7.2 Hz, 2 H, *o*-BC₆H₅), 7.59 (m, 2 H, *o*-SiC₆H₅), 7.55 (t, ³J_{HH} = 7.2 Hz, 2 H, *m*-BC₆H₅), 7.40 (t, ³J_{HH} = 7.2 Hz, 1 H, *p*-BC₆H₅), 7.11 (m, 3 H, *m*- and *p*-SiC₆H₅), 6.54 (d, ³J_{HH} = 1.8 Hz, 1 H, N₂C₃H₂Mes), 6.50 (s, 1 H, *m*-C₆H₂Me₃), 6.40 (s, 1 H, *m*-C₆H₂Me₃), 5.93 (d, ³J_{HH} = 1.8 Hz, 1 H, N₂C₃H₂Mes), 4.91 (d, ²J_{HH} = 6.0 Hz, ¹J_{SiH} = 170 Hz, 1 H, SiH), 4.43 (d, ²J_{HH} = 6.0 Hz, ¹J_{SiH} = 188 Hz, 1 H, SiH), 3.64 (d, ²J_{HH} = 7.8 Hz, 1 H, CNCMe₂CH₂O), 3.61 (d, ²J_{HH} = 8.4 Hz, 1 H, CNCMe₂CH₂O), 3.58 (d, ²J_{HH} = 8.4 Hz, 1 H, CNCMe₂CH₂O), 3.37 (d, ²J_{HH} = 8.4 Hz, 1 H, CNCMe₂CH₂O), 2.01 (s, 3 H, *o*-C₆H₂Me₃), 1.99 (s, 3 H, *o*-C₆H₂Me₃), 1.89 (s, 3 H, *p*-C₆H₂Me₃), 1.16 (s, 3 H, CNCMe₂CH₂O *trans* to H), 1.15 (s, 3 H, CNCMe₂CH₂O *trans* to H), 1.08 (s, 3 H, CNCMe₂CH₂O *trans* to Si), 1.02 (s, 3 H, CNCMe₂CH₂O *trans* to Si), -13.22 (dd, ¹J_{RhH} = 21.3 Hz, ³J_{HH} = 1.2 Hz, 1 H, RhH). ¹³C{¹H} NMR (benzene-*d*₆, 150 MHz): δ 194.53 (d, ¹J_{RhC} = 51.0 Hz, 2C-N₂C₃H₂Mes),

186 (br, CNCMe₂CH₂O), 178.39 (d, ¹J_{RhC} = 40.5 Hz, CO), 144 (br, *ipso*-BC₆H₅), 139.10 (*ipso*-SiC₆H₅), 138.63 (*p*-C₆H₂Me₃), 137.25 (*ipso*-C₆H₂Me₃), 136.98 (*o*-BC₆H₅), 136.45 (*o*-SiC₆H₅), 135.86 (*o*-C₆H₂Me₃), 135.84 (*o*-C₆H₂Me₃), 129.69 (*m*-C₆H₂Me₃), 129.68 (*m*-C₆H₂Me₃), 127.87 (*m*-BC₆H₅), 127.81 (*p*-BC₆H₅), 127.41 (*p*-SiC₆H₅), 127.37 (*m*-SiC₆H₅), 124.93 (4,5C-N₂C₃H₂Mes), 121.86 (4,5C-N₂C₃H₂Mes), 80.81 (CNCMe₂CH₂O), 80.65 (CNCMe₂CH₂O), 69.11 (CNCMe₂CH₂O *trans* to Si), 67.04 (CNCMe₂CH₂O *trans* to H), 28.72 (CNCMe₂CH₂O *trans* to Si), 28.39 (CNCMe₂CH₂O *trans* to Si), 28.15 (CNCMe₂CH₂O *trans* to H), 27.33 (CNCMe₂CH₂O *trans* to H), 21.51 (*p*-C₆H₂Me₃), 19.78 (*o*-C₆H₂Me₃), 19.40 (*o*-C₆H₂Me₃). ¹¹B NMR (benzene-*d*₆, 192 MHz): δ -9.9. ¹⁵N{¹H} NMR (benzene-*d*₆, 61 MHz): δ -161 (CNCMe₂CH₂O *trans* to Si), -172 (CNCMe₂CH₂O *trans* to H), -176 (N₂C₃H₂Mes), -187 (N₂C₃H₂Mes). ²⁹Si{¹H} NMR (benzene-*d*₆, 119 MHz): δ -21.37 (d, ¹J_{RhSi} = 30.2 Hz). IR (KBr, cm⁻¹): 2964 w, 2925 w, 2064 s (RhH), 2016 s (CO), 1998 s (SiH), 1593 m (CN), 1276 m, 967 m, 830 m. Anal. Calcd for C₃₅H₄₂BN₄O₃RhSi: C, 59.33; H, 5.98; N, 7.91. Found: C, 59.07; H, 5.64; N, 7.55. Mp, 124-127 °C.

{PhB(Ox^{Me2})₂Im^{Mes}}Ir(CO)CN^tBu (15). {PhB(Ox^{Me2})₂Im^{Mes}}Ir(CO)₂ (7, 0.254 g, 0.354 mmol) and *tert*-butyl isocyanide (40.0 μL, 0.354 mmol) were allowed to react in benzene (10 mL). The transparent green-yellow reaction mixture was stirred at room temperature for 3 h. The solvent and volatiles were evaporated, and the resulting solid was triturated with pentane and dried *in vacuo* to afford the product as greenish yellow solid (0.246 g, 0.318 mmol, 89.8%). ¹H NMR (benzene-*d*₆, 600 MHz): δ 7.95 (d, ³J_{HH} = 7.8 Hz, 2 H, *o*-C₆H₅), 7.67 (s, 1 H, N₂C₃H₂Mes), 7.44 (t, ³J_{HH} = 7.2 Hz, 2 H, *m*-C₆H₅), 7.25 (t, ³J_{HH} = 7.2 Hz, 1 H, *p*-C₆H₅), 6.76 (s, 2 H, *m*-C₆H₂Me₃), 6.32 (s, 1 H,

$\text{N}_2\text{C}_3\text{H}_2\text{Mes}$), 3.68 (m, 4 H, $\text{CNCMe}_2\text{CH}_2\text{O}$), 2.20 (s, 6 H, $o\text{-C}_6\text{H}_2\text{Me}_3$), 2.11 (s, 3 H, $p\text{-C}_6\text{H}_2\text{Me}_3$), 1.32 (s, 6 H, $\text{CNCMe}_2\text{CH}_2\text{O}$), 1.27 (s, 6 H, $\text{CNCMe}_2\text{CH}_2\text{O}$), 0.73 (s, 9 H, CMe_3). $^{13}\text{C}\{^1\text{H}\}$ NMR (benzene- d_6 , 150 MHz): δ 187 (br, $\text{CNCMe}_2\text{CH}_2\text{O}$), 177.53 (2C- $\text{N}_2\text{C}_3\text{H}_2\text{Mes}$), 176 (br, CO), 150 (br, *ipso*- C_6H_5), 138.49 ($p\text{-C}_6\text{H}_2\text{Me}_3$), 138.14 (*ipso*- $\text{C}_6\text{H}_2\text{Me}_3$), 136.84 ($o\text{-C}_6\text{H}_2\text{Me}_3$), 134.71 ($o\text{-C}_6\text{H}_5$), 129.64 ($m\text{-C}_6\text{H}_2\text{Me}_3$), 128.90 (CNCMe_3), 127.72 ($m\text{-C}_6\text{H}_5$), 126.38 ($p\text{-C}_6\text{H}_5$), 126.31 (4,5C- $\text{N}_2\text{C}_3\text{H}_2\text{Mes}$), 120.33 (4,5C- $\text{N}_2\text{C}_3\text{H}_2\text{Mes}$), 79.04 ($\text{CNCMe}_2\text{CH}_2\text{O}$), 68.89 ($\text{CNCMe}_2\text{CH}_2\text{O}$), 56.59 (CMe_3), 29.88 (CMe_3), 28.83 ($\text{CNCMe}_2\text{CH}_2\text{O}$), 28.68 ($\text{CNCMe}_2\text{CH}_2\text{O}$), 21.45 ($p\text{-C}_6\text{H}_2\text{Me}_3$), 19.30 ($o\text{-C}_6\text{H}_2\text{Me}_3$). ^{11}B NMR (benzene- d_6 , 192 MHz): δ -8.5. $^{15}\text{N}\{^1\text{H}\}$ NMR (benzene- d_6 , 61 MHz): δ -154 ($\text{CNCMe}_2\text{CH}_2\text{O}$), -176 ($\text{N}_2\text{C}_3\text{H}_2\text{Mes}$), -188 ($\text{N}_2\text{C}_3\text{H}_2\text{Mes}$), -196 (CNCMe_3). IR (KBr, cm^{-1}): 2959 w, 2920 w, 2852 w, 2144 m (CN), 1973 s (CO), 1616 w (CN), 1579 w (CN), 1461 w, 1185 w, 967 w, 731 w. Anal. Calcd for $\text{C}_{34}\text{H}_{43}\text{BIrN}_5\text{O}_3$: C, 52.84; H, 5.61; N, 9.06. Found: C, 53.27; H, 5.56; N, 9.35. Mp, 182-185 °C.

{PhB(Ox^{Me2})₂Im^{Mes}}Ir(CN^tBu)₂ (16). *tert*-Butyl isocyanide (175.0 μL , 1.547 mmol) was added to a benzene solution (10 mL) of {PhB(Ox^{Me2})₂Im^{Mes}}Ir($\eta^4\text{-C}_8\text{H}_{12}$) (6, 0.571 g, 0.742 mmol). The solution was stirred at room temperature for 3 h. Evaporation of the solvent and other volatile materials provided a solid that was triturated with pentane and immediately dried *in vacuo* to give the product as yellow solid (0.533 g, 0.644 mmol, 86.8%). ^1H NMR (benzene- d_6 , 600 MHz): δ 8.00 (d, $^3J_{\text{HH}} = 6.8$ Hz, 2 H, $o\text{-C}_6\text{H}_5$), 7.83 (s, 1 H, $\text{N}_2\text{C}_3\text{H}_2\text{Mes}$), 7.43 (t, $^3J_{\text{HH}} = 7.2$ Hz, 2 H, $m\text{-C}_6\text{H}_5$), 7.25 (t, $^3J_{\text{HH}} = 7.2$ Hz, 1 H, $p\text{-C}_6\text{H}_5$), 6.69 (s, 2 H, $m\text{-C}_6\text{H}_2\text{Me}_3$), 6.35 (s, 1 H, $\text{N}_2\text{C}_3\text{H}_2\text{Mes}$), 3.74 (m, 4 H, $\text{CNCMe}_2\text{CH}_2\text{O}$), 2.28 (s, 6 H, $o\text{-C}_6\text{H}_2\text{Me}_3$), 2.15 (s, 3 H, $p\text{-C}_6\text{H}_2\text{Me}_3$), 1.38 (s, 6 H, $\text{CNCMe}_2\text{CH}_2\text{O}$), 1.35 (s, 6 H, $\text{CNCMe}_2\text{CH}_2\text{O}$), 1.0 (br, 18 H, CMe_3). $^{13}\text{C}\{^1\text{H}\}$ NMR

(benzene-*d*₆, 150 MHz): δ 185 (br, CNCMe₂CH₂O), 181.35 (2C-N₂C₃H₂Mes), 151 (br, *ipso*-C₆H₅), 139.15 (*o*-C₆H₂Me₃), 136.96 (*p*-C₆H₂Me₃), 136.41 (*ipso*-C₆H₂Me₃), 135.02 (*o*-C₆H₅), 129.46 (*m*-C₆H₂Me₃), 127.46 (*m*-C₆H₅), 125.92 (*p*-C₆H₅), 125.84 (4,5C-N₂C₃H₂Mes), 119.86 (4,5C-N₂C₃H₂Mes), 78.89 (CNCMe₂CH₂O), 68.95 (CNCMe₂CH₂O), 54.7 (br, CMe₃), 30.8 (br, CMe₃), 28.96 (CNCMe₂CH₂O), 28.85 (CNCMe₂CH₂O), 21.38 (*p*-C₆H₂Me₃), 20.38 (*o*-C₆H₂Me₃). ¹¹B NMR (benzene-*d*₆, 192 MHz): δ -8.7. ¹⁵N{¹H} NMR (benzene-*d*₆, 61 MHz): δ -154 (CNCMe₂CH₂O), -176 (N₂C₃H₂Mes), -189 (N₂C₃H₂Mes), -231 (CNCMe₃). IR (KBr, cm⁻¹): 3137 w, 3044 w, 2979 s, 2962 s, 2926 m, 2865 m, 2124 s (CN), 2081 m, 2029 s (CN), 1653 w, 1616 m (CN), 1581 w (CN), 1559 w, 1492 m, 1458 m, 1401 m, 1365 m, 1338 m, 1324 m, 1284 m, 1230 s, 1211 s, 1185 m, 1162 m, 1130 m, 1000 m, 967 m, 851 w, 830 w, 729 m, 702 m. Anal. Calcd for C₃₈H₅₂BlrN₆O₂: C, 55.13; H, 6.33; N, 10.15. Found: C, 55.26; H, 6.61; N, 10.10. Mp, 174-177 °C.

{PhB(Ox^{Me2})₂Im^{Mes}}IrH(SiH₂Ph)CN^tBu (17). Phenylsilane (32.0 μ L, 0.259 mmol) was added to {PhB(Ox^{Me2})₂Im^{Mes}}Ir(CO)CN^tBu (**15**, 0.200 g, 0.258 mmol) dissolved in benzene (10 mL). The resulting yellow transparent solution was heated at 60 °C for 4 h. The solvent and the volatiles were removed *in vacuo*, and the resulting solid was triturated with pentane and dried to give the product as yellow solid (0.205 g, 0.240 mmol, 93.0%). ¹H NMR (benzene-*d*₆, 600 MHz): δ 8.53 (d, ³J_{HH} = 7.2 Hz, 2 H, *o*-BC₆H₅), 7.76 (d, ³J_{HH} = 7.2 Hz, 2 H, *o*-SiC₆H₅), 7.58 (t, ³J_{HH} = 7.2 Hz, 2 H, *m*-BC₆H₅), 7.42 (t, ³J_{HH} = 7.8 Hz, 1 H, *p*-BC₆H₅), 7.19 (m, 3 H, *m*- and *p*-SiC₆H₅), 6.60 (d, ³J_{HH} = 1.8 Hz, 1 H, N₂C₃H₂Mes), 6.50 (s, 1 H, *m*-C₆H₂Me₃), 6.47 (s, 1 H, *m*-C₆H₂Me₃), 6.00 (d, ³J_{HH} = 1.8 Hz, 1 H, N₂C₃H₂Mes), 4.61 (d, ²J_{HH} = 3.6 Hz, ¹J_{SiH} = 155 Hz, 1 H, SiH), 4.10 (d,

$^2J_{\text{HH}} = 3.6$ Hz, $^1J_{\text{SiH}} = 169$ Hz, 1 H, SiH), 3.76 (d, $^2J_{\text{HH}} = 7.8$ Hz, 1 H, $\text{CNCMe}_2\text{CH}_2\text{O}$), 3.68 (d, $^2J_{\text{HH}} = 3.6$ Hz, 1 H, $\text{CNCMe}_2\text{CH}_2\text{O}$), 3.67 (d, $^2J_{\text{HH}} = 3.0$ Hz, 1 H, $\text{CNCMe}_2\text{CH}_2\text{O}$), 3.47 (d, $^2J_{\text{HH}} = 7.8$ Hz, 1 H, $\text{CNCMe}_2\text{CH}_2\text{O}$), 2.13 (s, 6 H, $o\text{-C}_6\text{H}_2\text{Me}_3$), 1.92 (s, 3 H, $p\text{-C}_6\text{H}_2\text{Me}_3$), 1.26 (s, 3 H, $\text{CNCMe}_2\text{CH}_2\text{O}$ *trans* to H), 1.21 (s, 3 H, $\text{CNCMe}_2\text{CH}_2\text{O}$ *trans* to H), 1.18 (s, 3 H, $\text{CNCMe}_2\text{CH}_2\text{O}$ *trans* to Si), 1.13 (s, 3 H, $\text{CNCMe}_2\text{CH}_2\text{O}$ *trans* to Si), 0.92 (s, 9 H, CMe_3), -18.76 (s, 1 H, IrH). $^{13}\text{C}\{^1\text{H}\}$ NMR (benzene- d_6 , 150 MHz): δ 186 (br, $\text{CNCMe}_2\text{CH}_2\text{O}$), 185 (br, $\text{CNCMe}_2\text{CH}_2\text{O}$), 169.40 (2C- $\text{N}_2\text{C}_3\text{H}_2\text{Mes}$), 141.82 (*ipso*- $\text{C}_6\text{H}_2\text{Me}_3$), 138.03 ($p\text{-C}_6\text{H}_2\text{Me}_3$), 137.70 (*ipso*- SiC_6H_5), 137.08 ($o\text{-C}_6\text{H}_5$), 136.87 ($o\text{-C}_6\text{H}_5$), 136.13 ($o\text{-C}_6\text{H}_2\text{Me}_3$), 135.91 ($o\text{-C}_6\text{H}_2\text{Me}_3$), 129.49 ($m\text{-C}_6\text{H}_2\text{Me}_3$), 129.39 ($m\text{-C}_6\text{H}_2\text{Me}_3$), 127.79 ($m\text{-C}_6\text{H}_5$), 127.25 ($p\text{-C}_6\text{H}_5$), 126.70 ($m\text{-}$ and $p\text{-C}_6\text{H}_5$), 124.28 (4,5C- $\text{N}_2\text{C}_3\text{H}_2\text{Mes}$), 121.32 (4,5C- $\text{N}_2\text{C}_3\text{H}_2\text{Mes}$), 80.51 ($\text{CNCMe}_2\text{CH}_2\text{O}$), 77.97 ($\text{CNCMe}_2\text{CH}_2\text{O}$), 70.97 ($\text{CNCMe}_2\text{CH}_2\text{O}$ *trans* to H), 68.25 ($\text{CNCMe}_2\text{CH}_2\text{O}$ *trans* to Si), 55.98 (CMe_3), 30.60 (CMe_3), 28.65 ($\text{CNCMe}_2\text{CH}_2\text{O}$), 28.27 ($\text{CNCMe}_2\text{CH}_2\text{O}$), 27.81 ($\text{CNCMe}_2\text{CH}_2\text{O}$), 27.35 ($\text{CNCMe}_2\text{CH}_2\text{O}$), 21.58 ($p\text{-C}_6\text{H}_2\text{Me}_3$), 19.94 ($o\text{-C}_6\text{H}_2\text{Me}_3$), 19.70 ($o\text{-C}_6\text{H}_2\text{Me}_3$). ^{11}B NMR (benzene- d_6 , 192 MHz): δ -9.7 . $^{15}\text{N}\{^1\text{H}\}$ NMR (benzene- d_6 , 61 MHz): δ -176 ($\text{CNCMe}_2\text{CH}_2\text{O}$ *trans* to Si), -189 ($\text{CNCMe}_2\text{CH}_2\text{O}$ *trans* to H), -197 (CNCMe_3). $^{29}\text{Si}\{^1\text{H}\}$ NMR (benzene- d_6 , 119 MHz): δ -56.14 . IR (KBr, cm^{-1}): 3125 w, 3059 w, 3042 w, 2978 m, 2963 m, 2925 m, 2879 m, 2139 s (IrH), 2094 m (CN), 2029 m (SiH), 2005 m (SiH), 1608 sh (CN), 1592 m (CN), 1489 m, 1472 w, 1368 w, 1336 w, 1279 w, 1202 m, 1185 m, 1160 m, 1134 m, 967 m, 835 m, 706 m. Anal. Calcd for $\text{C}_{39}\text{H}_{51}\text{BIrN}_5\text{O}_2\text{Si}$: C, 54.92; H, 6.03; N, 8.21. Found: C, 54.64; H, 6.56; N, 8.28. Mp, 266-269 °C.

References

1. (a) Bergman, R. G., *Science* **1984**, *223*, 902-908. (b) Labinger, J. A.; Bercaw, J. E., *Nature* **2002**, *417*, 507-514.
2. Chaloner, P. A., *Homogeneous hydrogenation*. Kluwer Academic Publishers: Dordrecht; Boston, 1993.
3. Marciniak, B., *Hydrosilylation: a comprehensive review on recent advances*. Springer: Berlin, 2009.
4. Leeuwen, P. W. N. M.; Claver, C., Rhodium Catalyzed Hydroformylation. In *Catalysis by Metal Complexes*, Springer: Dordrecht, 2002.
5. (a) Bosnich, B., *Acc. Chem. Res.* **1998**, *31*, 667-674. (b) Leung, J. C.; Krische, M. J., *Chem. Sci.* **2012**, *3*, 2202-2209. (c) Roy, A. H.; Lenges, C. P.; Brookhart, M., *J. Am. Chem. Soc.* **2007**, *129*, 2082-2093.
6. Doughty, D. H.; Pignolet, L. H., *J. Am. Chem. Soc.* **1978**, *100*, 7083-7085.
7. Ho, H.-A.; Manna, K.; Sadow, A. D., *Angew. Chem. Int. Ed.* **2012**, *51*, 8607-8610.
8. (a) Janowicz, A. H.; Bergman, R. G., *J. Am. Chem. Soc.* **1982**, *104*, 352-354. (b) Hoyano, J. K.; Graham, W. A. G., *J. Am. Chem. Soc.* **1982**, *104*, 3723-3725.
9. Ho, H.-A.; Dunne, J. F.; Ellern, A.; Sadow, A. D., *Organometallics* **2010**, *29*, 4105-4114.
10. Pawlikowski, A. V.; Gray, T. S.; Schoendorff, G.; Baird, B.; Ellern, A.; Windus, T. L.; Sadow, A. D., *Inorg. Chim. Acta* **2009**, *362*, 4517-4525.
11. Purwoko, A. A.; Lees, A. J., *Inorg. Chem.* **1996**, *35*, 675-682.
12. Duckett, S. B.; Haddleton, D. M.; Jackson, S. A.; Perutz, R. N.; Poliakov, M.; Upmacis, R. K., *Organometallics* **1988**, *7*, 1526-1532.

13. (a) Ghosh, C. K.; Hoyano, J. K.; Krentz, R.; Graham, W. A. G., *J. Am. Chem. Soc.* **1989**, *111*, 5480-5481. (b) Perez, P. J.; Poveda, M. L.; Carmona, E., *Angew. Chem. Int. Ed. Engl.* **1995**, *34*, 231-233.
14. (a) Lian, T.; Bromberg, S. E.; Yang, H.; Proulx, G.; Bergman, R. G.; Harris, C. B., *J. Am. Chem. Soc.* **1996**, *118*, 3769-3770. (b) Bromberg, S. E.; Yang, H.; Asplund, M. C.; Lian, T.; McNamara, B. K.; Kotz, K. T.; Yeston, J. S.; Wilkens, M.; Frei, H.; Bergman, R. G.; Harris, C. B., *Science* **1997**, *278*, 260-263. (c) Yeston, J. S.; McNamara, B. K.; Bergman, R. G.; Moore, C. B., *Organometallics* **2000**, *19*, 3442-3446.
15. Clot, E.; Eisenstein, O.; Jones, W. D., *Proc. Natl. Acad. Sci.* **2007**, *104*, 6939-6944.
16. Blake, A. J.; George, M. W.; Hall, M. B.; McMaster, J.; Portius, P.; Sun, X. Z.; Towrie, M.; Webster, C. E.; Wilson, C.; Zarić, S. D., *Organometallics* **2007**, *27*, 189-201.
17. Köcher, C.; Herrmann, W. A., *J. Organomet. Chem.* **1997**, *532*, 261-265.
18. Xu, S.; Everett, W. C.; Ellern, A.; Windus, T. L.; Sadow, A. D., *Dalton Trans.* **2014**, *43*, 14368-14376.
19. (a) Mazet, C.; Köhler, V.; Pfaltz, A., *Angew. Chem. Int. Ed.* **2005**, *44*, 4888-4891. (b) Köhler, V.; Mazet, C.; Toussaint, A.; Kulicke, K.; Häussinger, D.; Neuburger, M.; Schaffner, S.; Kaiser, S.; Pfaltz, A., *Chem.–Eur. J.* **2008**, *14*, 8530-8539.
20. (a) Scepaniak, J. J.; Fulton, M. D.; Bontchev, R. P.; Duesler, E. N.; Kirk, M. L.; Smith, J. M., *J. Am. Chem. Soc.* **2008**, *130*, 10515-10517. (b) Scepaniak, J. J.; Young, J. A.; Bontchev, R. P.; Smith, J. M., *Angew. Chem. Int. Ed.* **2009**, *48*, 3158-3160.

21. Scepaniak, J. J.; Vogel, C. S.; Khusniyarov, M. M.; Heinemann, F. W.; Meyer, K.; Smith, J. M., *Science* **2011**, *331*, 1049-1052.
22. Gigler, P.; Bechlars, B.; Herrmann, W. A.; Kühn, F. E., *J. Am. Chem. Soc.* **2011**, *133*, 1589-1596.
23. Schneider, N.; Finger, M.; Haferkemper, C.; Bellemin-Lapponnaz, S.; Hofman, P.; Gade, L. H., *Chem.–Eur. J.* **2009**, *15*, 11515-11529.
24. Dunne, J. F.; Manna, K.; Wiench, J. W.; Ellern, A.; Pruski, M.; Sadow, A. D., *Dalton Trans.* **2010**, *39*, 641-653.
25. Dunne, J. F.; Su, J.; Ellern, A.; Sadow, A. D., *Organometallics* **2008**, *27*, 2399-2401.
26. Hernán-Gómez, A.; Herd, E.; Hevia, E.; Kennedy, A. R.; Knochel, P.; Koszinowski, K.; Manolikakes, S. M.; Mulvey, R. E.; Schnegelsberg, C., *Angew. Chem. Int. Ed.* **2014**, *53*, 2706-2710.
27. Bucher, U. E.; Currao, A.; Nesper, R.; Rügger, H.; Venanzi, L. M.; Younger, E., *Inorg. Chem.* **1995**, *34*, 66-74.
28. Northcutt, T. O.; Lachicotte, R. J.; Jones, W. D., *Organometallics* **1998**, *17*, 5148-5152.
29. Akita, M.; Ohta, K.; Takahashi, Y.; Hikichi, S.; Moro-oka, Y., *Organometallics* **1997**, *16*, 4121-4128.
30. (a) Herrmann, W. A.; Goossen, L. J.; Spiegler, M., *Organometallics* **1998**, *17*, 2162-2168. (b) Ren, L.; Chen, A. C.; Decken, A.; Crudden, C. M., *Can. J. Chem.* **2004**, *82*, 1781-1787.
31. Bonati, F.; Wilkinson, G., *J. Chem. Soc.* **1964**, 3156-3160.

32. Bucher, U. E.; Fässler, T. F.; Hunziker, M.; Nesper, R.; Rügger, H.; Venanzi, L. M., *Gazz. Chim. Ital.* **1995**, *125*, 181-188.
33. Jeletic, M. S.; Jan, M. T.; Ghiviriga, I.; Abboud, K. A.; Veige, A. S., *Dalton Trans.* **2009**, 2764-2776.
34. Bernskoetter, W. H.; Lobkovsky, E.; Chirik, P. J., *Organometallics* **2005**, *24*, 6250-6259.
35. Batsanov, S. S., *Inorg. Mater.* **2001**, *37*, 871-885.
36. Del Ministro, E.; Renn, O.; Rügger, H.; Venanzi, L. M.; Burckhardt, U.; Gramlich, V., *Inorg. Chim. Acta* **1995**, *240*, 631-639.
37. Albinati, A.; Bovens, M.; Rügger, H.; Venanzi, L. M., *Inorg. Chem.* **1997**, *36*, 5991-5999.
38. Netland, K. A.; Krivokapic, A.; Tilset, M., *J. Coord. Chem.* **2010**, *63*, 2909-2927.
39. Cotton, F. A.; Wilkinson, G. *Advanced Inorganic Chemistry*, 4th ed.; Wiley: New York, 1980; p 947.
40. Molinos, E.; Brayshaw, S. K.; Kociok-Köhn, G.; Weller, A. S., *Dalton Trans.* **2007**, 4829-4844.
41. (a) Scott, N. M.; Dorta, R.; Stevens, E. D.; Correa, A.; Cavallo, L.; Nolan, S. P., *J. Am. Chem. Soc.* **2005**, *127*, 3516-3526. (b) Dorta, R.; Stevens, E. D.; Nolan, S. P., *J. Am. Chem. Soc.* **2004**, *126*, 5054-5055. (c) Huang, J.; Stevens, E. D.; Nolan, S. P., *Organometallics* **2000**, *19*, 1194-1197.
42. Peters, J. C.; Feldman, J. D.; Tilley, T. D., *J. Am. Chem. Soc.* **1999**, *121*, 9871-9872.
43. Turculet, L.; Feldman, J. D.; Tilley, T. D., *Organometallics* **2004**, *23*, 2488-2502.

44. (a) Tanke, R. S.; Crabtree, R. H., *Inorg. Chem.* **1989**, *28*, 3444-3447. (b) Alvarado, Y.; Boutry, O.; Gutiérrez, E.; Monge, A.; Nicasio, M. C.; Poveda, M. L.; Pérez, P. J.; Ruíz, C.; Bianchini, C.; Carmona, E., *Chem.–Eur. J.* **1997**, *3*, 860-873.
45. Ho, H.-A.; Gray, T. S.; Baird, B.; Ellern, A.; Sadow, A. D., *Dalton Trans.* **2011**, *40*, 6500-6514.
46. Sexton, C. J.; Lopez-Serrano, J.; Lledos, A.; Duckett, S. B., *Chem. Commun.* **2008**, 4834-4836.
47. McGhee, W. D.; Bergman, R. G., *J. Am. Chem. Soc.* **1988**, *110*, 4246-4262.
48. (a) Scott, N. M.; Pons, V.; Stevens, E. D.; Heinekey, D. M.; Nolan, S. P., *Angew. Chem. Int. Ed.* **2005**, *44*, 2512-2515. (b) Corberán, R.; Sanaú, M.; Peris, E., *Organometallics* **2006**, *25*, 4002-4008. (c) Phillips, N.; Tang, C. Y.; Tirfoin, R.; Kelly, M. J.; Thompson, A. L.; Gutmann, M. J.; Aldridge, S., *Dalton Trans.* **2014**, *43*, 12288-12298.
49. (a) Keyes, M. C.; Young, V. G., Jr.; Tolman, W. B., *Organometallics* **1996**, *15*, 4133-4140. (b) Slugovc, C.; Mereiter, K.; Trofimenko, S.; Carmona, E., *Chem. Commun.* **2000**, 121-122. (c) Conejero, S.; Esqueda, A. C.; Valpuesta, J. E. V.; Álvarez, E.; Maya, C.; Carmona, E., *Inorg. Chim. Acta* **2011**, *369*, 165-172.
50. Cristóbal, C.; Hernández, Y. A.; López-Serrano, J.; Paneque, M.; Petronilho, A.; Poveda, M. L.; Salazar, V.; Vattier, F.; Álvarez, E.; Maya, C.; Carmona, E., *Chem.–Eur. J.* **2013**, *19*, 4003-4020.
51. Belt, S. T.; Grevels, F. W.; Klotzbuecher, W. E.; McCamley, A.; Perutz, R. N., *J. Am. Chem. Soc.* **1989**, *111*, 8373-8382.
52. Jones, W. D.; Hessell, E. T., *J. Am. Chem. Soc.* **1993**, *115*, 554-562.

53. (a) Behrens, U.; Dahlenburg, L., *J. Organomet. Chem.* **1976**, *116*, 103-111. (b) Whited, M. T.; Zhu, Y.; Timpa, S. D.; Chen, C.-H.; Foxman, B. M.; Ozerov, O. V.; Grubbs, R. H., *Organometallics* **2009**, *28*, 4560-4570. (c) Salomon, M. A.; Braun, T.; Krossing, I., *Dalton Trans.* **2008**, 5197-5206. (d) Franken, A.; McGrath, T. D.; Stone, F. G. A., *J. Am. Chem. Soc.* **2006**, *128*, 16169-16177. (e) Franken, A.; McGrath, T. D.; Stone, F. G. A., *Organometallics* **2008**, *27*, 148-151. (f) Carr, M. J.; McGrath, T. D.; Stone, F. G. A., *Inorg. Chem.* **2008**, *47*, 713-722.
54. Corey, J. Y., *Chem. Rev.* **2011**, *111*, 863-1071.
55. Rosenberg, L.; Davis, C. W.; Yao, J., *J. Am. Chem. Soc.* **2001**, *123*, 5120-5121.
56. (a) Drolet, D. P.; Lees, A. J., *J. Am. Chem. Soc.* **1992**, *114*, 4186-4194. (b) Lees, A. J.; Purwoko, A. A., *Coord. Chem. Rev.* **1994**, *132*, 155-160. (c) Ragaini, F.; Pizzotti, M.; Cenini, S.; Abboto, A.; Pagani, G. A.; Demartin, F., *J. Organomet. Chem.* **1995**, *504*, 107-113. (d) Purwoko, A. A.; Lees, A. J., *Inorg. Chem.* **1995**, *34*, 424-425. (e) Purwoko, A. A.; Tibensky, S. D.; Lees, A. J., *Inorg. Chem.* **1996**, *35*, 7049-7055. (f) Lees, A. J., *J. Organomet. Chem.* **1998**, *554*, 1-11. (g) Dunwoody, N.; Lees, A. J., *Organometallics* **1997**, *16*, 5770-5778. (h) Panesar, R. S.; Dunwoody, N.; Lees, A. J., *Inorg. Chem.* **1998**, *37*, 1648-1650. (i) Dunwoody, N.; Sun, S.-S.; Lees, A. J., *Inorg. Chem.* **2000**, *39*, 4442-4451.
57. Ghosh, C. K.; Rodgers, D. P. S.; Graham, W. A. G., *J. Chem. Soc., Chem. Commun.* **1988**, 1511-1512.
58. Gridnev, A. A.; Mihaltseva, I. M., *Synth. Commun.* **1994**, *24*, 1547-1555.
59. Occhipinti, G.; Jensen, V. R.; Törnroos, K. W.; Frøystein, N. Å.; Bjørsvik, H.-R., *Tetrahedron* **2009**, *65*, 7186-7194.

60. Giordano, G.; Crabtree, R. H., *Inorg. Synth.* **1979**, *19*, 218-220.
61. van der Ent, A.; Onderdelinden, A. L., *Inorg. Synth.* **1990**, *28*, 90-92.
62. Powell, J.; Shaw, B. L., *J. Chem. Soc. A*, **1968**, 211-212.
63. Herde, J. L.; Lambert, J. C.; Senoff, C. V., *Inorg. Synth.* **1974**, *15*, 18-20.

**CHAPTER 4. CATALYTIC PARTIAL DEOXYGENATION OF ESTERS WITH
AN OXAZOLINE-COORDINATED RHODIUM SILYLENE**

Modified from a paper submitted to *Chemical Science*

Songchen Xu, Jeffery S. Boschen, Takeshi Kobayashi, Marek Pruski, Theresa L. Windus,
and Aaron D. Sadow

Abstract

An electrophilic, coordinatively unsaturated rhodium complex supported by a borate-linked ligand containing *N*-heterocyclic carbene, oxazoline, and oxazoline-coordinated silylene donors [$\{\kappa^3\text{-N,Si,C-PhB(Ox}^{\text{Me}_2})\text{(Ox}^{\text{Me}_2}\text{SiHPh)Im}^{\text{Mes}}\}\text{Rh(H)CO}][\text{HB(C}_6\text{F}_5)_3]$ (**2**, Ox^{Me2} = 4,4-dimethyl-2-oxazoline; Im^{Mes} = 1-mesitylimidazole) is synthesized from the neutral rhodium silyl complex $\{\text{PhB(Ox}^{\text{Me}_2})_2\text{Im}^{\text{Mes}}\}\text{RhH(SiH}_2\text{Ph)CO}$ (**1**) and B(C₆F₅)₃. The unusual Rh–Si–N structure in **2** is proposed to form by rearrangement of an unobserved isomeric cationic rhodium silylene species [$\{\text{PhB(Ox}^{\text{Me}_2})_2\text{Im}^{\text{Mes}}\}\text{RhH(SiHPh)CO}][\text{HB(C}_6\text{F}_5)_3]$ generated by hydrogen abstraction. Complex **2** catalyzes reductions of organic carbonyl compounds with silanes to give hydrosilylation products or deoxygenation products. The pathway is primarily influenced by the degree of substitution of the silane. Primary silanes give deoxygenation of esters to ethers, amides to amines, and ketones and aldehydes to hydrocarbons, whereas tertiary silanes react to give 1,2-hydrosilylation of the carbonyl functionality. The products of reactions of carbonyls and phenylsilane as catalyzed by **2**

are distinguished from those of the strong Lewis acid $B(C_6F_5)_3$, demonstrating that the rhodium complex imparts selectivity to the reduction process.

Introduction

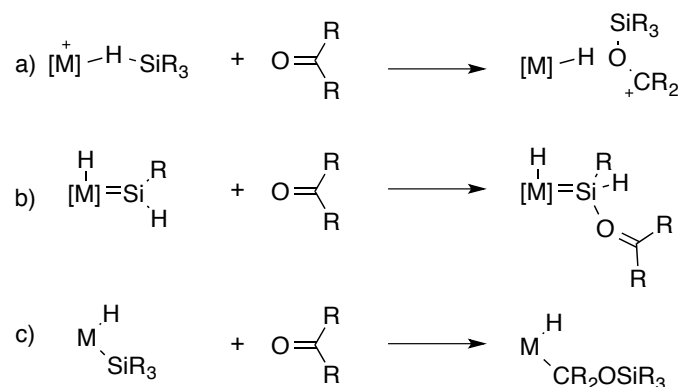
Carbon-oxygen cleavage reactions are critical for fuel and chemical applications of biologically-derived feedstocks.¹ Selective partial reductions are an important part of an overall strategy for biorenewable conversions,² and these transformations can be considered the counterpart to selective partial oxidation of hydrocarbons typically sought for petrochemical conversions. In this regard, recent advances have shown that complete deoxygenation of sugars and protected sugars into hydrocarbons may be affected by silanes in the presences of strong Lewis acid catalysts.³ Ester linkages are also common in renewable feedstock, for example in the methyl esters of biodiesel,⁴ in polylactic acid and other biorenewable polyesters,⁵ as well as in downstream chemicals obtained from lignin or carboxylic acid derivatives. Esters typically react under reducing conditions to give alcohols or protected alcohols through C–O cleavage, and complete C–O bond hydrogenolysis to alkanes is obtained under more forcing conditions. Thus, selective catalytic deoxygenations of esters could create new conversions of biorenewable chemicals, and new catalysts and processes are needed to facilitate these transformations.

A few stoichiometric methods, sought for application in synthesis, are available for the conversion of cyclic esters to ethers including the combination of $LiAlH_4$,⁶ or DIBAL and Et_3SiH with $BF_3 \cdot OEt_2$.⁷ Alternatively, a two-step procedure involves conversion of esters to thioesters followed by Raney nickel-catalyzed hydrosulfurization.⁸ Catalytic methods involving silanes as stoichiometric oxygen acceptors convert acyclic esters to ethers, led by a seminal manganese-catalyzed

hydrosilylation/deoxygenation that provides mixtures of ethers and alkoxy silanes with primary silanes as the reducing agent.⁹ More recently, group 8-based multimetallic carbonyl compounds also catalyze ether formation using trialkylsilanes (Ru) or tetramethyldisiloxane (Fe).¹⁰ However, the use of other metal precursors dramatically diverts the products to the more common ester reductive cleavage,¹¹ and even gives partial reduction to aldehydes in combination with choice of organosilane.¹² Likewise, titanium complexes catalyzed hydrosilylations to give ester cleavage or partial reduction of lactones to lactols, depending on catalytic conditions and silane reductant.¹³ Alternatively, gallium bromide¹⁴ and indium bromide¹⁵ Lewis acid catalysts employ tertiary silanes or disiloxanes for conversions of esters to ethers, whereas $B(C_6F_5)_3$ catalyzes hydrosilylation.¹⁶

Key organometallic-like intermediates in the above pathways include metal silane compounds,¹⁷ and metal silylene compounds (Scheme 1, a and b).¹⁸ Metal-coordinated silylenes are known to have Lewis acid character,¹⁹ and are proposed as catalytic intermediates in the hydrosilylation of carbonyls and olefins.^{18,20} The formation of metal-coordinated silylenes may involve α -hydrogen migration steps, while the reverse migrations of hydrogen to a metal-coordinated silylene or partial migrations of hydrogen give bridging M–H–Si structures in metal silyl or silane complexes. In this context, it is noteworthy that a number of alternatives to Chalk-Harrod or Ojima mechanisms for hydrosilylation are available, even with group 9 catalysts that might be readily anticipated to follow a classical oxidative addition/insertion pathway.²¹ For example, rhodium-coordinated silylenes are invoked as intermediates in a cationic carbene-oxazoline rhodium(I)-catalyzed carbonyl hydrosilylation.^{18a,22}

We synthesized the zwitterionic rhodium(III) silyl hydride containing the mixed carbene-oxazoline borate ligand $\{\text{PhB}(\text{Ox}^{\text{Me}2})_2\text{Im}^{\text{Mes}}\}\text{RhH}(\text{SiH}_2\text{Ph})\text{CO}$ (**1**, $\text{Ox}^{\text{Me}2}$ = 4,4-dimethyl-2-oxazoline; Im^{Mes} = 1-mesitylimidazole) in the previous chapter.²³ However, neither **1** nor its synthetic precursor $\{\text{PhB}(\text{Ox}^{\text{Me}2})_2\text{Im}^{\text{Mes}}\}\text{Rh}(\text{CO})_2$ show any catalytic hydrosilylation activity in the presence of ethyl acetate and phenylsilane. Therefore, we attempted to enhance the reactivity of **1** by reaction with $\text{B}(\text{C}_6\text{F}_5)_3$ to form a cationic complex. The resulting isolated material catalyzes the deoxygenation of esters to ethers, amides to amines, and ketones to alkanes in the presence of primary organosilanes as the reducing agent and oxygen-acceptors. Herein we describe the characterization of the base-stabilized silylene catalyst and its reactivity in carbonyl deoxygenation.

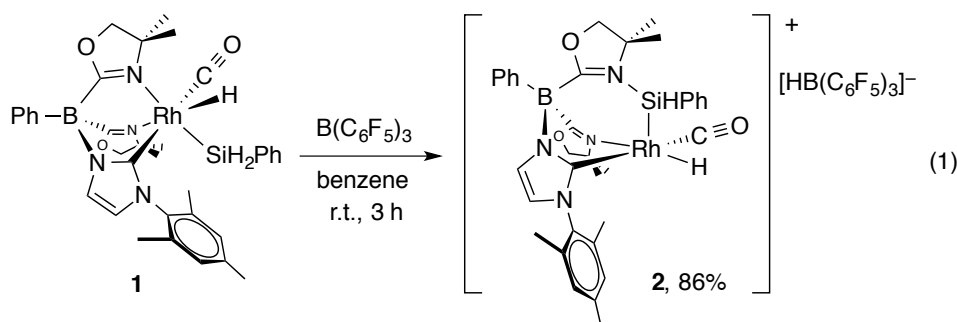


Scheme 1. Proposed steps for Si-O bond formation in carbonyl hydrosilylations.

Results and Discussion

The reaction of $\{\text{PhB}(\text{Ox}^{\text{Me}2})_2\text{Im}^{\text{Mes}}\}\text{RhH}(\text{SiH}_2\text{Ph})\text{CO}$ and $\text{B}(\text{C}_6\text{F}_5)_3$ in benzene at room temperature produces a dark oily precipitate **2** (eq. 1), and this material is purified to a black solid by washing with benzene and pentane. The NMR spectroscopic characterization is reported in bromobenzene-*d*₅, but the ¹H NMR spectra of **2** in

chloroform-*d* or methylene chloride-*d*₂ also provide evidence for the same species. Although pure material of the formulation of **2** is reproducibly obtained, its spectroscopic characterization proved challenging as described below.



The ¹H NMR spectrum of the isolated product contained one rhodium hydride resonance and one silicon hydride resonance, as well as a pattern of PhB(Ox^{Me2})₂Im^{Mes} resonances that indicated overall C₁ symmetry for the product and a set of phenyl resonances from the silyl moiety. In the isolated material, the rhodium hydride resonance was observed as a doublet of doublets at -12.92 ppm (¹J_{RhH} = 20.0 Hz, ³J_{HH} = 4.0 Hz) that integrated to 1 H in comparison to the PhB(Ox^{Me2})₂Im^{Mes} signals. For comparison, the rhodium hydride resonance of the rhodium starting material was observed at -13.36 ppm, also as a doublet of doublets (bromobenzene-*d*₅, ¹J_{RhH} = 21.3 Hz, ³J_{HH} = 1.2 Hz, 1 H). Silicon satellite signals were not detected for the rhodium hydride resonances in either **1** or **2**, and from this we rule out Rh–H–Si interactions. In **2**, a virtual triplet at 5.15 ppm (*J* = 4.0 Hz) was assigned to the single SiH, and notably that signal integrated to 1 H and interacted with the silicon center with a large one-bond coupling constant (¹J_{SiH} = 234.0 Hz). This signal was further downfield and exhibited a greater ¹J_{SiH} coupling constant than the diastereotopic SiHs in the rhodium starting material **1**, which were

observed as doublets at 4.23 and 4.68 ppm ($^2J_{\text{HH}} = 6.0$ Hz, $^1J_{\text{SiH}} = 170$ and 188 Hz, 1 H each). The increase in E–H one-bond coupling constant is typically attributed to greater *s*-character in the bond, which could result from greater *s/p* mixing in a three-coordinate silicon center or the interaction of the silicon center with a group of greater effective electronegativity than H. In line with the first possibility, a few SiH-containing metal silylene compounds with $^1J_{\text{SiH}}$ values > 200 Hz are reported.

In addition to the hydride, the rhodium coordination sphere includes the carbene and the carbonyl ligands. The $^{13}\text{C}\{^1\text{H}\}$ NMR spectrum provided evidence for coordination of these ligands based on the presence of two doublets at 186.33 ($^1J_{\text{RhC}} = 51$ Hz, NHC) and 169.23 ppm ($^1J_{\text{RhC}} = 37.5$ Hz, CO). Similar chemical shifts and splitting patterns were observed in the $^{13}\text{C}\{^1\text{H}\}$ NMR spectrum of the crystallographically characterized rhodium starting material **1** at 194.53 (d, $^1J_{\text{RhC}} = 51.0$ Hz) and 178.39 ppm (d, $^1J_{\text{RhC}} = 40.5$ Hz).

Furthermore, ^{11}B and ^{19}F NMR spectra provided support for the formation of the hydridoborate anion. Two resonances were observed in the ^{11}B NMR spectrum at -7.9 and -25 ppm assigned to the $\text{PhB}(\text{O}^{\text{Me}2})_2\text{Im}^{\text{Mes}}$ ligand and $\text{HB}(\text{C}_6\text{F}_5)_3$, respectively. The latter signal was broad (400 Hz peak width at half-height), and the $^1J_{\text{BH}}$ was not resolved. Three ^{19}F NMR resonances at -132.08 , -162.79 , and -165.72 ppm were distinguished from those of $\text{B}(\text{C}_6\text{F}_5)_3$ in bromobenzene-*d*₅, which appeared at -126.93 , -141.38 , and -158.88 ppm. The formation of $\text{HB}(\text{C}_6\text{F}_5)_3$ is further supported by mass spectral analysis in bromobenzene or chloroform in negative ion mode, which provided spectra dominated by a peak at 512.9 *m/z*.

Although the above data suggest that the hydrogen abstraction reaction with $\text{B}(\text{C}_6\text{F}_5)_3$ gives a three-coordinate silicon center bonded to phenyl, hydrogen, and rhodium, the ^{29}Si NMR chemical shift of 6.5 ppm ($^1J_{\text{RhSi}} = 42$ Hz) is not consistent with such an assignment (Table 1).^{20b-d,24-29} For comparison, the ^{29}Si NMR chemical shift of $[\text{PNP}(\text{H})\text{Ir}=\text{SiHMes}][\text{B}(\text{C}_6\text{F}_5)_4]$ (PNP = $\text{N}(2\text{-P}^i\text{Pr}_2\text{-4-MeC}_6\text{H}_3)_2$) is 246.7 ppm.^{20c}

To validate the chemical shift measured in solution, we also measured a ^{29}Si NMR spectrum of **2** in the solid state, using $^1\text{H} \rightarrow ^{29}\text{Si}$ cross-polarization under magic angle spinning (CPMAS), which similarly features a single resonance centered at 6 ppm. Calculations of ^{29}Si NMR chemical shifts for **1** and a plausible hydride abstracted product $[\{\text{PhB}(\text{Ox}^{\text{Me}_2})_2\text{Im}^{\text{Mes}}\}\text{Rh}(=\text{SiHPh})(\text{H})\text{CO}]^+$ provide additional evidence ruling out an unsaturated silicon center in **2**. The calculated atomic coordinates (**1-A**) and the coordinates of **1** determined by single crystal X-ray diffraction are in good agreement, and the calculated configuration of **1-A** maintains the *trans* disposed carbene and carbonyl ligands (Figure 1). The calculated ^{29}Si NMR chemical shift of **1-A** is 14 ppm, in reasonable agreement with the experimental value of -21 ppm. The calculated geometry of a putative rhodium silylene $[\{\text{PhB}(\text{Ox}^{\text{Me}_2})_2\text{Im}^{\text{Mes}}\}\text{Rh}(=\text{SiHPh})(\text{H})\text{CO}]^+$ (**2-A**) was optimized from a few starting configurations to the stationary point with carbene and carbonyl ligands *trans*, a hydride and oxazoline *trans*, and the SiHPh and oxazoline *trans* (Figure 1). However, the calculated ^{29}Si NMR chemical shift for **2-A** is 370 ppm as expected for a coordinatively unsaturated silicon center, and this is 364 ppm downfield from the experimental value for **2**. This difference prompted additional characterization efforts and further evaluation of possible structures of **2** that would be more consistent

with the data. Unfortunately, X-ray quality single crystals of **2** are not yet available, so we turned to additional spectroscopic tools.

Table 1. Characteristic δ_{SiH} and ^{29}Si NMR chemical shifts of the reported silylene complexes.

Complex	δ_{SiH} (ppm)	J_{SiH} (Hz)	^{29}Si (ppm)
1	4.23; 4.68	170; 188	-21.37
2	5.15	234.0	6.48
$[\text{PhBP}_3](\text{H})_2\text{Ir}=\text{SiH}(\text{Trip})^a$	11.16	-	-
$[\text{Cp}^*(i\text{Pr}_3\text{P})(\text{H})_2\text{Os}=\text{Si}(\text{H})\text{Si}(\text{SiMe}_3)_3][\text{B}(\text{C}_6\text{F}_5)_4]^b$	12.05	147.6	417.5
$\text{Cp}^*(\text{dmpe})\text{Mo}(\text{H})\text{Si}(\text{H})\text{Ph}^c$	9.45	130	250
$\text{Cp}^*(i\text{Pr}_3\text{P})(\text{H})\text{Os}=\text{SiH}(\text{trip})^d$	12.1	144	229
$[(\text{PNP})(\text{H})\text{Ir}=\text{SiH}(\text{Mes})][\text{B}(\text{C}_6\text{F}_5)_4]^e$	10.65	202	246.7
$[(\text{PNP})(\text{H})\text{Ir}=\text{SiH}(\text{Trip})][\text{B}(\text{C}_6\text{F}_5)_4]^f$	10.76	206.2	233.9
$\text{Cp}^*(i\text{Pr}_2\text{MeP})(\text{H})\text{Ru}=\text{SiH}(\text{trip})^g$	9.41	-	-
$\text{Cp}^*(i\text{Pr}_2\text{MeP})(\text{H})\text{Ru}=\text{SiH}(\text{dmp})^{g,h}$	8.00	151	204
$[\text{Cp}^*(\text{PiPr}_3)\text{Ru}(\text{H})_2(=\text{SiHMe})][\text{B}(\text{C}_6\text{F}_5)_4]^i$	7.99	226.5	228.9
$[\text{Cp}^*(\text{PiPr}_3)\text{Ru}(\text{H})_2(=\text{SiHSi}(\text{SiMe}_3)_3)][\text{B}(\text{C}_6\text{F}_5)_4]^i$	7.42	214.9	241.0
$\text{Cp}^*(\text{IXy})\text{Ru}(\mu\text{-H})(\mu\text{-AgOTf})\text{SiHTrip}^j$	7.99	175	182.2
$\text{Cp}^*(\text{IXy})\text{Ru}(\mu\text{-H})(\mu\text{-CuOTf})\text{SiHTrip}^j$	7.80	174	176.0

^a See reference 24; $[\text{PhBP}_3] = \text{PhB}(\text{CH}_2\text{PPh}_2)_3^-$; Trip = 2,4,6-triisopropylphenyl. ^b See reference 25; Cp* = 1,2,3,4,5-pentamethylcyclopentadienyl. ^c See reference 26; dmpe = 1,2-bis(dimethylphosphino)ethane. ^d See reference 20d. ^e See reference 20c; PNP = [N(2-

$P^iPr_2-4-MeC_6H_3)_2]^-$; Mes = 2,4,6- $C_6H_2Me_3$.^f See reference 20b. ^g See reference 27. ^h dmp = 2,6-Mes₂-C₆H₃. ⁱ See reference 28. ^j See reference 29; IXy = 1,3-bis(2,6-dimethylphenyl)imidazol-2-ylidene.

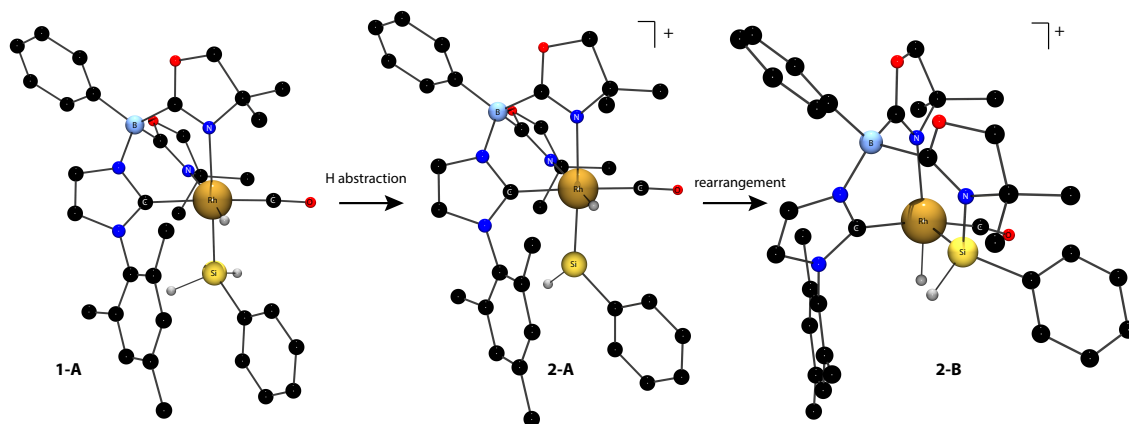


Figure 1. Calculated structure of $[\{PhB(Ox^{Me_2})_2Im^{Mes}\}Rh(SiH_2Ph)(H)CO]$ (**1-A**), $[\{PhB(Ox^{Me_2})_2Im^{Mes}\}Rh(=SiHPh)(H)CO]^+$ (**2-A**), and $[\{\kappa^3-N,Si,C-PhB(Ox^{Me_2})(Ox^{Me_2}SiHPh)Im^{Mes}\}Rh(H)CO]^+$ (**2-B**). H atoms on Si and Rh are illustrated, and all other H atoms are not included in the picture for clarity.

Mass spectrometry, in positive ion mode, provided a spectrum with the major peak at 707.21 m/z which corresponds to the calculated mass of $[\{PhB(Ox^{Me_2})_2Im^{Mes}\}RhSiH_2PhCO]^+$, indicating a monomeric species is present in the gas phase. In addition, peaks with $M^{\pm} \pm 27.99$ m/z were observed, corresponding to $[\{PhB(Ox^{Me_2})_2Im^{Mes}\}RhSiH_2Ph(CO)_2]^+$ and $[\{PhB(Ox^{Me_2})_2Im^{Mes}\}RhSiH_2Ph]^+$, which may come from gas-phase rearrangements or fragmentation of dimeric, CO bridged $[\{PhB(Ox^{Me_2})_2Im^{Mes}\}RhSiH_2PhCO]_2^{+2}$ into dicarbonyl, monocarbonyl and carbonyl-free species. There was also a peak at 601.18 m/z that corresponds to

$[\{\text{PhB}(\text{Ox}^{\text{Me}_2})_2\text{Im}^{\text{Mes}}\}\text{RhH}(\text{CO})]^+$, resulting from loss of a SiHPh group. Some evidence for the appearance of the dicarbonyl through a gas phase rearrangement comes from the reaction of **2** with CO to give $[\{\text{PhB}(\text{Ox}^{\text{Me}_2})_2\text{Im}^{\text{Mes}}\}\text{Rh}(\text{H})\text{SiHPh}(\text{CO})_2]^+$, which gives an identical parent ion m/z as the minor signals observed in the MS of **2**. The coordination of CO to **2** indicates that there is an open coordination site in the complex. Unfortunately, $[\{\text{PhB}(\text{Ox}^{\text{Me}_2})_2\text{Im}^{\text{Mes}}\}\text{Rh}(\text{H})\text{SiHPh}(\text{CO})_2]^+$ is too short-lived at room temperature for isolation or detailed NMR characterization.

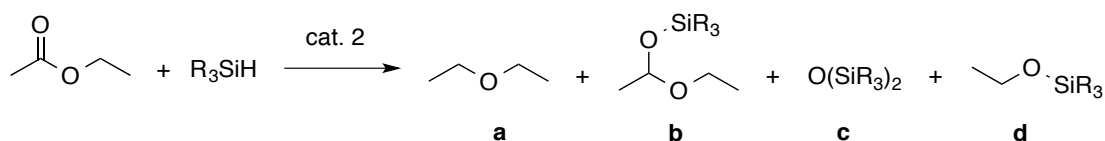
Fortunately, analysis of chemical shifts and correlations in a ^1H - ^{15}N HMBC experiments offered insight into the identity of **2**. Correlations between ^{15}N and ^1H NMR resonances assigned to 4,4-dimethyl-2-oxazoline provided ^{15}N NMR chemical shifts of -199 and -167 ppm. These chemical shifts strongly suggest that both oxazolines are coordinated in **2**. In the precursor **1**, ^{15}N NMR chemical shifts of -161 and -172 ppm were observed for rhodium-coordinated oxazolines *trans* to SiH_2Ph and hydride, respectively. One of these signals shifts 30 to 40 ppm upfield in the cationic compound **2**. Significantly, a correlation between the upfield ^{15}N signal at -199 ppm and the SiH ^1H NMR signal suggests a N-Si bond has formed in **2**. In contrast, no correlation between the RhH and its *trans*-disposed oxazoline nitrogen was detected even after extended acquisition times.

On the basis of this correlation, the isomer $[\{\kappa^3\text{-N,Si,C-PhB}(\text{Ox}^{\text{Me}_2})(\text{Ox}^{\text{Me}_2}\text{SiHPh})\text{Im}^{\text{Mes}}\}\text{Rh}(\text{H})\text{CO}]^+$ (**2-B**) was calculated (Figure 1). The optimized structure is 17 kcal/mol lower in energy than the silylene isomer **2-A**. The calculated ^{29}Si NMR chemical shift of **2-B** is 73 ppm. The remaining difference in calculated vs. experimental ^{29}Si NMR chemical shifts may be related to the cationic

charge in the gas phase vs. a solvated ionic species. In addition, the calculated ^{15}N NMR chemical shifts of the oxazolines are consistent with experiment, with the chemical shifts of the oxazoline N bonded to Si calculated to be -191 ppm and the N coordinated to Rh at -167 ppm.

Complex **2** is a precatalyst for the selective reduction of esters to ethers (**a**), silyl-protected acetals (**b**), or silyl-protected alcohols (**d**). The catalysis conditions are screened using ethyl acetate as the substrate, and the results are summarized below (Table 2). Notably, the pathway for conversion of the ester to ether vs hydrosilylation depends on the silane, with primary silanes giving selective deoxygenation and tertiary silanes giving 1,2-addition.

Phenylsilane, methylphenylsilane, and benzyldimethylsilane are representative primary, secondary, and tertiary silanes. These reagents have a dramatic effect on the chemoselectivity, as determined by micromolar scale reactions. The primary silane PhSiH_3 gives diethyl ether as the product through deoxygenation process, while the tertiary silane BnMe_2SiH gives the hydrosilylation product (**b**) and a small amount of ester cleavage product benzyl(ethoxy)dimethylsilane (**d**). The yield of ester cleavage increases with 8 equiv. of BnMe_2SiH . The secondary silane reagent PhMeSiH_2 gives a mixture of both products. In this case, the cleavage product **d** is not formed, as determined by comparison of the ^1H NMR spectrum of the reaction to an authentic sample prepared by zinc-catalyzed dehydrocoupling of PhMeSiH_2 and EtOH .³⁰ The relative amounts of diethyl ether and disiloxane byproduct from PhMeSiH_2 reduction are $\sim 1:1$ as expected by stoichiometry, while PhSiH_3 gives unquantified, presumably oligomeric siloxanes as the byproduct.

Table 2. Catalytic deoxygenation of ethyl acetate using **2**.

Entry ^a	Silane	Solvent	Time (h)	Conv. (%)	Yield (%) ^b			
					a	b	c	d
1	PhSiH ₃	C ₆ D ₅ Br	24	79	55	n.d.	n.a. ^c	n.d.
2	PhMeSiH ₂	C ₆ D ₅ Br	24	98	46	50	48 ^d	n.d.
3	BnMe ₂ SiH	C ₆ D ₅ Br	12	100	n.d.	77 (68) ^e	n.d.	8
4	BnMe ₂ SiH ^f	C ₆ D ₅ Br	12	100	n.d.	n.d.	n.d.	88
5	PhSiH ₃	CDCl ₃	0.5	100	75	n.d.	n.a. ^c	n.d.
6	PhMeSiH ₂	CDCl ₃	24	96	37	46	41 ^d	n.d.
7	BnMe ₂ SiH	CDCl ₃	24	0 ^g	n.d.	n.d.	n.d.	n.d.
8 ^h	PhSiH ₃	CDCl ₃	0.5	100	70	n.d.	n.a. ^c	n.d.

^a Reaction conditions: 1.48 mM **2**, 295 mM silane, 148 mM EtOAc, 3.12 mM Si(SiMe₃)₄ as an internal standard, r.t. ^b n.d.: not detected; n.a.: not applicable. ^c These disiloxane products are oligomeric materials and are not quantified. ^d Yield is calculated based on EtOAc, and diethyl ether (product **a**) and disiloxane (product **c**) are co-produced. ^e Isolated yield. ^f 8 equiv. of BnMe₂SiH vs. EtOAc. ^g Only starting materials observed. ^h 0.328 mM **2**.

Halogenated solvents effectively solubilize the cationic catalyst, and the solvent affects hydrosilylation and deoxygenation inequivalently. Bromobenzene is a superior

solvent than chloroform for hydrosilylation using the tertiary silane BnMe_2SiH , as the latter solvent gives no detectable conversion. In contrast, ethyl acetate deoxygenation to diethyl ether proceeds significantly more rapidly and gives a higher yield in chloroform or methylene chloride than in bromobenzene. In fact, a lower catalyst loading (0.1 mol %) gives full conversion and equivalent yields at equal reaction times to 1 mol % for the deoxygenation reaction. Unexpectedly, the effects of chloroform vs. bromobenzene are minor in reactions of ethyl acetate and PhMeSiH_2 .

On the basis of these optimized conditions for diethyl ether synthesis, compound **2** was studied as a deoxygenation catalyst for a variety of ester substrates in the presence of 2.0 equiv. of PhSiH_3 in chloroform, and the results are summarized below (Table 3).

Table 3. Reactions of esters and PhSiH_3 catalyzed by **2** or $\text{B}(\text{C}_6\text{F}_5)_3$.

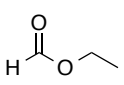
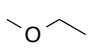
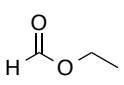
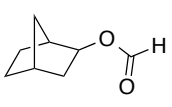
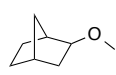
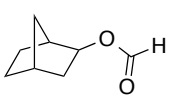

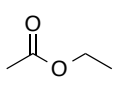
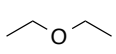
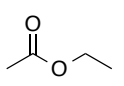
Entry ^{a,b,c}	cat. (loading, mol %)	Substrate	Temp. (°C)	Time (h)	Product	Yield (%) ^d
1 ^e	2 (0.1)		25	2.5		54
2	$\text{B}(\text{C}_6\text{F}_5)_3$ (1.0)		25	0.5	CH_4 and C_2H_6	100 ^f
3 ^g	2 (0.1)		25	25		56 (49)
4	$\text{B}(\text{C}_6\text{F}_5)_3$ (1.0)		25	0.5	 and CH_4	95 ^h
5 ^e	2 (0.1)		25	0.5		70
6	$\text{B}(\text{C}_6\text{F}_5)_3$ (1.0)		25	0.5	C_2H_6	100 ^f

Table 3 continued.

Entry ^{a,b,c}	cat. (loading, mol %)	Substrate	Temp. (°C)	Time (h)	Product	Yield (%) ^d
7	2 (1.0)		25	6		87 (62)
8	B(C ₆ F ₅) ₃ (1.0)		25	0.5	CH ₃ (CH ₂) ₁₄ CH ₃ and CH ₄	94 ^h
9 ⁱ	2 (1.0)		80	72		82 (75)
10	B(C ₆ F ₅) ₃ (1.0)		25	0.5	Br(CH ₂) ₅ CH ₃ and C ₂ H ₆	95 ^h
11 ^{ij}	2 (1.0) ^c		80	24		54 (50)
12	B(C ₆ F ₅) ₃ (1.0)		25	0.5		93 ^h
13 ⁱ	2 (1.0)		60	72		86 (62)
14	2 (1.0)		80	24		65
15	2 (1.0)		25	8		60 (55)
16	2 (2.0)		25	6		50

^a General conditions for **2**-catalyzed micromolar scale reactions: 0.5 mL chloroform-*d*, 1.64 mM **2**, 326 mM silane, 3.14 mM Si(SiMe₃)₄ (internal standard). ^b General conditions for ether isolation: 3 mL methylene chloride, 4.10 mM **2**, 837 mM silane. ^c General conditions for B(C₆F₅)₃-catalyzed micromolar scale reactions: 0.5 mL chloroform-*d*, 1.95 mM B(C₆F₅)₃, 392 mM silane, 3.14 mM Si(SiMe₃)₄ (internal standard). ^d NMR yield,

isolated yield in parentheses. ^e 0.328 mM **2**, 656 mM PhSiH₃, 328 mM EtOCHO. ^f Substrate conversion. ^g 10 mL methylene chloride, 1.23 mM **2**, 2510 mM silane. ^h NMR yield of the less volatile alkane product. ⁱ 3 mL chloroform. ^j 8367 mM silane (20 equiv. with respect to the substrate).

Typically, 1 mol % catalyst is required for conversion of most esters to ethers in Table 3, and the lower catalyst loading (0.1 mol %) determined for ethyl acetate above is effective for less sterically-demanding substrates such as ethyl formate and *exo*-2-norbornyl formate. Substrates with long alkyl chains such as methyl palmitate, or substituents with heteroatoms, such as 6-bromohexanoate and 2-thiopheneacetate, require 1 mol % catalyst loading and elevated temperature to give the ether products. The low yield for the deoxygenation of ethyl formate is probably due the volatility of the gaseous methyl ethyl ether product.

The catalysis product of *exo*-2-norbornyl formate is *exo*-2-methoxybicyclo[2.2.1]heptane (Table 3), indicating that the R–O bond in R'CO₂R is not broken during reduction. The isolated yield of the deoxygenation is comparable to the yield from *exo*-norbornol and iodomethane using sodium hydride via the Williamson ether method.³¹ Olefins are unaffected by catalytic ester deoxygenation conditions. Methyl oleate and methyl *trans*-3-pentenoate are effectively and selectively deoxygenated to their corresponding ethers in good yield, although elevated temperature is required. The stereochemistry of the C=C double bond is maintained as suggested by the ¹³C{¹H} NMR spectrum of the isolated products. The cyclic ester γ -butyrolactone is deoxygenated quickly at room temperature with moderate yield of the product, while

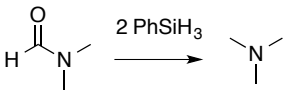
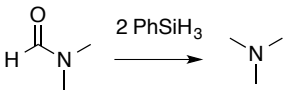
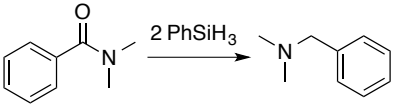
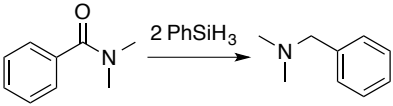
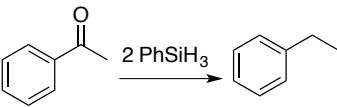
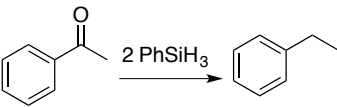
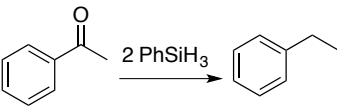
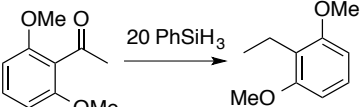
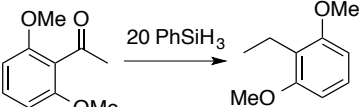
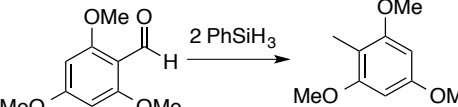
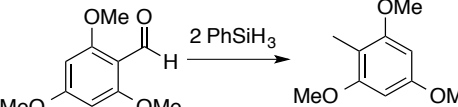
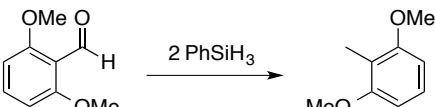
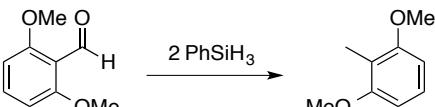
elevated temperatures result in ring opening. Both carbonyl groups in trifluoroacetic anhydride are deoxygenated with 2.0 mol % of the catalyst loading at room temperature.

Tris(perfluorophenyl)borane is a catalyst for carbonyl hydrosilylation and C–O bond cleavage in the presence of tertiary and secondary silanes,³ and might be involved in the present deoxygenation since InBr₃ and GaBr₃ are known catalysts with tertiary silanes.^{14,15} However to the best of our knowledge, B(C₆F₅)₃-catalyzed reactions of esters and primary silanes are not yet reported, and the above studies demonstrate a significant effect of silane upon the product of ester conversion. Although the ¹¹B NMR and mass spectrometry results indicated that the precatalyst contains HB(C₆F₅)₃, and no B(C₆F₅)₃ was detected by ¹¹B or ¹⁹F NMR spectroscopy, a small amount of that Lewis acid could form during catalysis. Therefore, the interaction of PhSiH₃ and esters in the presence of catalytic B(C₆F₅)₃ was tested as a possible background reaction, and the results are given for comparison to the catalytic action of **2** in Table 3. Interestingly, the combination of PhSiH₃ and B(C₆F₅)₃ with esters provides hydrocarbons (complete deoxygenation) through C–O bond cleavage rather than the selective deoxygenation to ethers observed with **2**. These experiments indicate that trace B(C₆F₅)₃, as a unilateral catalytic actor, is not responsible for selective conversion of esters to ethers.

As noted above, the common reaction pathway for esters in their reactions with hydridic reagents involves reductive cleavage of the C–O linkage. In contrast, deoxygenation of amides to amines is readily mediated by metal hydride reagents.³² Catalytic hydrosilylation of esters and amides also tend to follow the pathways established for metal hydrides, with ester hydrosilylation giving reductive cleavage and amide hydrosilylation providing amines. Thus, catalytic reactions of phenylsilane with

amides, employing **2** or B(C₆F₅)₃ as catalysts, provide further insight into the pathway for ester deoxygenation. Interestingly, both precatalysts mediate amide deoxygenation to tertiary amines (Table 4). These experiments were then extended to ketones and aldehydes, which generally give complete deoxygenation to alkane.

Table 4. Catalytic deoxygenation of aldehydes, ketones, and amides using 1 mol% **2** or B(C₆F₅)₃ as catalyst.

Entry ^{a,b,c}	cat.	Reaction	Temp. (°C)	Time (h)	Yield (%) ^d
1	2		80	3	85
2	B(C ₆ F ₅) ₃		80	3	88
3 ^e	2		80	24	86 (80) ^f
4	B(C ₆ F ₅) ₃		80	18	84
5	2		25	7	65 (58)
6	B(C ₆ F ₅) ₃		25	0.5	87
7 ^g	1		25	18	n.d. ^h
8 ⁱ	2 ^b		25	24	57 (55)
9	B(C ₆ F ₅) ₃		25	18	65
10	2		25	7	65 (48)
11	B(C ₆ F ₅) ₃		25	18	n.d. ^h
12	2		25	4	77
13	B(C ₆ F ₅) ₃		25	4	n.d. ^j

^a General conditions for **2**-catalyzed micromolar scale reactions: 0.5 mL chloroform-*d*,

1.64 mM **2**, 326 mM silane, 3.14 mM Si(SiMe₃)₄ (internal standard). ^b General conditions

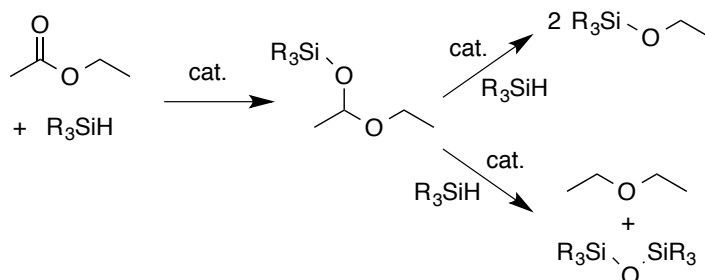
for **2**-catalyzed scaled-up reactions: 3 mL methylene chloride, 4.10 mM **2**, 837 mM silane. ^c General conditions for B(C₆F₅)₃-catalyzed micromolar scale reactions: 0.5 mL chloroform-*d*, 1.95 mM B(C₆F₅)₃, 392 mM silane, 3.14 mM Si(SiMe₃)₄ (internal standard). ^d NMR yield, isolated yield in parentheses. ^e 3 mL chloroform. ^f Isolated as the hydrochloric salt. ^g Conditions for **1**-catalyzed micromolar scale reaction: 0.5 mL chloroform-*d*, 2.54 mM **1**, 507 mM silane, 3.14 mM Si(SiMe₃)₄ (internal standard). ^h Not Detected (starting material recovered). ⁱ 8370 mM silane (20 equiv. with respect to the substrate). ^j Starting material decomposed.

Both **2** and B(C₆F₅)₃ catalyze the conversion of acetophenone to ethylbenzene, with the B(C₆F₅)₃-catalyzed reaction occurring in a shorter time. However, the dimethoxy-substituted electron-rich ketone is deoxygenated with similar reaction times with **2** or B(C₆F₅)₃, while the 2,4,6-trimethoxybenzaldehyde is selectively deoxygenated by **2** but is unreactive under B(C₆F₅)₃-catalyzed conditions at room temperature. Furthermore, the dimethoxy-substituted aldehyde decomposes under the B(C₆F₅)₃-catalyzed conditions, but is selectively deoxygenated in the presence of **2**. The neutral hydrosilyl hydridorhodium compound, which might be envisioned to catalyze ketone hydrosilylation via an oxidative addition and insertion pathway,^{21c} is not reactive under the tested catalytic conditions.

The combined results from the background reactions using B(C₆F₅)₃ and the deoxygenation reactions using **2** (Tables 3 and 4) shed some light on the pathways and active species involved in the catalyses. First, B(C₆F₅)₃ catalyzes the C–O bond cleavage reactions of ketones and amides in the presence of phenylsilane to give the same products

that are observed with **2**. However, the relative rates observed from the two catalysts vary significantly with the substrates, indicating that the reactive species in the two systems are not equivalent. That is, compound **2** is not providing free $B(C_6F_5)_3$ as the catalyst, nor is the reaction of $PhSiH_3$ with $B(C_6F_5)_3$ or **2** affording an equivalent activated organosilane species that interacts with the carbonyl substrate. This point is further emphasized by the distinct products observed from reaction of $PhSiH_3$ and esters or aldehydes, as catalyzed by **2** or $B(C_6F_5)_3$.

A possible pathway for the catalytic processes involves stepwise carbonyl hydrosilylation to give a silyl-protected acetal followed by C–O bond cleavage to provide either two silyl ethers or the ether/disiloxane products (Scheme 2).



Scheme 2. Two C–O bond cleavage pathways for the carbonyl hydrosilylation product.

A few additional points emerge from these experiments that clarifies the effect of the silane on C–O bond cleavage. First, the addition of $PhSiH_3$ to a mixture of the silyl-protected acetal $BnMe_2SiOCHMeOEt$ and $BnMe_2SiH$ increases the yield of $BnMe_2SiOEt$. This likely occurs through exchange of PhH_2SiOEt -type species with $BnMe_2SiH$, as suggested by new yet transient OEt resonances in the 1H NMR spectrum of the reaction mixture. This ester cleavage side reaction may be responsible for the

difference between conversion and yield of ethers from deoxygenation. However, the ether yield is lower when $\text{BnMe}_2\text{SiOCHMeOEt}$ is allowed to react with PhSiH_3 in comparison to the reaction of EtOAc and PhSiH_3 . The difference in ether yield may result from steric effects due to the large BnMe_2Si group, or it may reflect a different pathway accessible to SiH -substituted acetals vs. tertiary silyl substituted acetals. Regardless, these results suggest that 1,2-hydrosilylation is the first step for either ester cleavage or ester deoxygenation pathways. A related experiment with acetophenone shows that the hydrosilylation product $\text{PhMeHCOSiH}_2\text{Ph}$, obtained by reaction of PhSiH_3 and acetophenone with $\text{To}^{\text{M}}\text{ZnH}$, reacts in the presence of excess PhSiH_3 and catalytic quantities of **2** to give ethylbenzene.

Conclusions

The reaction of rhodium silyl $\{\text{PhB}(\text{Ox}^{\text{Me}_2})_2\text{Im}^{\text{Mes}}\}\text{RhH}(\text{SiH}_2\text{Ph})\text{CO}$ and $\text{B}(\text{C}_6\text{F}_5)_3$ give **2** which contains a silicon bonded to both rhodium and an oxazoline nitrogen. This species can be formulated as a rhodium-bonded silylene that is coordinated by an oxazoline donor, leaving a coordinatively unsaturated rhodium site. The preference for N–Si bonding vs. N–Rh coordination suggest that the putative silylene is more electrophilic than the rhodium center in **2**. Compound **2** is an excellent catalyst for the deoxygenation of carbonyl-containing compounds with organosilanes. Unlike many coordinatively unsaturated late-metal catalysts for hydrosilylation, redistribution of organosilanes is not observed with **2**. However, the selective conversion of substrates through hydrosilylation or deoxygenation is systematically affected by the substitution of the silane. Primary silanes give deoxygenation and tertiary silanes give hydrosilylation

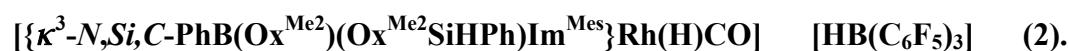
products, while secondary silanes giving mixtures of both processes. This trend is followed with $B(C_6F_5)_3$ -catalyzed reactions of silanes and carbonyls, with primary silanes giving complete deoxygenation and tertiary silanes giving addition chemistry.¹⁶ However, the selectivity, rates, and in many cases, products of **2**-catalyzed conversions are inequivalent from those of $B(C_6F_5)_3$, suggesting that the unsaturated rhodium-silyl moiety is central to the conversions observed here.

Experimental

General considerations. All reactions were performed under a dry argon atmosphere using standard Schlenk techniques or under a nitrogen atmosphere in a glovebox, unless otherwise indicated. Benzene, pentane, methylene chloride, and diethyl ether were dried and deoxygenated using an IT PureSolv system. Chloroform was heated to reflux over CaH_2 , and then distilled before use. Bromobenzene and bromobenzene- d_5 were degassed under vacuum and stored with activated molecular sieves. Benzene- d_6 was stirred over Na/K alloy and then vacuum transferred. Compound **1** was synthesized according to the previously published work.²³ Tris(perfluorophenyl)borane was synthesized from boron trichloride and bromopentafluorobenzene.³³ Phenylsilane was synthesized by reduction of trichlorophenylsilane with $LiAlH_4$. Benzyldimethylsilane was purchased from Gelest and stored over 4 Å molecular sieves in the glovebox. Ethyl acetate was purchased from Fisher Scientific, distilled over K_2CO_3 , and stored over 4 Å molecular sieves in the glovebox. Commercial esters, amides, ketones and aldehydes were degassed and stored in the glovebox. Liquid samples were stored over 4 Å molecular sieves.

^1H , $^{13}\text{C}\{^1\text{H}\}$, and ^{11}B NMR spectra were collected on an Avance II 600 MHz NMR spectrometer. ^{15}N NMR chemical shifts were determined by ^1H - ^{15}N HMBC experiments on an Avance II 600 MHz NMR spectrometer or a Bruker Avance II 700 MHz spectrometer with a Bruker Z-gradient inverse TXI $^1\text{H}/^{13}\text{C}/^{15}\text{N}$ 5 mm cryoprobe. ^{15}N chemical shifts were originally referenced to an external liquid NH_3 standard and recalculated to the CH_3NO_2 chemical shift scale by adding -381.9 ppm. ^{29}Si NMR chemical shift was determined by ^1H - ^{29}Si HMBC experiment on an Avance II 600 MHz NMR spectrometer. Infrared spectra were recorded on a Bruker Vertex spectrometer. Mass spectrometry data for the catalyst were acquired on an Agilent 6540 QTOF accurate mass spectrometer equipped with 1200 series U-HPLC system and ESI ion source. Mass spectrometry data of the isolated organic substances were acquired from an Agilent Technologies 7890A GC system coupled with 5975C inert MSD with Triple-Axis detector. Elemental analyses were performed using a Perkin-Elmer 2400 Series II CHN/S in Iowa State Chemical Instrumentation Facility.

The ^1H - ^{29}Si cross-polarization magic angle spinning (CPMAS) and ^1H MAS spectra of **2** were acquired on a 600 MHz Varian spectrometer equipped with a 1.6-mm FastMASTM T3 probe. The rotor was packed in a glove box to provide protection from air and moisture contamination and was spun using dry nitrogen gas. The experimental parameters are given in figure captions, where ν_R is the MAS rate, $\nu_{\text{RF}}(\text{X})$ is the magnitude of the RF magnetic field applied to X spins, τ_{CP} is the cross-polarization time, τ_{RD} is the recycle delay, and NS is the number of scans.



Tris(perfluorophenyl)borane (0.0895 g, 0.175 mmol) and

{PhB(Ox^{Me2})₂Im^{Mes}}RhH(SiH₂Ph)CO (**1**, 0.124 g, 0.175 mmol) were mixed in benzene (5 mL). Dark brown oily precipitate formed in a few minutes, and the solution was then stirred at room temperature for another 3 h. The top clear brown solution was decanted, and the oil was then washed with benzene (5 mL × 2) and pentane (5 mL × 1), and dried under vacuum to give the product as black solid (0.184 g, 0.151 mol, 86.3%). ¹H NMR (bromobenzene-*d*₅, 600 MHz): δ 7.65 (d, ³J_{HH} = 6.8 Hz, 2 H, *o*-BC₆H₅), 7.43 (m, 4 H, C₆H₅), 7.14 (m, 3 H, C₆H₅), 6.81 (d, ³J_{HH} = 6.8 Hz, 2 H, *o*-SiC₆H₅), 6.72 (s, 1 H, *m*-C₆H₂Me₃), 6.64 (s, 1 H, *m*-C₆H₂Me₃), 6.34 (d, ³J_{HH} = 2.0 Hz, 1 H, 4,5H-N₂C₃H₂Mes), 6.25 (d, ³J_{HH} = 2.0 Hz, 1 H, 4,5H-N₂C₃H₂Mes), 5.15 (vt, ²J_{RhH} = 4.0 Hz, ¹J_{SiH} = 234.0 Hz, 1 H, SiH), 3.89 (m, 3 H, CNCMe₂CH₂O), 3.80 (d, ²J_{HH} = 9.6 Hz, 1 H, CNCMe₂CH₂O), 2.06 (s, 3 H, *p*-C₆H₂Me₃), 1.68 (s, 3 H, *o*-C₆H₂Me₃), 1.10 (s, 3 H, CNCMe₂CH₂O), 1.07 (s, 3 H, CNCMe₂CH₂O), 1.04 (s, 3 H, CNCMe₂CH₂O), 0.76 (s, 3 H, *o*-C₆H₂Me₃), 0.68 (s, 3 H, CNCMe₂CH₂O), -12.92 (dd, ¹J_{RhH} = 20.0 Hz, ³J_{HH} = 4.0 Hz, 1 H, RhH). ¹³C{¹H} NMR (bromobenzene-*d*₅, 150 MHz): δ 186.33 (d, ¹J_{RhC} = 51 Hz, 2C-N₂C₃H₂Mes), 169.23 (d, ¹J_{RhC} = 37.5 Hz, CO), 148 (br, C₆F₅), 147 (br, C₆F₅), 138.06 (*p*-C₆H₂Me₃), 137.6 (br, *ipso*-C₆H₅), 136.4 (br, C₆F₅), 136.0 (br, *ipso*-C₆H₅), 135 (br, C₆F₅), 133.89 (*o*-BC₆H₅), 133.76 (*ipso*-C₆H₂Me₃), 133.38 (*o*-SiC₆H₅), 132.91 (*o*-C₆H₂Me₃), 131.73 (*o*-C₆H₂Me₃), 128.36 (2 *m*-C₆H₂Me₃, overlapped with C₆D₅Br), 127.03 (C₆H₅), 126.85 (C₆H₅), 126.68 (C₆H₅), 126.52 (C₆H₅), 125.18 (4,5C-N₂C₃H₂Mes, overlapped with C₆D₅Br), 122.92 (4,5C-N₂C₃H₂Mes), 80.68 (CNCMe₂CH₂O), 78.95 (CNCMe₂CH₂O), 68.39 (CNCMe₂CH₂O), 66.94 (CNCMe₂CH₂O), 26.98 (CNCMe₂CH₂O), 26.43 (CNCMe₂CH₂O), 25.04 (CNCMe₂CH₂O), 23.21 (CNCMe₂CH₂O), 19.63 (*p*-C₆H₂Me₃), 18.26 (*o*-C₆H₂Me₃), 15.12 (*o*-C₆H₂Me₃). ¹¹B NMR (bromobenzene-*d*₅, 192 MHz): δ -7.9

(PhB(Im^{Mes})(Ox^{Me2})Ox^{Me2}SiHPh), -25 (br, HB(C₆F₅)₃). ¹⁵N{¹H} NMR (bromobenzene-*d*₅, 61 MHz): δ -167.7 (CNCMe₂CH₂O), -180.7 (N₂C₃H₂Mes), -183.1 (N₂C₃H₂Mes), -199.5 (CN(SiHPh)CMe₂CH₂O). ¹⁹F NMR (bromobenzene-*d*₅, 545 MHz): δ -132.08 (*o*-C₆F₅), -162.79 (*p*-C₆F₅), -165.72 (*m*-C₆F₅). ²⁹Si NMR (bromobenzene-*d*₅, 119 MHz): δ 6.5 (¹*J*_{RhSi} = 42 Hz). IR (KBr, cm⁻¹): 3398 w, 2972 w, 2928 w, 2859 w, 2386 w, 2162 w, 2076 s, 2016 m, 2000 br, 1652 m, 1639 m, 1560 m, 1508 s, 1464 s, 1373 m, 1301 m, 1274 m, 1209 m, 1184 m, 1162 m, 1110 s, 1075 s, 968 s, 852 m, 827 m, 750 w, 738 w, 705 w, 681 w, 639 w, 567 w. EIMS (positive ion mode): 707.2 M⁺, 679.2 M⁺-CO, 629.2 M⁺-C₇H₆O, 601.2 M⁺-SiC₇H₆O, 471.3 M⁺-RhSiC₇H₇O. EIMS (negative ion mode): 512.9 HB(C₆F₅)₃⁻. Anal. Calcd for C₅₃H₄₂B₂F₁₅N₄O₃RhSi: C, 52.16; H, 3.47; N, 4.59. Found: C, 51.45; H, 3.20; N, 4.55. Mp, 89-91 °C.

Benzyl(1-ethoxyethoxy)dimethylsilane. A bromobenzene solution of **2** (0.0150 g, 0.0123 mmol, 3 mL) was added to ethyl acetate (0.120 mL, 1.23 mmol) and benzyldimethylsilane (0.390 mL, 2.46 mmol). The solution was stirred at room temperature for 12 h and then filtered through a short plug of celite (5 mL). The celite was washed with bromobenzene (3 mL × 2), the colorless filtrates were combined, and the mixture was purified by distillation. The product was distilled at 75 °C (15 mmHg) as a colorless liquid (0.200 g, 0.839 mmol, 68.2%). ¹H NMR (benzene-*d*₆, 600 MHz): δ 7.14 (m, overlapped with benzene-*d*₆, C₆H₅), 7.02 (m, 3 H, C₆H₅), 4.83 (q, ³*J*_{HH} = 4.8 Hz, 1 H, CH₃CH), 3.56 (pent, ³*J*_{HH} = 7.5 Hz, 1 H, OCH₂CH₃), 3.18 (pent, ³*J*_{HH} = 7.5 Hz, 1 H, OCH₂CH₃), 2.14 (s, 2 H, SiCH₂Ph), 1.29 (d, ³*J*_{HH} = 4.8 Hz, 3 H, CH₃CH), 1.10 (t, ³*J*_{HH} = 7.2 Hz, 3 H, OCH₂CH₃), 0.09 (s, 3 H, SiMe), 0.08 (s, 3 H, SiMe). ¹³C{¹H} NMR (benzene-*d*₆, 150 MHz): δ 139.69 (*ipso*-C₆H₅), 129.18 (*o*-C₆H₅), 128.91 (*m*-C₆H₅), 125.00

(*p*-C₆H₅), 95.85 (CH₃CH), 62.19 (OCH₂CH₃), 28.00 (SiCH₂Ph), 24.67 (CH₃CH), 15.82 (OCH₂CH₃), -0.95 (SiMe), -1.01 (SiMe). ²⁹Si{¹H} NMR (benzene-*d*₆, 119 MHz): δ 10.18. EIMS: C₁₃H₂₂O₂Si m/z 238 M⁺.

Methoxyethane. Complex **2** (0.0010 g, 0.000819 mmol) was dissolved in chloroform-*d* (0.5 mL), and the clear brown solution was added to the mixture of ethyl formate (6.5 μL, 0.0808 mmol) and phenylsilane (20.2 μL, 0.163 mmol) in a J. Young NMR tube. The internal standard solution (Si(SiMe₃)₄ in chloroform-*d*, 5.0 μL, 0.314 M) was then added before the NMR tube was sealed. The progress was monitored through ¹H NMR, and all ester was consumed after 2.5 h to give ethyl methyl ether (54.2%). The spectra matched the literature report.³⁴ ¹H NMR (chloroform-*d*, 600 MHz): δ 3.46 (q, ³J_{HH} = 6.8 Hz, 2 H, CH₂CH₃), 3.36 (s, 3 H, OMe), 1.23 (t, ³J_{HH} = 6.8 Hz, 3 H, CH₂CH₃).

exo-2-Methoxybicyclo[2.2.1]heptane. Complex **2** (0.0150 g, 0.0123 mmol) was dissolved in methylene chloride (10 mL), and the clear brown solution was added to the mixture of *exo*-2-norbornylformate (1.60 mL, 12.0 mmol) and phenylsilane (3.10 mL, 25.1 mmol). The solution was then stirred at room temperature for 24 h before it was filtered through a short plug of celite (5 mL), and the celite was further washed with methylene chloride (5 mL × 2). The clear and colorless filtrate was combined with the wash, and distilled at 760 mmHg, 167 °C to give the product as a clear and colorless liquid (0.740 g, 5.86 mmol, 48.8%). The experimental ¹H and ¹³C{¹H} NMR spectra matched those reported in the literature.³¹ ¹H NMR (chloroform-*d*, 600 MHz): δ 3.27 (s, 3 H, OMe), 3.25 (m, 1 H, 2H-C₆H₉), 2.34 (m, 1 H, 1H-C₆H₉), 2.24 (m, 1 H, 4H-C₆H₉), 1.34-1.56 (m, 5 H, C₆H₉(1,4-*η*-CH₂)), 0.96-1.10 (m, 3 H, C₆H₉(1,4-*η*-CH₂)). ¹³C{¹H} NMR (chloroform-*d*, 150 MHz): δ 84.39 (2C-C₆H₉), 56.01 (OMe), 40.06 (1C-C₆H₉),

39.49 (3C-C₆H₉), 35.30 (C₆H₉(1,4- η -CH₂), 34.90 (4C-C₆H₉), 28.67 (5C-C₆H₉), 24.77 (6C-C₆H₉). EIMS: C₈H₁₄O m/z 126 M⁺.

Diethylether. Complex **2** (0.0002 g, 0.000164 mmol) was dissolved in chloroform-*d* (0.5 mL), and the clear brown solution was added to the mixture of ethyl acetate (16.0 μ L, 0.164 mmol) and phenylsilane (40.5 μ L, 0.328 mmol) in a J. Young NMR tube. The internal standard solution (Si(SiMe₃)₄ in chloroform-*d*, 5.0 μ L, 0.314 M) was then added before the NMR tube was sealed. The progress was monitored through ¹H NMR, and all ester was consumed after 0.5 h to give the product in 70.0% yield. The NMR spectra matched those acquired using an authentic sample of diethyl ether. ¹H NMR (chloroform-*d*, 600 MHz): δ 3.51 (q, ³J_{HH} = 7.2 Hz, 4 H, CH₂CH₃), 1.24 (t, ³J_{HH} = 7.2 Hz, 6 H, CH₂CH₃).

1-Methoxyhexadecane. Complex **2** (0.0150 g, 0.0123 mmol) was dissolved in methylene chloride (3 mL), and the clear brown solution was added to the mixture of methyl palmitate (0.330 g, 1.22 mmol) and phenylsilane (0.310 mL, 2.51 mmol). The solution was then stirred at room temperature for 6 h before it was filtered through a short plug of celite (5 mL), and the celite was further washed with methylene chloride (3 mL \times 2). The clear and colorless filtrate was combined with the wash, and distilled at 0.1 mmHg, 88 °C to give the product as a clear colorless liquid (0.195 g, 0.760 mmol, 62.3%). The spectra matched the literature report.³⁵ ¹H NMR (chloroform-*d*, 600 MHz): δ 3.37 (t, ³J_{HH} = 6.6 Hz, 2 H, CH₃(CH₂)₁₄CH₂OMe), 3.34 (s, 3 H, OMe), 1.57 (m, 2 H, CH₃(CH₂)₁₃CH₂CH₂OMe), 1.3 (br, 26 H, CH₃(CH₂)₁₃CH₂CH₂OMe), 0.89 (t, ³J_{HH} = 6.6 Hz, 3 H, CH₃(CH₂)₁₅OMe). ¹³C{¹H} NMR (chloroform-*d*, 150 MHz): δ 73.14 (CH₃(CH₂)₁₄CH₂OMe), 58.67 (OMe), 32.09 (CH₃CH₂CH₂(CH₂)₁₃OMe), 29.52-29.85

(CH₃CH₂CH₂(CH₂)₁₀CH₂CH₂CH₂OMe), 26.31 (CH₃(CH₂)₁₂CH₂(CH₂)₂OMe), 22.85 (CH₃CH₂(CH₂)₁₄OMe), 14.27 (CH₃(CH₂)₁₅OMe). EIMS: C₁₇H₃₆O m/z 224 M⁺-OMe.

1-Bromo-6-ethoxyhexane. Complex **2** (0.0150 g, 0.0123 mmol) was dissolved in chloroform (3 mL), and the clear brown solution was added to the mixture of ethyl 6-bromohexanoate (0.218 mL, 1.23 mmol) and phenylsilane (0.310 mL, 2.51 mmol). The solution was then heated to 80 °C for 72 h before it was filtered through a short plug of celite (5 mL), and the celite was further washed with chloroform (3 mL × 2). The clear and colorless filtrate was combined with the wash, and distilled at 10 mmHg, 101 °C to give the product as a clear colorless liquid (0.193 g, 0.923 mmol, 75.0%). The experimental spectra matched the literature report.³⁶ ¹H NMR (chloroform-*d*, 600 MHz): δ 3.48 (q, ³J_{HH} = 6.6 Hz, 2 H, OCH₂CH₃), 3.42 (m, 4 H, BrCH₂(CH₂)₄CH₂OEt), 1.88 (m, 2 H, BrCH₂CH₂(CH₂)₄OEt), 1.57 (m, 2 H, Br(CH₂)₄CH₂CH₂OEt), 1.47 (m, 2 H, Br(CH₂)₃CH₂(CH₂)₂OEt), 1.39 (m, 2 H, Br(CH₂)₂CH₂(CH₂)₃OEt), 1.21 (t, ³J_{HH} = 6.6 Hz, 3 H, OCH₂CH₃). ¹³C {¹H} NMR (chloroform-*d*, 150 MHz): δ 70.63 (Br(CH₂)₅CH₂OEt), 66.27 (OCH₂CH₃), 34.05 (BrCH₂(CH₂)₅OEt), 32.90 (BrCH₂CH₂(CH₂)₄OEt), 29.78 (Br(CH₂)₄CH₂CH₂OEt), 28.18 (Br(CH₂)₃CH₂(CH₂)₂OEt), 25.59 (Br(CH₂)₂CH₂(CH₂)₃OEt), 15.38 (OCH₂CH₃). EIMS: C₁₈H₁₇BrO m/z 164 M⁺-OEt.

2-(2-Ethoxyethyl)thiophene. Complex **2** (0.0150 g, 0.0123 mmol) was dissolved in chloroform (3 mL), and the clear brown solution was added to the mixture of ethyl 2-thiopheneacetate (0.184 mL, 1.23 mmol) and phenylsilane (3.10 mL, 25.1 mmol). The solution was then heated to 80 °C for 24 h before it was filtered through a short plug of celite (5 mL), and the celite was further washed with chloroform (3 mL × 2). The clear and colorless filtrate was combined with the wash, and distilled at 10 mmHg, 69 °C to

give the product as a clear colorless liquid (0.0958 g, 0.613 mmol, 49.8%). The spectra of the isolated material matched the literature report.¹⁵ ¹H NMR (chloroform-*d*, 600 MHz): δ 7.15 (d, $^3J_{\text{HH}} = 4.8$ Hz, 1 H, 5H-C₄H₃S), 6.94 (t, $^3J_{\text{HH}} = 4.2$ Hz, 1 H, 4H-C₄H₃S), 6.86 (d, $^3J_{\text{HH}} = 3.0$ Hz, 1 H, $^3J_{\text{HH}} = 3.0$ Hz, 3H-C₄H₃S), 3.68 (t, $^3J_{\text{HH}} = 7.2$ Hz, 2 H, CH₂CH₂OEt), 3.53 (q, $^3J_{\text{HH}} = 7.2$ Hz, 2 H, OCH₂CH₃), 3.11 (t, $^3J_{\text{HH}} = 7.2$ Hz, 2 H, CH₂CH₂OEt), 1.24 (t, $^3J_{\text{HH}} = 7.2$ Hz, 3 H, OCH₂CH₃). ¹³C{¹H} NMR (chloroform-*d*, 150 MHz): δ 141.52 (2C-C₄H₃S), 126.78 (3C-C₄H₃S), 125.15 (4C-C₄H₃S), 123.70 (5C-C₄H₃S), 71.31 (CH₂CH₂OEt), 66.44 (OCH₂CH₃), 30.67 (CH₂CH₂OEt), 15.32 (OCH₂CH₃). EIMS: C₁₈H₁₂OS *m/z* 156 M⁺.

(Z)-1-Methoxyoctadec-9-ene. Complex **2** (0.0150 g, 0.0123 mmol) was dissolved in chloroform (3 mL), and the clear brown solution was added to the mixture of methyl oleate (0.417 mL, 1.23 mmol) and phenylsilane (0.310 mL, 2.51 mmol). The solution was then heated to 60 °C for 72 h before it was filtered through a short plug of celite (5 mL), and the celite was further washed with chloroform (3 mL × 2). The clear and colorless filtrate was combined with the wash, and distilled at 0.1 mmHg, 200 °C to give the product as a clear colorless liquid (0.215 g, 0.761 mmol, 61.9%). The spectra of the isolated material matched the literature report.¹⁴ ¹H NMR (chloroform-*d*, 600 MHz): δ 5.36 (m, 2 H, CH=CH), 3.38 (t, $^3J_{\text{HH}} = 6.6$ Hz, 2 H, CH₂OMe), 3.34 (s, 3 H, OMe), 2.03 (m, 4 H, CH₂CH=CHCH₂), 1.58 (m, 2 H, CH₂CH₂OMe), 1.3 (br, 22 H, CH₃(CH₂)₆CH₂CH=CHCH₂(CH₂)₅CH₂CH₂OMe), 0.90 (t, $^3J_{\text{HH}} = 6.6$ Hz, 3 H, CH₃(CH₂)₇CH=CH(CH₂)₈OMe). ¹³C{¹H} NMR (chloroform-*d*, 150 MHz): δ 130.00 (*cis*-CH=CH), 129.99 (*cis*-CH=CH), 73.13 (CH₂OMe), 58.69 (OMe), 32.07 (CH₃CH₂CH₂), 29.33-29.93 (CH₃CH₂CH₂(CH₂)₄CH₂CH=CHCH₂(CH₂)₆CH₂OMe), 27.37

(CH₂CH=CHCH₂), 27.36 (CH₂CH=CHCH₂), 22.84
 (CH₃CH₂(CH₂)₆CH=CH(CH₂)₈OMe), 14.27 (CH₃(CH₂)₇CH=CH(CH₂)₈OMe). EIMS:
 C₁₉H₃₈O m/z 283 M⁺.

(E)-5-Methoxypent-2-ene. Complex **2** (0.0010 g, 0.000819 mmol) was dissolved in chloroform-*d* (0.5 mL), and the clear brown solution was added to the mixture of methyl *trans*-3-pentenoate (10.0 μL, 0.0815 mmol) and phenylsilane (20.2 μL, 0.163 mmol) in a J. Young NMR tube. The internal standard solution (Si(SiMe₃)₄ in chloroform-*d*, 5.0 μL, 0.314 M) was then added. The NMR tube was sealed, and then heated to 80 °C. The progress was monitored through ¹H NMR, and all ester was consumed after 24 h. The spectra matched the literature report.³⁷ ¹H NMR (chloroform-*d*, 600 MHz): δ 5.48-5.53 (m, 2 H, CH=CH), 3.42 (t, ³J_{HH} = 10.2 Hz, 2 H, CH₂OMe), 3.37 (s, 3 H, OMe), 2.31 (m, 2 H, CH₂CH₂OMe), 1.69 (m, 3 H, CH₃CH=CH).

Tetrahydrofuran. Complex **2** (0.0300 g, 0.0246 mmol) was dissolved in methylene chloride (3 mL), and the clear brown solution was added to the mixture of γ-butyrolactone (0.200 mL, 2.60 mmol) and phenylsilane (0.640 μL, 5.19 mmol). The solution was then stirred at room temperature for 8 h before it was filtered through a short plug of celite (5 mL). The product was distilled at 65 °C (760 mmHg) to give a sample of THF (0.0520 g, 0.721 mmol, 55.4%) that matched authentic samples of tetrahydrofuran by ¹H and ¹³C{¹H} NMR spectroscopy. ¹H NMR (chloroform-*d*, 600 MHz): δ 3.7 (br, 4 H, 2,5H-C₄H₈O), 1.8 (br, 4 H, 3,4H-C₄H₈O). ¹³C{¹H} NMR (chloroform-*d*, 150 MHz): δ 68.08 (2,5C-C₄H₈O), 25.73 (3,4C-C₄H₈O). EIMS: C₄H₈O m/z 72 M⁺.

1,1,1-Trifluoro-2-(2,2,2-trifluoroethoxy)ethane. Complex **2** (0.0005 g, 0.000410 mmol) was dissolved in chloroform-*d* (0.5 mL), and the clear brown solution

was added to the mixture of trifluoroacetic anhydride (28.4 μL , 0.204 mmol) and phenylsilane (100.8 μL , 0.817 mmol) in a J. Young NMR tube. The internal standard solution ($\text{Si}(\text{SiMe}_3)_4$ in chloroform-*d*, 5.0 μL , 0.314 M) was then added. The NMR tube was sealed, and then heated to 80 °C. The progress was monitored through ^1H NMR, and all ester was consumed after 48 h. The spectra matched the literature report.³⁸ ^1H NMR (chloroform-*d*, 600 MHz): δ 3.84 (q, $^3J_{\text{HF}} = 8.0$ Hz, CH_2). ^{19}F NMR (chloroform-*d*, 376 MHz): δ -76.36 (t, $^3J_{\text{HF}} = 8.6$ Hz, CF_3).

Trimethylamine. Complex **2** (0.0010 g, 0.000819 mmol) was dissolved in chloroform-*d* (0.5 mL), and the clear brown solution was added to the mixture of *N,N*-dimethylformamide (6.3 μL , 0.0814 mmol) and phenylsilane (20.2 μL , 0.163 mmol) in a J. Young NMR tube. The internal standard solution ($\text{Si}(\text{SiMe}_3)_4$ in chloroform-*d*, 5.0 μL , 0.314 M) was then added. The NMR tube was sealed, and then heated to 80 °C. The progress was monitored through ^1H NMR, and all amide was consumed after 3 h. The spectra matched the literature report.³⁹ ^1H NMR (chloroform-*d*, 600 MHz): δ 2.24 (s, Me).

***N,N*-Dimethylbenzylammonium chloride.** Complex **2** (0.0150 g, 0.0123 mmol) was dissolved in chloroform (3 mL), and the clear brown solution was added to the mixture of *N,N*-dimethylbenzamide (0.183 g, 1.23 mmol) and phenylsilane (0.310 mL, 2.51 mmol). The solution was then heated to 80 °C for 24 h before it was filtered through a short plug of celite (5 mL), and the celite was further washed with diethylether (3 mL \times 2). The filtrate was combined with the wash, and the diethylether solution of hydrochloric acid (2.0 M, 5 mL) was added. The slightly cloudy solution was then evaporated to remove solvent and excess hydrochloric acid, and the residual white solid was washed

with more diethylether (5 mL \times 3), and dried under vacuum to give the product as a white solid (0.168 g, 0.979 mmol, 79.6%). The NMR spectra of this material matched the literature report.⁴⁰ ^1H NMR (chloroform-*d*, 600 MHz): δ 12.8 (br, 1 H, NH), 7.6 (br, 2 H, C_6H_5), 7.5 (br, 3 H, C_6H_5), 4.17 (s, 2 H, CH_2Ph), 2.75 (s, 6 H, Me). $^{13}\text{C}\{^1\text{H}\}$ NMR (chloroform-*d*, 150 MHz): δ 131.20 (*ipso*- C_6H_5), 130.41 (*o*- C_6H_5), 129.59 (*m*- C_6H_5), 128.51 (*p*- C_6H_5), 61.39 (CH_2Ph), 42.29 (Me). EIMS: $\text{C}_9\text{H}_{14}\text{ClN}$ m/z 135 $\text{M}^+ - \text{Cl}$. For *N,N*-dimethyl-1-phenylmethanamine, a chloroform-*d* solution (0.5 mL) of **2** (0.0010 g, 0.000819 mmol) was added to *N,N*-dimethylbenzamide (0.0122 g, 0.0818 mmol), phenylsilane (20.2 μL , 0.163 mmol), and $\text{Si}(\text{SiMe}_3)_4$ (0.314 M) as an internal standard. The solution was heated to 80 $^\circ\text{C}$, and the reaction progress was monitored using ^1H NMR spectroscopy which indicated the amide was consumed after 24 h (86.3%). ^1H NMR (chloroform-*d*, 600 MHz): δ 7.31-7.20 (m, 5 H, C_6H_5), 3.37 (s, 2 H, CH_2), 2.20 (s, 6 H, Me).

Ethylbenzene. Complex **2** (0.0150 g, 0.0123 mmol) was dissolved in methylene chloride (3 mL), and the clear brown solution was added to the mixture of acetophenone (0.140 mL, 1.20 mmol) and phenylsilane (0.310 mL, 2.51 mmol). The solution was then stirred at room temperature for 7 h before it was filtered through a short plug of celite (5 mL), and the celite was further washed with more methylene chloride (3 mL \times 2). The clear and colorless filtrate was combined with the wash, and distilled at 760 mmHg, 132 $^\circ\text{C}$ to give the product as a clear colorless liquid (0.0739 g, 0.696 mmol, 58.0%). The spectra matched those acquired from an authentic sample of ethylbenzene. ^1H NMR (chloroform-*d*, 600 MHz): δ 7.34 (m, 2 H, C_6H_5), 7.23 (m, 3 H, C_6H_5), 2.70 (m, 2 H, CH_2CH_3), 1.30 (m, 3 H, CH_2CH_3). $^{13}\text{C}\{^1\text{H}\}$ NMR (chloroform-*d*, 150 MHz): δ 144.38

(*ipso*-C₆H₅), 128.44 (*m*-C₆H₅), 127.99 (*o*-C₆H₅), 125.72 (*p*-C₆H₅), 29.03 (CH₂CH₃), 15.76 (CH₂CH₃). EIMS: C₈H₁₀ m/z 106 M⁺.

2-Ethyl-1,3-dimethoxybenzene. Complex **2** (0.0150 g, 0.0123 mmol) was dissolved in methylene chloride (3 mL), and the clear brown solution was added to the mixture of 2',6'-dimethoxyacetophenone (0.220 g, 1.22 mmol) and phenylsilane (3.10 mL, 25.1 mmol). The solution was then stirred at room temperature for 24 h before it was filtered through a short plug of celite (5 mL), and the celite was further washed with more methylene chloride (3 mL × 2). The clear and colorless filtrate was combined with the wash, and the product was isolated from it through column chromatography (ethyl acetate : hexane = 1 : 9, R_f = 0.85) as a white solid (0.112 g, 0.674 mmol, 55.2%). The NMR spectra of the isolated material matched the literature report.⁴¹ ¹H NMR (chloroform-*d*, 600 MHz): δ 7.13 (t, ³J_{HH} = 8.4 Hz, 1 H, 5H-C₆H₃), 6.56 (d, ³J_{HH} = 8.4 Hz, 2 H, 4,6H-C₆H₃), 3.83 (s, 6 H, OMe), 2.68 (q, ³J_{HH} = 7.2 Hz, 2 H, CH₂CH₃), 1.10 (t, ³J_{HH} = 7.2 Hz, 3 H, CH₂CH₃). ¹³C {¹H} NMR (chloroform-*d*, 150 MHz): δ 158.27 (1,3C-C₆H₃), 126.55 (5C-C₆H₃), 121.07 (2C-C₆H₃), 103.91 (4,6-C₆H₃), 55.88 (OMe), 16.43 (CH₂CH₃), 13.93 (CH₂CH₃). EIMS: C₁₀H₁₄O₂ m/z 166 M⁺.

1,3,5-Trimethoxy-2-methylbenzene. Complex **2** (0.0150 g, 0.0123 mmol) was dissolved in methylene chloride (3 mL), and the clear brown solution was added to the mixture of 2,4,6-trimethoxybenzaldehyde (0.241 g, 1.23 mmol) and phenylsilane (0.310 mL, 2.51 mmol). The solution was then stirred at room temperature for 7 h before it was filtered through a short plug of celite (5 mL). The celite was further washed with more methylene chloride (3 mL × 2). The colorless filtrates were combined, and the mixture was purified by distillation. The product was distilled at 74 °C (0.1 mmHg) as a clear

colorless liquid (0.107 g, 0.587 mmol, 47.8%). The spectra matched the literature report.⁴² ¹H NMR (chloroform-*d*, 600 MHz): δ 6.15 (s, 2 H, 4,6H-C₆H₂), 3.82 (s, 9 H, OMe), 2.03 (s, 3 H, Me). ¹³C{¹H} NMR (chloroform-*d*, 150 MHz): δ 159.07 (5C-C₆H₂), 158.95 (1,3C-C₆H₂), 106.94 (2C-C₆H₂), 90.68 (4,6C-C₆H₂), 55.86 (1,3-OMe), 55.52 (5-OMe), 7.80 (Me). EIMS: C₁₀H₁₄O₃ m/z 182 M⁺.

1,3-Dimethoxy-2-methylbenzene. A chloroform-*d* solution (0.5 mL) of **2** (0.0010 g, 0.000819 mmol) was added to 2,6-dimethoxybenzaldehyde (0.0136 g, 0.0818 mmol), phenylsilane (20.2 μ L, 0.163 mmol), and Si(SiMe₃)₄ (0.314 M) as an internal standard. The progress was monitored through ¹H NMR, and all aldehyde was consumed after 4 h to give the hydrocarbon in 77% yield. The products spectra matched the literature report.⁴¹ ¹H NMR (chloroform-*d*, 600 MHz): δ 7.15 (t, ³J_{HH} = 8.4 Hz, 1 H, 5H-C₆H₃), 6.57 (d, ³J_{HH} = 8.4 Hz, 2 H, 4,6H-C₆H₃), 3.85 (s, 6 H, OMe), 2.14 (s, 3 H, Me). ¹³C NMR (chloroform-*d*, 150 MHz): δ 158.53 (1,3C-C₆H₃), 128.41 (5C-C₆H₃), 114.67 (2C-C₆H₃), 103.67 (4,6C-C₆H₃), 55.86 (OMe), 8.27 (Me). EIMS: C₉H₁₂O₂ m/z 152 M⁺.

Computational Details. Structure optimizations were performed in TURBOMOLE⁴⁴ using B3LYP⁴⁵ density functional theory. The Stuttgart 1997 relativistic small core basis set plus effective core potential (ECP)⁴⁶ was used for Rh, and the 6-311G(d,p) basis set⁴⁷ was used for all other atoms. NMR calculations were performed in NWChem⁴⁸ using the gauge independent atomic orbital method. The same level of theory and basis sets were used as for the structure optimizations except an all electron basis, ATZP,⁴⁹ was used for Rh. The reported energies and NMR chemical shifts were obtained with the ATZP basis for Rh, but NMR results using the Stuttgart basis and ECP are included in the SI.

References

1. (a) Corma, A.; Iborra, S.; Velty, A. *Chem. Rev.* **2007**, *107*, 2411-2502. (b) Zakzeski, J.; Bruijninx, P. C. A.; Jongerius, A. L.; Weckhuysen, B. M. *Chem. Rev.* **2010**, *110*, 3552-3599. (c) Huber, G. W.; Iborra, S.; Corma, A. *Chem. Rev.* **2006**, *106*, 4044-4098. (d) Bozell, J. J.; Peterson, G. R. *Green Chem.* **2010**, *12*, 539-554.
2. (a) Rahimi, A.; Ulbrich, A.; Coon, J. J.; Stahl, S. S. *Nature* **2014**, *515*, 249-252. (b) Ahmad, I.; Chapman, G.; Nicholas, K. M. *Organometallics* **2011**, *30*, 2810-2818. (c) Sergeev, A. G.; Hartwig, J. F. *Science* **2011**, *332*, 439-443. (d) Hanson, S. K.; Baker, R. T.; Gordon, J. C.; Scott, B. L.; Thorn, D. L. *Inorg. Chem.* **2010**, *49*, 5611-5618. (e) Nichols, J. M.; Bishop, L. M.; Bergman, R. G.; Ellman, J. A. *J. Am. Chem. Soc.* **2010**, *132*, 12554-12555. (f) Arceo, E.; Ellman, J. A.; Bergman, R. G. *J. Am. Chem. Soc.* **2010**, *132*, 11408-11409. (g) Vkuturi, S.; Chapman, G.; Ahmad, I.; Nicholas, K. M. *Inorg. Chem.* **2010**, *49*, 4744-4746. (h) Ziegler, J. E.; Zdilla, M. J.; Evans, A. J.; Abu-Omar, M. M. *Inorg. Chem.* **2009**, *48*, 9998-10000. (i) Schlaf, M.; Ghosh, P.; Fagan, P. J.; Hauptman, E.; Bullock, R. M. *Adv. Synth. Catal.* **2009**, *351*, 789-800. (j) Schlaf, M.; Ghosh, P.; Fagan, P. J.; Hauptman, E.; Bullock, R. M. *Angew. Chem. Int. Ed.* **2001**, *40*, 3887-3890.
3. (a) Adduci, L. L.; McLaughlin, M. P.; Bender, T. A.; Becker, J. J.; Gagné, M. R. *Angew. Chem. Int. Ed.* **2014**, *53*, 1646-1649. (b) Robert, T.; Oestreich, M. *Angew. Chem. Int. Ed.* **2013**, *52*, 5216-5218.
4. Ma, F. R.; Hanna, M. A. *Bioresour. Technol.* **1999**, *70*, 1-15.

5. Dechy-Cabaret, O.; Martin-Vaca, B.; Bourissou, D. *Chem. Rev.* **2004**, *104*, 6147-6176.
6. (a) Pettit, G.; Ghatak, U.; Green, B.; Kasturi, T.; Piatak, D. *J. Org. Chem.* **1961**, *26*, 1685-1686. (b) Pettit, G.; Kasturi, T. *J. Org. Chem.* **1960**, *25*, 875-876. (c) Pettit, G. R.; Piatak, D. M. *J. Org. Chem.* **1962**, *27*, 2127-2130.
7. Kraus, G. A.; Frazier, K. A.; Roth, B. D.; Taschner, M. J.; Neuenschwander, K. J. *Org. Chem.* **1981**, *46*, 2417-2419.
8. Baxter, S. L.; Bradshaw, J. S. *J. Org. Chem.* **1981**, *46*, 831-832.
9. Mao, Z.; Gregg, B. T.; Cutler, A. R. *J. Am. Chem. Soc.* **1995**, *117*, 10139-10140.
10. Das, S.; Li, Y.; Junge, K.; Beller, M. *Chem. Commun.* **2012**, *48*, 10742-10744.
11. Junge, K.; Wendt, B.; Zhou, S.; Beller, M. *Eur. J. Org. Chem.* **2013**, 2061-2065.
12. Li, H.; Misal Castro, L. C.; Zheng, J.; Roisnel, T.; Dorcet, V.; Sortais, J.-B.; Darcel, C. *Angew. Chem. Int. Ed.* **2013**, *52*, 8045-8049.
13. (a) Berk, S. C.; Kreutzer, K. A.; Buchwald, S. L. *J. Am. Chem. Soc.* **1991**, *113*, 5093-5095. (b) Verdaguer, X.; Berk, S. C.; Buchwald, S. L. *J. Am. Chem. Soc.* **1995**, *117*, 12641-12642.
14. Biermann, U.; Metzger, J. O. *ChemSusChem* **2014**, *7*, 644-649.
15. Sakai, N.; Moriya, T.; Konakahara, T. *J. Org. Chem.* **2007**, *72*, 5920-5922.
16. (a) Blackwell, J. M.; Morrison, D. J.; Piers, W. E. *Tetrahedron* **2002**, *58*, 8247-8254. (b) Parks, D. J.; Blackwell, J. M.; Piers, W. E. *J. Org. Chem.* **2000**, *65*, 3090-3098. (c) Parks, D. J.; Piers, W. E. *J. Am. Chem. Soc.* **1996**, *118*, 9440-9441.
17. (a) Lipke, M. C.; Tilley, T. D. *J. Am. Chem. Soc.* **2014**, *136*, 16387-16398. (b) Park, S.; Brookhart, M. *Organometallics* **2010**, *29*, 6057-6064.

18. (a) Schneider, N.; Finger, M.; Haferkemper, C.; Bellemin-Lapponnaz, S.; Hofmann, P.; Gade, L. H. *Angew. Chem. Int. Ed.* **2009**, *48*, 1609-1613. (b) Calimano, E.; Tilley, T. D. *Organometallics* **2010**, *29*, 1680-1692.
19. Waterman, R.; Hayes, P. G.; Tilley, T. D. *Acc. Chem. Res.* **2007**, *40*, 712-719.
20. (a) Fasulo, M. E.; Lipke, M. C.; Tilley, T. D. *Chem. Sci.* **2013**, *4*, 3882-3887. (b) Calimano, E.; Tilley, T. D. *J. Am. Chem. Soc.* **2009**, *131*, 11161-11173. (c) Calimano, E.; Tilley, T. D. *J. Am. Chem. Soc.* **2008**, *130*, 9226-9227. (d) Hayes, P. G.; Beddie, C.; Hall, M. B.; Waterman, R.; Tilley, T. D. *J. Am. Chem. Soc.* **2006**, *128*, 428-429. (e) Glaser, P. B.; Tilley, T. D. *J. Am. Chem. Soc.* **2003**, *125*, 13640-13641.
21. (a) Marciniak, B. *Hydrosilylation: A comprehensive review on recent advances*. Springer: Berlin, 2009; p xxiv, 408 p. (b) Marciniak, B. *Comprehensive handbook on hydrosilylation*. Pergamon Press: Oxford; New York, 1992; p xi, 754 p. (c) Ojima, I.; Kogure, T.; Kumagai, M. *J. Org. Chem.* **1977**, *42*, 1671-1679.
22. (a) César, V.; Bellemin-Lapponnaz, S.; Wadepohl, H.; Gade, L. H. *Chem. Eur. J.* **2005**, *11*, 2862-2873. (b) Gade, L. H.; César, V.; Bellemin-Lapponnaz, S. *Angew. Chem. Int. Ed.* **2004**, *43*, 1014-1017. (c) Cheng, C.; Brookhart, M. *Angew. Chem. Int. Ed.* **2012**, *51*, 9422-9424.
23. Xu, S.; Manna, K.; Ellern, A.; Sadow, A. D. *Organometallics* **2014**, *33*, 6840-6860.
24. Feldman, J. D.; Peters, J. C.; Tilley, T. D. *Organometallics* **2002**, *21*, 4065-4075.
25. Glaser, P. B.; Tilley, T. D. *Organometallics* **2004**, *23*, 5799-5812.

26. Mork, B. V.; Tilley, T. D.; Schultz, A. J.; Cowan, J. A. *J. Am. Chem. Soc.* **2004**, *126*, 10428-10440.
27. Hayes, P. G.; Waterman, R.; Glaser, P. B.; Tilley, T. D. *Organometallics* **2009**, *28*, 5082-5089.
28. Fasulo, M. E.; Glaser, P. B.; Tilley, T. D. *Organometallics* **2011**, *30*, 5524-5531.
29. Liu, H.-J.; Raynaud, C.; Eisenstein, O.; Tilley, T. D. *J. Am. Chem. Soc.* **2014**, *136*, 11473-11482.
30. Mukherjee, D.; Thompson, R. R.; Ellern, A.; Sadow, A. D. *ACS Catal.* **2011**, 698-702.
31. Hirai, T.; Hamasaki, A.; Nakamura, A.; Tokunaga, M. *Org. Lett.* **2009**, *11*, 5510-5513.
32. Dodds, D. L.; Cole-Hamilton, D. J. Catalytic Reduction of Amides Avoiding LiAlH_4 or B_2H_6 . In *Sustainable catalysis: Challenges and practices for the pharmaceutical and fine chemical industries*, Dunn, P. J.; Hii, K. K.; Krische, M. J.; Williams, M. T., Eds. Wiley: Hoboken NJ, 2013; pp1-36.
33. Massey, A. G.; Park, A. J., *J. Organomet. Chem.* **1964**, *2*, 245-250.
34. Champion, C. L.; Li, W.; Lucht, B. L. *J. Electrochem. Soc.* **2005**, *152*, A2327-A2334.
35. Gasparrini, F.; Caglioti, L.; Misiti, D.; Palmieri, G.; Ballini, R. *Tetrahedron* **1982**, *38*, 3609-3613.
36. Matsubara, K.; Iura, T.; Maki, T.; Nagashima, H. *J. Org. Chem.* **2002**, *67*, 4985-4988.
37. Smith, M. B.; Hrubiec, R. T.; Zezza, C. A. *J. Org. Chem.* **1985**, *50*, 4815-4821.

38. Wu, K.; Chen, Q.-Y. *J. Fluorine Chem.* **2002**, *113*, 79-83.
39. Pohl, R.; Dračinský, M.; Slavětinská, L.; Buděšínský, M., *Magn. Reson. Chem.* **2011**, *49*, 320-327.
40. Hanada, S.; Tsutsumi, E.; Motoyama, Y.; Nagashima, H., *J. Am. Chem. Soc.* **2009**, *131*, 15032-15040.
41. Azzena, U.; Denurra, T.; Melloni, G.; Piroddi, A. M. *J. Org. Chem.* **1990**, *55*, 5386-5390.
42. de Haro, T.; Nevado, C. *J. Am. Chem. Soc.* **2010**, *132*, 1512-1513.
43. Ahlrichs, R.; Baer, M.; Haeser, M.; Horn, H.; Kölmel, C. *Chem. Phys. Lett.* **1989**, *162*, 165-169.
44. Ahlrichs, R.; Bär, M.; Häser, M.; Horn, H.; Kölmel, C. *Chem. Phys. Lett.* **1989**, *162*, 165-169.
45. (a) Becke, A. D. *J. Chem. Phys.* **1993**, *98*, 5648-5652. (b) Lee, C.; Yang, W.; Parr, R. G. *Phys. Rev. B* **1988**, *37*, 785-789. (c) Vosko, S. H.; Wilk, L.; Nusair, M. *Can. J. Phys.* **1980**, *58*, 1200-1211. (d) Stephens, P. J.; Devlin, F. J.; Chabalowski, C. F.; Frisch, M. J. *J. Phys. Chem.* **1994**, *98*, 11623-11627.
46. Andrae, D.; Häußermann, U.; Dolg, M.; Stoll, H.; Preuß, H. *Theor. Chim. Acta* **1990**, *77*, 123-141.
47. (a) Krishnan, R.; Binkley, J. S.; Seeger, R.; Pople, J. A. *J. Chem. Phys.* **1980**, *72*, 650-654. (b) McLean, A. D.; Chandler, G. S. *J. Chem. Phys.* **1980**, *72*, 5639-5648.

48. Valiev, M.; Bylaska, E. J.; Govind, N.; Kowalski, K.; Straatsma, T. P.; Van Dam, H. J. J.; Wang, D.; Nieplocha, J.; Apra, E.; Windus, T. L.; de Jong, W. A. *Comput. Phys. Commun.* **2010**, *181*, 1477-1489.
49. Martins, L. S. C.; de Souza, F. A. L.; Ceolin, G. A.; Jorge, F. E.; de Berrêdo, R. C.; Campos, C. T. *Comput. Theor. Chem.* **2013**, *1013*, 62-69.

**CHAPTER 5. ORGANOMETALLIC COMPLEXES OF
BULKY AND OPTICALLY ACTIVE C₃-SYMMETRIC TRIS(4*S*-ISOPROPYL-
5,5-DIMETHYL-2-OXAZOLINYL)PHENYLBORATE (To^{P*})**

Modified from a paper accepted by *Organometallics*

Songchen Xu, Yitzhak Magoon, Regina R. Reinig, Bradley M. Schmidt, Arkady Ellern,
and Aaron D. Sadow

Abstract

A new bulky, optically active monoanionic scorpionate ligand tris(4*S*-isopropyl-5,5-dimethyl-2-oxazolinyl)phenylborate (To^{P*}) is synthesized from the naturally occurring amino acid L-valine as its lithium salt Li[To^{P*}] (**1**). That species is readily converted to a thallium complex Tl[To^{P*}] (**2**) and to the acid derivative H[To^{P*}] (**3**). Group 7 tricarbonyl complexes To^{P*}M(CO)₃ (M = Mn, **4**; Re, **5**) are synthesized by reaction of MBr(CO)₅ and Li[To^{P*}] and are crystallographically characterized. The ν_{CO} bands in their infrared spectra indicate that π -back donation in the rhenium compounds is greater with To^{P*} than with non-methylated tris(4*S*-isopropyl-2-oxazolinyl)phenylborate (To^P). Reaction of H[To^{P*}] and ZnEt₂ gives To^{P*}ZnEt (**6**), while To^{P*}ZnCl (**7**) is synthesized from Li[To^{P*}] and ZnCl₂. Reaction of To^{P*}ZnCl and KO*t*Bu, followed by addition of PhSiH₃, provides zinc hydride complex, To^{P*}ZnH (**8**). Compound **8** the first example of a crystallographically characterized optically active zinc hydride. We have tested its catalytic reactivity in the cross-dehydrocoupling of silanes and alcohols, which provides *Si*-chiral silanes with moderate enantioselectivity.

Introduction

Bulky scorpionate borate ligands, such as Tp^{Ms} (tris(3-mesitylpyrazolyl)hydridoborate), Tp^* (tris(3,5-dimethylpyrazolyl)hydridoborate), and $\text{Tp}^{\text{tBu,Me}}$ (tris(3-*tert*-butyl-5-methylpyrazolyl)hydridoborate),¹ stabilize reactive groups in transition metal,² lanthanide,³ and main group metal complexes.⁴ Optically active tris(pyrazolyl)borate ligands also offer the opportunity to explore C_3 -symmetry in stereoselective reactions and as catalysts (see Tp^{menth} or $\text{B}(\text{camphpz})_4$ in Chart 1).⁵

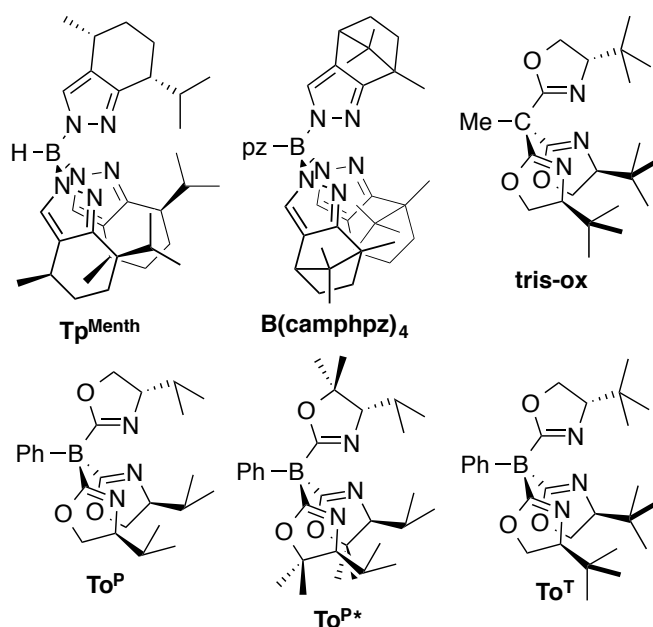


Chart 1. C_3 -symmetric pyrazolyl and oxazoline-based scorpionate ligands.

However, unsymmetrically substituted pyrazoles may form either B–1N or B–2N linkages, and combinations of these linkages give diastereomeric mixtures rather than stereochemically pure compounds. In addition, the B–N bond in pyrazolylborate ligands is susceptible toward isomerization or cleavage.^{5c,6} This process can be mediated by

metal ions,⁷ and it may limit the application of optically active tris(pyrazolyl)borates in enantioselective catalysis. Oxazolinyborate-based ligands with 2C–B linkages circumvent these isomerization issues, and a series of oxazolinyborate-based scorpionate ligands have previously been reported including achiral To^M (tris(4,4-dimethyl-2-oxazolinyl)phenylborate),⁸ optically active To^P (tris(4*S*-isopropyl-2-oxazolinyl)phenylborate),⁹ and To^T (tris(4*S*-*tert*-butyl-2-oxazolinyl)phenylborate).¹⁰ Alternatively, neutral C_3 -symmetric tris-ox ligands $RC(Ox^R)_3$ also circumvent the isomerization issues associated with optically active pyrazolylborates.¹¹ The anionic nature of tris(oxazolinyl)borates, however, also impacts the electronic properties and reactivity of the resulting complexes.

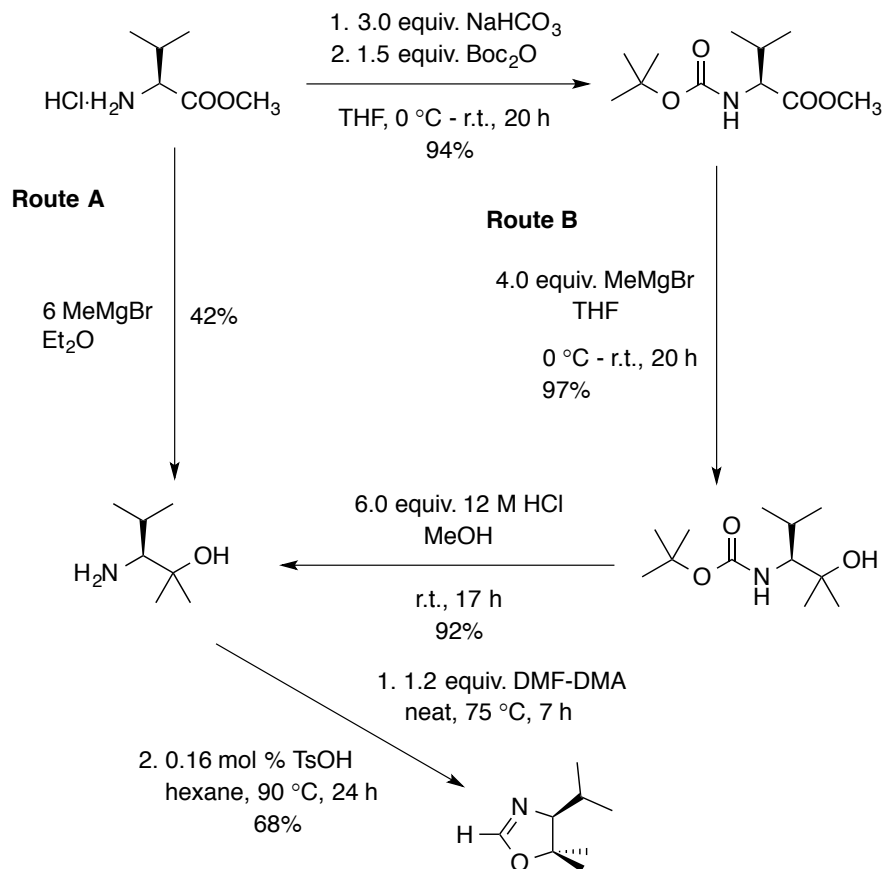
The 4*S*-isopropyl-5,5-dimethyl-2-oxazoline group (Ox^{iPr,Me_2}) has been widely used in a variety of chiral ligands in catalytic reactions such as cyclopropanation,¹² allylic oxidation,¹³ α -tosyloxylation,¹⁴ and the Henry reaction (nitro Aldol reaction),¹⁵ and other enantioselective syntheses.¹⁶ This group has a potential advantage over 4-*tert*-butyl-2-oxazoline-based ligands in that it is synthesized from naturally occurring L-valine. In addition, the mixed cyclopentadienyl-bis(oxazolinyl)borate ligand containing Ox^{iPr,Me_2} is highly effective in enantioselective hydroamination/cyclization of aminoalkenes,¹⁷ and more active than the analogue derived from 4-*S*-*tert*-butyl-2-oxazoline. We were therefore motivated to synthesize the C_3 -symmetric tridentate tris(4*S*-isopropyl-5,5-dimethyl-2-oxazolinyl)phenylborate (To^{P*}) and compare its coordination compounds and reactivity to previously synthesized achiral and chiral tris(oxazolinyl)borate complexes.

Here, we describe the preparation of To^{P*} and its salts as precursors to organometallic compounds. These compounds allow the evaluation of electronic and

steric properties of the $\text{To}^{\text{P}*}$ through single-crystal X-ray diffraction and infrared spectroscopic studies of group 7 tricarbonyl compounds. In addition, we have compared the reactivity and capability of $\text{To}^{\text{P}*}$ to support monomeric zinc compounds, including zinc hydride and zinc alkylperoxide, and the application of the former in catalytic cross-dehydrocoupling of silanes and alcohols.

Results and Discussion

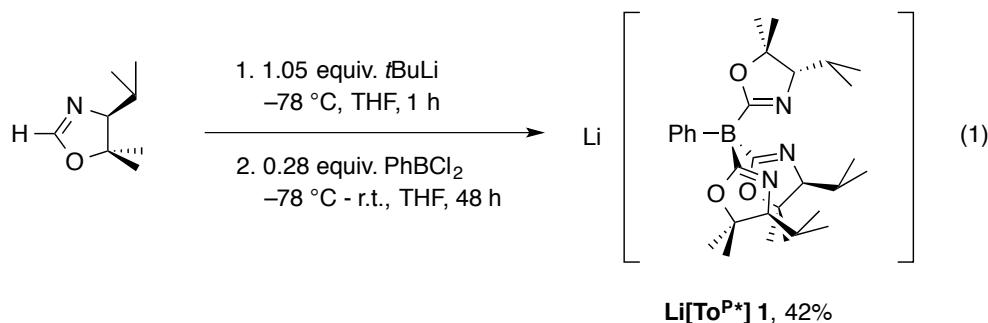
Synthesis of 4*S*-isopropyl-5,5-dimethyl-2-oxazoline ($2\text{H-Ox}^{\text{iPr,Me}_2}$). The synthesis of 4*S*-isopropyl-5,5-dimethyl-2-oxazoline ($2\text{H-Ox}^{\text{iPr,Me}_2}$) was previously communicated as part of the preparation of $\text{H}[\text{PhB}(\text{Ox}^{\text{iPr}_2,\text{Me}_2})_2\text{C}_5\text{H}_5]$.^{17a} However, the previous synthesis involves the direct methylation of L-valine methyl ester that gives the intermediate 2*S*-amino-1,1,3-trimethylbutanol in low yield and requires a large excess of MeMgBr, limiting the overall yield of $2\text{H-Ox}^{\text{iPr,Me}_2}$ (Scheme 1, Route A). Instead, we tested an alternative route (Route B), which begins with the reported preparation of L-valine methyl ester hydrochloride.¹⁸



Scheme 1. Synthesis of 4*S*-isopropyl-5,5-dimethyl-2-oxazoline through direct methylation (route A) or protection/methylation/deprotection (route B).

Instead of its direct methylation with MeMgBr , L-valine methyl ester hydrochloride is neutralized and protected by di-*tert*-butyl dicarbonate (Boc_2O).¹⁹ The protected ester is then converted to the alcohol by methyl magnesium bromide, purified through column chromatography, and deprotected.¹⁹ Although the second preparation involves more steps than the first, the overall yield is higher than obtained from direct methylation. Cyclization of the amino alcohol to 2*H*-Ox^{*i*Pr,Me₂} follows the classical synthesis.²⁰

Synthesis and characterization of tris(4*S*-isopropyl-5,5-dimethyl-2-oxazoliny)phenylborate (To^{P*}) transfer agents. The preparation of Li[To^{P*}] (**1**) is based on the general route for the syntheses of tris(oxazoliny)borate ligands and involves deprotonation of 2H-Ox^{*i*Pr,Me²} followed by reaction with 0.3 equiv. of PhBCl₂ (eq. 1).

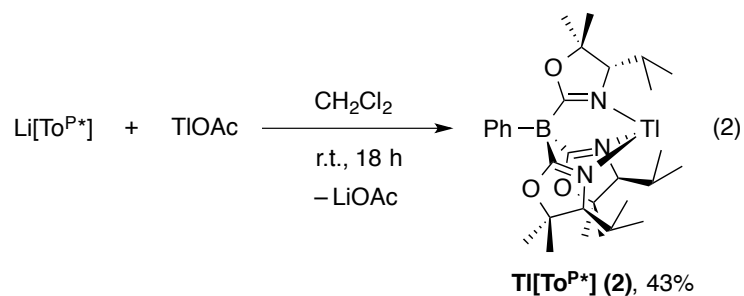


However, the oxazoline's substituents affect the optimal base, reaction concentration, and reaction time needed to prepare tris(2-oxazoliny)borates. In our experience, bulkier substituents require more aggressive bases to quantitatively deprotonate the 2H-2-oxazoline to 2-lithio-2-oxazolide. For this reason, the preparation of bulky To^{P*} employs *t*BuLi to generate 2-lithio-4*S*-isopropyl-5,5-dimethyl-2-oxazolide (2Li-Ox^{*i*Pr,Me²}). A second key to good yield is a concentrated reaction mixture ([2H-Ox^{*i*Pr,Me²}] ~ 0.5 M), because the deprotonation reaction appears slow and dilute conditions give impure products. Quantitative deprotonation of the oxazoline is critical because mixtures of 2H-oxazoline, 2-lithio-oxazolide, and dichlorophenylborane produce unidentified and inseparable side-products.⁸ Moreover, 2Li-Ox^{*i*Pr,Me²} is employed in a slight excess (0.28 equiv. PhBCl₂) because the separation of bis(oxazoliny)phenylborane and **1** is difficult. The yellow crude Li[To^{P*}] purifies to a white solid after pentane washes. The To^{P*} ligand is the permethylated derivative of tris(4*S*-isopropyl-2-

oxazoliny)phenylborate (To^{P}) and is named in analogy to isoelectronic pentamethylcyclopentadiene (Cp^*) and tris(3,5-dimethylpyrazolyl)hydridoborate (Tp^*).

The ^1H NMR spectrum of a benzene- d_6 solution of $\text{Li}[\text{To}^{\text{P}*}]$ contained broad alkyl and aryl resonances. In contrast, a sharp and well-defined ^1H NMR spectrum was obtained for $\text{Li}[\text{To}^{\text{P}*}]$ dissolved in acetonitrile- d_3 . One set of 4*S*-isopropyl-5,5-dimethyl-2-oxazoline ^1H NMR resonances suggests a C_3 -symmetric structure in which the stereochemical integrity of the 4*S*-isopropyl moiety is maintained (*i.e.*, $S,S,S\text{-To}^{\text{P}*}$ is obtained from $2\text{H-Ox}^{4S\text{-}i\text{Pr,Me}2}$). The integrated ratio between the alkyl and phenyl groups indicates that three oxazolines and one phenyl group are bonded to boron. This conclusion is also supported by the ^{11}B chemical shift of -17.8 ppm, which is in the region typical of four coordinate anionic borates.²¹ Similar ^{11}B NMR chemical shifts were observed for $\text{Li}[\text{To}^{\text{M}}]$ (-16.9 ppm),⁸ $\text{Li}[\text{To}^{\text{P}}]$ (-16.8 ppm),⁹ and $\text{Li}[\text{To}^{\text{T}}]$ (-17.0 ppm).¹⁰ A broad peak in the $^{13}\text{C}\{^1\text{H}\}$ NMR spectrum at 185 ppm was assigned to the oxazoline 2C that is bonded to boron. The IR spectrum (KBr) contained only one strong, broad peak in the ν_{CN} region at 1583 cm^{-1} . Although the carbon elemental analysis was consistently lower than calculated, this material is sufficiently pure to use for the synthetic applications described in this chapter.

$\text{Li}[\text{To}^{\text{P}*}]$ may be used directly for some preparations, but a few other reagents were synthesized to facilitate coordination of $\text{To}^{\text{P}*}$ to reactive metals centers. The thallium reagent, $\text{Tl}[\text{To}^{\text{P}*}]$ (**2**), is synthesized by reaction of $\text{Li}[\text{To}^{\text{P}*}]$ and thallium(I) acetate in methylene chloride at room temperature (eq. 2).



The initially yellow suspension becomes milky gray over 30 min. as a result of the formation of the insoluble lithium acetate. Crude Tl[To^{P*}] is obtained as a brown solid after work-up, and it is further purified by pentane washes to an off-white solid. Compound **2** is partially soluble in benzene-*d*₆ and acetonitrile-*d*₃, and, like Li[To^{P*}], it gives broad ¹H NMR signals in benzene-*d*₆ and sharp resonances of a C₃-symmetric species in acetonitrile-*d*₃. The oxazoline resonances of **2** were shifted slightly with respect to Li[To^{P*}], but the overall NMR and IR spectroscopy of the two compounds were very similar. The identity of **2** and the tridentate interaction of To^{P*} and Tl are supported by a single crystal X-ray diffraction study. X-ray quality single crystals are obtained from a toluene/pentane solution of Tl[To^{P*}] at -30 °C (Figure 1).

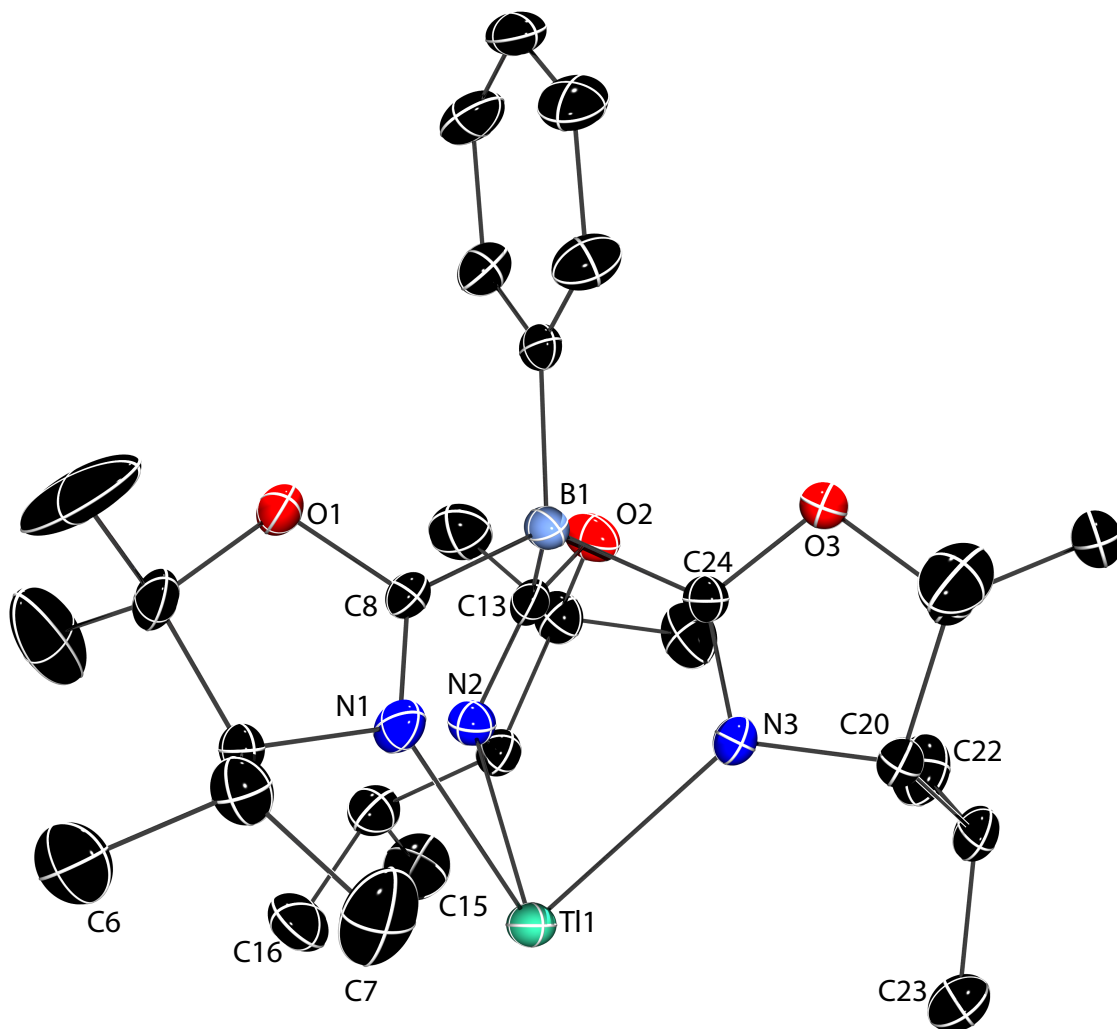


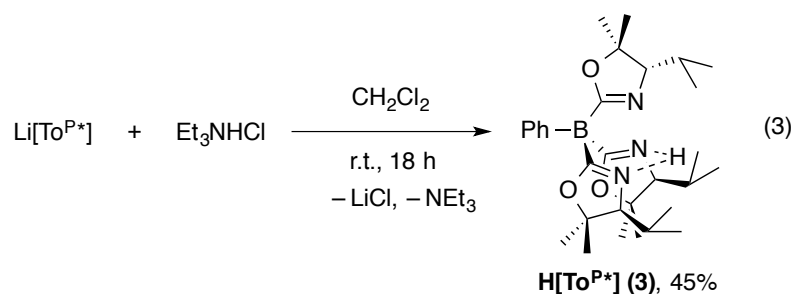
Figure 1. Rendered thermal ellipsoid plot of Tl[To^{P*}] (**2**) with ellipsoids at 35% probability. H atoms are not plotted for clarity. Selected interatomic distances (Å): Tl1-N1, 2.493(2); Tl1-N2, 2.647(2); Tl1-N3, 2.493(2). Selected interatomic angles (°): N1-Tl1-N2, 78.09(6); N2-Tl1-N3, 81.37(7); N3-Tl1-N1, 75.27(7).

In the crystallographically determined solid-state structure, nitrogen atoms of the three oxazolines are coordinated to the Tl center in a tridentate bonding motif. In each oxazoline, one methyl in each isopropyl group points toward the thallium atom. The geometry is not pseudo- C_3 symmetric because the Tl1–N2 distance (2.647(2) Å) is

significantly longer than the Tl1–N1 and Tl1–N3 distances (2.493(2) Å). In addition, one of the oxazolines coordinates through N3 such that the three *N*-bonded atoms (Tl1, C24, and C20) and the boron center are essentially planar (e.g., the Tl1–N3–C24–B1 torsion is 4.6(4)°, whereas the Tl1 coordinates to the other two oxazolines in a canted fashion. This twist is characterized by large Tl1–N1–C8–B1 and Tl1–N2–C13–B1 torsion angles of –35.3(4) and –37.3(4)°. Finally, the conformation of the isopropyl groups are inequivalent in the three oxazolines. The isopropyl group on the N3 ring is oriented with one methyl group (C23) pointing in front of the ligand, whereas the isopropyl substituents of N1 and N2 rings have both methyl groups (C6, C7, C15, C16) pointing forward.

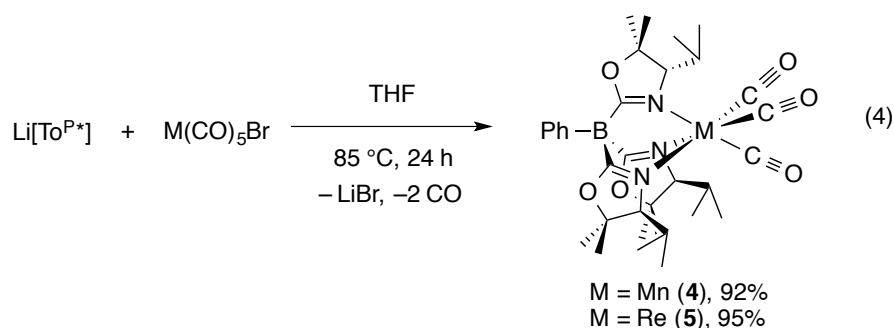
The steric properties of $\text{To}^{\text{P}*}$ are assessed using solid angles, which describe the surface area resulting from the projection of the ligand in question onto a sphere surrounding the complex.²² The solid angle of $\text{To}^{\text{P}*}$, determined based on the X-ray crystallographic coordinates of **2** analyzed by Solid-G,²³ is 6.67 steradians, which corresponds to 53.1% of a sphere's surface area. For comparison, the solid angle of To^{M} , also bonded to Tl, is 6.09 steradians (48.5%). Thus, a greater percentage of the area around Tl is occupied by $\text{To}^{\text{P}*}$ than To^{M} .

The protonated ligand $\text{H}[\text{To}^{\text{P}*}]$ (**3**) is formed after $\text{Li}[\text{To}^{\text{P}*}]$ is subjected to flash column chromatography using bench-grade solvents in air or upon exposure of $\text{Li}[\text{To}^{\text{P}*}]$ to air or bench-grade solvents. $\text{H}[\text{To}^{\text{P}*}]$ is most quickly and conveniently prepared by the reaction of $\text{Li}[\text{To}^{\text{P}*}]$ and triethylammonium chloride (eq. 3).



H[To^{P*}] is isolated in moderate yield as a slightly sticky white solid, and it is readily soluble in benzene-*d*₆. In contrast to the characteristic two doublets and two singlets for the methyl groups in the ¹H NMR spectra of 2H-Ox^{*i*Pr,Me₂}, Li[To^{P*}] and Ti[To^{P*}], three broad resonances at 0.75 (9 H), 1.1 (18 H), and 1.2 ppm (9 H) were observed for H[To^{P*}]. A ¹H–¹³C HMQC experiment indicated that the broad singlet at 1.1 ppm resulted from the overlap of one of the isopropyl methyl groups and one 5-methyl group. A signal in the ¹¹B NMR spectrum at –17.8 ppm indicated that the four B–C bonds were unaffected by the acidic treatment. In addition, two intense IR absorption bands at 1601 and 1583 cm^{–1} indicate that two types of oxazoline rings are present in the molecule. These bands are assigned to non-protonated and *N*-protonated oxazoline groups, respectively.

Synthesis and characterization of To^{P*}M(CO)₃ (M = Mn (4), Re (5)). Monovalent group 7 carbonyl compounds provide a metric for comparing electron-donating ability of *fac*-coordinating tridentate ligands through the IR frequency of the carbonyl stretching modes. Complexes To^{P*}Mn(CO)₃ (4) and To^{P*}Re(CO)₃ (5) are synthesized by reaction of Li[To^{P*}] with manganese or rhenium pentacarbonyl bromide (eq. 4).



The NMR spectra of **4** and **5** in benzene- d_6 confirm their anticipated pseudo C_3 -symmetry. The ^1H NMR spectrum of the manganese compound **4** is well resolved. In the ^1H NMR spectrum of **5**, a large virtual doublet at 1.06 ppm integrating to 27 H resulted from overlapping singlet and doublet signals assigned to methyls of the 5-dimethyl and 4-isopropyl groups. A ^1H - ^{13}C HMQC experiment supported this assignment. The $^{13}\text{C}\{^1\text{H}\}$ NMR spectra of **4** and **5** contained broad downfield signals for the carbonyl carbons at 223 and 199 ppm, respectively, in addition to $\text{To}^{\text{P}*}$ resonances. The ^{15}N NMR chemical shifts of **5**, obtained from ^1H - ^{15}N HMBC experiments, were upfield of the $\text{To}^{\text{M}}\text{Re(CO)}_3$ but similar to $\text{To}^{\text{P}}\text{Re(CO)}_3$. The IR spectra (KBr) contained the expected symmetric and asymmetric carbonyl bands ($2000\text{-}1800\text{ cm}^{-1}$) and oxazoline ν_{CN} ($\sim 1600\text{ cm}^{-1}$). The spectral data, as well as data for previously reported isoelectronic To^{M} , To^{P} , Tp , and Tp^* compounds are summarized in Table 1.²⁴

The two symmetric CO stretching modes of complexes **4** and **5**, measured both in the solid state and in CH_2Cl_2 solution, were slightly lower energy than the corresponding group 7 compounds of To^{M} and To^{P} . The asymmetric stretches of **5** in CH_2Cl_2 are also slightly lower energy than $\text{To}^{\text{M}}\text{Re(CO)}_3$ and $\text{To}^{\text{P}}\text{Re(CO)}_3$. The ν_{CO} data from the

symmetric and asymmetric modes suggest that π -back donation from manganese or rhenium to the carbonyl ligands is affected by 5,5-methylation of the oxazoline. The average of the symmetric and asymmetric stretching frequencies for the ligands, across the series of rhenium compounds, indicates that the tris(oxazolinyl)borate complexes are lower in energy than their Tp and Tp* analogues. By this measure, the tris(oxazolinyl)borate ligands are more electron-donating than Tp and Tp*, while To^{P*} is the most electron-donating among the five borate ligands following the trend: To^{P*} > To^P > To^M > Tp* > Tp.

Table 1. Summary of the characteristic data of manganese and rhenium tricarbonyl complexes bearing To^{P*}, with related To^M, To^P, Tp, and Tp* given for comparison.

Compound	ν_{CO}^a	Avg. $\nu_{\text{CO}}^{a,b}$	ν_{CN}^c	$E_{1/2}^d$	¹⁵ N NMR ^e
To ^{P*} Mn(CO) ₃ (4) ^f	2013, 1903 (KBr) 2016, 1911 (CH ₂ Cl ₂)	1946	1592	n.a.	n.d. ^g
To ^{P*} Re(CO) ₃ (5) ^f	2008, 1886 (KBr) 2012, 1894 (CH ₂ Cl ₂)	1933	1584	0.97	-197
To ^M Mn(CO) ₃ ^h	2018, 1899 (KBr) 2020, 1912 (CH ₂ Cl ₂)	1948	1592	n.a.	-172
To ^M Re(CO) ₃ ^h	2012, 1892 (KBr) 2019, 1898 (CH ₂ Cl ₂)	1938	1582	1.00	-177
To ^P Mn(CO) ₃ ^h	2016, 1961 (KBr) 2017, 1908 (THF)	1944	1601	n.a.	n.d. ^g
To ^P Re(CO) ₃ ^h	2010, 1892 (KBr) 2014, 1897 (CH ₂ Cl ₂)	1936	1589	0.97	-196
TpMn(CO) ₃ ⁱ	2026, 1932, 1915 (KBr) 2035, 1932 (CH ₂ Cl ₂) ^h	1966	n.a.	n.a.	n.a.
TpRe(CO) ₃ ⁱ	2020, 1896 (KBr) 2026, 1912 (CH ₂ Cl ₂) ^h	1950	n.a.	0.98	n.a.

Table 1 continued.

Compound	ν_{CO}^a	Avg. $\nu_{\text{CO}}^{a,b}$	ν_{CN}^c	$E_{1/2}^d$	$^{15}\text{N NMR}^e$
Tp* $\text{Mn}(\text{CO})_3^i$	2023, 1912 (KBr)	1957	n.a.	n.a.	n.a.
	2027, 1922 (CH_2Cl_2) ^h				
Tp* $\text{Re}(\text{CO})_3^i$	2017, 1893 (KBr)	1941	n.a.	0.82	n.a.
	2018, 1903 (CH_2Cl_2) ^h				

^a cm^{-1} . ^b Avg. $\nu_{\text{CO}} = (\nu_{\text{sym}} + 2\nu_{\text{asym}})/3$. ^c KBr, cm^{-1} . ^d V vs $\text{Cp}_2\text{Fe}^{0+}$. ^e ppm. ^f This work. ^g

Not detected. ^h See reference 24b. ⁱ See reference 24a.

To^P* $\text{Re}(\text{CO})_3$ may be reversibly oxidized and reduced by one electron, as demonstrated by a cyclic voltammetry (CV) experiment (Figure 2). The $E_{1/2}$ of To^P* $\text{Re}(\text{CO})_3$ is identical to To^P $\text{Re}(\text{CO})_3$, and the additional methyl groups in To^P* do not affect the redox potential of the rhenium center.

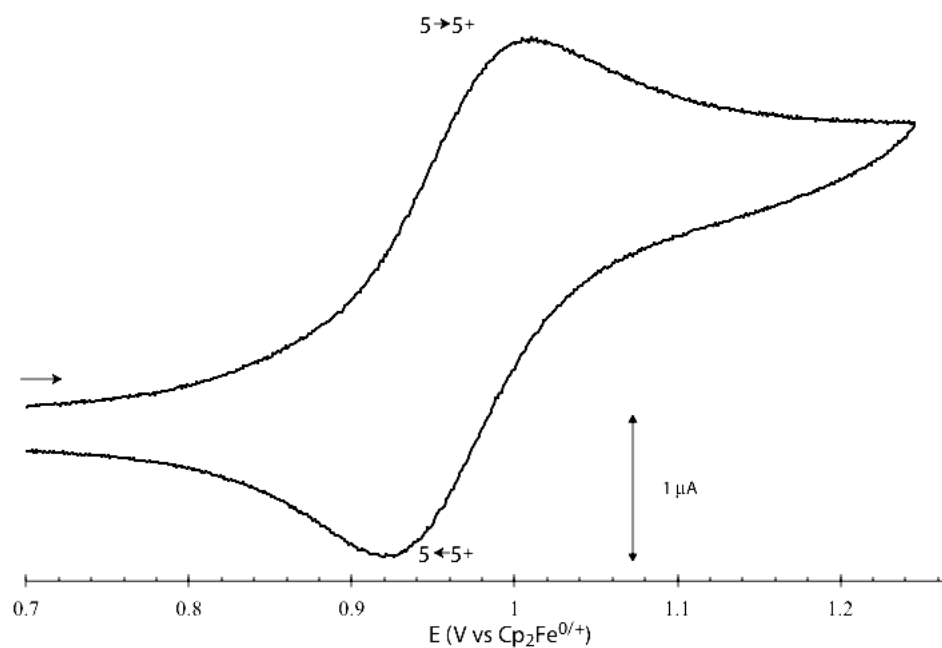


Figure 2. CV of 1.0 mM **5** in $\text{CH}_2\text{Cl}_2/0.10 \text{ M } [\text{NBu}_4][\text{BF}_4]$. Condition: 298 K, 2 mm Pt electrode, 10 mV/s.

X-ray quality crystals of **4** or **5** are obtained from concentrated solutions containing a mixture of toluene and pentane cooled at $-30 \text{ }^\circ\text{C}$ (Figures 3 and 4).

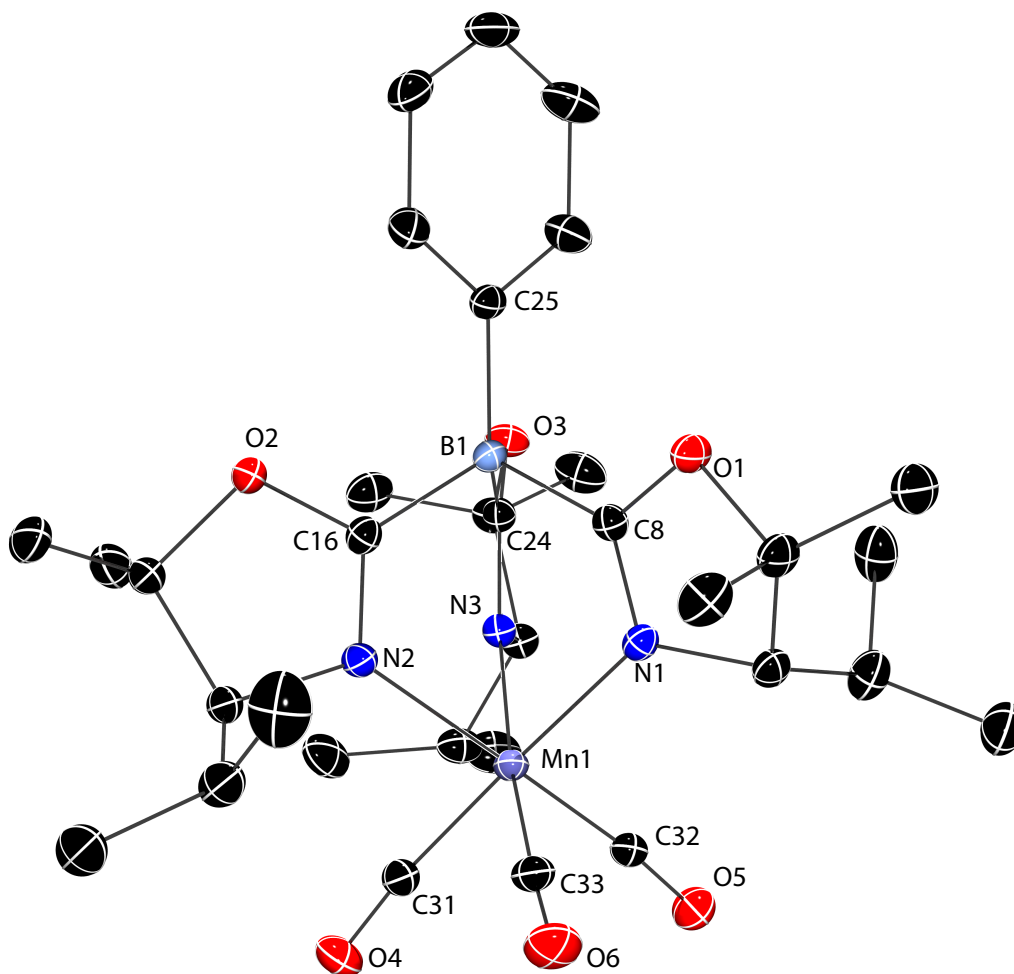


Figure 3. Rendered thermal ellipsoid plot of $[\text{To}^{\text{P}^*}]\text{Mn}(\text{CO})_3$ (**4**) with ellipsoids at 35% probability. H atoms are not plotted for clarity. Selected interatomic distances (Å): Mn1-N1, 2.067(1); Mn1-N2, 2.082(1); Mn1-N3, 2.074(1); Mn1-C31, 1.808(2); Mn1-C32, 1.808 (1); Mn1-C33, 1.800(2); N1-C32, 2.868(3); N3-C32, 2.804(3); N3-C31, 2.967(3); N2-C31, 2.774(3); N2-C33, 2.873(3); N1-C33, 2.648(3). Selected interatomic angles (°): N1-Mn1-N2, 88.58(5); N2-Mn1-N3, 82.70(4); N3-Mn1-N1, 85.98(5); C31-Mn1-C32, 86.01(7); C32-Mn1-C33, 90.43(7); C33-Mn1-C31, 88.38(7); Mn1-N1-C8-B1, $-15.4(2)$; Mn1-N2-C16-B1, $-3.8(3)$; Mn1-N3-C24-B1, $-8.3(2)$.

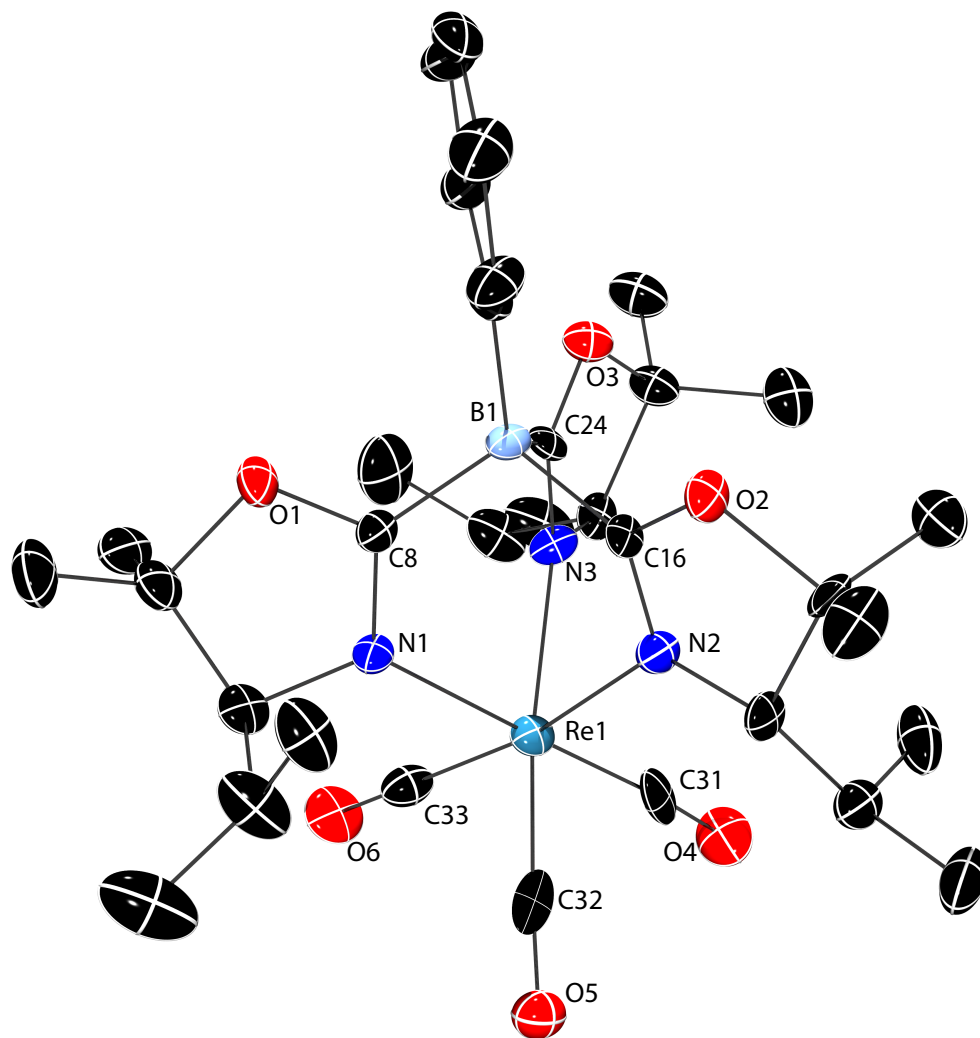
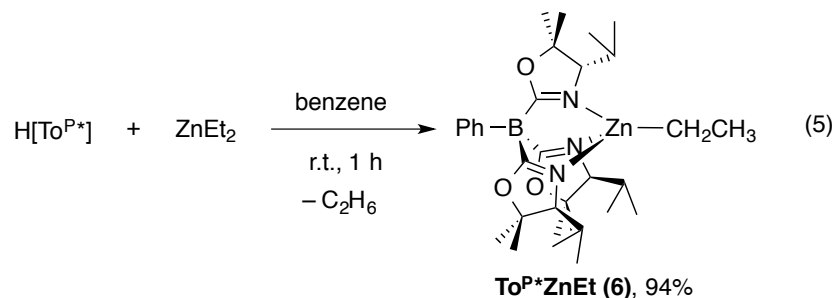


Figure 4. Rendered thermal ellipsoid plot of $[\text{To}^{\text{P}*}]\text{Re}(\text{CO})_3$ (**5**) with ellipsoids at 35% probability. H atoms are not plotted for clarity. Selected interatomic distances (\AA): Re1-N1, 2.186(8); Re1-N2, 2.203(7); Re1-N3, 2.189(7); Re1-C31, 1.93(1); Re1-C32, 1.87(1); Re1-C33, 1.94(1). Selected interatomic angles ($^\circ$): N1-Re1-N2, 83.6(3); N2-Re1-N3, 80.1(3); N3-Re1-N1, 84.8(3); C31-Re1-C32, 86.1(4); C32-Re1-C33, 90.1(4); C33-Re1-C31, 89.4(4); Re1-N1-C8-B1, $-15(2)$; Re1-N2-C16-B1, $-10(2)$; Re1-N3-C24-B1, $-6(2)$.

The manganese and rhenium compounds are isostructural and crystallize in the same orthorhombic space group ($P2_12_12_1$). The primary difference between **4** and **5** is

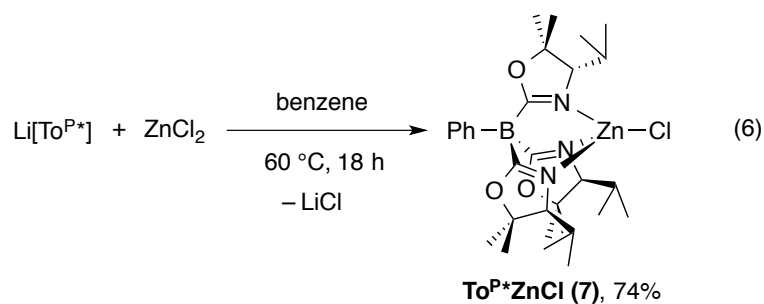
related to the M–L distances and unit cell sizes. The *a* and *c* dimensions of $\text{To}^{\text{P}^*}\text{Re}(\text{CO})_3$ are 0.05 and 0.25 Å longer than those of the manganese complex. The Re–C and Re–N interatomic distances are ca. 0.1 Å longer than the distances associated with the manganese center. Apart from these minor differences, the two compounds adopt similar molecular structures. The metal centers are coordinated in a distorted octahedral environment, and the carbonyl groups are positioned between the oxazoline rings. However, the carbonyls are not equally situated between the oxazoline nitrogen, as determined by the interligand distances between atoms in the metal's first coordination sphere. For example in **4**, the C33 carbon of the carbonyl is 2.65 Å from N1 and 2.87 Å from N2. These distances may be readily rationalized by the observation that the isopropyl group on the N2 oxazoline ring is pointing at the C33 carbonyl ligand. This distortion is repeated for N2–C31–N3, but the carbonyl (C32, *trans* to N2) between N1 and N3 is nearly equidistance to the two oxazoline nitrogen.

Synthesis and characterization of $\text{To}^{\text{P}^*}\text{ZnX}$ (X = Et (6**), Cl (**7**), H (**8**)).** The reaction of diethylzinc and $\text{H}[\text{To}^{\text{P}^*}]$ affords $\text{To}^{\text{P}^*}\text{ZnEt}$ (**6**; eq. 5).



Ethane is formed within 5 min. in a micromolar scale reaction monitored by ^1H NMR spectroscopy. The product forms in essentially quantitative yield and is easily isolated as an analytically pure white solid after evaporation of volatile materials. The ^1H NMR spectrum contained the expected integrated ratio of ethyl and pseudo- C_3 -symmetric $\text{To}^{\text{P}*}$ signals, supporting the assigned ligand ratio. As in the group 7 compounds, a ^1H - ^{15}N HMBC experiment revealed one nitrogen signal at -177 ppm that correlated to the oxazoline and isopropyl methine ^1H NMR resonances. The IR spectrum (KBr) contained one strong CN stretching band at 1585 cm^{-1} . These data indicate that all three oxazoline rings are equivalent and coordinated to zinc.

$\text{To}^{\text{P}*}\text{ZnEt}$ is converted to $\text{To}^{\text{P}*}\text{ZnCl}$ (**7**) by reaction with triethylammonium chloride. A more direct synthetic route of $\text{To}^{\text{P}*}\text{ZnCl}$ involves the reaction of $\text{Li}[\text{To}^{\text{P}*}]$ and zinc chloride in benzene at elevated temperature (eq. 6).



The well-resolved features of the ^1H NMR spectrum of $\text{To}^{\text{P}*}\text{ZnCl}$ were readily distinguished from the broad signals of the $\text{Li}[\text{To}^{\text{P}*}]$ starting materials. Two sharp doublets at 0.94 and 1.22 ppm ($^3J_{\text{HH}} = 6.6$ Hz, 9 H each) and two singlets observed at 0.98 and 1.03 ppm (9 H each), respectively assigned to the CHMe_2 and 5-dimethyl groups, were distinct from the broad signals obtained for the ^1H NMR spectrum of

Li[To^{P*}]. The IR spectrum (KBr) showed one strong band at 1579 cm⁻¹ assigned to a CN stretch supported the structural assignment.²⁵ This assignment is confirmed by a single crystal X-ray diffraction study (Figure 5).

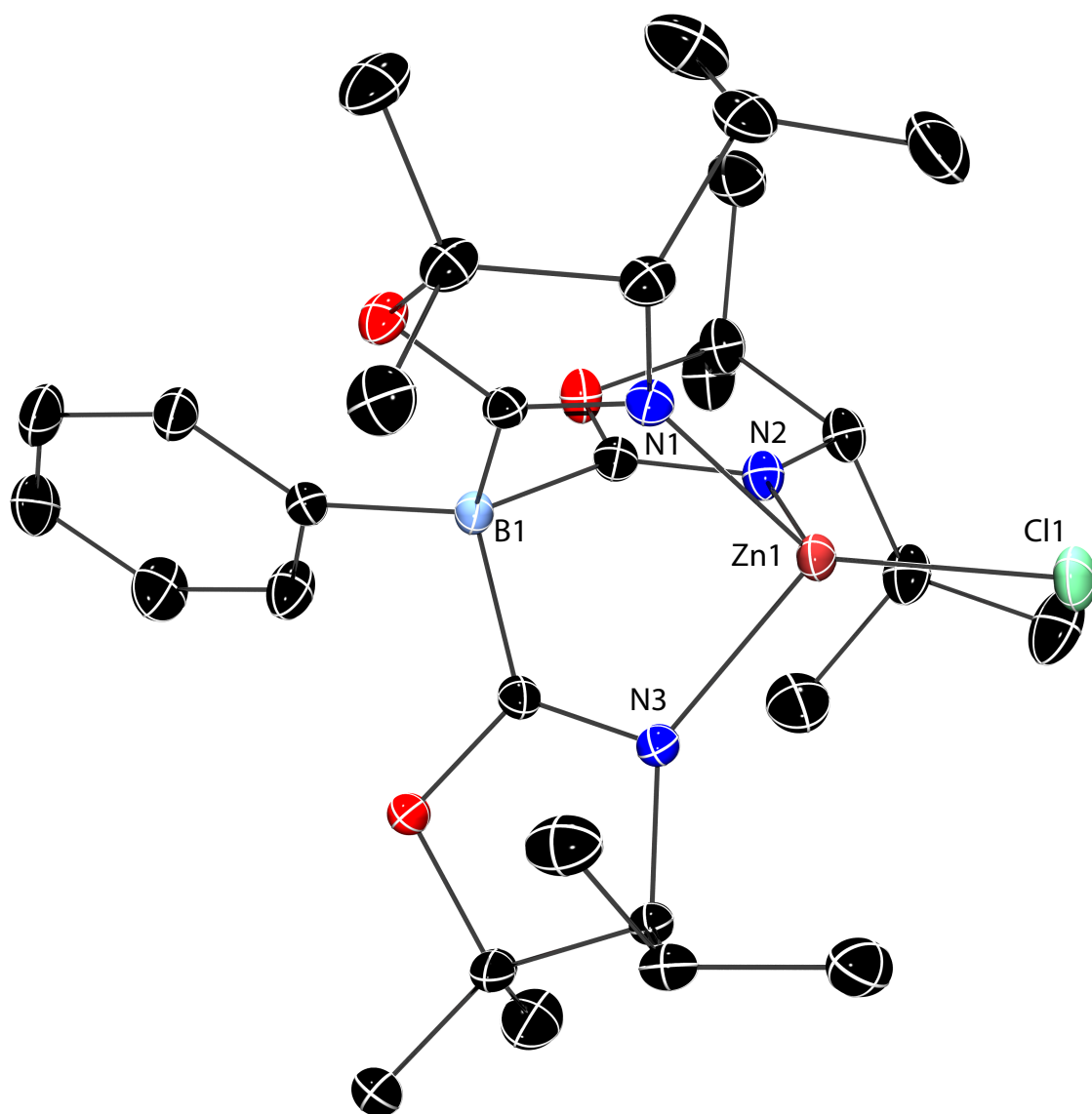
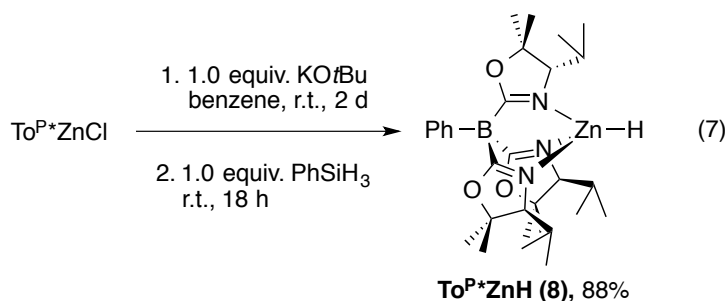


Figure 5. Rendered thermal ellipsoid plot of To^{P*}ZnCl (7) with ellipsoids at 35% probability. H atoms are not plotted for clarity. Selected interatomic distances (Å): Zn1-N1, 2.047(1); Zn1-N2, 2.0249(9); Zn1-N3, 2.023(1); Zn1-Cl1, 2.1831(4). Selected

interatomic angles (°): N1-Zn1-N2, 93.70(4); N2-Zn1-N3, 93.81(4); N3-Zn1-N1, 94.21(4); N1-Zn1-Cl1, 121.15(3); N2-Zn1-Cl1, 121.63(3); N3-Zn1-Cl1, 124.53(3).

In the solid-state structure, the isopropyl groups on the oxazoline are oriented to place one methyl group in each oxazoline (C3, C11, and C17) in front of the metal center. The ligand's conformation, particularly the orientation of the isopropyl groups in $Tl[To^{P*}]$, $To^{P*}ZnCl$, and $To^{P*}M(CO)_3$ changes with the changing coordination number of the metal center. The conformation in this complex is similar to that observed in the X-ray crystal structure of $To^{P*}ZnH$ and will be discussed in the structure of that compound (below).

Compound **7** reacts with potassium *tert*-butoxide at room temperature to give $To^{P*}ZnOtBu$. 1H NMR spectra of $To^{P*}ZnOtBu$ dissolved in benzene- d_6 or methylene chloride- d_2 , however, contained broad peaks in the alkyl region, and the species did not provide a characteristic set of signals. Instead $To^{P*}ZnOtBu$ is assigned based on its reactivity toward $PhSiH_3$ to form $To^{P*}ZnH$ (**8**) and $PhH_2SiOtBu$ (eq. 7).



The 1H NMR spectrum of **8**, acquired in benzene- d_6 , contained a singlet at 4.61 ppm characteristic of a zinc hydride resonance.²⁶ The C_3 -symmetric molecule provided a

spectrum that contained one set of oxazoline resonances. A ^1H - ^{15}N HMBC experiment correlated the oxazoline nitrogen signal at -179 ppm to the zinc hydride resonance, the oxazoline 4-H, and the isopropyl methine at 1.63 ppm. The IR spectrum (KBr) revealed one strong band at 1587 cm^{-1} assigned to the oxazoline C=N stretching mode and a medium intensity peak at 1766 cm^{-1} assigned to the ν_{ZnH} . The related compounds $\text{To}^{\text{M}}\text{ZnH}$ (1745 cm^{-1}) and $\text{Tp}^{\text{tBu}}\text{ZnH}$ (1770 cm^{-1}) have ν_{ZnH} bands in a similar range.

X-ray quality crystals of $\text{To}^{\text{P}}\text{ZnH}$ are grown from a concentrated pentane solution at $-30\text{ }^\circ\text{C}$ (Figure 6).

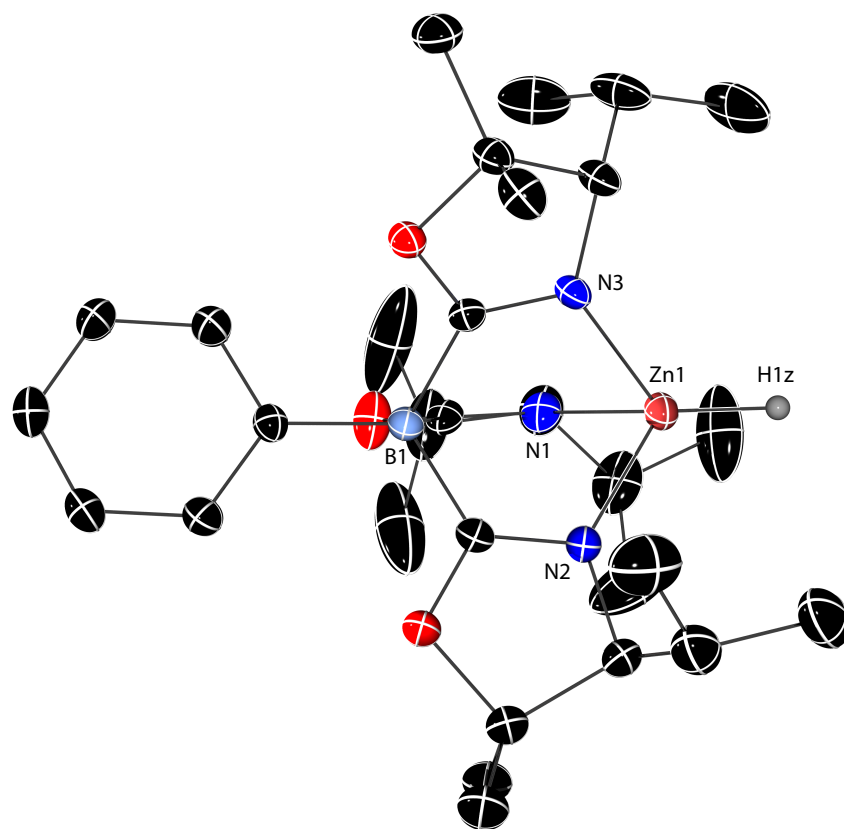


Figure 6. Rendered thermal ellipsoid plot of $\text{To}^{\text{P}}\text{ZnH}$ (**8**) with ellipsoids at 35% probability. H atoms are not plotted for clarity, except the hydride. Selected interatomic

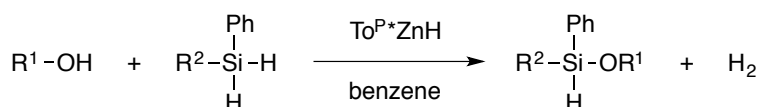
distances (Å): Zn1-N1, 2.071(2); Zn1-N2, 2.062(2); Zn1-N3, 2.060(2); Zn1-H1Z, 1.44(3). Selected interatomic angles (°): N1-Zn1-N2, 90.53(9); N2-Zn1-N3, 91.95(9); N3-Zn1-N1, 90.85(8); N1-Zn1-H1Z, 126(1); N2-Zn1-H1Z, 123(1); N3-Zn1-H1Z, 124(1).

To the best of our knowledge, $\text{To}^{\text{P}}\text{ZnH}$ is the first example of a crystallographically characterized optically active mononuclear zinc hydride compound. The Zn–H interatomic distance (1.44(3) Å) is the shortest crystallographically characterized terminal zinc hydride compounds reported in the Cambridge Structural Database. For comparison, the Zn–H distance in TptmZnH is 1.51(3) Å (Tptm = tris(2-pyridylthio)methyl),^{26e} the *C*-metalated dimeric compound $[\{\mu\text{-}\kappa^3\text{-HC(NHC)}_2\}\text{ZnH}]_2$ (NHC = methylidyne-3,3'-bis(*N*-*tert*-butylimidazol-2-ylidene)) has a Zn–H distance of 1.61(3) Å,²⁷ while the distance in aminophenolate-support ZnH (L = 2,4-di-*tert*-butyl-6-[[2'-dimethylaminoethyl)methylamino]-methyl}phenolate) is 1.75(3) Å.²⁸ Like $\text{To}^{\text{P}}\text{ZnCl}$, the zinc atom in $\text{To}^{\text{P}}\text{ZnH}$ is coordinated in a distorted tetrahedral geometry, with the N–Zn–H angles (average, $125 \pm 1^\circ$, see Figure 5 for individual values and crystallographic E.S.D.s) are much larger than the N–Zn–N bond angles (average, $91 \pm 1^\circ$). These angles show an increased distortion from $\text{To}^{\text{P}}\text{ZnCl}$ which have smaller N–Zn–Cl angles (average $122 \pm 1^\circ$) and larger N–Zn–N (average, 93.9 ± 0.2). This distortion is also manifested in the B–Zn distance, which is longer in $\text{To}^{\text{P}}\text{ZnH}$ than in $\text{To}^{\text{P}}\text{ZnCl}$ by ca 0.1 Å. Moreover, the three isopropyl groups inherit the same conformation as in **7**, in which only one methyl group from each isopropyl is placed in front of the metal, and the other methyl group of the isopropyl points at the next

oxazoline donor. Overall, the isopropyl groups' conformation conform to the C_3 symmetry associated with this ligand in the solid-state structure.

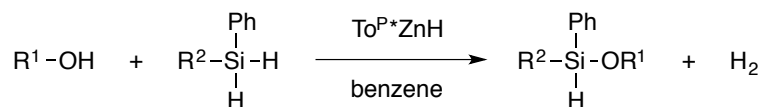
Enantioselective dehydrogenative silylation of alcohols. The achiral tris(oxazolinyl)borato zinc hydride complex $To^M ZnH$ is a catalyst for the dehydrogenative silylation of alcohols with silanes.²⁹ Complex **8** was tested as catalyst for the dehydrogenative coupling of alcohols and the prochiral silanes, phenylmethylsilane and 1-naphthylphenylsilane, as a catalytic route to enantioenriched *Si*-chiral silanes (Table 2). This transformation might provide an alternative approach to such silicon-centered optically active molecules to complement kinetic resolutions of racemic chiral tertiary silanes via dehydrocoupling,³⁰ and other synthetic routes to compounds containing stereogenic silicon centers.³¹ A previous example of asymmetric dehydrocoupling employed a chiral rhodium complex as the catalyst.³²

Table 2. Enantioselective dehydrogenative silylation of alcohols with prochiral silanes catalyzed by **8**.



Trial	R ¹	R ²	Cat. loading (mol %)	Temp. (°C)	Time	Conv. (%)	Yield (%) ^a	ee (%) ^b
1 ^c	Me	Me ^d	1.0	25	4 h	100	79	6
2 ^e	Et	Me ^d	1.0	25	8 h	100	75	56

Table 2 continued.



Trial	R ¹	R ²	Cat. loading (mol %)	Temp. (°C)	Time	Conv. (%)	Yield (%) ^a	ee (%) ^b
3 ^e	3,5-C ₆ H ₃ Me ₂	Me	2.0	25	4 d	100	81	24
4 ^c	Me	1-Np ^d	1.0	25	6 h	100	90	16
5 ^e	Et	1-Np ^d	1.0	25	10 h	100	91	22
6 ^g	<i>i</i> Pr	1-Np	1.0	25	14 d	91	67	4
7 ^f	3,5-C ₆ H ₃ Me ₂	1-Np	2.0	25	14 d	100	80	7
8 ^f	3,5-C ₆ H ₃ Me ₂	1-Np ^c	2.0	35	26 h	100	80	8
9 ^f	3,5-C ₆ H ₃ Me ₂	1-Np ^c	2.0	60	12 h	100	80	11

^a Isolated yield. ^b Determined by HPLC (Chiracel-ODH) with hexane as eluent. ^c 10 mL benzene, 2.61 mM **8**, 524 mM silane, 259 mM alcohol. ^d 10 mL benzene, 1.74 mM **8**, 350 mM silane, 172 mM alcohol. ^e 2 mL benzene, 8.70 mM **8**, 437 mM silane, 434 mM C₆H₃Me₂OH. ^f 2 mL benzene, 8.70 mM **8**, 865 mM silane, 850 mM *i*PrOH.

Low enantioselectivity was observed for the combination of methanol and phenylmethylsilane (entry 1), however an encouragingly increase in enantioselectivity was obtained from ethanol and PhMeSiH₂ (entry 2). An excess amount of silane was used in these two experiments, as well as some of the following trials, in order to suppress the formation of dialkoxysiloxanes through another dehydrogenative silylation of the desired products.

However, the dehydrogenative coupling of 3,5-dimethylphenol and phenylmethylsilane gives lower enantiomeric excess (trial 3). In addition, the reactions of 1-naphthylphenylsilane and methanol, ethanol, isopropanol and 3,5-dimethylphenol give low % ee. In the end, $To^{P*}ZnH$ is most effective for the specific combination of EtOH and $PhMeSiH_2$, and trends for extending and enhancing this activity are not currently obvious with this ligand-metal combination. However, a number of first row metal compounds catalyze the dehydrocoupling of silanes and protic reagents, and we are currently investigating $To^{P*}M$ -complexes in this capacity.

Conclusions

To^{P*} is a new, C_3 -symmetric tridentate monoanionic ligand that forms related coordination compounds as the reported tris(oxazolanyl)borate ligands, namely achiral To^M and chiral To^P and To^T ligands. In particular, octahedral group 7 tricarbonyl compounds and tetrahedral zinc To^{P*} -supported compounds may be readily prepared, as well as lithium, thallium, and protonated ligand for transmetalation. The 5,5-dimethyl substitution affects the steric profile of the tris(oxazolanyl)borate ligand as described by the larger solid angle of To^{P*} than To^P . The 5,5-methylation in To^{P*} also affects the ν_{CO} in group 7 tricarbonyls, although the redox potentials are similar for To^M , To^P and To^{P*} . $To^{P*}ZnH$ also provides some stereoselectivity in the cross-coupling of alcohols and silanes to give *Si*-chiral siloxanes, although the results were highly substrate dependent.

Experimental

General procedures. All reactions were performed under a dry argon atmosphere using standard Schlenk techniques or under a nitrogen atmosphere in a glovebox, unless otherwise indicated. Benzene, pentane, tetrahydrofuran, and methylene chloride were dried and deoxygenated using an IT PureSolv system. Benzene- d_6 was heated to reflux over Na/K alloy and vacuum transferred. Acetonitrile- d_3 and chloroform- d were heated to reflux over CaH₂ and vacuum transferred. Thionyl chloride, *N,N*-dimethylformamide dimethyl acetal (DMF-DMA), and dichlorophenylborane were purchased from Sigma-Aldrich, and were distilled then stored in separate storage flasks equipped with resealable Teflon valves under inert atmosphere before use. Methyl magnesium bromide solution (3.0 M in diethyl ether), *tert*-butyl lithium solution (1.7 M in pentane), and dimethylzinc solution (2.0 M in toluene) were purchased from Sigma-Aldrich, and were transferred then stored in separate storage flasks equipped with resealable Teflon valves under inert atmosphere before use. L-Valine was purchased from Acros Organics. Di-*tert*-butyl dicarbonate (Boc₂O) was purchased from TCI America. *p*-Toluenesulfonic acid monohydrate was purchased from Fisher Scientific. Thallium(I) acetate and 1-naphthylphenylsilane were purchased from Sigma-Aldrich, and stored in a glovebox in their original bottles. Diethylzinc was purchased from Strem Chemicals, Inc., and stored inside a glovebox in its original Swagelok cylinder. Zinc chloride was purchased from Fluka Analytical, and stored in a glovebox. Potassium *tert*-butoxide and 3,5-dimethylphenol were purchased from Sigma-Aldrich, and were sublimed then stored in a glovebox. Manganese and rhenium pentacarbonyl bromide were synthesized according to the literature procedures,³³ starting from manganese(0) carbonyl and dirhenium

decarbonyl, respectively. Manganese pentacarbonyl bromide was used without further sublimation, while rhenium pentacarbonyl bromide was further purified with sublimation. Triethylammonium chloride was synthesized from triethylamine and hydrochloric acid. Phenylsilane and phenylmethylsilane were synthesized by reduction of trichlorophenylsilane and dichloro(methyl)phenylsilane with LiAlH_4 , respectively. Methanol, ethanol, and isopropanol for the catalysis were heated to reflux with the activated magnesium metal, and then distilled and stored over 4 Å molecular sieves in a glovebox.

^1H , $^{13}\text{C}\{^1\text{H}\}$, and ^{11}B NMR spectra were collected on a Varian VRX 300 MHz, a Varian MR 400 MHz, and a Bruker Avance II 600 MHz NMR spectrometer. ^{15}N NMR chemical shifts were determined by ^1H - ^{15}N HMBC experiments on an Avance II 600 MHz NMR spectrometer. ^{15}N chemical shifts were originally referenced to an external liquid NH_3 standard and recalculated to the CH_3NO_2 chemical shift scale by adding -381.9 ppm. ^{29}Si chemical shifts were determined by ^1H - ^{29}Si HMBC experiments collected on an Avance II 600 MHz spectrometer. Infrared spectra were recorded on a Bruker Vertex spectrometer. Elemental analyses were performed using a Perkin-Elmer 2400 Series II CHN/S in Iowa State Chemical Instrumentation Facility. $[\alpha]_{\text{D}}$ values were measured on an ATAGO AP-300 polarimeter with a wavelength of 589 nm in a 50 mm observation tube at 20 °C. HPLC analyses were carried out on a Waters Alliance HPLC system with an e2695 separation module and a 2489 dual wavelength detector. The electrochemistry was performed in a glovebox under a nitrogen atmosphere, using a Princeton Applied Research (PAR) VersaSTAT 3 potentiostat interfaced to a personal computer. Voltammetry scans were recorded using a platinum working electrode disk of

2 mm diameter (PAR). The disk was polished with 0.05 μm micropolish alumina suspension (Buehler), and then washed with distilled water and acetone, and finally sonicated for 5 min before use. Ag/AgCl pseudo-reference electrode was employed, and the system was calibrated against the $\text{Cp}_2\text{Fe}^{0/+}$ redox couple.

L-Valine methyl ester hydrochloride. Following the literature procedure,¹⁸ into a three-necked round bottom flask connected to an oil bubbler was added methanol (300 mL), and the flask was cooled in an ice-salt bath. Under nitrogen purge, thionyl chloride (47.6 mL, 0.653 mol) was added dropwise over 2 h. L-Valine (70.0 g, 0.598 mol) was then added in one portion to the solution, and the mixture was heated to 60 °C to dissolve all of the solids. The solution was then heated for another hour. The solvent and excess reagents were removed by distillation. The resulting white solid was dried *in vacuo* for several hours and then dissolved in minimal amount of methanol (90 mL). Diethyl ether (900 mL) was then poured into the methanol solution, and the mixture was cooled to -30 °C overnight, during which the product crystallized as white crystals. The solid was collected, washed with cold diethyl ether and dried *in vacuo* to give L-valine methyl ester hydrochloride as a white solid (90.7 g, 0.541 mol, 90.4%). ¹H NMR (chloroform-*d*, 300 MHz): δ 8.9 (br, 3 H, $\text{HCl}\cdot\text{H}_2\text{NCH}(\text{CHMe}_2)\text{COOCH}_3$), 3.93 (d, $^3J_{\text{HH}} = 4.5$ Hz, 1 H, $\text{HCl}\cdot\text{H}_2\text{NCH}(\text{CHMe}_2)\text{COOCH}_3$), 3.84 (s, 3 H, $\text{HCl}\cdot\text{H}_2\text{NCH}(\text{CHMe}_2)\text{COOCH}_3$), 2.47 (m, 1 H, $\text{HCl}\cdot\text{H}_2\text{NCH}(\text{CHMe}_2)\text{COOCH}_3$), 1.16 (vt, 6 H, $\text{HCl}\cdot\text{H}_2\text{NCH}(\text{CHMe}_2)\text{COOCH}_3$).

Boc-L-valine methyl ester. Following the literature procedure,¹⁹ L-valine methyl ester hydrochloride (70.0 g, 0.418 mol) was dissolved in tetrahydrofuran/methanol (4:1, 750 mL), and cooled to 0 °C. Solid NaHCO_3 (105.4 g, 1.255 mol) was added to the solution in one portion, immediately followed by the addition of solid Boc_2O (137 g,

0.628 mol). The mixture was then warmed up to room temperature, and stirred for 20 h. Then it was quenched with water (500 mL). The organic layer was extracted with diethyl ether (3 × 300 mL). The ether extracts were combined and washed with saturated aqueous NaHCO₃ solution (3 × 100 mL), then brine (3 × 100 mL), and dried over MgSO₄ for several hours, filtered, and then concentrated under reduced pressure to give the crude product as an oil. Purification of the crude product with flash column chromatography (silica gel; hexane/ethyl acetate = 9:1 → 6:1) gave the pure product as a clear colorless oil (90.7 g, 0.392 mol, 93.8%). R_f = 0.4 (silica gel; hexane/ethyl acetate = 9:1). ¹H NMR (chloroform-*d*, 300 MHz): δ 5.03 (d, ³J_{HH} = 8.4 Hz, 1 H, Me₃COC(O)NHCH(CHMe₂)COOCH₃), 4.20 (dd, ³J_{HH} = 4.8, 9.0 Hz, 1 H, Me₃COC(O)NHCH(CHMe₂)COOCH₃), 3.71 (s, 3 H, Me₃COC(O)NHCH(CHMe₂)COOCH₃), 2.09 (m, 1 H, Me₃COC(O)NHCH(CHMe₂)COOCH₃), 1.42 (s, 9 H, Me₃COC(O)NHCH(CHMe₂)COOCH₃), 0.93 (d, ³J_{HH} = 6.9 Hz, 3 H, Me₃COC(O)NHCH(CHMe₂)COOCH₃), 0.87 (d, ³J_{HH} = 6.9 Hz, 3 H, Me₃COC(O)NHCH(CHMe₂)COOCH₃).

3S-(Boc-amino)-2,4-dimethyl-2-pentanol. Following the literature procedure,³⁴ Boc-L-valine methyl ester (70.0 g, 0.303 mol) was degassed through “freeze-pump-thaw” cycle (3 ×), and dissolved in tetrahydrofuran (1.5 L). The solution was cooled to 0 °C, and methyl magnesium bromide solution (400.0 mL, 3.0 M in diethyl ether, 1.2 mol) was added dropwise over 3 h. The resulting brown solution with some white precipitate was warmed up to room temperature and stirred for 20 h, during which the precipitate dissolved. The solution was cooled to 0 °C again and carefully quenched with saturated

aqueous solution of NH_4Cl (800 mL). The aqueous layer was extracted with diethyl ether (2×250 mL), and the ether extracts were combined with the organic layer and washed with brine (2×600 mL), dried over Na_2SO_4 for several hours, filtered, and concentrated under reduced pressure to give the crude product as a slightly yellow oil. The crude product was then purified with flash column chromatography (silica gel; hexane/ethyl acetate = 9:1 \rightarrow 4:1) to give the pure product as a white solid (67.7 g, 0.293 mol, 96.7%). $R_f = 0.4$ (silica gel; hexane/ethyl acetate = 4:1). $^1\text{H NMR}$ (chloroform-*d*, 400 MHz): δ 4.87 (d, $^3J_{\text{HH}} = 10.0$ Hz, 1 H, $\text{Me}_3\text{COC}(\text{O})\text{NHCH}(\text{CHMe}_2)\text{CMe}_2\text{OH}$), 3.37 (dd, $^3J_{\text{HH}} = 2.4, 10.4$ Hz, 1 H, $\text{Me}_3\text{COC}(\text{O})\text{NHCH}(\text{CHMe}_2)\text{CMe}_2\text{OH}$), 2.08 (m, 1 H, $\text{Me}_3\text{COC}(\text{O})\text{NHCH}(\text{CHMe}_2)\text{CMe}_2\text{OH}$), 1.43 (s, 9 H, $\text{Me}_3\text{COC}(\text{O})\text{NHCH}(\text{CHMe}_2)\text{CMe}_2\text{OH}$), 1.24 (s, 3 H, $\text{Me}_3\text{COC}(\text{O})\text{NHCH}(\text{CHMe}_2)\text{CMe}_2\text{OH}$), 1.21 (s, 3 H, $\text{Me}_3\text{COC}(\text{O})\text{NHCH}(\text{CHMe}_2)\text{CMe}_2\text{OH}$), 0.93 (d, $^3J_{\text{HH}} = 6.8$ Hz, 3 H, $\text{Me}_3\text{COC}(\text{O})\text{NHCH}(\text{CHMe}_2)\text{CMe}_2\text{OH}$), 0.89 (d, $^3J_{\text{HH}} = 6.8$ Hz, 3 H, $\text{Me}_3\text{COC}(\text{O})\text{NHCH}(\text{CHMe}_2)\text{CMe}_2\text{OH}$).

2S-Amino-1,1,3-trimethylbutanol. Following a modified literature procedure,¹⁸ 3S-(Boc-amino)-2,4-dimethyl-2-pentanol (50.0 g, 0.216 mol) was dissolved in methanol (1 L) and cooled to 0 °C. Hydrochloric acid (108.0 mL, 12.1 M, 1.307 mol) was diluted with methanol (500 mL) and added dropwise to the solution in 30 min. The resulting solution was warmed up to room temperature and stirred for 17 h. The volatiles were then removed under reduced pressure, and diluted with diethyl ether (500 mL). The mixture was cooled to 0 °C and NaOH powder (80 g, 2.0 mol) was added in portions. The resulting yellow solution with white precipitate was stirred at room temperature for

another hour after it cooled down. The mixture was then filtered, concentrated under reduced pressure to give the crude product as a red oil, which was purified by distillation at 97 °C, 30 mmHg to give a clear colorless oil (26.0 g, 0.198 mol, 91.7%). ¹H NMR (chloroform-*d*, 400 MHz): δ 2.41 (d, ³J_{HH} = 2.8 Hz, 1 H, H₂NCH(CHMe₂)CMe₂OH), 1.92 (m, 1 H, H₂NCH(CHMe₂)CMe₂OH), 1.19 (s, 3 H, H₂NCH(CHMe₂)CMe₂OH), 1.11 (s, 3 H, H₂NCH(CHMe₂)CMe₂OH), 0.97 (d, ³J_{HH} = 7.2 Hz, 3 H, H₂NCH(CHMe₂)CMe₂OH), 0.88 (d, ³J_{HH} = 6.8 Hz, 3 H, H₂NCH(CHMe₂)CMe₂OH).

4*S*-Isopropyl-5,5-dimethyl-2-oxazoline. A modification of Meyers' procedure for 2-H oxazoline synthesis using 2*S*-amino-1,1,3-trimethylbutanol was implemented.²⁰ DMF-DMA (13.7 mL, 103 mmol) was added to degassed 2*S*-amino-1,1,3-trimethylbutanol (11.1 g, 84.6 mmol). This mixture was allowed to reflux at 75 °C for 7 h. The volatiles were removed under reduced pressure, and the mixture was triturated with hexane (4 × 30 mL). Then *p*-toluenesulfonic acid monohydrate (26.5 mg, 0.139 mmol) and hexane (40 mL) were added, and an addition funnel with approximately 40 mL of activated 4 Å molecular sieves inside was placed on top of the flask, and a condenser was placed on top of the addition funnel. The solution was heated at 90 °C for 24 h and the condensed liquid was washed over the sieves as the reaction proceeded. The reaction mixture was washed with saturated aqueous NaHCO₃ solution (30 mL) and then with brine (50 mL). The aqueous layers were combined, back-extracted with diethyl ether (6 × 25 mL), and then the organic extracted were combined with the organic layer and dried over Na₂SO₄ overnight and filtered. Concentration of the filtrate gave a dark red oil which was distilled at 85 °C, 18 mmHg to provide 4*S*-isopropyl-5,5-dimethyl-2-oxazoline as a clear colorless oil (8.11 g, 57.4 mmol, 67.8%). ¹H NMR (chloroform-*d*,

600 MHz): δ 6.74 (s, 1 H, $\text{CHNCH}(\text{CHMe}_2)\text{CMe}_2\text{O}$), 3.23 (d, $^3J_{\text{HH}} = 8.4$ Hz, 1 H, $\text{CHNCH}(\text{CHMe}_2)\text{CMe}_2\text{O}$), 1.80 (m, 1 H, $\text{CHNCH}(\text{CHMe}_2)\text{CMe}_2\text{O}$), 1.45 (s, 3 H, $\text{CHNCH}(\text{CHMe}_2)\text{CMe}_2\text{O}$), 1.29 (s, 3 H, $\text{CHNCH}(\text{CHMe}_2)\text{CMe}_2\text{O}$), 1.08 (d, $^3J_{\text{HH}} = 6.6$ Hz, 3 H, $\text{CHNCH}(\text{CHMe}_2)\text{CMe}_2\text{O}$), 0.98 (d, $^3J_{\text{HH}} = 6.6$ Hz, 3 H, $\text{CHNCH}(\text{CHMe}_2)\text{CMe}_2\text{O}$). $^{13}\text{C}\{^1\text{H}\}$ NMR (benzene- d_6 , 150 MHz): δ 152.74 ($\text{CHNCH}(\text{CHMe}_2)\text{CMe}_2\text{O}$), 85.17 ($\text{CHNCH}(\text{CHMe}_2)\text{CMe}_2\text{O}$), 80.07 ($\text{CHNCH}(\text{CHMe}_2)\text{CMe}_2\text{O}$), 29.56 ($\text{CHNCH}(\text{CHMe}_2)\text{CMe}_2\text{O}$), 29.48 ($\text{CHNCH}(\text{CHMe}_2)\text{CMe}_2\text{O}$), 21.53 ($\text{CHNCH}(\text{CHMe}_2)\text{CMe}_2\text{O}$), 21.48 ($\text{CHNCH}(\text{CHMe}_2)\text{CMe}_2\text{O}$), 21.20 ($\text{CHNCH}(\text{CHMe}_2)\text{CMe}_2\text{O}$). $^{15}\text{N}\{^1\text{H}\}$ NMR (benzene- d_6 , 71 MHz): δ -143. IR (KBr, cm^{-1}): 3069 w, 2973 s, 2874 m, 1686 w, 1632 s (CN), 1471 m, 1462 m, 1386 m, 1372 m, 1336 w, 1304 w, 1272 w, 1243 w, 1202 w, 1172 m, 1134 m, 1114 m, 1082 s, 1015 m, 934 m, 894 m, 856 w, 813 w, 769 w. $[\alpha]_{\text{D}}^{20} = -35.2$ (C_6H_6).

Li[To^P] (1). 4*S*-Isopropyl-5,5-dimethyl-2-oxazoline (0.966 g, 6.84 mmol) was degassed through “freeze-pump-thaw” cycle (3×) and dissolved in tetrahydrofuran (15 mL). The solution was cooled to -78 °C, and *t*BuLi solution (4.40 mL, 1.7 M in pentane, 7.48 mmol) was added dropwise. The resulting bright yellow solution was stirred at -78 °C for another hour. PhBCl₂ (0.250 mL, 1.93 mmol) was then added dropwise and the solution was stirred at -78 °C for another hour and gradually warmed up to room temperature and stirred for 48 h. The solvent was then removed *in vacuo* and the resulting yellow solid was extracted with benzene (2 × 15 mL). The benzene extracts were combined, evaporated *in vacuo*, and the crude product was then washed with pentane (2 × 5 mL), and dried *in vacuo* to give the product as a white solid (0.417 g, 0.809 mmol,

41.9%). ^1H NMR (acetonitrile- d_3 , 600 MHz): δ 7.5 (br, 2 H, *o*-C₆H₅), 7.04 (t, $^3J_{\text{HH}} = 6.6$ Hz, 2 H, *m*-C₆H₅), 6.96 (t, $^3J_{\text{HH}} = 6.6$ Hz, 1 H, *p*-C₆H₅), 3.2 (br, 3 H, CNCH(CHMe₂)CMe₂O), 1.76 (m, 3 H, CNCH(CHMe₂)CMe₂O), 1.21 (s, 9 H, CNCH(CHMe₂)CMe₂O), 1.16 (s, 9 H, CNCH(CHMe₂)CMe₂O), 0.99 (d, $^3J_{\text{HH}} = 6.6$ Hz, 9 H, CNCH(CHMe₂)CMe₂O), 0.95 (d, $^3J_{\text{HH}} = 6.6$ Hz, 9 H, CNCH(CHMe₂)CMe₂O). $^{13}\text{C}\{^1\text{H}\}$ NMR (acetonitrile- d_3 , 150 MHz): δ 185 (br, CNCH(CHMe₂)CMe₂O), 150 (br, *ipso*-C₆H₅), 135.33 (*o*-C₆H₅), 126.88 (*m*-C₆H₅), 125.02 (*p*-C₆H₅), 83.48 (CNCH(CHMe₂)CMe₂O), 79.81 (CNCH(CHMe₂)CMe₂O), 30.05 (CNCH(CHMe₂)CMe₂O and CNCH(CHMe₂)CMe₂O), 22.13 (CNCH(CHMe₂)CMe₂O), 21.78 (CNCH(CHMe₂)CMe₂O), 20.48 (CNCH(CHMe₂)CMe₂O). ^{11}B NMR (acetonitrile- d_3 , 128 MHz): δ -17.8. $^{15}\text{N}\{^1\text{H}\}$ NMR (acetonitrile- d_3 , 71 MHz): δ -163. IR (KBr, cm^{-1}): 3068 w, 3044 w, 2970 s, 2932 m, 2875 m, 1653 w, 1635 w, 1583 s (CN), 1560 w, 1471 m, 1432 w, 1386 m, 1369 m, 1247 w, 1213 m, 1194 m, 1173 m, 1138 m, 1096 w, 1019 m, 948 m, 895 w, 742 w, 709 w. Anal. Calcd for C₃₀H₄₇BLiN₃O₃: C, 69.90; H, 9.19; N, 8.15. Found: C, 65.02; H, 8.79; N, 7.51. Mp, 238-241 °C.

Tl[To^{P*}] (2). Thallium(I) acetate (0.182 g, 0.691 mmol) was added to the solution of Li[To^{P*}] (**1**, 0.293 g, 0.568 mmol) in methylene chloride (15 mL). The resulting yellow suspension with white precipitate was stirred at room temperature for 18 h, during which it turned to a gray suspension. The suspension was then filtered, and the filtrate was evaporated *in vacuo* to give the crude product as a brown solid, which was then washed with pentane (3 × 10 mL) to give the product as an off-white solid (0.174 g, 0.244 mmol, 43.0%). ^1H NMR (acetonitrile- d_3 , 600 MHz): δ 7.6 (br, 2 H, *o*-C₆H₅), 7.02 (t, $^3J_{\text{HH}} = 6.6$ Hz, 2 H, *m*-C₆H₅), 6.94 (t, $^3J_{\text{HH}} = 6.6$ Hz, 1 H, *p*-C₆H₅), 3.2 (br, 3 H,

CNCH(CHMe₂)CMe₂O), 1.71 (m, 3 H, CNCH(CHMe₂)CMe₂O), 1.20 (s, 9 H, CNCH(CHMe₂)CMe₂O), 1.15 (s, 9 H, CNCH(CHMe₂)CMe₂O), 0.98 (d, ³J_{HH} = 5.4 Hz, 9 H, CNCH(CHMe₂)CMe₂O), 0.92 (d, ³J_{HH} = 5.4 Hz, 9 H, CNCH(CHMe₂)CMe₂O). ¹³C{¹H} NMR (acetonitrile-*d*₃, 150 MHz): δ 185 (br, CNCH(CHMe₂)CMe₂O), 151 (br, *ipso*-C₆H₅), 135.70 (*o*-C₆H₅), 126.60 (*m*-C₆H₅), 124.65 (*p*-C₆H₅), 82.80 (CNCH(CHMe₂)CMe₂O), 80.13 (CNCH(CHMe₂)CMe₂O), 30.21 (CNCH(CHMe₂)CMe₂O), 30.12 (CNCH(CHMe₂)CMe₂O), 22.09 (CNCH(CHMe₂)CMe₂O), 21.88 (CNCH(CHMe₂)CMe₂O), 20.43 (CNCH(CHMe₂)CMe₂O). ¹¹B NMR (acetonitrile-*d*₃, 128 MHz): δ -18.0. ¹⁵N{¹H} NMR (acetonitrile-*d*₃, 71 MHz): δ -160. IR (KBr, cm⁻¹): 3068 w, 3044 w, 2971 s, 2932 m, 2875 m, 1653 w, 1584 s (CN), 1458 m, 1436 m, 1386 m, 1368 m, 1274 w, 1247 w, 1215 m, 1173 w, 1141 m, 1096 w, 1019 w, 989 w, 964 w, 948 m, 895 w, 809 w, 742 w, 709 m. Anal. Calcd for C₃₀H₄₇BN₃O₃Tl: C, 50.54; H, 6.65; N, 5.89. Found: C, 53.76; H, 7.05; N, 6.15. Mp, 249-251 °C.

H[To^{P*}] (3). Triethylammonium chloride (0.174 g, 1.26 mmol) was added to the solution of Li[To^{P*}] (1, 0.539 g, 1.05 mmol) in methylene chloride (15 mL). The resulting yellow suspension with white precipitate was stirred at room temperature for 18 h, during which it turned to a white suspension. The suspension was then filtered, and the filtrate was evaporated *in vacuo* to give the crude product, which was extracted with pentane (2 × 10 mL). The pentane extracts were combined and cooled to -30 °C, and the white precipitate was isolated and dried *in vacuo* to give the product as a sticky slightly yellow solid (0.242 g, 0.475 mmol, 45.2%). ¹H NMR (benzene-*d*₆, 600 MHz): δ 8.06 (d, ³J_{HH} = 6.6 Hz, 2 H, *o*-C₆H₅), 7.44 (t, ³J_{HH} = 6.6 Hz, 2 H, *m*-C₆H₅), 7.24 (t, ³J_{HH} = 6.6 Hz,

1 H, *p*-C₆H₅), 3.07 (d, $^3J_{\text{HH}} = 8.4$ Hz, 3 H, CNCH(CHMe₂)CMe₂O), 1.63 (m, 3 H, CNCH(CHMe₂)CMe₂O), 1.24 (s, 9 H, CNCH(CHMe₂)CMe₂O), 1.1 (br, 18 H, CNCH(CHMe₂)CMe₂O (9 H) and CNCH(CHMe₂)CMe₂O (9 H)), 0.75 (d, $^3J_{\text{HH}} = 5.4$ Hz, 9 H, CNCH(CHMe₂)CMe₂O). $^{13}\text{C}\{^1\text{H}\}$ NMR (benzene-*d*₆, 150 MHz): δ 187 (br, CNCH(CHMe₂)CMe₂O), 147 (br, *isop*-C₆H₅), 134.96 (*o*-C₆H₅), 127.72 (*m*-C₆H₅), 126.04 (*p*-C₆H₅), 86.18 (CNCH(CHMe₂)CMe₂O), 77.77 (CNCH(CHMe₂)CMe₂O), 29.59 (CNCH(CHMe₂)CMe₂O), 29.28 (CNCH(CHMe₂)CMe₂O), 21.57 (CNCH(CHMe₂)CMe₂O), 21.42 (CNCH(CHMe₂)CMe₂O), 21.25 (CNCH(CHMe₂)CMe₂O). ^{11}B NMR (benzene-*d*₆, 128 MHz): δ -17.8. $^{15}\text{N}\{^1\text{H}\}$ NMR (benzene-*d*₆, 71 MHz): -173. IR (KBr, cm⁻¹): 3074 w, 3047 w, 2971 s, 2932 m, 2871 m, 2836 w, 1653 w, 1624 m, 1601 s (CN), 1583 m (CN), 1559 w, 1489 m, 1471 m, 1409 m, 1380 m, 1368 m, 1334 m, 1277 w, 1200 w, 1141 m, 1117 w, 1096 w, 1024 m, 970 m, 930 w, 888 w, 852 w, 792 w, 756 m. Anal. Calcd for C₃₀H₄₈BN₃O₃: C, 70.72; H, 9.50; N, 8.25. Found: C, 71.03; H, 9.91; N, 8.29. Mp, 126-128 °C.

To^P*Mn(CO)₃ (4). Manganese pentacarbonyl bromide (0.0567 g, 0.206 mmol) was added to the solution of Li[To^P*] (**1**, 0.106 g, 0.206 mol) in tetrahydrofuran (15 mL). The solution was heated to 85 °C for 24 h. The solvent was then removed under reduced pressure, and the resulting solid was extracted with benzene (2 × 15 mL). The benzene extracts were combined, filtered through a short plug of grade III neutral alumina (1.5 mL). The filtrate was evaporated *in vacuo* to give the product as a yellow solid (0.123 g, 0.190 mol, 92.2%). ^1H NMR (benzene-*d*₆, 600 MHz): δ 8.23 (d, $^3J_{\text{HH}} = 7.2$ Hz, 2 H, *o*-C₆H₅), 7.48 (t, $^3J_{\text{HH}} = 7.2$ Hz, 2 H, *m*-C₆H₅), 7.25 (t, $^3J_{\text{HH}} = 7.2$ Hz, 1 H, *p*-C₆H₅), 3.6 (br, 3 H, CNCH(CHMe₂)CMe₂O), 2.67 (m, 3 H, CNCH(CHMe₂)CMe₂O), 1.12 (s, 9 H,

CNCH(CHMe₂)CMe₂O), 1.11 (s, 9 H, CNCH(CHMe₂)CMe₂O), 1.05 (d, ³J_{HH} = 7.2 Hz, 9 H, CNCH(CHMe₂)CMe₂O), 0.90 (d, ³J_{HH} = 7.2 Hz, 9 H, CNCH(CHMe₂)CMe₂O). ¹³C{¹H} NMR (benzene-*d*₆, 150 MHz): δ 223 (br, CO), 189 (br, CNCH(CHMe₂)CMe₂O), 143 (br, *ipso*-C₆H₅), 136.20 (*o*-C₆H₅), 127.30 (*m*-C₆H₅), 126.11 (*p*-C₆H₅), 88.38 (CNCH(CHMe₂)CMe₂O), 80.09 (CNCH(CHMe₂)CMe₂O), 31.69 (CNCH(CHMe₂)CMe₂O), 30.23 (CNCH(CHMe₂)CMe₂O), 23.11 (CNCH(CHMe₂)CMe₂O), 18.85 (CNCH(CHMe₂)CMe₂O), 17.35 (CNCH(CHMe₂)CMe₂O). ¹¹B NMR (benzene-*d*₆, 128 MHz): δ -18.7. IR (KBr, cm⁻¹): 3074 w, 3046 w, 3019 w, 2975 m, 2935 m, 2878 m, 2013 s (CO), 1903 s (CO), 1592 m (CN), 1470 w, 1391 w, 1371 w, 1258 m, 1147 w, 1127 w, 1024 m. Anal. Calcd for C₃₃H₄₇BMnN₃O₆: C, 61.21; H, 7.32; N, 6.49. Found: C, 61.40; H, 7.41; N, 6.38. Mp, 164-167 °C.

To^{P*}Re(CO)₃ (5). Rhenium pentacarbonyl bromide (0.0800 g, 0.197 mmol) was added to the solution of Li[To^{P*}] (**1**, 0.102 g, 0.198 mmol) in tetrahydrofuran (15 mL). The solution was heated to 85 °C for 24 h. The solvent was then removed under reduced pressure, and the resulting solid was extracted with benzene (2 × 15 mL). The benzene extracts were combined, filtered through a short plug of grade III neutral alumina (1.5 mL). The filtrate was evaporated *in vacuo* to give the product as a yellow solid (0.146 g, 0.187 mmol, 94.9%). ¹H NMR (benzene-*d*₆, 600 MHz): δ 8.19 (d, ³J_{HH} = 7.2 Hz, 2 H, *o*-C₆H₅), 7.48 (t, ³J_{HH} = 7.2 Hz, *m*-C₆H₅), 7.26 (t, ³J_{HH} = 7.2 Hz, 1 H, *p*-C₆H₅), 3.6 (br, 3 H, CNCH(CHMe₂)CMe₂O), 2.63 (m, 3 H, CNCH(CHMe₂)CMe₂O), 1.07-1.05 (m, 27 H, CNCH(CHMe₂)CMe₂O (9 H) and CNCH(CHMe₂)CMe₂O (18 H)), 0.86 (d, ³J_{HH} = 7.2 Hz, 9 H, CNCH(CHMe₂)CMe₂O). ¹³C{¹H} NMR (benzene-*d*₆, 150 MHz): δ 199 (br,

CO), 189 (br, CNCH(CHMe₂)CMe₂O), 142 (br, *ipso*-C₆H₅), 136.15 (*o*-C₆H₅), 127.36 (*m*-C₆H₅), 126.35 (*p*-C₆H₅), 89.04 (CNCH(CHMe₂)CMe₂O), 80.53 (CNCH(CHMe₂)CMe₂O), 31.43 (CNCH(CHMe₂)CMe₂O), 30.19 (CNCH(CHMe₂)CMe₂O), 22.84 (CNCH(CHMe₂)CMe₂O), 18.49 (CNCH(CHMe₂)CMe₂O), 17.60 (CNCH(CHMe₂)CMe₂O). ¹¹B NMR (benzene-*d*₆, 128 MHz): δ -18.2. ¹⁵N{¹H} NMR (benzene-*d*₆, 71 MHz): δ -197. IR (KBr, cm⁻¹): 3074 w, 3047 w, 3003 w, 2974 m, 2934 m, 2877 m, 2008 s (CO), 1886 s (CO), 1584 m (CN), 1553 w, 1463 w, 1391 m, 1372 m, 1296 m, 1261 m, 1201 m, 1154 m, 1125 m. Anal. Calcd for C₃₃H₄₇BN₃O₆Re: C, 50.90; H, 6.08; N, 5.40. Found: C, 50.97; H, 6.47; N, 5.36. Mp, 189-191 °C.

To^P*ZnEt (6). Diethyl zinc (22.0 μL, 0.215 mmol) was added to the solution of H[To^P*] (**3**, 0.109 g, 0.214 mmol) in benzene (10 mL). The resulting solution was stirred at room temperature for 1 h. The solvent was then removed *in vacuo* to give the product as a white solid (0.122 g, 0.202 mmol, 94.4%). ¹H NMR (benzene-*d*₆, 600 MHz): δ 8.27 (d, ³J_{HH} = 6.6 Hz, 2 H, *o*-C₆H₅), 7.50 (t, ³J_{HH} = 6.6 Hz, 2 H, *m*-C₆H₅), 7.26 (t, ³J_{HH} = 6.6 Hz, 1 H, *p*-C₆H₅), 3.3 (br, 3 H, CNCH(CHMe₂)CMe₂O), 1.83 (t, ³J_{HH} = 6.6 Hz, 3 H, ZnCH₂CH₃), 1.65 (m, 3 H, CNCH(CHMe₂)CMe₂O), 1.08 (s, 9 H, CNCH(CHMe₂)CMe₂O), 1.0 (br, 18 H, CNCH(CHMe₂)CMe₂O (9 H) and CNCH(CHMe₂)CMe₂O (9 H)), 0.92 (d, ³J_{HH} = 6.0 Hz, 9 H, CNCH(CHMe₂)CMe₂O), 0.8 (br, 2 H, ZnCH₂CH₃). ¹³C{¹H} NMR (benzene-*d*₆, 150 MHz): δ 191 (br, CNCH(CHMe₂)CMe₂O), 144 (br, *ipso*-C₆H₅), 136.45 (*o*-C₆H₅), 127.15 (*m*-C₆H₅), 125.86 (*p*-C₆H₅), 87.61 (CNCH(CHMe₂)CMe₂O), 77.40 (CNCH(CHMe₂)CMe₂O), 30.09 (CNCH(CHMe₂)CMe₂O), 29.89 (CNCH(CHMe₂)CMe₂O), 21.96

(CNCH(CHMe₂)CMe₂O), 21.62 (CNCH(CHMe₂)CMe₂O), 18.99 (CNCH(CHMe₂)CMe₂O), 14.26 (ZnCH₂CH₃), 0.51 (ZnCH₂CH₃). ¹¹B NMR (benzene-*d*₆, 128 MHz): -18.0. ¹⁵N{¹H} NMR (benzene-*d*₆, 71 MHz): δ -177. IR (KBr, cm⁻¹): 3080 w, 3047 m, 2970 s, 2932 s, 2851 m, 1585 s (CN), 1558 w, 1495 w, 1466 m, 1386 m, 1371 m, 1336 w, 1254 s, 1231 s, 1202 m, 1191 m, 1139 s, 1109 w, 1019 m, 993 m, 947 m, 888 w, 839 w, 816 m, 747 m, 703 m. Anal. Calcd for C₃₂H₅₂BN₃O₃Zn: C, 63.74; H, 8.69; N, 6.97. Found: C, 63.30; H, 8.65; N, 6.96. Mp, 130-132 °C.

To^P*ZnCl (7). Zinc chloride (0.108 g, 0.792 mmol) was added to the solution of Li[To^P*] (**1**, 0.406 g, 0.788 mmol) in benzene (20 mL). The solution was then heated at 60 °C for 18 h. The resulting yellow solution with white precipitate was filtered, and the filtrate was evaporated *in vacuo* to give a yellow solid, which was triturated with pentane and dried *in vacuo* to give the product as a yellow solid (0.355 g, 0.583 mmol, 74.0%). ¹H NMR (benzene-*d*₆, 600 MHz): δ 8.22 (d, ³J_{HH} = 7.2 Hz, 2 H, *o*-C₆H₅), 7.49 (t, ³J_{HH} = 7.2 Hz, 2 H, *m*-C₆H₅), 7.26 (t, ³J_{HH} = 7.2 Hz, 1 H, *p*-C₆H₅), 3.42 (d, ³J_{HH} = 3.0 Hz, 3 H, CNCH(CHMe₂)CMe₂O), 1.65 (m, 3 H, CNCH(CHMe₂)CMe₂O), 1.22 (d, ³J_{HH} = 6.6 Hz, 9 H, CNCH(CHMe₂)CMe₂O), 1.03 (s, 9 H, CNCH(CHMe₂)CMe₂O), 0.98 (s, 9 H, CNCH(CHMe₂)CMe₂O), 0.94 (d, ³J_{HH} = 6.6 Hz, 9 H, CNCH(CHMe₂)CMe₂O). ¹³C{¹H} NMR (benzene-*d*₆, 150 MHz): δ 191 (br, CNCH(CHMe₂)CMe₂O), 142.25 (*ipso*-C₆H₅), 136.30 (*o*-C₆H₅), 127.30 (*m*-C₆H₅), 126.26 (*p*-C₆H₅), 88.91 (CNCH(CHMe₂)CMe₂O), 76.86 (CNCH(CHMe₂)CMe₂O), 29.99 (CNCH(CHMe₂)CMe₂O), 29.66 (CNCH(CHMe₂)CMe₂O), 22.51 (CNCH(CHMe₂)CMe₂O), 21.47 (CNCH(CHMe₂)CMe₂O), 18.94 (CNCH(CHMe₂)CMe₂O). ¹¹B NMR (benzene-*d*₆, 128 MHz): δ -17.9. ¹⁵N{¹H} NMR (benzene-*d*₆, 71 MHz): δ -184. IR (KBr, cm⁻¹): 3079 w,

3046 w, 2969 s, 2932 m, 2875 m, 1579 s (CN), 1466 m, 1390 m, 1372 m, 1339 w, 1290 m, 1257 s, 1192 w, 1141 s, 1110 w, 1023 m, 951 m, 885 m. Anal. Calcd for $C_{30}H_{47}BClN_3O_3Zn$: C, 59.13; H, 7.77; N, 6.90. Found: C, 58.78; H, 8.05; N, 6.80. Mp, 249-251 °C.

To^P*ZnH (8). Potassium *tert*-butoxide (0.0393 g, 0.350 mmol) was added to the solution of To^P*ZnCl (7, 0.213 g, 0.350 mmol) in benzene (15 mL). The solution was then stirred at room temperature for 2 d. Phenylsilane (43.5 μL, 0.353 mmol) was then added, and the resulting solution was stirred at room temperature for another 18 h. The solution was then filtered, and the filtrate was evaporated *in vacuo*. The resulting was washed with pentane (2 × 5 mL), and dried *in vacuo* to give the product as a white solid (0.177 g, 0.308 mmol, 88.0%). ¹H NMR (benzene-*d*₆, 600 MHz): δ 8.29 (d, ³*J*_{HH} = 7.2 Hz, 2 H, *o*-C₆H₅), 7.52 (t, ³*J*_{HH} = 7.2 Hz, 2 H, *m*-C₆H₅), 7.27 (t, ³*J*_{HH} = 7.2 Hz, 1 H, *p*-C₆H₅), 4.61 (s, 1 H, ZnH), 3.4 (br, 3 H, CNCH(CHMe₂)CMe₂O), 1.63 (m, 3 H, CNCH(CHMe₂)CMe₂O), 1.19 (d, ³*J*_{HH} = 7.2 Hz, 9 H, CNCH(CHMe₂)CMe₂O), 1.07 (s, 9 H, CNCH(CHMe₂)CMe₂O), 1.02 (s, 9 H, CNCH(CHMe₂)CMe₂O), 0.98 (d, ³*J*_{HH} = 6.6 Hz, 9 H, CNCH(CHMe₂)CMe₂O). ¹³C{¹H} NMR (benzene-*d*₆, 150 MHz): δ 191 (br, CNCH(CHMe₂)CMe₂O), 144 (br, *ipso*-C₆H₅), 136.47 (*o*-C₆H₅), 127.18 (*m*-C₆H₅), 125.96 (*p*-C₆H₅), 87.84 (CNCH(CHMe₂)CMe₂O), 77.62 (CNCH(CHMe₂)CMe₂O), 30.15 (CNCH(CHMe₂)CMe₂O), 29.78 (CNCH(CHMe₂)CMe₂O), 22.81 (CNCH(CHMe₂)CMe₂O), 21.46 (CNCH(CHMe₂)CMe₂O), 19.16 (CNCH(CHMe₂)CMe₂O). ¹¹B NMR (benzene-*d*₆, 128 MHz): δ -18.0. ¹⁵N{¹H} NMR (benzene-*d*₆, 71 MHz): δ -179. IR (KBr, cm⁻¹): 3082 w, 3045 w, 2964 m, 2931 m, 2873 m, 1766 m (ZnH), 1587 s (CN), 1464 m, 1389 w, 1371 m, 1286 w, 1254 m, 1234 m,

1202 w, 1194 w, 1140 m, 1112 w, 1022 m, 1001 w, 950 m, 885 w. Anal. Calcd for $C_{30}H_{48}BN_3O_3Zn$: C, 62.67; H, 8.42; N, 7.31. Found: C, 62.53; H, 8.30; N, 7.10. Mp, 186-189 °C.

PhMeHSiOMe. Phenylmethylsilane (0.720 mL, 5.24 mmol) and To^P*ZnH (0.0150 g, 0.0261 mmol) were dissolved in benzene (10 mL), and methanol (0.105 mL, 2.59 mmol) was added to the solution. Bubbles formed immediately, and the resulting clear and colorless solution was stirred at room temperature for 4 h before it was filtered through a short plug of celite (5 mL). The celite plug was further washed with benzene (3 mL \times 2). The clear and colorless filtrates were combined with the wash, and the mixture was purified by distillation. The product was distilled at 53 °C (15 mmHg) to give the product as a clear colorless liquid (0.312 g, 2.05 mmol, 79.2%). 1H NMR (benzene- d_6 , 600 MHz): δ 7.56 (m, 2 H, *o*-C₆H₅), 7.20 (m, 3 H, *p*- and *m*-C₆H₅), 5.17 (q, $^3J_{HH} = 3.0$ Hz, $^1J_{SiH} = 207$ Hz, 1 H, SiH), 3.30 (s, 3 H, OMe), 0.33 (d, $^3J_{HH} = 2.4$ Hz, 3 H, SiMe). $^{13}C\{^1H\}$ NMR (benzene- d_6 , 150 MHz): δ 136.38 (*ipso*-C₆H₅), 134.55 (*o*-C₆H₅), 130.71 (*p*-C₆H₅), 128.65 (*m*-C₆H₅), 52.04 (OMe), -2.59 (SiMe). $^{29}Si\{^1H\}$ NMR (benzene- d_6 , 119 MHz): δ -0.61. GC-MS: $C_8H_{12}OSi$ m/e 152 (M^+). $[\alpha]_D^{20} = -212.42$ (C₆H₆).

PhMeHSiOEt. Phenylmethylsilane (0.480 mL, 3.49 mmol) and To^P*ZnH (0.0100 g, 0.0174 mmol) were dissolved in benzene (10 mL), and ethanol (0.100 mL, 1.71 mmol) was added to the solution. Bubbles formed immediately, and the resulting clear and colorless solution was stirred at room temperature for 8 h before it was filtered through a short plug of celite (5 mL). The celite plug was further washed with benzene (3 mL \times 2). The clear and colorless filtrates were combined with the wash, and the mixture was purified by distillation. The product was distilled at 61 °C (10 mmHg) to give the

product as a clear colorless liquid (0.213 g, 1.28 mmol, 74.9%). ^1H NMR (benzene- d_6 , 600 MHz): δ 7.60 (m, 2 H, *o*-C₆H₅), 7.20 (m, 3 H, *p*- and *m*-C₆H₅), 5.25 (q, $^3J_{\text{HH}} = 3.0$ Hz, $^1J_{\text{SiH}} = 206$ Hz, 1 H, SiH), 3.60 (q, $^3J_{\text{HH}} = 7.2$ Hz, 2 H, OCH₂CH₃), 1.08 (t, $^3J_{\text{HH}} = 7.2$ Hz, 3 H, OCH₂CH₃), 0.36 (d, $^3J_{\text{HH}} = 2.4$ Hz, 3 H, SiMe). $^{13}\text{C}\{^1\text{H}\}$ NMR (benzene- d_6 , 150 MHz): δ 136.87 (*ipso*-C₆H₅), 134.56 (*o*-C₆H₅), 130.64 (*p*-C₆H₅), 128.63 (*m*-C₆H₅), 60.47 (OCH₂CH₃), 18.72 (OCH₂CH₃), -2.12 (SiMe). $^{29}\text{Si}\{^1\text{H}\}$ NMR (benzene- d_6 , 119 MHz): δ -3.45. GC-MS: C₉H₁₄OSi m/e 166 (M⁺). $[\alpha]_{\text{D}}^{20} = +22.01$ (C₆H₆).

PhMeHSi(O-3,5-C₆H₃Me₂). Phenylmethylosilane (0.120 mL, 0.874 mmol) and To^P*ZnH (0.0100 g, 0.0174 mmol) were dissolved in benzene (2 mL), and 3,5-dimethylphenol (0.106 g, 0.868 mmol) was added to the solution. The resulting clear and colorless solution was stirred at room temperature for 4 d before it was filtered through a short plug of celite (5 mL). The celite plug was further washed with benzene (3 mL × 2). The clear and colorless filtrates were combined with the wash, and the mixture was purified by distillation. The product was distilled at 101 °C (0.1 mmHg) to give the product as a clear colorless oil (0.170 g, 0.701 mmol, 80.8%). ^1H NMR (benzene- d_6 , 600 MHz): δ 7.63 (m, 2 H, *o*-C₆H₅), 7.16 (m, *p*- and *m*-C₆H₅, overlapped with benzene- d_6), 6.73 (s, 2 H, *o*-C₆H₃Me₂), 6.50 (s, 1 H, *p*-C₆H₃Me₂), 5.55 (q, $^3J_{\text{HH}} = 3.0$ Hz, $^1J_{\text{SiH}} = 213$ Hz, 1 H, SiH), 2.06 (s, 6 H, C₆H₃Me₂), 0.44 (d, $^3J_{\text{HH}} = 3.0$ Hz, 3 H, SiMe). $^{13}\text{C}\{^1\text{H}\}$ NMR (benzene- d_6 , 150 MHz): δ 156.32 (*ipso*-C₆H₃Me₂), 139.79 (*m*-C₆H₃Me₂), 135.72 (*ipso*-C₆H₅), 134.56 (*o*-C₆H₅), 130.95 (*p*-C₆H₅), 128.73 (*m*-C₆H₅), 124.39 (*p*-C₆H₃Me₂), 117.90 (*o*-C₆H₃Me₂), 21.62 (C₆H₃Me₂), -2.01 (SiMe). $^{29}\text{Si}\{^1\text{H}\}$ NMR (benzene- d_6 , 119 MHz): δ -5.23. GC-MS: C₁₅H₁₈OSi m/e 242 (M⁺). $[\alpha]_{\text{D}}^{20} = -198.31$ (C₆H₆).

1-NpPhHSiOMe. 1-Naphthylphenylsilane (1.150 mL, 5.25 mmol) and $\text{To}^{\text{P}}\text{*ZnH}$ (0.0150 g, 0.0261 mmol) were dissolved in benzene (10 mL), and methanol (0.105 mL, 2.59 mmol) was added to the solution. Bubbles formed immediately, and the resulting clear and colorless solution was stirred at room temperature for 6 h before it was filtered through a short plug of celite (5 mL). The celite plug was further washed with benzene (3 mL \times 2). The clear and colorless filtrates were combined with the wash, and the mixture was purified by distillation. The product was distilled at 120 °C (0.1 mmHg) to give the product as a clear colorless oil (0.617 g, 2.33 mmol, 90.0%). ^1H NMR (benzene- d_6 , 600 MHz): δ 8.38 (m, 1 H, C_{10}H_7), 7.93 (d, $^3J_{\text{HH}} = 6.6$ Hz, 1 H, C_{10}H_7), 7.70 (d, $^3J_{\text{HH}} = 7.8$ Hz, 2 H, *o*- C_6H_5), 7.67 (d, $^3J_{\text{HH}} = 7.8$ Hz, 1 H, C_{10}H_7), 7.61 (m, 1 H, C_{10}H_7), 7.27 (t, $^3J_{\text{HH}} = 7.8$ Hz, 1 H, *p*- C_6H_5), 7.20 (m, 2 H, C_{10}H_7), 7.11 (m, 3 H, *m*- C_6H_5 (2 H) and C_{10}H_7 (1 H)), 5.94 (s, $^1J_{\text{SiH}} = 212$ Hz, 1 H, SiH), 3.44 (s, 3 H, OMe). $^{13}\text{C}\{^1\text{H}\}$ NMR (benzene- d_6 , 150 MHz): δ 138.05 (C_{10}H_7), 137.61 (C_{10}H_7), 136.34 (*ipso*- C_6H_5), 135.29 (*o*- C_6H_5), 134.20 (C_{10}H_7), 134.09 (C_{10}H_7), 131.91 (C_{10}H_7), 131.69 (C_{10}H_7), 130.90 (C_{10}H_7), 130.45 (C_{10}H_7), 128.85 (*m*- C_6H_5), 127.11 (C_{10}H_7), 126.49 (C_{10}H_7), 125.96 (*p*- C_6H_5), 52.68 (OMe). $^{29}\text{Si}\{^1\text{H}\}$ NMR (benzene- d_6 , 119 MHz): δ -7.86. GC-MS: $\text{C}_{17}\text{H}_{16}\text{OSi}$ m/e 264 (M^+). $[\alpha]_{\text{D}}^{20} = +9.20$ (C_6H_6).

1-NpPhHSiOEt. 1-Naphthylphenylsilane (0.770 mL, 3.51 mmol) and $\text{To}^{\text{P}}\text{*ZnH}$ (0.0100 g, 0.0174 mmol) were dissolved in benzene (10 mL), and ethanol (0.100 mL, 1.71 mmol) was added to the solution. Bubbles formed immediately, and the resulting clear and colorless solution was stirred at room temperature for 10 h before it was filtered through a short plug of celite (5 mL). The celite plug was further washed with benzene (3 mL \times 2). The clear and colorless filtrates were combined with the wash, and the mixture

was purified by distillation. The product was distilled at 140 °C (0.1 mmHg) to give the product as a clear colorless oil (0.435 g, 1.56 mmol, 91.2%). ^1H NMR (benzene- d_6 , 600 MHz): δ 8.42 (m, 1 H, C_{10}H_7), 7.97 (d, $^3J_{\text{HH}} = 6.6$ Hz, 1 H, C_{10}H_7), 7.73 (d, $^3J_{\text{HH}} = 7.2$ Hz, 2 H, $o\text{-C}_6\text{H}_5$), 7.67 (d, $^3J_{\text{HH}} = 7.8$ Hz, 1 H, C_{10}H_7), 7.61 (m, 1 H, C_{10}H_7), 7.29 (t, $^3J_{\text{HH}} = 7.2$ Hz, 1 H, $p\text{-C}_6\text{H}_5$), 7.20 (m, 2 H, C_{10}H_7), 7.13 (m, 3 H, $m\text{-C}_6\text{H}_5$ (2 H) and C_{10}H_7 (1 H)), 5.99 (s, $^1J_{\text{SiH}} = 211$ Hz, 1 H, SiH), 3.74 (m, 2 H, OCH_2CH_3), 1.12 (t, $^3J_{\text{HH}} = 6.6$ Hz, 3 H, OCH_2CH_3). $^{13}\text{C}\{^1\text{H}\}$ NMR (benzene- d_6 , 150 MHz): δ 138.05 (C_{10}H_7), 137.61 (C_{10}H_7), 136.34 (*ipso*- C_6H_5), 135.31 ($o\text{-C}_6\text{H}_5$), 134.22 (C_{10}H_7), 134.10 (C_{10}H_7), 131.86 (C_{10}H_7), 131.69 (C_{10}H_7), 130.82 (C_{10}H_7), 130.45 (C_{10}H_7), 128.85 ($m\text{-C}_6\text{H}_5$), 127.01 (C_{10}H_7), 126.47 (C_{10}H_7), 125.97 ($p\text{-C}_6\text{H}_5$), 61.22 (OCH_2CH_3), 18.66 (OCH_2CH_3). $^{29}\text{Si}\{^1\text{H}\}$ NMR (benzene- d_6 , 119 MHz): δ -10.96. GC-MS: $\text{C}_{18}\text{H}_{18}\text{OSi}$ m/e 278 (M^+). $[\alpha]_{\text{D}}^{20} = +3.66$ (C_6H_6).

1-NpPhHSiOiPr. 1-Naphthylphenylsilane (0.380 mL, 1.73 mmol) and $\text{To}^{\text{P}}\text{*ZnH}$ (0.0100 g, 0.0174 mmol) were dissolved in benzene (2 mL), and isopropanol (0.130 mL, 1.70 mmol) was added to the solution. The resulting clear and colorless solution was stirred at room temperature for 14 d before it was filtered through a short plug of celite (5 mL). The celite plug was further washed with benzene (3 mL \times 2). The clear and colorless filtrates were combined with the wash, and the mixture was purified by distillation. The product was distilled at 146 °C (0.1 mmHg) to give the product as a clear colorless oil (0.333 g, 1.14 mmol, 67.1%). ^1H NMR (benzene- d_6 , 600 MHz): δ 8.43 (m, 1 H, C_{10}H_7), 8.01 (d, $^3J_{\text{HH}} = 6.6$ Hz, 1 H, C_{10}H_7), 7.75 (d, $^3J_{\text{HH}} = 7.8$ Hz, 2 H, $o\text{-C}_6\text{H}_5$), 7.70 (d, $^3J_{\text{HH}} = 8.4$ Hz, 1 H, C_{10}H_7), 7.62 (m, 1 H, C_{10}H_7), 7.30 (t, $^3J_{\text{HH}} = 7.2$ Hz, 1 H, $p\text{-C}_6\text{H}_5$), 7.20 (m, 2 H, C_{10}H_7), 7.13 (m, 3 H, $m\text{-C}_6\text{H}_5$ (2 H) and C_{10}H_7 (1 H)), 6.02 (s, $^1J_{\text{SiH}} = 211$

Hz, 1 H, SiH), 4.11 (m, 1 H, OCHMe₂), 1.19 (d, ³J_{HH} = 6.0 Hz, 3 H, OCHMe₂), 1.13 (d, ³J_{HH} = 6.0 Hz, 3 H, OCHMe₂). ¹³C{¹H} NMR (benzene-*d*₆, 150 MHz): δ 138.01 (C₁₀H₇), 136.32 (C₁₀H₇), 135.75 (*ipso*-C₆H₅), 135.29 (*o*-C₆H₅), 134.24 (C₁₀H₇), 133.73 (C₁₀H₇), 131.81 (C₁₀H₇), 130.74 (C₁₀H₇), 129.48 (C₁₀H₇), 129.07 (C₁₀H₇), 128.69 (*m*-C₆H₅), 126.90 (C₁₀H₇), 126.44 (C₁₀H₇), 125.81 (*p*-C₆H₅), 68.18 (OCHMe₂), 25.76 (OCHMe₂), 25.70 (OCHMe₂). ²⁹Si{¹H} NMR (benzene-*d*₆, 119 MHz): δ -13.70. GC-MS: C₁₉H₂₀OSi m/e 292 (M⁺). [α]_D²⁰ = +17.18 (C₆H₆).

1-NpPhHSi(O-3,5-C₆H₃Me₂). 1-Naphthylphenylsilane (0.190 mL, 0.867 mmol) and To^P*ZnH (0.0100 g, 0.0174 mmol) were dissolved in benzene (2 mL), and 3,5-dimethylphenol (0.106 g, 0.868 mmol) was added to the solution. The resulting clear and colorless solution was stirred at room temperature for 14 d before it was filtered through a short plug of celite (5 mL). The celite plug was further washed with benzene (3 mL × 2). The clear and colorless filtrates were combined with the wash, and the mixture was purified by distillation. The product was distilled at 250 °C (0.1 mmHg) to give the product as a clear colorless oil (0.246 g, 0.694 mmol, 80.0%). ¹H NMR (benzene-*d*₆, 600 MHz): δ 8.44 (m, 1 H, C₁₀H₇), 8.01 (d, ³J_{HH} = 6.6 Hz, 1 H, C₁₀H₇), 7.76 (d, ³J_{HH} = 7.8 Hz, 2 H, *o*-C₆H₅), 7.67 (d, ³J_{HH} = 7.8 Hz, 1 H, C₁₀H₇), 7.59 (m, 1 H, C₁₀H₇), 7.23 (t, ³J_{HH} = 7.2 Hz, 1 H, *p*-C₆H₅), 7.18 (m, 2 H, C₁₀H₇), 7.11 (m, 3 H, *m*-C₆H₅ (2 H) and C₁₀H₇ (1 H)), 6.83 (s, 2 H, *o*-C₆H₃Me₂), 6.47 (s, 1 H, *p*-C₆H₃Me₂), 6.34 (s, ¹J_{SiH} = 218 Hz, 1 H, SiH), 1.99 (s, 6 H, C₆H₃Me₂). ¹³C{¹H} NMR (benzene-*d*₆, 150 MHz): δ 156.48 (*ipso*-C₆H₃Me₂), 139.87 (*m*-C₆H₃Me₂), 139.69 (C₁₀H₇), 137.86 (C₁₀H₇), 136.47 (*ipso*-C₆H₅), 135.42 (*o*-C₆H₅), 134.31 (C₁₀H₇), 134.23 (C₁₀H₇), 132.21 (C₁₀H₇), 132.13 (C₁₀H₇), 131.16 (*p*-C₆H₅), 129.57 (*m*-C₆H₅), 127.24 (C₁₀H₇), 126.57 (C₁₀H₇), 125.86 (*p*-C₆H₃Me₂),

124.62 (C₁₀H₇), 118.48 (C₁₀H₇), 117.82 (*o*-C₆H₃Me₂), 21.56 (C₆H₃Me₂). ²⁹Si{¹H} NMR (benzene-*d*₆, 119 MHz): δ -13.32. GC-MS: C₂₄H₂₂OSi m/e 354 (M⁺). [α]_D²⁰ = +11.96 (C₆H₆).

References

1. (a) Trofimenko, S., *Acc. Chem. Res.* **1971**, *4*, 17-22. (b) Trofimenko, S., *Chem. Rev.* **1993**, *93*, 943-980.
2. (a) Fujisawa, K.; Tanaka, M.; Moro-oka, Y.; Kitajima, N., *J. Am. Chem. Soc.* **1994**, *116*, 12079-12080. (b) Kersten, J. L.; Kucharczyk, R. R.; Yap, G. P. A.; Rheingold, A. L.; Theopold, K. H., *Chem. Eur. J.* **1997**, *3*, 1668-1674. (c) Komatsuzaki, H.; Sakamoto, N.; Satoh, M.; Hikichi, S.; Akita, M.; Moro-oka, Y., *Inorg. Chem.* **1998**, *37*, 6554-6555. (d) Kisko, J. L.; Hascall, T.; Parkin, G., *J. Am. Chem. Soc.* **1998**, *120*, 10561-10562. (e) Shirasawa, N.; Nguyet, T. T.; Hikichi, S.; Moro-oka, Y.; Akita, M., *Organometallics* **2001**, *20*, 3582-3598. (f) Qin, K.; Incarvito, C. D.; Rheingold, A. L.; Theopold, K. H., *Angew. Chem. Int. Ed.* **2002**, *41*, 2333-2335. (g) Thyagarajan, S.; Shay, D. T.; Incarvito, C. D.; Rheingold, A. L.; Theopold, K. H., *J. Am. Chem. Soc.* **2003**, *125*, 4440-4441. (h) Hikichi, S.; Okuda, H.; Ohzu, Y.; Akita, M., *Angew. Chem. Int. Ed.* **2009**, *48*, 188-191.
3. (a) Ferrence, G. M.; McDonald, R.; Takats, J., *Angew. Chem. Int. Ed.* **1999**, *38*, 2233-2237. (b) Zimmermann, M.; Takats, J.; Kiel, G.; Törnroos, K. W.; Anwender, R., *Chem. Commun.* **2008**, 612-614.
4. (a) Gorrell, I. B.; Looney, A.; Parkin, G.; Rheingold, A. L., *J. Am. Chem. Soc.* **1990**, *112*, 4068-4069. (b) Alsfasser, R.; Trofimenko, S.; Looney, A.; Parkin, G.;

- Vahrenkamp, H., *Inorg. Chem.* **1991**, *30*, 4098-4100. (c) Han, R.; Parkin, G., *J. Am. Chem. Soc.* **1992**, *114*, 748-757.
5. (a) Brunner, H.; Singh, U. P.; Boeck, T.; Altmann, S.; Scheck, T.; Wrackmeyer, B., *J. Organomet. Chem.* **1993**, *443*, C16-C18. (b) LeCloux, D. D.; Tolman, W. B., *J. Am. Chem. Soc.* **1993**, *115*, 1153-1154. (c) LeCloux, D. D.; Keyes, M. C.; Osawa, M.; Reynolds, V.; Tolman, W. B., *Inorg. Chem.* **1994**, *33*, 6361-6368. (d) Kitajima, N.; Tolman, W. B., Coordination Chemistry with Sterically Hindered Hydrotris(Pyrazolyl)Borate Ligand: Organometallic and Bioinorganic Perspectives. In *Prog. Inorg. Chem.*, 1995; Vol. 43, pp 419-531. (e) Keyes, M. C.; Young, V. G., Jr.; Tolman, W. B., *Organometallics* **1996**, *15*, 4133-4140. (f) Keyes, M. C.; Chamberlain, B. M.; Caltagirone, S. A.; Halfen, J. A.; Tolman, W. B., *Organometallics* **1998**, *17*, 1984-1992. (g) Singh, U. P.; Babbar, P.; Hassler, B.; Nishiyama, H.; Brunner, H., *J. Mol. Catal. A: Chem.* **2002**, *185*, 33-39.
6. (a) Trofimenko, S.; Calabrese, J. C.; Domaille, P. J.; Thompson, J. S., *Inorg. Chem.* **1989**, *28*, 1091-1101. (b) Murtuza, S.; Casagrande, O. L.; Jordan, R. F., *Organometallics* **2002**, *21*, 1882-1890. (c) Marques, N.; Sella, A.; Takats, J., *Chem. Rev.* **2002**, *102*, 2137-2159. (d) Michiue, K.; Jordan, R. F., *Organometallics* **2004**, *23*, 460-470.
7. Lee, H.; Jordan, R. F., *J. Am. Chem. Soc.* **2005**, *127*, 9384-9385.
8. Dunne, J. F.; Su, J.; Ellern, A.; Sadow, A. D., *Organometallics* **2008**, *27*, 2399-2401.
9. Baird, B.; Pawlikowski, A. V.; Su, J.; Wiench, J. W.; Pruski, M.; Sadow, A. D., *Inorg. Chem.* **2008**, *47*, 10208-10210.

10. Neal, S. R.; Ellern, A.; Sadow, A. D., *J. Organomet. Chem.* **2011**, *696*, 228-234.
11. (a) Gade, L. H.; César, V.; Bellemin-Lapponnaz, S., *Angew. Chem. Int. Ed.* **2004**, *43*, 1014-1017. (b) Gade, L. H.; Marconi, G.; Dro, C.; Ward, B. D.; Poyatos, M.; Bellemin-Lapponnaz, S.; Wadepohl, H.; Sorace, L.; Poneti, G., *Chem. Eur. J.* **2007**, *13*, 3058-3075. (c) Gade, L. H.; Bellemin-Lapponnaz, S., *Chem. Eur. J.* **2008**, *14*, 4142-4152.
12. Denmark, S. E.; Stavenger, R. A.; Faucher, A.-M.; Edwards, J. P., *J. Org. Chem.* **1997**, *62*, 3375-3389.
13. Dugal-Tessier, J.; Dake, G. R.; Gates, D. P., *Org. Lett.* **2010**, *12*, 4667-4669.
14. Guilbault, A.-A.; Basdevant, B.; Wanie, V.; Legault, C. Y., *J. Org. Chem.* **2012**, *77*, 11283-11295.
15. Lang, K.; Park, J.; Hong, S., *J. Org. Chem.* **2010**, *75*, 6424-6435.
16. Stohler, R.; Wahl, F.; Pfaltz, A., *Synthesis* **2005**, 1431-1436.
17. (a) Manna, K.; Xu, S.; Sadow, A. D., *Angew. Chem. Int. Ed.* **2011**, *50*, 1865-1868. (b) Manna, K.; Everett, W. C.; Schoendorff, G.; Ellern, A.; Windus, T. L.; Sadow, A. D., *J. Am. Chem. Soc.* **2013**, *135*, 7235-7250.
18. Applewhite, T. H.; Waite, H.; Niemann, C., *J. Am. Chem. Soc.* **1958**, *80*, 1465-1469.
19. Gibson, S. E.; Mainolfi, N.; Kalindjian, S. B.; Wright, P. T.; White, A. J. P., *Chem. Eur. J.* **2005**, *11*, 69-80.
20. Leonard, W. R.; Romine, J. L.; Meyers, A. I., *J. Org. Chem.* **1991**, *56*, 1961-1963.
21. Kidd, R. G., *NMR of Newly Accessible Nuclei*. Academic Press: New York, 1983; Vol. 2, p 49-77.

22. (a) White, D.; Taverner, B. C.; Leach, P. G. L.; Coville, N. J., *J. Comp. Chem.* **1993**, *14*, 1042-1049. (b) Guzei, I. A.; Wendt, M., *Dalton Trans.* **2006**, 3991-3999.
23. Guzei, I. A.; Wendt, M. *Solid-G*, 2004.
24. (a) Joachim, J. E.; Apostolidis, C.; Kanellakopulos, B.; Maier, R.; Marques, N.; Meyer, D.; Müller, J.; Pires de Matos, A.; Nuber, B.; Rebizant, J.; Ziegler, M. L., *J. Organomet. Chem.* **1993**, *448*, 119-129. (b) Wu, K.; Mukherjee, D.; Ellern, A.; Sadow, A. D.; Geiger, W. E., *New J. Chem.* **2011**, *35*, 2169-2178.
25. Mukherjee, D.; Ellern, A.; Sadow, A. D., *J. Am. Chem. Soc.* **2012**, *134*, 13018-13026.
26. (a) Han, R.; Gorrell, I. B.; Looney, A. G.; Parkin, G., *J. Chem. Soc., Chem. Commun.* **1991**, 717-719. (b) Bergquist, C.; Parkin, G., *Inorg. Chem.* **1999**, *38*, 422-423. (c) Rombach, M.; Brombacher, H.; Vahrenkamp, H., *Eur. J. Inorg. Chem.* **2002**, 153-159. (d) Mukherjee, D.; Ellern, A.; Sadow, A. D., *J. Am. Chem. Soc.* **2010**, *132*, 7582-7583. (e) Sattler, W.; Parkin, G., *J. Am. Chem. Soc.* **2011**, *133*, 9708-9711.
27. Rit, A.; Spaniol, T. P.; Okuda, J., *Chem. Asian J.* **2014**, *9*, 612-619.
28. Brown, N. J.; Harris, J. E.; Yin, X.; Silverwood, I.; White, A. J. P.; Kazarian, S. G.; Hellgardt, K.; Shaffer, M. S. P.; Williams, C. K., *Organometallics* **2014**, *33*, 1112-1119.
29. Mukherjee, D.; Thompson, R. R.; Ellern, A.; Sadow, A. D., *ACS Catal.* **2011**, *1*, 698-702.

30. Rendler, S.; Plefka, O.; Karatas, B.; Auer, G.; Fröhlich, R.; Mück-Lichtenfeld, C.; Grimme, S.; Oestreich, M., *Chem. Eur. J.* **2008**, *14*, 11512-11528.
31. Xu, L.-W.; Li, L.; Lai, G.-Q.; Jiang, J.-X., *Chem. Soc. Rev.* **2011**, *40*, 1777-1790.
32. Ohta, T.; Ito, M.; Tsuneto, A.; Takaya, H., *J. Chem. Soc., Chem. Commun.* **1994**, 2525-2526.
33. Schmidt, S. P.; Trogler, W. C.; Basolo, F.; Urbancic, M. A.; Shapley, J. R., Pentacarbonylrhenium Halides. In *Inorg. Syn.*, John Wiley & Sons, Inc.1985; pp 41-46.
34. Delair, P.; Einhorn, C.; Einhorn, J.; Luche, J. L., *J. Org. Chem.* **1994**, *59*, 4680-4682.

CHAPTER 6. CONCLUSION

The previous chapters have demonstrated the effect of the modification of the electronic and steric properties of the ancillary ligand upon the reactivity of the organometallic complexes. The replacement of one of the oxazoline rings in To^M ($To^M = \text{tris}(4,4\text{-dimethyl-2-oxazoliny})\text{phenylborate}$) with an imidazole ring enhances the electron-donating ability of the ligand by generating a carbene moiety upon deprotonation while maintaining the *fac*-coordination mode of the scorpionate ligand. The heteroleptic monoanionic mixed *N*-heterocyclic carbene–oxazolinyborate ligands, $\text{PhB}(\text{Ox}^{\text{Me}2})_2(\text{Im}^{\text{tBu}}\text{H})$ and $\text{PhB}(\text{Ox}^{\text{Me}2})_2(\text{Im}^{\text{Mes}}\text{H})$ ($\text{Ox}^{\text{Me}2} = 4,4\text{-dimethyl-2-oxazoline}$; $\text{Im}^{\text{tBu}}\text{H} = 1\text{-tert-butylimidazole}$; $\text{Im}^{\text{Mes}}\text{H} = 1\text{-mesitylimidazole}$), are readily deprotonated by dialkylzinc reagents to form the zinc alkyl complexes $\{\text{PhB}(\text{Ox}^{\text{Me}2})_2\text{Im}^{\text{Mes}}\}\text{ZnR}$ ($R = \text{Me}$ and Et). Like $To^M\text{ZnEt}$, the zinc ethyl complex $\{\text{PhB}(\text{Ox}^{\text{Me}2})_2\text{Im}^{\text{Mes}}\}\text{ZnEt}$ reacts with oxygen at atmospheric pressure to give the zinc ethylperoxide complex $\{\text{PhB}(\text{Ox}^{\text{Me}2})_2\text{Im}^{\text{Mes}}\}\text{ZnOOEt}$, which is only the second crystallographically characterized example of a ligand that supports a monoanionic zinc alkylperoxide formed from oxygen. Even though the zinc methyl complex $\{\text{PhB}(\text{Ox}^{\text{Me}2})_2\text{Im}^{\text{Mes}}\}\text{ZnMe}$ remains inert toward oxygen as $To^M\text{ZnMe}$ does, and unlike $To^M\text{ZnEt}$, $\{\text{PhB}(\text{Ox}^{\text{Me}2})_2\text{Im}^{\text{Mes}}\}\text{ZnEt}$ is too unstable toward *t*-BuOOH to give isolable $\{\text{PhB}(\text{Ox}^{\text{Me}2})_2\text{Im}^{\text{Mes}}\}\text{ZnOOt-Bu}$, the carbene moiety is notably stable in the presence of oxygen and any $\cdot\text{OOR}$ that gives the alkylperoxide product. In addition, the significant and systematic distortion of the alkyl groups observed in the X-ray structures of $\{\text{PhB}(\text{Ox}^{\text{Me}2})_2\text{Im}^{\text{Mes}}\}\text{ZnR}$ ($R = \text{Me}$, Et , and

OOEt) helps the understanding of the electronic, as well as the steric effect of the carbene substituent of the ligand toward the reactivity of the organometallic complexes.

Enhanced reactivity of the metal complexes bearing the mixed *N*-heterocyclic carbene–oxazolinyborate ligand is also observed in the case of the rhodium and iridium complexes. Phenylsilane reacts cleanly with $\{\text{PhB}(\text{Ox}^{\text{Me}_2})_2\text{Im}^{\text{Mes}}\}\text{Rh}(\text{CO})_2$ and $\{\text{PhB}(\text{Ox}^{\text{Me}_2})_2\text{Im}^{\text{Mes}}\}\text{Ir}(\text{CO})\text{CN}^t\text{Bu}$ to displace CO and CN^tBu , respectively, and forms $\{\text{PhB}(\text{Ox}^{\text{Me}_2})_2\text{Im}^{\text{Mes}}\}\text{RhH}(\text{SiH}_2\text{Ph})\text{CO}$ and $\{\text{PhB}(\text{Ox}^{\text{Me}_2})_2\text{Im}^{\text{Mes}}\}\text{IrH}(\text{SiH}_2\text{Ph})\text{CN}^t\text{Bu}$, respectively, under thermal conditions, while the oxidative addition of Si–H bond to $\text{To}^{\text{M}}\text{Rh}(\text{CO})_2$, $\text{TpRh}(\text{CO})_2$, and $\text{CpM}(\text{CO})_2$ ($\text{M} = \text{Rh}, \text{Ir}$) requires photochemical conditions and sometimes gives multiple unidentified products. It is also observed that, compared to the *tert*-butylimidazole substituted borate ligand, the mesitylimidazole substituted one shows much richer reactivity, which indicates that the substituent on the imidazole ring also affects the reactivity of the organometallic complexes. The rich reactivity of $\{\text{PhB}(\text{Ox}^{\text{Me}_2})_2\text{Im}^{\text{Mes}}\}$ -supported rhodium and iridium complexes has deepened the understanding of the electronic and the steric properties of the ligand. For example, the ligand gives $\{\kappa^4\text{-PhB}(\text{Ox}^{\text{Me}_2})\text{Im}^{\text{Mes}'}\text{CH}_2\}\text{Rh}(\mu\text{-H})(\mu\text{-Cl})\text{Rh}(\eta^2\text{-C}_8\text{H}_{14})_2$ with $[\text{Rh}(\mu\text{-Cl})(\eta^2\text{-C}_8\text{H}_{14})_2]_2$, while $\{\text{PhB}(\text{Ox}^{\text{Me}_2})_2\text{Im}^{\text{Mes}}\}\text{IrH}(\eta^3\text{-C}_8\text{H}_{13})$ is formed when the ligand is treated with $[\text{Ir}(\mu\text{-Cl})(\eta^2\text{-C}_8\text{H}_{14})_2]_2$. In another occasion, the nonanalogous products have been observed as well when $\{\text{PhB}(\text{Ox}^{\text{Me}_2})_2\text{Im}^{\text{Mes}}\}\text{Ir}(\text{CO})_2$ C–H activates benzene under photolytic conditions to give $\{\text{PhB}(\text{Ox}^{\text{Me}_2})_2\text{Im}^{\text{Mes}}\}\text{IrH}(\text{Ph})\text{CO}$, while $\{\text{PhB}(\text{Ox}^{\text{Me}_2})_2\text{Im}^{\text{Mes}}\}\text{Rh}(\text{CO})_2$ formed $\{\kappa^4\text{-PhB}(\text{Ox}^{\text{Me}_2})_2\text{Im}^{\text{Mes}'}\text{CH}_2\}\text{RhH}(\text{CO})$ through intramolecular C–H activation under the same conditions.

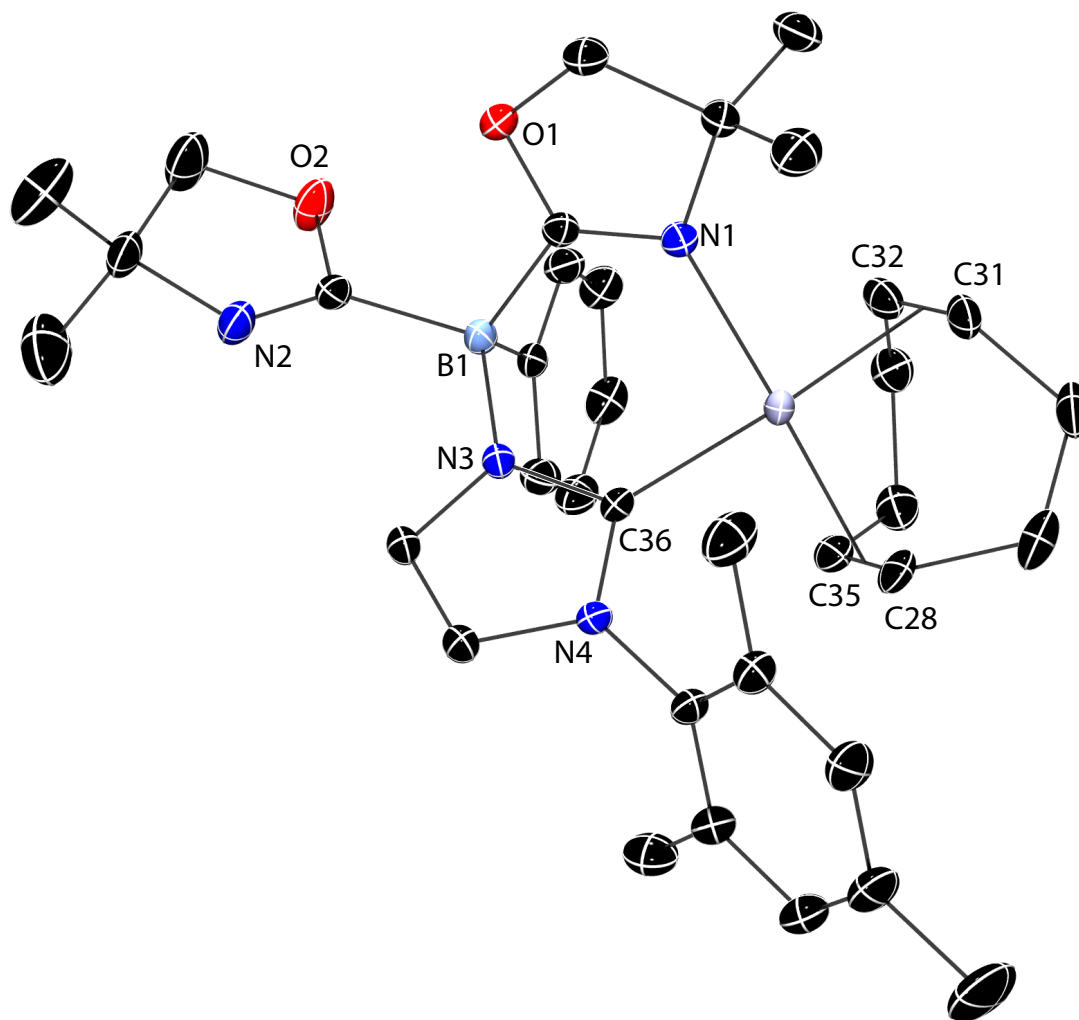
The rhodium silyl complex $\{\text{PhB}(\text{Ox}^{\text{Me}_2})_2\text{Im}^{\text{Mes}}\}\text{RhH}(\text{SiH}_2\text{Ph})\text{CO}$ leads to the formation of an electrophilic, coordinatively unsaturated rhodium silylene complex when treated with tris(perfluorophenyl)borane. The resulting rhodium complex has unique spectroscopic features that separate itself from other rhodium silylene complexes as the characteristic ^{29}Si chemical shift is quite more upfield which results from the silicon rearrangement to bond to both rhodium and an oxazoline nitrogen after the H-abstraction. The complex shows catalytic ability toward deoxygenation of carbonyl-containing compounds especially esters in the presence of phenylsilane, which, to the best of our knowledge, no other catalyst can with primary silanes. The carbene–oxazolinyborate ligand steers the property of the catalyst such that even though the Lewis acid generated during the catalysis catalyzes the hydrosilylation of the substrate, the hydrosilylation intermediate is then deoxygenated by the rhodium catalyst in the presence of primary silane through C–O bond cleavage in a tandem fashion.

Although the modification on the steric property of the tris(oxazoliny)borate ligand by incorporating enantiomerically enriched oxazoline moieties, 4*S*-isopropyl-5,5-dimethyl-2-oxazoline, gives moderate enantioselectivity in catalytic cross-dehydrocoupling of alcohols with silanes, it is noteworthy that the catalyst for this catalysis, $\text{To}^{\text{P}*}\text{ZnH}$ ($\text{To}^{\text{P}*}$ = tris(4*S*-isopropyl-5,5-dimethyl-2-oxazoliny)phenylborate), is the first crystallographically characterized terminal zinc hydride on a chiral ligand. However, the incorporation of this oxazoline moiety onto the ligand still opens possibilities for achieving excellent enantioselectivity as demonstrated by the zirconium catalyst of $\{\text{PhB}(\text{C}_5\text{H}_4)(\text{Ox}^{\text{iPr,Me}_2})_2\}\text{Zr}(\text{NMe}_2)_2$ (C_5H_4 = cyclopentadienyl, $\text{Ox}^{\text{iPr,Me}_2}$ = 4*S*-isopropyl-5,5-dimethyl-2-oxazoliny), which shows excellent enantioselectivity in

catalytic hydroamination/cyclization of olefinic amines. In addition, the comparative study on the C–O stretching frequencies of the rhenium and manganese tricarbonyl complexes shows that $\text{To}^{\text{P}*}$ is more electron-donating than To^{M} , To^{P} , Tp , and Tp^* (Tp = tris(1-pyrazolyl)hydroborate, Tp^* = tris(3,5-dimethylpyrazolyl)hydroborate). Moreover, one of the advantages of the tris(oxazoliny)borate ligand is that, besides its steric property, the electronic property of the ligand is also tunable. We have demonstrated that the incorporation of the imidazole moiety significantly enhances the electron-donating ability of the ligand in the previous chapters, therefore it opens the opportunity of the synthesis of a new hybrid *N*-heterocyclic carbene–oxazolinyborate ligand, $\text{PhB}(\text{Ox}^{\text{iPr,Me}_2})_2(\text{Im}^{\text{RH}})$, which combines the modified electronic and steric properties of the tris(oxazoliny)borate ligand demonstrated before. Hence, the moiety of 4*S*-isopropyl-5,5-dimethyl-2-oxazoline may still be beneficial for other organometallic complexes.

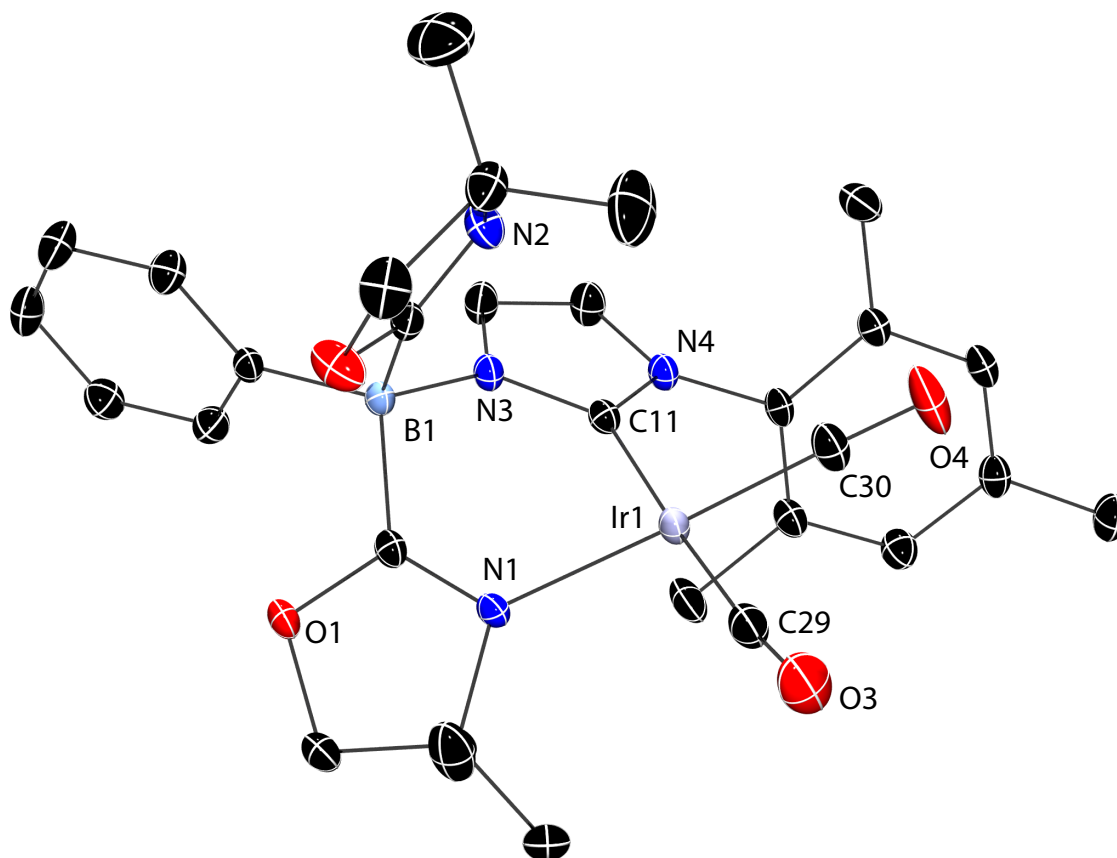
Both borate ligands ($\text{PhB}(\text{Ox}^{\text{Me}_2})_2\text{Im}^{\text{R}}$ ($\text{R} = \text{tBu, Mes}$) and $\text{To}^{\text{P}*}$) can be metalated with more metal precursors other than the ones presented in this thesis. Magnesium, calcium, scandium, cobalt, yttrium, ruthenium, lutetium, and gold precursors have been tested with these ligands, and the resulting organometallic complexes have shown interesting spectroscopic and crystallographic features, as well as remarkable chemical reactivity that could lead to a broader understanding of the ligands and significant discoveries. In addition, more in-depth study of the ligands could also be derived from the work presented in this thesis as the kinetic study of the CO dissociation reaction of $\{\text{PhB}(\text{Ox}^{\text{Me}_2})_2\text{Im}^{\text{Mes}}\}\text{Rh}(\text{CO})_2$ and phenylsilane is underway.

APPENDIX A. X-RAY STRUCTURE OF THE IRIDIUM CYCLOOCTADIENE
COMPLEX



Rendered thermal ellipsoid plot of $\{\text{PhB}(\text{Ox}^{\text{Me}_2})_2\text{Im}^{\text{Mes}}\}\text{Ir}(\eta^4\text{-C}_8\text{H}_{12})$ (Chapter 3, **6**) with ellipsoids at 35% probability. A co-crystallized pentane solvent molecule and H atoms are not plotted for clarity. Selected interatomic distances (Å): Ir1-C36, 2.069(3); Ir1-N1, 2.116(2); Ir1-C28, 2.124(3); Ir1-C35, 2.126(3); Ir1-C31, 2.192(3); Ir1-C32, 2.161(3). Selected interatomic angle (°): C36-Ir1-N1, 84.85(10).

APPENDIX B. X-RAY STRUCTURE OF THE IRIDIUM DICARBONYL COMPLEX



Rendered thermal ellipsoid plot of $\{\text{PhB}(\text{Ox}^{\text{Me}_2})_2\text{Im}^{\text{Mes}}\}\text{Ir}(\text{CO})_2$ (Chapter 3, 7) with ellipsoids at 35% probability. A co-crystallized benzene solvent molecule and H atoms are not plotted for clarity. Selected interatomic distances (Å): Ir1-C11, 2.074(3); Ir1-N1, 2.085(2); Ir1-C29, 1.891(3); Ir1-C30, 1.836(3). Selected interatomic angles (°): C11-Ir1-N1, 86.78(10); N1-Ir1-C29, 95.57(11); C29-Ir1-C30, 85.69(13); C30-Ir1-C11, 91.93(12).